Molecular Characterisation of the Polyhistidine Triad Proteins of *Streptococcus pneumoniae*

THE UNIVERSITY of ADELAIDE

Charles Deveron Plumptre, BA (Hons)

A thesis submitted in fulfilment of the requirements for the degree of Doctor of Philosophy from the University of Adelaide

February 2013

Research Centre for Infectious Diseases
School of Molecular and Biomedical Science
The University of Adelaide
Adelaide, S.A., Australia

Table of Contents

Abstract

The polyhistidine triad (Pht) proteins are a family of proteins defined by the presence of multiple copies of the histidine triad motif (HxxHxH). There are four members of this family in *Streptococcus pneumoniae*: PhtA, B, D and E. The proteins are found on the cell surface and immunisation with them has been shown to elicit protective immunity against disease caused by this Gram positive pathogen.

The aim of the work presented in this thesis was to extend our understanding of the structure and functions of these proteins, as well as to explore their potential use in vaccines. Firstly, the previously reported interaction of the Pht proteins with factor H (a negative regulator of the alternative pathway of the complement system) was investigated by testing binding of the proteins to different regions of factor H by ELISA and flow cytometry. This revealed that the Pht proteins bind to the first seven domains of factor H more strongly than they do to the full length protein.

Pht proteins have also been implicated in binding to zinc ions. In this work the proteins were found to interact to a certain extent with a number of transition metal ions. However, measurements of metal ion content of wild-type and Δ*phtABDE* mutant strains only showed decreases in zinc and nickel content of the mutant relative to the wild-type. Growth of the mutant strain was impaired relative to wild-type in media with low concentrations of available zinc. Further work indicated that this phenotype is linked to the zinc-specific ABC transporter substrate binding proteins AdcA and AdcAII, and implied that the Pht proteins may facilitate acquisition of zinc by AdcAII.

It is not clear which region or regions of the Pht proteins are required for protective immunity to be induced against pneumococcal disease when used as immunogens. To investigate this, truncated derivatives of PhtA and PhtD were cloned, expressed and purified and analysed for their capacity to bind antibodies that had been generated against the full length protein. This led to the identification of immunogenic regions in both proteins which were subsequently tested as immunogens in mouse models of pneumococcal disease and colonisation. However, significant protective effects were not found in almost all cases, including for control groups immunised with the full length proteins, leading to the conclusion that PhtA and PhtD are not effective vaccine candidates in the models tested.

Lastly, the mechanism of attachment of PhtD to the cell surface was examined by deletion of regions near the N-terminus of the protein and subsequent analysis of the surface accessibilities of the mutant forms of the protein. These experiments identified a short stretch of amino acids that are required for the protein to be cell-associated. Furthermore, a considerable proportion of the total amount of wild-type PhtD produced was found to be released into culture supernatants. Further experiments revealed that the released protein could not re-attach to the surface and that PhtD release occurs in a number of different pneumococcal strains.

Declaration

This work contains no material which has been accepted for the award of any other degree or diploma in any university or other tertiary institution to Charles Deveron Plumptre and, to the best of my knowledge and belief, contains no material previously published or written by another person, except where due reference has been made in the text.

I give consent to this copy of my thesis, when deposited in the University Library, being made available for loan and photocopying, subject to the provisions of the Copyright Act 1968.

I also give permission for the digital version of my thesis to be made available on the web, via the University's digital research repository, the Library catalogue, and also through web search engines, unless permission has been granted by the University to restrict access for a period of time.

……

Charles Deveron Plumptre

……/……/…….

Abbreviations

°C	degrees Celsius
µg	microgram/s
µl	microlitre/s
µM	micromolar
ABC transporter	ATP-binding cassette transporter
ATP	adenosine triphosphate
bp	base pairs
C+Y	casein hydrolysate medium with yeast extract
CFU	colony forming units
cml	chloramphenicol
DNA	deoxyribonucleic acid
EDTA	ethylenediaminetetraacetic acid disodium salt
ELISA	enzyme-linked immunosorbent assay
ery	erythromycin
FITC	fluorescein-5-isothiocyanate
g	relative centrifugal force
h	hour/s
HEPES	4-(2-hydroxyethyl)-1-piperazineethanesulphonic acid
ICPMS	inductively-coupled plasma mass spectrometry
IPTG	isopropyl-β-D-thio-galactopyranoside
kb	kilobase/s
K_D	dissociation constant
kDa	kilodalton/s
kg	kilogram/s
kpsi	kilopounds per square inch
l	litre/s
LB	Luria Bertani broth
M	molar
mg	milligram/s
min	minute/s

ml	millilitre/s
mM	millimolar
MOPS	3-(N-morpholino)propanesulphonic acid
ng	nanogram/s
Ni-NTA	nickel-nitrilotriacetic acid
nm	nanometres
OD_{600}	optical density at 600 nm
PAGE	polyacrylamide gel electrophoresis
PBS	phosphate buffered saline
PCR	polymerase chain reaction
PMSF	phenylmethylsulphonyl fluoride
RT	room temperature
s	second/s
SBP	solute-binding protein
SDS	sodium dodecyl sulphate
spec	spectinomycin
spp	species
TBE	tris-borate EDTA buffer
tet	tetracycline
TPEN	N,N,N′,N′-Tetrakis(2-pyridylmethyl)ethylenediamine
TTBS	Tween tris buffered saline
v/v	volume per volume
w/v	weight per volume
WT	wild-type

Acknowledgements

Firstly I would like to thank my principal supervisor Professor James Paton for giving me the opportunity to come to Australia to do a PhD, as well as for all of the time and effort he has put in to help me complete it and to develop as a scientist. Thanks also to my co-supervisor Dr David Ogunniyi for all of the encouragement, help and advice he has given me, both in the lab and on the soccer pitch.

I would like to thank Dr Chris McDevitt for the large contributions he has made to many aspects of my project, as well as all of the members of the Paton group for their help and friendship throughout my project. To the alpha males Dr Richard Harvey, Brock Herdman and Dr Adam 'TGM' Potter, thank you for introducing me ever more to Australian culture, and to the afternoon tea club of Dr Catherine Hughes, Stephanie Philp, Dr Lauren McAllister and Melissa Chai, thank you for always inviting me, especially for when there was cake! Thanks to Dr Claudia Trappetti, Dr Layla Mahdi and Dr Austen Chen for hysterical, delightful and incomprehensible conversation respectively. Thanks also to Dr Adrienne Paton, Zarina Amin, Dr Hui Wang, Dr Trisha Rogers, Dr Miranda Ween, Dr Bart Eijkelkamp, Victoria Lewis, Jacqui Morey, Jon Whittall, Stephanie Begg, Ursula Talbot and Dr Tony Focareta. I feel lucky to have landed in a lab filled with so many friendly and helpful people and that I get to work in such a relaxed and productive environment.

I would also like to thank a number of others who have helped me along the way. Thanks to Dr Stephen Kidd for help with zeta potential measurements, to Dr Alistair Standish for anti-CpsD antibody, to Tatiana Soares Da Costa, Dr Emma Parkinson-Lawrence, Shee Chee Ong and Dr Briony Forbes for help with surface plasmon resonance experiments and to Sarah Wilkinson for help with circular dichroism spectroscopy. I am also very grateful to the Northcote Trust for their financial support throughout my PhD.

Lastly thanks to my amazing fiancée Rachel for putting up with me talking about Pht proteins for three years, and I am looking forward to many more together.

Chapter 1: Introduction

1.1 Significance of *Streptococcus pneumoniae* for human health

Streptococcus pneumoniae (the pneumococcus) is a major human pathogen. It is a leading cause of bacterial pneumonia, meningitis, sepsis and otitis media, and is estimated to have caused 14.5 million episodes of serious disease in 2000 (O'Brien *et al*., 2009). Bacterial pneumonia and meningitis, of which the pneumococcus is the principal cause, are responsible for the loss of around 105 million disability-adjusted life years (a measure of disease burden designed by the World Health Organization to capture both death and disease) per annum, which is significantly larger than that of any other infectious disease grouping (WHO, 2004; Enserink, 2009). Furthermore, the bacterium is of particular importance for children under the age of five years, in whom it has been estimated to cause around 11% of all deaths worldwide (O'Brien *et al*., 2009). Pneumococcal otitis media is the most common reason for the prescription of antibiotics for children in the United States of America (USA), where over five million episodes of this condition occur each year, at a cost of around US $3 billion (American Academy of Pediatrics and American Academy of Family Physicians, 2004; Rodgers *et al*., 2009; Agency for Healthcare Research and Quality (AHRQ), 2010). Lastly, co-infections of *S. pneumoniae* and other pathogens have a very significant impact on human health, notably in the cases of human immunodeficiency virus (HIV) and pandemic influenza. For instance, the majority of deaths during the 1918-1919 'Spanish flu' pandemic are now thought to have been caused by secondary bacterial pneumonia, principally caused by the pneumococcus (Morens *et al*., 2008). Thus, the impact of this pathogen on global human health is enormous.

1.2 Pathogenesis of pneumococcal disease and underlying molecular mechanisms

Streptococcus pneumoniae is a Gram-positive encapsulated diplococcus which readily colonises the nasopharynx of humans; this is its main niche as there are no animal or environmental reservoirs in which the bacteria can survive. Events subsequent to colonisation are determined by a complex interplay between environmental and genetic (of both host and pathogen) factors; the bacteria may be eliminated, or persist for weeks or

months in the upper airway, or invade deeper body tissues such as the lungs, blood, brain or middle ear. Whilst nasopharyngeal colonisation and persistence alone do not cause pathology, the process of invasion and the subsequent inflammation lead to pneumococcal diseases such as pneumonia, sepsis, meningitis and otitis media. The propensity to cause invasive disease in different niches is in part also determined by the serotype of the bacteria, of which over 90 have now been identified. Serotypes are defined based on the chemical structure of the polysaccharides that make up the layer of capsule that pneumococci produce and attach to the outside of their cell wall.

1.2.1 Colonisation

Pneumococci are generally transmitted to a new nasopharyngeal niche, that is, to a new host, through contaminated respiratory secretions, usually from a close contact. The 'donor' individual is generally just a carrier of the pneumococcus, rather than an individual experiencing any form of invasive disease. In most cases, the recipient nasopharynx already harbours commensal microorganisms, such as α-haemolytic streptococci, which inhibit colonisation by *S. pneumoniae* (Tano *et al*., 2000). Furthermore, there can be competition between the pneumococcus and other pathogenic species such as *Haemophilus influenzae*, *Neisseria meningitidis* or even other strains of *S. pneumoniae* in the nasopharynx that affect the ability of the incoming bacteria to successfully colonise (Bogaert *et al*., 2004).

Colonisation depends on adherence of pneumococci to the epithelial cells lining the upper respiratory tract. This is thought to occur via specific binding of pneumococcal surface proteins to host cell surface carbohydrates, as well as via non-specific physicochemical interactions (Swiatlo *et al*., 2002). Interestingly, reversible phenotypic variation of pneumococci (colonies of which can be identified as being in either an opaque or transparent form) also affects adherence properties. Transparent phase variants show superior adherence, and this is associated with lower expression of polysaccharide capsule and higher expression of certain cell-surface proteins, whereas opaque variants express more capsule and are more virulent (Weiser *et al*., 1994; Kim and Weiser, 1998).

The prevalence of colonisation by *S. pneumoniae* across human populations is dependent on age, increasing from birth to a peak at around 2 years of age. This is followed by a decline for the majority of life and another rise in the elderly. A number of

studies around the world have examined carriage rates, revealing large differences in the percentage of people colonised, from only a few percent up to 70% or even more (reviewed in Bogaert *et al*., 2004). There are a number of different risk factors that affect carriage rates and could account for these differences, such as ethnicity, crowding, family size, income, smoking and antibiotic use (Principi *et al*., 1999; Bogaert *et al*., 2004).

1.2.2 Progression to invasive disease

Disease occurs when pneumococci penetrate into niches beyond the nasopharynx, such as the lungs, blood, brain or middle ear. Invasion is usually the result of acquisition of a new serotype, as opposed to a serotype that has stably colonised the nasopharynx for some time (Gray and Dillon, 1986). After initial contact of the bacteria with the respiratory epithelium, an inflammatory reaction leads to a change in the expression and distribution of receptors on host cells. These mediate new interactions between the pneumococcus and the host cell, such as between phosphorylcholine in the bacterial cell wall and the platelet-activating-factor receptor, and between pneumococcal surface protein C (see section 1.4.3) and the polymeric immunoglobulin receptor. Both of these interactions contribute to pneumococci invading into and through the nasopharyngeal epithelium (Cundell *et al*., 1995; Rosenow *et al*., 1997; Zhang *et al*., 2000). A number of pneumococcal transcriptional regulators and two-component signal transduction systems have been identified and are thought to be involved in progression to invasive disease (Hava *et al*., 2003). Alteration in gene expression emanating from the phase variation phenomenon mentioned above is also thought to play a role in disease progression, but the molecular basis of this is not understood. Finally, host genetics and other factors such as viral infections of the respiratory tract, physical injury, alcoholism and diabetes can also contribute to the development of invasive pneumococcal disease (Willey *et al*., 2008).

1.2.3 Host immune response to pneumococci

Recognition of pneumococci by the host innate immune system occurs via several mechanisms. The complement system is a crucial component of the innate immune response and acts to opsonise the bacteria and promote neutrophil chemotaxis. This has traditionally been thought to occur primarily via the classical and alternate pathways of complement deposition (Brown *et al*., 2002); however, more recent data have indicated

that the lectin pathway also plays an important role (Ali *et al*., 2012). The polysaccharide capsule, which is regarded as the major virulence determinant of the pneumococcus, confers resistance to complement deposition by both the classical and alternate pathways, as well as protecting the pneumococcus from other immune mechanisms such as entrapment in mucus and neutrophil extracellular traps (Paterson and Orihuela, 2010). Pneumococci also use multiple surface-localised proteins to evade complement deposition and its effects (see Section 1.4).

In addition to the complement system, a number of pathogen recognition receptors can initiate inflammation in response to the presence of pneumococci, such as through recognition of lipoteichoic acid by Toll-like receptor (TLR) 2, pneumolysin by TLR4 and bacterial DNA by TLR9 (Koppe *et al.*, 2012; Malley *et al*., 2003; Paterson and Orihuela, 2010). These events lead to the release of many cytokines, amongst which the effects of TNF-α and IL-1 are considered to be of central importance. Over time, innate immune responses are supplanted by adaptive mechanisms, such as the generation of high-affinity antibodies against pneumococcal capsule and surface proteins and the actions of CD4+ T cells. Developing a better understanding of these mechanisms is of great importance to the development of effective vaccines (see Section 1.3.3.3) (Malley, 2010).

1.3 Treatment and prevention of pneumococcal disease

1.3.1 Antibiotics

Penicillin has been the treatment of choice against the pneumococcus since the 1940s (Watson *et al*., 1993). However, penicillin-resistant strains of pneumococci emerged in the late 1960s (Hansman *et al*., 1971) and have now spread worldwide. The mechanism of resistance is based on structural alterations to penicillin-binding proteins that allow the synthesis of peptidoglycan even in the presence of the antibiotic. Furthermore, resistance to other antibiotics such as macrolides, fluoroquinolones and trimethoprim is increasing (Van der Poll and Opal, 2009), and this is facilitated by the natural genetic transformability of the pneumococcus (Reichmann *et al*., 1997). The level of antibiotic resistance in pneumococci shows significant geographical variability (Felmingham *et al*., 2007), and is a particular problem in developing countries. Here the issue is compounded by high rates of colonisation and disease, inappropriate use of drugs, low quality of generic drugs,

overcrowding and poor sanitation, all of which may hasten the spread of antibiotic resistant strains (Kunin, 1993). Whilst several new drugs are in development, almost all are new derivatives of existing antibiotics, and the emergence of cross-resistance seems inevitable (Van Bambeke *et al*., 2007). Thus the prevention of pneumococcal disease via vaccination will become even more critical in the future.

1.3.2 Vaccines in current use and their limitations

Vaccination against *Streptococcus pneumoniae* is the most important measure used to fight pneumococcal disease. Vaccines currently in use are based on the capsular polysaccharide of the bacteria. The oldest of these, Pneumovax® 14 (Merck), was made up of purified polysaccharide from 14 different serotypes, and while a revised 23-valent formulation (Pneumovax® 23) is still used in certain populations, the lack of immunogenicity of polysaccharides in children under 2 years of age limits its effectiveness in this crucial group (Douglas *et al*., 1983). The most extensively used vaccine worldwide to date is Prevnar® (Pfizer), the original formulation of which was composed of seven different capsular polysaccharides conjugated to a carrier protein (CRM197™, a diphtheria toxoid) which improves its immunogenicity in infants. Since the introduction of this vaccine in 2000 there has been a significant decrease in the incidence of invasive pneumococcal disease in vaccinees, as well as a significant herd immunity effect in older people who have not received the vaccine (Poehling *et al*., 2006; Pilishvili *et al*., 2010).

There are, however, several problems associated with Prevnar®, and, indeed, with vaccines based on capsular polysaccharide in general. Firstly, they are expensive to manufacture relative to other vaccine types due to the number of steps involved in producing the polysaccharides, conjugating them to the carrier protein, balancing the levels of polysaccharide from the different serotypes of pneumococci, and carrying out the large amount of quality control required (Wilson, 2010). A complex tiered pricing structure is used to sell pneumococcal vaccines in different countries under different agreements with prices per dose ranging from US $7 to US $91.75 (Wilson, 2010; Moon *et al*., 2011). Despite this, it is apparent that worldwide access to the vaccines is hindered by the cost. The second main problem faced by Prevnar® is that vaccines based on capsular polysaccharide only confer protection against the limited number of serotypes whose polysaccharides are included in the formulation. This is compounded by the geographical

variation in serotype prevalence, meaning that many countries derive a much smaller benefit from immunisation programs since the prevalent serotypes in the area do not match those covered by the vaccines. Whilst several 'second generation' conjugated polysaccharide vaccines have been licensed that increase the number of serotypes that are protected against (13-valent Prevnar®, Pfizer; 10-valent Synflorix™, GlaxoSmithKline Biologicals), it is not feasible to include polysaccharides covering all pneumococcal serotypes due to the complexity and expense of manufacture that that would entail (Moffitt and Malley, 2011). The third major drawback of conjugate vaccines is serotype replacement, whereby non-vaccine serotypes fill the niche vacated by vaccine serotypes. This was predicted to be a potential problem before the introduction of conjugate vaccines (Lipsitch, 1997), and its occurrence is now well documented (Singleton *et al*., 2007; Hsu *et al*., 2009). This phenomenon will inevitably lead to a significant decrease in the impact of conjugate vaccines as non-vaccine serotypes increase in prevalence.

1.3.3 Alternative vaccination strategies

Given these limitations, a number of alternatives to previous capsular polysaccharide-based vaccines are under investigation. These include improvements to the conjugate vaccine approach, whole-cell pneumococcal vaccines, and protein-based vaccines (Moffitt and Malley, 2011).

1.3.3.1 Conjugate vaccines

The international non-profit organisation Program for Appropriate Technology in Health (PATH) is exploring two separate adaptations of the conjugate vaccine approach: firstly, a collaboration is underway aiming to develop pneumococcal conjugate vaccines that target serotypes prevalent in low-resource countries using cheaper, more efficient methods to conjugate the antigens to the carrier proteins (PATH, 2011). A second strategy involves the use of conserved pneumococcal proteins (see section 1.3.4) as carrier proteins for capsular polysaccharides of targeted serotypes (Paton *et al*., 1991; Moffitt and Malley, 2011; PATH, 2011).

1.3.3.2 Whole cell vaccines

Investigations into the use of a killed whole cell pneumococcal vaccine date back to 1911, and interest in this strategy increased greatly during and after the 1918 influenza pandemic, since the majority of deaths during this event were caused by secondary bacterial pneumonia (Brundage and Shanks, 2008; Chien *et al*., 2009). A recent meta-analysis has found, however, that due to serious methodological flaws, little can be concluded from the early studies of the 1910s regarding the potential for whole-cell inactivated pneumococcal vaccines to confer cross-protection to multiple serotypes (Chien *et al*., 2010). Nevertheless, the whole cell approach is attractive since it bypasses the need to identify individual protein antigens that confer protection, allows the presentation of a large number of antigens simultaneously, is relatively cheap and has the potential to provide serotype-independent protection against both colonisation and invasive disease (Moffitt and Malley, 2011). Recent studies with a more sophisticated approach than those of a century ago have shown promising efficacy, and approval for human trials is currently being sought (Malley *et al*., 2001; Lu *et al*., 2010a, 2010b).

1.3.3.3 Mechanisms of immunity

Work on pneumococcal whole cell vaccines has led to an increased understanding of the mechanisms of immunity to the pneumococcus. The major correlate of immunity induced by capsular polysaccharide vaccines is IgG that binds to the pneumococcal surface, facilitating adherence by phagocytes, and this type of opsonophagocytic protection has traditionally been the target of novel vaccination strategies. However, whole cell vaccines that are effective against colonisation have been shown to rely on CD4+ T cells and the cytokine IL-17, and not on any antibody response (Malley *et al*., 2005; Lu *et al*., 2008b). Such vaccines can also protect mice against invasive disease when given by injection, in which case protection depends on serum antibodies and not T cells (Lu *et al*., 2010a). Thus immunity elicited by pneumococcal whole cell vaccines appears bipartite, with CD4+ T cells and IL-17 effective against nasopharyngeal colonisation, and antibodies effective against invasive disease, and there is some evidence that this mimics the development of natural immunity in humans (Malley and Anderson, 2012).

1.3.4 Protein-based vaccines

The focus of research into alternative vaccine strategies has been in the identification and characterisation of protein antigens that could elicit protection against pneumococcal disease. An ideal candidate protein should be surface-exposed, immunogenic, and conserved amongst different pneumococcal serotypes. On this basis, many virulence factors have been found to be vaccine candidates, since they are often located on the bacterial surface in order to mediate interactions with the host. Furthermore, antibodies against virulence factors may be able to neutralise their function, thus inhibiting the disease-related effects they would normally cause, in addition to any opsonic activity that the antibodies may have.

1.3.4.1 Identification of candidate proteins

Prior to the advent of genomic sequencing, laborious biochemical and genetic methods or empirical approaches were mainly used to identify candidate proteins (Jedrzejas, 2007). There are a number of examples showing the diversity of approaches employed, such as pneumolysin (Paton *et al*., 1983), pneumococcal surface protein A (PspA) (McDaniel *et al*., 1984, 1986), pneumococcal surface protein C (PspC; also known as choline-binding protein A (CbpA) and *S. pneumoniae* surface protein A (SpsA)) (Rosenow *et al*., 1997), and pneumococcal surface adhesin A (PsaA) (Russell *et al*., 1990). Such approaches have now been superseded by new techniques.

The publication of pneumococcal genome sequence data led to a slew of new protein vaccine candidates being identified. Several studies have used genome-wide bioinformatic analysis to search for open reading frames predicted to encode surface-localised proteins (Tettelin *et al*., 2001; Wizemann *et al*., 2001; Rigden *et al*., 2003). An alternative approach employs signature-tagged mutagenesis to create libraries of mutants, which can be screened to identify genes whose disruption results in defects in ability to colonise and/or cause invasive disease. Whilst the results must be considered in the context of a few caveats (Paton and Giammarinaro, 2001), four such studies have been successfully performed and reported in *S. pneumoniae* (Polissi *et al*., 1998; Lau *et al*., 2001; Hava and Camilli, 2002; Chen *et al*., 2008). Other strategies include comparative genomic hybridisation of virulent and non-virulent strains (Harvey *et al*., 2011b; McAllister *et al*., 2011), microarray transciptomics (Orihuela *et al*., 2004; Ogunniyi *et al*., 2012), *in vivo*

expression technology (Meng *et al*., 2008), differential fluorescence induction (Marra *et al*., 2002), antigenome technology (Giefing *et al*., 2008), genomic array footprinting (Molzen *et al*., 2011) and protein expression library screening (Moffitt *et al*., 2011). Taken together, the number of protein vaccine candidates identified by these methods in the post-genomic era is vast, and the major challenge for researchers now lies in characterisation of these candidates and comparative assessment of their protective efficacies.

1.4 Protein vaccine candidates

Amongst all of the proteins identified, a small selection have been more extensively characterised and are currently the most likely to be incorporated into protein-based vaccines that proceed to clinical trials. These include pneumolysin, PspA, PspC, PsaA and Pht proteins. The structure, functions and vaccine potential of each of these will be discussed below (for reviews, see Kadioglu *et al*., 2008; Jedrzejas, 2007; Mitchell and Mitchell, 2010; Ferreira *et al*., 2011).

1.4.1 Pneumolysin

Pneumolysin is a member of the cholesterol-dependent cytolysin family of toxins found in many Gram-positive species of bacteria. As such it is able to form oligomers in the membranes of target cells that contain cholesterol, creating a large pore that leads to cell lysis (Tilley *et al*., 2005). Furthermore, pneumolysin has a number of other activities at sub-lytic concentrations that contribute to pneumococcal virulence, such as inhibition of the beating of cilia on the respiratory epithelium, downregulation of the respiratory burst of phagocytes, induction of cytokine production and activation of CD4+ T cells, and activation of the classical pathway of complement, although it is also a target of effective immune responses against the pneumococcus (Marriott *et al*., 2008). Unlike other cholesterol-dependant cytolysins, pneumolysin does not contain a signal peptide. It has historically been thought to be released from pneumococci by lysis of the bacteria caused by autolysin (LytA amidase); however this has been disputed, at least for some strains (Balachandran *et al*., 2001). Instead, in strain D39 pneumolysin has been shown to be released via the action of a caseinolytic protease (Ibrahim *et al*., 2005). Furthermore, pneumolysin has also been found to be attached to the cell wall of pneumococci,

challenging the traditional view that the protein is held intracellularly until release (Price and Camilli, 2009).

Pneumolysin has been shown many times to be critical for pneumococcal virulence in mouse models of pneumonia (Berry *et al*., 1989, 1995; Paton, 1996). It is found in almost all pneumococcal isolates with little variation. Interestingly, some variants associated with low haemolytic activity are found in highly virulent strains, highlighting the importance of the non-lytic functions mentioned above (Lock *et al*., 1996; Kirkham *et al*., 2006). Several studies have found pneumolysin and toxoid variants to be effective in conferring protection against invasive pneumococcal disease, including against strains expressing pneumolysin with low haemolytic activity (Paton *et al*., 1983; Alexander *et al*., 1994; Harvey *et al*., 2011a).

1.4.2 Pneumococcal surface protein A (PspA)

PspA is a member of the choline-binding family of pneumococcal proteins. These use choline-binding domains, usually at their C-termini, to anchor themselves to the pneumococcal surface by binding to phosphorylcholine moieties that are a component of surface-localised teichoic acids. It was recently demonstrated that PspA competes for binding of phosphocholine moieties with C-reactive protein (CRP), and therefore defends against the enhancement of complement C3 deposition via the classical pathway that CRP promotes (Mukerji *et al*., 2012). In addition to the choline-binding domain, PspA also contains a proline-rich domain, whilst its N-terminus is made up of repeated α-helices that form anti-parallel coiled coils. PspA can bind lactoferrin, an iron-sequestering glycoprotein that is found predominantly at host mucosal surfaces (Hammerschmidt *et al*., 1999). This interaction protects *S. pneumoniae* from the anti-microbial activity of apolactoferrin (Shaper *et al*., 2004).

PspA, like pneumolysin, has been extensively characterised in terms of its potential to be used as a vaccine, since it can provide protection in several mouse models of pneumococcal disease (Briles *et al*., 1996). The delivery of PspA via a DNA vaccine has also been investigated, since this may allow enhanced protection against pneumococcal colonisation (Ferreira *et al*., 2010). However, a serious drawback of PspA as a vaccine candidate is its high level of variability amongst pneumococcal strains: the *pspA* gene has been classified into three families, which in turn fall into six clades (Hollingshead *et al*.,

2000). Nevertheless, there are some conserved cross-protective epitopes such that immunisation with one PspA elicits a degree of protection against pneumococci with heterologous PspA types (Nabors *et al*., 2000; Moreno *et al*., 2010).

1.4.3 Pneumococcal surface protein C (PspC)

PspC is another member of the choline-binding family of pneumococcal proteins. It is closely related to PspA in that it also contains a proline-rich domain and an α-helical N-terminus. Three major functions have been attributed to PspC: firstly, it binds to the polymeric immunoglobulin receptor to allow pneumococci to adhere to and invade mucosal epithelia (Hammerschmidt *et al*., 1997; Zhang *et al*., 2000). Secondly, it binds factor H, a negative regulator of the alternate pathway of complement activation (Dave *et al*., 2001). This interaction contributes to both evasion of complement deposition and adherence of pneumococci (Jarva *et al*., 2002; Quin *et al*., 2007). Lastly, PspC binds the laminin receptor, allowing invasion of endothelial cells and crossing of the blood-brain barrier (Orihuela *et al*., 2009). The *pspC* gene is not present in all pneumococcal isolates, but strains lacking it contain *hic*, the N-terminal domain of which is homologous to the N-terminal portion of PspC. Hic lacks the choline binding domain of PspC, but is instead anchored to the cell surface in a sortase-dependent fashion (Janulczyk *et al*., 2000). Despite the polymorphic nature of PspC and it not being present in all pneumococcal isolates, it remains an important vaccine candidate (Brooks-Walter *et al*., 1999; Ricci *et al*., 2011).

1.4.4 Pneumococcal surface adhesin A (PsaA)

PsaA is a surface-localised lipoprotein which was originally thought to be an adhesin because of its homology to putative adhesins from other streptococci and the observation of reduced adherence of *psaA* mutants to mammalian cell lines *in vitro* (Sampson *et al*., 1994; Berry and Paton, 1996). The protein has been reported to bind to E-cadherin, which could act as a receptor mediating adherence (Anderton *et al*., 2007). However, subsequent analyses revealed that PsaA is in fact the solute-binding protein (SBP) of an ABC transporter system that is specific for the import of manganese ions into the pneumococcus (Dintilhac *et al*., 1997; McAllister *et al*., 2004). The effects relating to adherence are now thought to be due to altered expression of adherence factors under conditions of low

intracellular manganese. High-affinity manganese transport by PsaA has now been shown to be important in a range of processes, most notably resistance to oxidative stress (Tseng *et al*., 2002; McAllister *et al*., 2004; Ogunniyi *et al*., 2010). PsaA has been successfully used to protect against experimental pneumococcal infection of mice in a number of models and using various delivery routes (Talkington *et al*., 1996; Briles *et al*., 2000; Wang *et al*., 2010; Xu *et al*., 2011).

1.4.5 Combination vaccines

From the many studies that have been performed evaluating protein antigens of *S. pneumoniae* as vaccine candidates, it has become clear that no one antigen alone is sufficiently immunogenic and conserved amongst serotypes to be able to provide the broad and effective protection required for a next-generation vaccine. Furthermore, certain candidates may provide superior protection against pneumococci in certain niches, whilst failing to protect elsewhere. Several studies have therefore examined immunisation with combinations of protein vaccine candidates, often using high doses of virulent pneumococci as the challenge strain in order to distinguish between proteins conferring moderate and strong protection (Briles *et al*., 2000, 2003; Ogunniyi *et al*., 2000, 2001, 2007; Wu *et al*., 2010). To date, a combination of Ply, PspA and PspC is one of the most promising formulations in terms of strength of protection, at least against invasive disease (Ogunniyi *et al*., 2007).

1.5 Polyhistidine triad proteins

Notwithstanding the above, the combination of Ply, PspA and PspC is still not 100% protective, nor is its superiority universally accepted, and attempts at identifying and characterizing new candidates are ongoing. This includes the polyhistidine triad (Pht) proteins (also known as pneumococcal histidine triad proteins), a family of four members (PhtA, B, D and E) that range in size from 96 to 115 kDa. These proteins were independently discovered via a genomic search for a signal peptidase II motif (Adamou *et al*., 2001), a genomic search for a putative C3b peptidase sequence (Zhang *et al*., 2001), and an immunoscreen of an *S. pneumoniae* genomic library (Hamel *et al*., 2004). These initial analyses found the Pht proteins to be surface-localised, highly conserved amongst pneumococcal strains, and to confer protective immunity in mouse models of

pneumococcal colonisation, pneumonia and sepsis. The proteins are very similar to one another (32 to 87% amino acid identity), particularly at their N-termini, and are characterised by the presence of five (PhtA, B and D) or six (PhtE) unusual histidine triad (HxxHxH) motifs (Adamou *et al*., 2001). Since the discovery of Pht proteins in *S. pneumoniae*, homologues have been described in *S. pyogenes* (two different proteins named streptococcal leucine rich protein [Slr] and histidine triad protein A [HtpA]) (Reid *et al*., 2003; Kunitomo *et al*., 2008), *S. agalacticae* (group B leucine-rich protein [Blr] and streptococcal histidine triad surface protein [Sht]) (Waldemarsson *et al*., 2006; Maruvada *et al*., 2009) and *S. suis* (histidine triad protein of *S. suis* [HtpS]) (Shao *et al*., 2011). Searches of genomic databases for further homologues has revealed the presence of genes encoding polyhistidine triad proteins in almost all of the streptococci (see Figure 1.1a) (Plumptre *et al*., 2012). These can be categorised into three groups. The first two are distinguishable by the absence (group 1) or presence (group 2) of regions with homology to leucine-rich repeat (LRR) domains. The remaining Pht proteins have not been studied apart from PhtE, and have simply been labelled as group 3. The arrangements of histidine triad motifs and secondary structural elements in a prototypical protein from each group (PhtD, Slr and PhtE for groups 1, 2 and 3, respectively) are shown in Figure 1.1b.

1.5.1 Structural features of Pht proteins

To date, attempts to solve the structures of intact Pht proteins by X-ray crystallography have been unsuccessful. However, a fragment of PhtA (residues 166-220) containing its second histidine triad (HIT) motif has been crystallised and its structure solved to 1.2 angstrom resolution (Riboldi-Tunnicliffe *et al*., 2004, 2005). The HIT motif in this structure was complexed with a zinc ion (Zn^{2+}), as was predicted would be the case based on the known affinity of metal ions for histidine residues. The structure was unlike that of any other known protein and the HIT motif represents a novel Zn^{2+}-binding domain. However, modelling of the other four HIT motifs in PhtA suggested that they may not all have the correct geometry to permit Zn^{2+} binding (Riboldi-Tunnicliffe *et al*., 2005).

Further crystallographic studies will be required to obtain a full understanding of Pht protein structure, including determination of whether Zn^{2+} can bind to all of the HIT motifs. In the meantime, however, useful topographical information can be inferred from

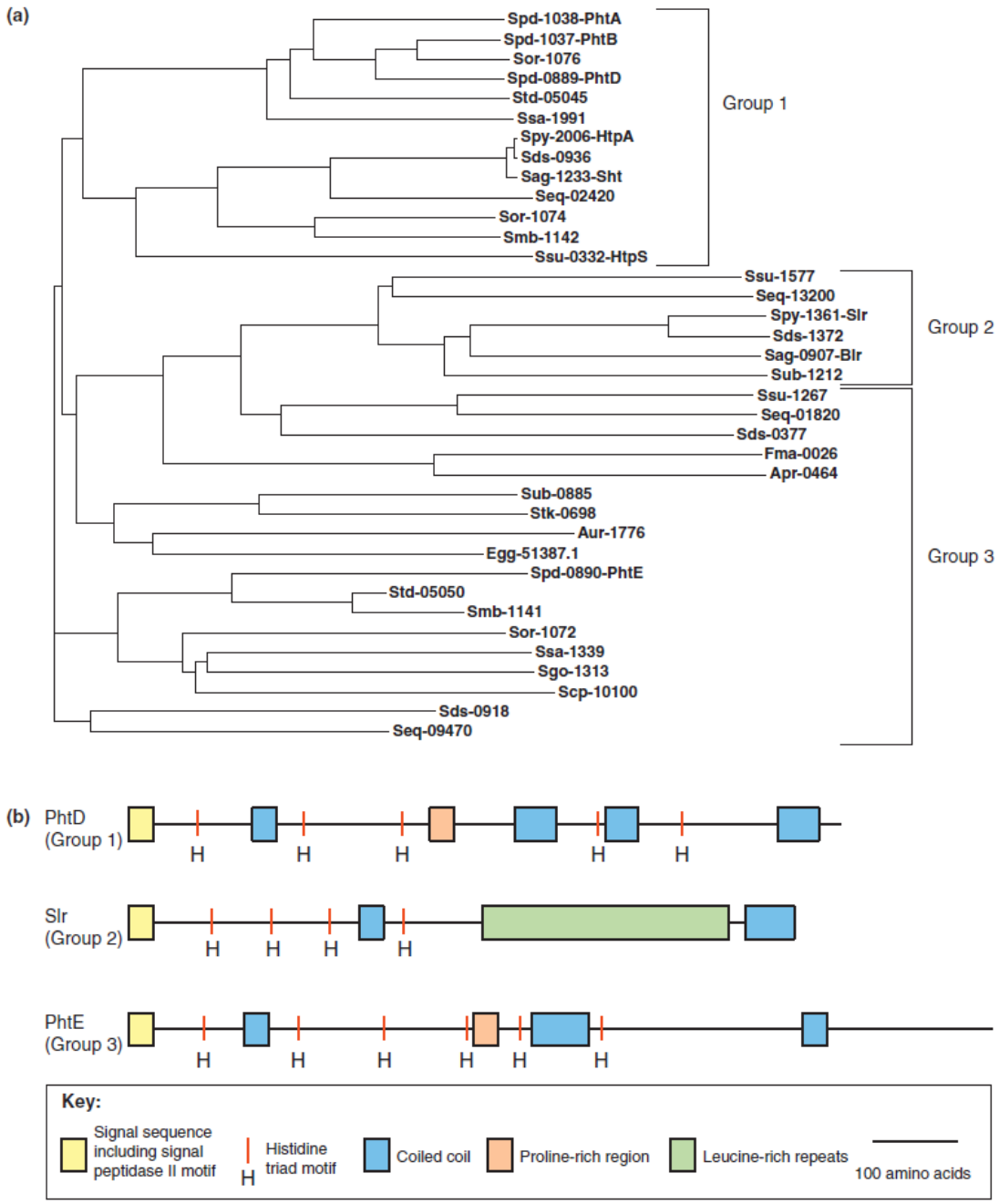

Figure 1.1: Genetic and structural relationships of polyhistidine triad (Pht) proteins.

(a) Dendogram of Pht proteins based on sequence alignment using the program ClustalW2 (Larkin *et al*., 2007). The Pht proteins are shown in three groups based on sequence identity. Proteins from only one representative strain of each species are shown. Proteins are labelled by a three-letter organism code and gene number according to the Kyoto Encyclopedia of Genes and Genomes (KEGG), followed by the name of the protein in the cases where it has been identified in the literature. Abbreviations: Apr, *Anaerococcus prevotii* DSM 20548; Aur, *Aerococcus urinae* ACS-120-V-Col10a; Egg, *Enterococcus faecalis* TX1467 (NB found in NCBI (National Center for Biotechnology Information) database; not present in KEGG]; Fma, *Finegoldia magna* ATCC 29328; Sag, *Streptococcus agalactiae* 2603 (serotype V); Scp, *Streptococcus parasanguinis* ATCC 15912; Sds, *Streptococcus dysgalactiae subsp. equisimilis* GGS_124; Seq, *Streptococcus equi subsp.*

zooepidemicus H70; Sgo, *Streptococcus gordonii* Challis; Smb, *Streptococcus mitis* B6; Sor, *Streptococcus oralis* Uo5; Spd, *Streptococcus pneumoniae* D39; Spy, *Streptococcus pyogenes* SF370 (serotype M1); Ssa, *Streptococcus sanguinis* SK36; Ssu, *Streptococcus suis* 05ZYH33; Std, *Streptococcus pseudopneumoniae* IS7493; Stk, *Streptococcus parauberis* KCTC 11537; Sub, *Streptococcus uberis* 0140J. **(b)** Arrangements of histidine triad motifs and secondary structural elements in prototypical Pht proteins from groups 1 to 3. The N termini are to the left. Reproduced with permission from Plumptre *et al*., 2012.

other observations. PhtA, PhtB, PhtD and PhtE show a high level of amino acid identity and similarity, and this is concentrated in the N-terminal region, with the C-termini being more divergent. Flow cytometric analyses have also shown that the C-terminal regions are more accessible to exogenous antibodies (Adamou *et al*., 2001; Hamel *et al*., 2004). This evidence points to the Pht proteins being anchored to the pneumococcal surface via their N-termini, with the C-termini, which are predicted to contain coiled-coil regions, protruding from the surface. The mechanism of attachment to the surface is also unclear. Although their signal peptides all contain an N-terminal signal peptidase II (LxxC) motif, this does not appear to function as a true lipobox, as the proteins are not labelled by [^{3}H]-palmitate (Hamel *et al*., 2004). Moreover, cell fractionation experiments indicate that, for PhtD at least, the protein is predominantly associated with the cell wall rather than the membrane (as would have been expected for a lipoprotein) (Loisel *et al*., 2011). There was also no difference in size between PhtD produced by wild-type *S. pneumoniae* and that produced by a signal peptidase II (Lsp) mutant (Loisel *et al*., 2011). Early studies also showed evidence of anti-Pht-reactive species in concentrated culture supernatants of several *S. pneumoniae* strains, although the possibility that this was due to autolysis rather than genuine secretion was not addressed (Zhang *et al*., 2001).

1.5.2 Genetic organisation and regulation of expression of *pht* genes

The *pht* genes are arranged in two pairs in the pneumococcal chromosome (see Figure 1.2), with *phtA* and *phtB* forming one pair and *phtD* and *phtE* the other (Adamou *et al*., 2001; Rioux *et al*., 2010). Expression of each gene is monocistronic, with the exception of *phtD*, which is co-transcribed in an operon with *ccdA* (which is involved in the biogenesis of cytochrome c), *spr0904* (which shows homology with thioredoxin), *yfnA* (a putative amino acid transporter), and *adcAII* (also known as *lmb*; discussed in Section 1.6.1). Transcription of each of the *pht* genes, as well as that of *adcAII*, has been shown to be

under the control of AdcR, a transcriptional repressor of the MarR family. This was first predicted *in silico* due to the presence of AdcR binding sites upstream of the these genes (Panina *et al*., 2003), and later demonstrated experimentally by measurements of gene expression in Δ*adcR* mutant strains (Ogunniyi *et al*., 2009; Shafeeq *et al*., 2011). Binding of purified AdcR to the promoter regions of each of the *pht* genes has also been shown using an electrophoretic mobility shift assay (Ogunniyi *et al*., 2009). The level of expression of *pht* genes in the presence of AdcR has been found to be regulated by [Zn^{2+}], but there are conflicting reports regarding the direction of influence (Ogunniyi *et al*., 2009; Rioux *et al*., 2010; Loisel *et al*., 2011; Shafeeq *et al*., 2011). It has been suggested that this apparent disagreement may be explained by taking the level of expression of AdcR itself into account, since its expression is also controlled by [Zn^{2+}] (Shafeeq *et al*., 2011; Plumptre *et al*., 2012). *In vivo*, expression of *pht* genes is higher than when pneumococci are grown *in vitro*, with higher mRNA concentrations being found in pneumococcal transcripts recovered from the nasopharynx as compared to samples from the lungs and blood (Ogunniyi *et al*., 2009), potentially indicative of the proteins playing a major role in colonisation. Aside from regulation by zinc, the concentration of arginine has recently been reported to influence expression of *phtD* by up to twofold (Kloosterman and Kuipers, 2011).

1.5.3 Use in vaccines

A number of studies have examined the potential for proteins from the Pht family to be used as vaccines to prevent streptococcal diseases (summarised in Plumptre *et al*., 2012). Pht proteins have broadly been successful in eliciting significant protective immunity in these experiments, which have tested a number of disease models (such as invasive disease, sepsis and nasopharyngeal colonisation) using a diverse range of pneumococcal challenge strains.

The effectiveness of Pht proteins as immunogens compared to other pneumococcal protein antigens is debatable. One study reported that, amongst PdB (a toxoid derivative of pneumolysin), PspA, PspC, PhtB and PhtE, combinations of proteins that included PhtB or PhtE generally elicited inferior protection compared with other combinations (Ogunniyi *et al*., 2007). However, more recent work found PhtD to provide better protection than PspA, PspC or PsaA in a lethal intranasal challenge mouse model, especially when serotype 3 or

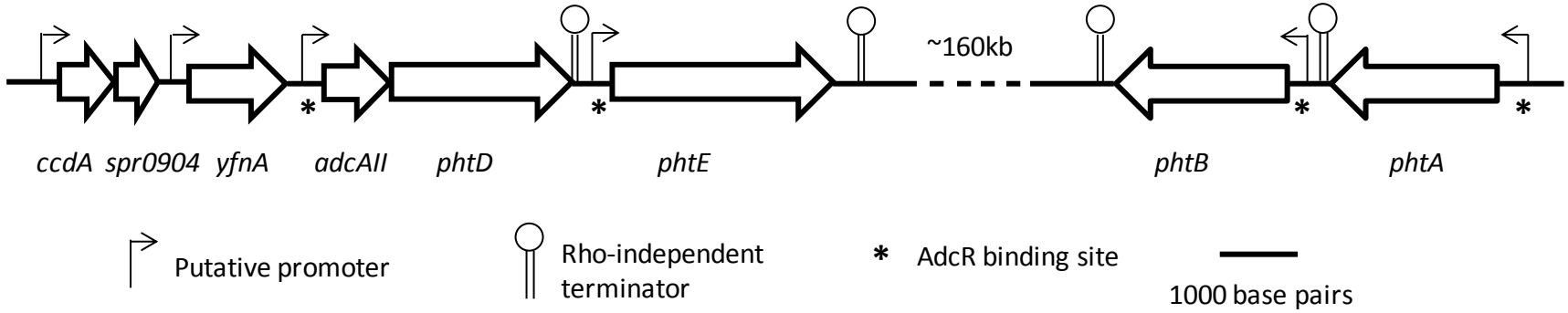

Figure 1.2: Genetic and transcriptional organisation of *pht* genes.

Genetic organisation of the *pht* genes in *S. pneumoniae* strain TIGR4. The genes are arranged in two pairs, with *phtD* and *phtE* forming one pair and *phtB* and *phtA* the other. *phtD* is co-transcribed with *ccdA*, *spr0904*, *yfnA* and *adcAII*; the other three *pht* genes are monocistronic. Positions of promoters, rho-independent terminators and AdcR binding sites are indicated. Reproduced with permission from Plumptre *et al*. 2012.

4 strains were used for the challenge (Godfroid *et al*., 2011). This study also suggested PhtD to be the best member of the Pht protein family in terms of vaccine potential due to it having the highest level of conservation amongst pneumococcal strains and its superior efficacy in a nasopharyngeal colonisation model compared to PhtA, PhtB or PhtE. Furthermore, significant protection against lung colonisation was found to be elicited by vaccination with PhtD; in some cases this was superior to that elicited by PspA, PspC or PsaA (Godfroid *et al*., 2011). This group has also demonstrated strong protection against lethal intranasal challenge of mice after a combination of vaccination with PhtD and passive transfer of capsular polysaccharide-specific antibodies (Denoël *et al*., 2011a), as well as protective immunity against pneumococcal pneumonia in rhesus macaques immunised with PhtD and detoxified Ply (Denoël *et al*., 2011b). Protective epitopes appear to be located mainly at the C-terminal ends of the proteins**,** in keeping with observations suggesting that these regions are exposed to the immune system on the pneumococcal surface (Adamou *et al*., 2001; Hamel *et al*., 2004). However, the histidine triad motif administered alone as a short peptide does not appear to be immunogenic (Kunitomo *et al*., 2008).

Immunogenicity of Pht proteins in humans has been demonstrated by observations of anti-Pht antibodies in sera from patients infected by *S. pneumoniae* (Adamou *et al*., 2001; Holmlund *et al*., 2007, 2009; Simell *et al*., 2009; Godfroid *et al*., 2011), the finding that children prone to otitis media have a smaller percentage of memory B cells specific to PhtD and PhtE, as well as lower antigen-specific IgG concentrations, compared to non-otitis-prone children (Sharma *et al*., 2012) and recent phase 1 clinical trials using PhtD in vaccine formulations (Bologa *et al*., 2012; Seiberling *et al*., 2012). Since naturally-occurring human anti-PhtD antibodies are able to provide passive protection in mice in an intranasal sepsis model (Godfroid *et al*., 2011), it is assumed that the mechanism of immunity to *S. pneumoniae* elicited by immunisation with Pht protein involves antibody recognition of the surface-exposed Pht antigens (most likely their C-terminal ends), leading to blockade of their functions(s) and/or opsonophagocytosis. It is unclear whether Pht-specific CD4+ T cells are involved in the protective immunity that can be elicited against colonisation. Whilst further work is required to fully understand these issues, phase 2 clinical trials are underway with both PhtD and a fusion of PhtB and PhtE (Ferreira *et al*.,

2011). Thus Pht proteins are well advanced in terms of vaccine development for use against the pneumococcus.

1.5.4 Roles and functions of Pht proteins in pathogenesis

The earliest evidence for a role for pneumococcal Pht proteins in disease pathogenesis was a large scale signature-tagged mutagenesis screen, which demonstrated reduced *in vivo* fitness of *phtA*, *phtB* and *phtD* mutants in a lung infection model (Hava and Camilli, 2002). More recently, a panel of single and double *pht* deletion mutants, as well as a quadruple mutant in which all four *pht* genes were deleted, were tested in intraperitoneal and intranasal murine infection models. After intraperitoneal infection, only the quadruple *phtABDE* mutant was significantly attenuated in virulence. However, in the intranasal challenge model, the quadruple mutant, the *phtAB* deletion and the *phtD* deletion all showed statistically significant attenuation, although only the *phtABDE* mutant was completely avirulent (Ogunniyi *et al*., 2009). These results suggest that there is a degree of functional redundancy amongst the four Pht proteins, and also that they may have a role in the pathogenesis of pneumococcal sepsis, in addition to nasopharyngeal colonisation and early lung disease.

The fact that *pht* gene expression is regulated by Zn^{2+} through AdcR (whose regulon also includes the primary Zn^{2+} ABC transporter operon *adcCBA*), and the known association of histidine residues in other proteins with metal and/or nucleoside binding, raises the possibility that the Pht proteins are somehow involved in Zn^{2+} homeostasis, perhaps acting as metal ion scavengers. Alternatively, Zn^{2+} binding by Pht proteins might be structurally important or the metal may act as a co-factor in other functions. ICPMS has been used to show that Zn^{2+} binds purified PhtD *in vitro* at a molar ratio of 4.6:1 (consistent with occupation of all five HIT motifs), and that metal binding leads to thermal stabilisation of the protein structure (Loisel *et al*., 2011). As mentioned previously, *phtD* is cotranscribed with *adcAII*. Despite the characterisation of its homologues in other streptococci as laminin-binding proteins involved in adhesion to, and invasion of, host cell surfaces (Spellerberg *et al*., 1999; Elsner *et al*., 2002; Tenenbaum *et al*., 2007), AdcAII in *S. pneumoniae* is an orphan SBP of an ABC transporter system. It is specific for Zn^{2+} and appears to be redundant with AdcA in import of Zn^{2+} via the transmembrane protein AdcB (Dintilhac and Claverys, 1997; Dintilhac *et al*., 1997; Loisel *et al*., 2008; Bayle *et al*.,

2011). Loisel *et al*. suggested that PhtD and AdcAII could have a joint function in Zn^{2+} uptake, given their co-expression, as well as evidence of apparent colocalisation at the bacterial surface, and ability of the two purified proteins to be cross-linked *in vitro*. However, these data have been criticized by Plumptre *et al*. (2012), who note that, in the cross-linking experiment, only a small proportion of the purified PhtD became associated with AdcAII, in spite of AdcAII being present at eightfold molar excess. Furthermore, it was suggested that the two proteins would be unlikely to be close enough to one another to interact *in vivo*, since the majority of the PhtD was found in the cell wall fraction whilst AdcAII was found exclusively in the cell membrane (Plumptre *et al*., 2012).

Regardless of whether or not PhtD directly interacts with AdcAII, there is evidence that Pht proteins play a role in metal ion homeostasis, as a quadruple *phtABDE* mutant was not able to grow in a synthetic culture medium unless Zn^{2+} or Mn^{2+} were added (Rioux *et al*., 2010). It was suggested that the proteins may act as metal ion scavengers, storing the ions when they are abundant and releasing them to membrane transporters when the environmental concentration diminishes (Rioux *et al*., 2010). As noted previously in virulence studies (Ogunniyi *et al*., 2009), single *phtD*, double *phtBD* or *phtDE*, or triple *phtBDE* mutants were not growth-attenuated under ion-limiting conditions, indicating functional redundancy (Rioux *et al*., 2010).

The Pht proteins have also been reported to decrease the deposition of complement protein C3 on the pneumococcal surface via the recruitment of factor H, a negative regulator of the alternative pathway of complement deposition (Giannakis *et al*., 2001; Ogunniyi *et al*., 2009). Flow cytometry was used to show that when pneumococci were incubated with fresh naïve mouse serum, significantly more C3 was deposited on the surface of a *phtABDE* quadruple deletion mutant, compared to either the wild-type or any of the single or double deletion mutants. Direct binding of purified human factor H to purified PhtA, PhtB, PhtD and PhtE was also demonstrated by ELISA and Western blotting (Ogunniyi *et al*., 2009). Factor H specifically protects the host from potentially damaging spontaneous activation of complement by binding to sialic acid residues on host cells, and subsequently displacing factor B from C3b:Bb convertases, as well as acting as a co-factor for factor I, a protease that cleaves C3b to the inactive iC3b (Buhé *et al*., 2010). Evasion of complement deposition onto its surface is clearly critical for survival of *S.*

pneumoniae in the host environment, and it uses multiple and in some cases apparently redundant strategies for this purpose. The polysaccharide capsule is an important inhibitor of complement deposition, as are PspC, PspA and Ply, as discussed in Section 1.4. However, binding of factor H by Pht proteins is controversial, and Ogunniyi *et al*. (2009) showed that purified PspC bound much more factor H *in vitro* than similar concentrations of any of the purified Pht proteins. Using flow cytometry, Melin *et al*. (2010) detected significantly reduced factor H binding and concomitant increased C3 deposition on the surface of a quadruple *pht* mutant relative to the wild-type in only one out of five pneumococcal strains tested. Moreover, although weak binding of purified human factor H to PhtD was demonstrated by surface plasmon resonance, no binding to other Pht proteins was detected using this technology, nor could significant binding be demonstrated by ELISA, whereas strong factor H binding could be found with PspC. The authors concluded that pneumococcal Pht proteins play a much lesser role in factor H binding than PspC, and that their overall contribution to complement evasion could be heavily influenced by the presence of other pneumococcal proteins and by genetic background (Melin *et al*., 2010). Interestingly, however, a Pht homologue produced by type III group B streptococci (GBS), referred to as Sht, which is 52% identical to PhtD, has also been shown to be capable of binding factor H and inhibiting deposition of C3 on the GBS surface (Maruvada *et al*., 2009).

Pht proteins may therefore have roles in Zn^{2+} homeostasis and in evasion of complement deposition. Interestingly, Zn^{2+} has been reported to cause oligomerisation of factor H (Nan *et al*., 2008; Perkins *et al*., 2010), and although direct evidence is lacking, it is tempting to speculate that there is a mechanistic link between Zn^{2+} binding and recruitment of factor H by Pht proteins. A recent study also suggested that Pht proteins may contribute to adherence to host epithelial cells. Deletion of either *phtD* or *phtE* reduced *in vitro* adherence of *S. pneumoniae* to Detroit 562 (nasopharyngeal) or A549 (type II pneumocyte) cells by about 50%, while expression of PhtD or PhtE on the surface of recombinant *Escherichia coli* significantly increased adherence to both cell lines (Khan and Pichichero, 2012). Adherence of wild-type pneumococci was also inhibited by IgG Fab fragments derived from human sera containing Pht antibodies, but not when the Fab preparations were preabsorbed with purified PhtD or PhtE (Khan and Pichichero, 2012). Thus, Pht proteins appear to be a further example of pneumococcal virulence proteins

playing multiple roles in disease pathogenesis. The apparently similar contributions of PhtD and PhtE to adherence supports the concept of there being functional redundancy within the Pht family, and it remains to be determined whether there are any functional differences between the four pneumococcal Pht proteins, perhaps mediated via their more divergent C-terminal regions.

1.6 Zinc homeostasis in *S. pneumoniae*

Whatever relationship Pht proteins may have with zinc, it must fit in with the overall picture of zinc homeostasis in *S. pneumoniae*; the limited amount that is known about this is summarised below. Epidemiological evidence shows that zinc is an important nutritional factor for humans, deficiency in which leads to an increased risk of pneumococcal (and other) infections (Prasad, 2003; Fischer Walker and Black, 2004). To explain this phenomenon, some studies have examined the links between zinc and the immune system, and have indeed found adequate zinc levels to be important for a range of immunological cell types such as macrophages, neutrophils, and B and T lymphocytes to function correctly (Shankar and Prasad, 1998; Rink and Gabriel, 2001). However, zinc is known to be both essential for and toxic to bacteria *in vitro*, so the host's zinc status may have a direct effect on the ability of pathogens to survive and grow *in vivo*. Indeed, it is thought that the host manipulates the levels of zinc to which bacteria have access, in some cases to deprive the pathogen of this essential nutrient, and in some cases to overwhelm it with an excess of the metal to cause toxicity (Kehl-Fie *et al*., 2011; McDevitt *et al*., 2011; Hood and Skaar, 2012).

1.6.1 Requirement for zinc and its import and export

Bacteria are estimated to incorporate zinc into 4 - 6% of all proteins (Andreini *et al*., 2006), including those with roles in diverse processes such as control of gene expression, metabolism and virulence (Kehl-Fie and Skaar, 2010). Its intracellular availability is tightly controlled; proteins within the cell have a very high zinc binding capacity that prevents the formation of a free cytosolic pool of Zn^{2+}, and changes in intracellular [Zn^{2+}] even in the femtomolar range induce changes in transcription of uptake or efflux machinery to restore normal levels (Outten and O'Halloran, 2001). In *S. pneumoniae* specifically, zinc import has been shown to be required for competence, septation during

cell division, and the ability to colonise and cause pneumonia and sepsis in mice (Dintilhac *et al*., 1997; Bayle *et al*., 2011). Dintilhac and Claverys (1997) identified AdcA as a metal-binding lipoprotein and proposed that it be the founding member of a new family of external SBPs which are specific for metal ions, originally referred to as cluster 9. Based on their homology to AdcA, this family includes PsaA and AdcAII of *S. pneumoniae*, as well as a number of proteins from related streptococci that have been characterised as adhesins, such as Lmb of *S. agalacticae* and Lsp of *S. pyogenes* (Spellerberg *et al*., 1999; Elsner *et al*., 2002). This family has now been re-classified as cluster A-1 (Berntsson *et al*., 2010). AdcA and AdcAII are both capable of mediating zinc import via the transmembrane protein AdcB, and they appear to be largely redundant, with loss of both *adcA* and *adcAII* genes being required for large decreases in zinc import and consequent impairment of growth (Bayle *et al*., 2011). This system is thought to be the only specific zinc importer for the pneumococcus; the only protein that has been identified as a zinc exporter is CzcD, the expression of which is regulated by the TetR family protein SczA (Kloosterman *et al*., 2007).

1.6.2 Mechanism of zinc toxicity

The systems described above can only maintain normal zinc homeostasis up to a certain concentration of zinc, above which the growth rate of the pneumococcus is impaired. For bacteria in general, toxicity of zinc has been assumed to be due to an elevated intracellular concentration of Zn^{2+} leading to the replacement of other metal ion co-factors from the enzymes that require them with zinc, leading to these enzymes being unable to function. However, more recent data have shown that, in *S. pneumoniae*, the toxicity could in fact be due to an extracellular mechanism whereby zinc ions irreversibly bind to the SBP PsaA (described in Section 1.4.4), blocking it from performing its usual function of binding manganese ions and delivering them to the PsaBC importer complex (McDevitt *et al*., 2011; Shafeeq *et al*., 2011). The bacteria are then starved of manganese, which is an essential co-factor for proteins involved in oxidative stress responses and carbon metabolism, and this leads to impaired growth and greater susceptibility to polymorphonuclear leukocyte killing (Ogunniyi *et al*., 2010; McDevitt *et al*., 2011). The ratio of extracellular $[Zn^{2+}]$:$[Mn^{2+}]$ thus determines the ability of PsaA to perform its function; interestingly, this ratio is greatly increased in the brain, lungs, nasopharynx and

blood of mice after infection with *S. pneumoniae*, implying that release of zinc could be a mechanism employed by the host innate immune system to interfere with bacterial growth (McDevitt *et al.*, 2011).

As described in Section 1.5.4, Pht proteins are known to bind zinc. However, it is not yet clear whether the purpose of this binding could be to aid import of the metal ion, defend against a toxic excess of zinc, or whether the binding does not play a role in zinc homeostasis *per se*, but is required for Pht proteins to fold in the correct conformation to perform other functions (such as binding of factor H).

1.7 Project aims

It is clear that characterisation of the Pht proteins is far from complete, particularly in terms of their structure and function. Such information is critical for understanding how Pht proteins act as virulence factors, and will help to show how and why their incorporation into vaccine formulations provides protective immunity. At the commencement of this project, further details on the interaction of Pht proteins with factor H were needed, and there was no information published describing if and how the Pht proteins might play a role in pneumococcal metal ion homeostasis. As the project developed and new information was published, it was decided that the relationship of Pht proteins with AdcAII should also be investigated. In separate work designed to gain an understanding of the topology of Pht proteins, different regions of the proteins were examined in terms of their secondary structural elements, surface exposure, necessity for attachment of the protein to the cell surface and potential for use in vaccines. The specific aims are therefore as follows:

1. Identify which region(s) of factor H are involved in binding Pht proteins.
2. Determine the relative contributions of Pht proteins, PspA and PspC to pneumococcal evasion of complement deposition.
3. Investigate whether Pht proteins contribute to acquisition of zinc ions or to defence against an excess of extracellular zinc.
4. Determine whether Pht proteins have a joint function with AdcAII.

5. Identify immunodominant epitopes of PhtA and PhtD and compare their ability to induce protective immunity in mouse models of pneumococcal disease with that of the full length proteins.
6. Identify amino acids in PhtD that are required for attachment of the protein to the pneumococcal surface.

Chapter 2: Materials and Methods

2.1 Strains and plasmids

The bacterial strains and plasmids used in this study are listed in Table 2.1.

Table 2.1: Strains and plasmids used in the work of this thesis.

Strain	Description	Reference/Source
D39	Serotype 2	Avery *et al*., 1944
D39 Δ*phtABDE*	Replacement of *phtA* with ery^R; *phtD* with tet^R; null mutant of *phtB* and *phtE*	Ogunniyi *et al*., 2009
D39 Δ*pspA*	Null mutant of *pspA*	Graham and Paton, 2006
D39 Δ*adcR*	Replacement of *adcR* with cml^R	Ogunniyi *et al*., 2009
D39 Δ*adcR*Δ*phtABDE*	Replacement of *adcR* with cml^R; *phtA* with ery^R; *phtD* with tet^R; null mutant of *phtB* and *phtE*	This study
BL21 (DE3) *lpxM*−	A lipid A mutant of *E. coli* expression strain BL21	Cognet *et al*., 2003
pQE-30	QIAexpress vector for His_6-tagged protein fusion	Qiagen [VIC, Australia]
pQE-31	QIAexpress vector for His_6-tagged protein fusion	Qiagen [VIC, Australia]
pQE-32	QIAexpress vector for His_6-tagged protein fusion	Qiagen [VIC, Australia]
D39 Δ*pspC*	Replacement of *pspC* with spec^R	Graham and Paton, 2006
D39 Δ*phtABDE*Δ*pspA*	Replacement of *phtA* with ery^R; *phtD* with tet^R; null mutant of *phtB, phtE* and *pspA*	This study
D39 Δ*phtABDE*Δ*pspC*	Replacement of *phtA* with ery^R; *phtD* with tet^R; *pspC* with spec^R; null mutant of *phtB* and *phtE*	This study
D39 Δ*pspA*Δ*pspC*	Replacement of *pspC* with spec^R; null mutant of *pspA*	This study

D39 Δ*phtABDE*Δ*pspA*Δ*pspC*	Replacement of *phtA* with ery^R; *phtD* with tet^R; *pspC* with spec^R; null mutant of *phtB, phtE* and *pspA*	This study
WCH43	Serotype 4	Women's and Children's Hospital, North Adelaide
WCH43 Δ*phtABDE*	Replacement of *phtA* with ery^R; *phtD* with tet^R; null mutant of *phtB* and *phtE*	This study
D39 Δ*adcA*	Replacement of *adcA* with cml^R	This study
D39 Δ*adcAII*	Null mutant of *adcAII*	This study
D39 Δ*adcCBA*	Replacement of *adcCBA* with cml^R	This study
D39 Δ*adcA*Δ*adcAII*	Replacement of *adcA* with cml^R; null mutant of *adcAII*	This study
D39 Δ*adcAII*Δ*adcCBA*	Replacement of *adcCBA* with cml^R; null mutant of *adcAII*	This study
D39 Δ*adcA*Δ*phtABDE*	Replacement of *adcA* with cml^R; *phtA* with ery^R; *phtD* with tet^R; null mutant of *phtB* and *phtE*	This study
D39 Δ*adcAII*Δ*phtABDE*	Replacement of *phtA* with ery^R; *phtD* with tet^R; null mutant of *phtB, phtE* and *adcAII*	This study
D39 Δ*adcA*Δ*adcAII*Δ*phtABDE*	Replacement of *adcA* with cml^R; *phtA* with ery^R; *phtD* with tet^R; null mutant of *phtB, phtE* and *adcAII*	This study
P9	Serotype 6A	PATH
D39 N full	Replacement of *phtA* with ery^R; null mutant of *phtB* and *phtE*. Wild-type *phtD*.	This study
D39 N50	Replacement of *phtA* with ery^R; null mutant of *phtB* and *phtE*. *phtD* altered to lack Ser40 to Pro95.	This study
D39 SP+	Replacement of *phtA* with ery^R; null mutant of *phtB* and *phtE*. *phtD* altered to lack Val32 to Val39.	This study
D39 SP-	Replacement of *phtA* with ery^R; null mutant of *phtB* and *phtE*. *phtD* altered to lack Arg26 to Val39.	This study
D39 3 alanine	Replacement of *phtA* with ery^R; null mutant of *phtB* and *phtE*. *phtD* altered with amino acid substitutions R26A, H27A and Q28A.	This study
WU2	Serotype 3	(Briles *et al*., 1981)

2.2 Growth media

S. pneumoniae strains were routinely grown in Todd–Hewitt broth [Oxoid, Hampshire, UK] with 1% Bacto yeast extract [Becton, Dickinson and Company (BD), New Jersey, USA] (THY), on blood agar (39 g/l Columbia base agar [Oxoid], 5% v/v defibrinated horse blood), or, for challenge of mice, in serum broth (10% v/v horse serum, 10 g/l peptone [Oxoid], 10 g/l Lab Lemco [Oxoid] and 5 g/l NaCl). For growth curve and ICPMS analyses, bacteria were grown in a semisynthetic casein hydrolysate medium with 0.5% yeast extract (C+Y) according to the recipe of Lacks and Hotchkiss, 1960, with the addition of 1 μM manganese sulphate.

For growth of *E. coli* for cloning, Luria Broth (LB) was used (10 g/l tryptone, 5 g/l yeast extract, 5 g/l NaCl). For protein expression, bacteria were grown in Terrific Broth (12 g/l Tryptone, 24 g/l yeast extract, 0.4% v/v glycerol, 17 mM KH_2PO_4, 72 mM K_2HPO_4).

Growth media were supplemented with erythromycin (0.2 μg/ml), tetracycline (5 μg/ml), chloramphenicol (6 μg/ml), spectinomycin (200 μg/ml), gentamycin (5 μg/ml), ampicillin (200 μg/ml) or kanamycin (50 μg/ml) as appropriate.

For storage of pneumococci or *E. coli*, strains were harvested from blood or LB agar plates into THY or LB respectively. 15% v/v glycerol was added and the sample was frozen at −80°C.

2.3 Oligonucleotide primers

Primers used in this study, which were purchased from Sigma [NSW, Australia], are listed in Table 2.2.

Table 2.2: Primers used in the work of this thesis.

Primer	Sequence (5'→3')	Description
AD84	AGCATCCAAGGCTTCCTTGTCTTTA	Amplification of *phtAB*
AD85	GACCTGGTCCGTGATAGGGGTCT	Amplification of *phtAB*
AD79	TATCCCAGTTCTTTATGATACCAAAGC	Amplification of *phtDE*

AD82	GTCAATGCCCTTCAGCTAGCAATTG	Amplification of *phtDE*
PspC Flank F	CAATTCTAGGTGGTGTTGGTCTAGT	Amplification of *pspC*
PspC Flank R	ACATCAAACCCAAGCTAGCTCAAC	Amplification of *pspC*
CP1	GAGGTGATTTTGCAGGCGGAAAATC	Mutagenesis of *adcA* – upstream flank
CP2	CAATTTTCGGTCACGCTGTTGGTTCGTCTCCTATTTGATAAAACGTC	Mutagenesis of *adcA* – overlap with chloramphenicol acetyltransferase
CP3	GCCCAAAACCTTCTCCAAGAAACC	Mutagenesis of *adcAII* – upstream flank
CP4	TATGTATTCATATATATCCTCCTCGAACAACTCCTTAACCATTTAATTAAC	Mutagenesis of *adcAII* – overlap with spectinomycin adenyltransferase
CP5	GGATAGTATGGGAACGGTTGAGTT	Mutagenesis of *adcCBA* – upstream flank
CP6	CAATTTTCGGTCACGCTGTTGTTATTTGATTTCTCCTACTAAAGCAGTC	Mutagenesis of *adcCBA* – overlap with chloramphenicol acetyltransferase
CP7	GACGTTGAGCCTCGGAACCCTGAGAAATCGACTAGTTCATAAGAGC	Mutagenesis of *adcA* – overlap with chloramphenicol acetyltransferase
CP8	CAATTTGTGCTATAATATAGTTGAAATG	Mutagenesis of *adcA* –downstream flank
CP9	AAATAACAGATTGAAGAAGGTATAATGAGTATTCTAGCAGAAGAATTAAAGTGA	Mutagenesis of *adcAII* – overlap with spectinomycin adenyltransferase
CP10	CATGAGGAACGATATAAGCATTACC	Mutagenesis of *adcAII* – downstream flank
CP11	GACGTTGAGCCTCGGAACCCTGAGAAATCGACTAGTTCATAAGAGC	Mutagenesis of *adcCBA* – overlap with chloramphenicol acetyltransferase
CP12	CTGATAGCCTTTTGTATAGTAAGCC	Mutagenesis of *adcCBA* – downstream flank
CP13	CAACAGCGTGACCGAAAATTG	Amplification of chloramphenicol acetyltransferase
CP14	GGGTTCCGAGGCTCAACGTC	Amplification of chloramphenicol acetyltransferase
CP15	GCTAGAATACTCAGAACAACTCCTTAACCATTTAATTAAC	Mutagenesis of *adcAII* – removal of spectinomycin adenyltransferase
CP16	TAAGGAGTTGTTCTGAGTATTCTAGCAGAAGAATTAAAGTGA	Mutagenesis of *adcAII* – removal of spectinomycin adenyltransferase
J253	GAGGAGGATATATATGAATACATACG	Amplification of spectinomycin adenyltransferase
J254	TTATACCTTCTTCAATCTGTTATTTAAATAGTTTATAGTTA	Amplification of spectinomycin adenyltransferase

PhtE Spec Y	AAATAACAGATTGAAGAAGGTATAAGGAATAG CAGTAGAAAAAGTCTGAA	Mutagenesis of *adcAIIphtDE* – overlap with spectinomycin adenyltransferase
PhtA F	GATTTTAAGTGTTGGATCCTACGAGTTGGGAC	Cloning of PhtA truncated derivatives
PhtA R	GAAAGCCTCTTTATCGAAGCTTTCATTTTTCA	Cloning of PhtA truncated derivatives
PhtA C1 R	ACGATTGTAAAAAGCTTCTGCACTATCT	Cloning of PhtA C1
PhtA C2 R	GTTTCAGATGGTAAAGCTTTCGCAAAG	Cloning of PhtA C2
PhtA C3 R	CTAGCTGATAACTCAAGCTTAGGAATG	Cloning of PhtA C3
PhtA C4 R	TCTTGGAGTCCAAGCTTCACGATGTTG	Cloning of PhtA C4
PhtA N1 F	CATAGAGGATCCTGGTGATGCTTATATC	Cloning of PhtA N1
PhtA N2 F	GGCCTTGTTTTGGATCCAGCGCAAAT	Cloning of PhtA N2
PhtA N3 F	CAATTAGCTGATAAGGATCCAACGTCA	Cloning of PhtA N3
PhtA N4 F	CACACATACAAGGATCCAAATGGCTAT	Cloning of PhtA N4
PhtD F	GCCCTAAGTGTTGGATCCTATGAACTTG	Cloning of PhtD truncated derivatives
PhtD R	TCTCCATAAAATAAGCTTCATTCATTTTAC	Cloning of PhtD truncated derivatives
PhtD C1 R	TGCCTCATAAAAGCTTTCGTCAAACCA	Cloning of PhtD C1
PhtD C2 R	TAAGCCTTATTGTAAGCTTCTCTATCACTAGAT	Cloning of PhtD C2
PhtD C3 R	TCTCTGACAAGCTTGGTTGAGCTGGA	Cloning of PhtD C3
PhtD N1 F	TAGTCATAATGCGGATCCAGCTCAACCA	Cloning of PhtD N1
PhtD N2 F	CCATCTAGGGATCCAGAATTTTACAATAAG	Cloning of PhtD N2
PhtD N3 F	GGCCTTTATGAGGATCCTAAGGGGTATAG	Cloning of PhtD N3
CP17	GCCTATTCTTGTCTTGGTCTTGGT	Cloning of *phtD* derivatives for surface attachment study: primer F
CP18	AACTCGATTAGACTCTTTCTTAACCTG	Cloning of *phtD* derivatives for surface attachment study: primer X

CP19	CAGGTTAAGAAAGAGTCTAATCGAGTTTATGATGCCATCATCAGTGAAGA	Cloning of *phtD* derivatives for surface attachment study: primer Y (N50)
CP20	GACTTTCTACTTCTTCCTTGCTATCTGT	Cloning of *phtD* derivatives for surface attachment study: primer R
CP21	CTGACCAGCTTGGTGACGACCA	Cloning of *phtD* derivatives for surface attachment study: primer X (SP+)
CP22	ACCAAGTTCATAGGAACAAACACTTAG	Cloning of *phtD* derivatives for surface attachment study: primer X (SP-)
CP23	TGGTCGTCACCAAGCTGGTCAGTCTTATATAGATGGTGATCAGGCTG	Cloning of *phtD* derivatives for surface attachment study: primer Y (SP+)
CP24	CTAAGTGTTTGTTCCTATGAACTTGGTTCTTATATAGATGGTGATCAGGCTG	Cloning of *phtD* derivatives for surface attachment study: primer Y (SP-)
CP25	CCTATGAACTTGGTGCTGCCGCAGCTGGTCAGGTT	Cloning of *phtD* derivatives for surface attachment study: primer Y (3 ala)
CP26	AACCTGACCAGCTGCGGCAGCACCAAGTTCATAGG	Cloning of *phtD* derivatives for surface attachment study: primer X (3 ala)

2.4 Manipulation of DNA

2.4.1 PCR, agarose gel electrophoresis and DNA sequencing

PCR was performed using Phusion High Fidelity DNA Polymerase [Thermo Fisher Scientific, VIC, Australia] or Expand Long Range [Roche, NSW, Australia] according to the manufacturers' instructions. For overlap PCR in which one large product was to be amplified from multiple smaller pieces, equimolar amounts of each smaller piece were used as template, with approximately 20 ng of template DNA used in total. Agarose gel electrophoresis was performed using gels composed of 0.6 – 1.2% w/v agarose dissolved in TBE (44.5 mM Tris, 44.5 mM boric acid, 1.25 mM EDTA, pH 8.4). These were immersed in TBE and run at 180 V. DNA was mixed with $1/10^{th}$ volume of loading buffer (15% w/v Ficoll, 0.1% w/v bromophenol blue, 100 ng/ml RNAse A) prior to loading. Staining was performed using GelRed^{TM} [Biotium, California, USA] according to the manufacturer's instructions and DNA was visualised by transillumination with short wavelength ultraviolet light using the Gel Doc XR system [Bio-Rad, NSW, Australia]. DNA was purified from PCR reactions using a QIAquick PCR purification kit [Qiagen] according to the manufacturer's instructions. Purified DNA was submitted to the Australian Genome Research Facility for sequencing.

2.4.2 Restriction digestion and ligation

Restriction enzymes and T4 DNA ligase were purchased from New England Biolabs [Mass., USA] and used according to the manufacturer's instructions.

2.5 Transformation of bacteria

2.5.1 THY method for pneumococcal transformation

For standard transformations in which antibiotic selection could be used, pneumococci were grown in THY to OD_{600} 0.5. A $1/10^{th}$ dilution of this culture was made with THY competence medium (THY supplemented with 0.2% w/v BSA, 0.2% w/v glucose and 0.02% w/v $CaCl_2$) and 100 ng/ml of competence-stimulating peptide 1 (CSP-1) [Chriontech, VIC, Australia] was added. After 14 min at 37°C, 10 – 100 ng/ml of DNA was added and the culture was incubated for 2 – 4 h at 37°C followed by plating onto blood agar containing the appropriate antibiotic. This was incubated overnight at 37°C in 95% air, 5% CO_2. Transformants were checked by PCR, DNA sequencing and (in cases where appropriate antibodies were available) Western blotting.

2.5.2 Preparation of pneumococcal competent cells and back transformation

For back transformations in which a higher transformation efficiency than the THY method could provide was required, competent cells were prepared. Pneumococci were first grown in cCAT medium (10 g/l Bacto Casamino acids [BD], 5 g/l Bacto tryptone, 5 g/l NaCl, 10 g/l Bacto yeast extract, 4% v/v 0.4 M K_2HPO_4, 0.002% w/v glucose, 150 mg/l glutamine) to OD_{600} 0.6, then diluted to OD_{600} 0.02 in CTM medium (cCAT supplemented with 0.2% w/v BSA, 1% v/v 0.01 M $CaCl_2$) and grown to OD_{600} 0.2. Cells were centrifuged at 3,200 × *g* for 20 min and resuspended in $1/10^{th}$ volume CTM adjusted to pH 7.8. 15% v/v glycerol was added and 50 µl aliquots were stored at −80°C.

For transformation, 500 µl of CTM pH 7.8 and CSP-1 to a final concentration of 100 ng/ml were added to a thawed aliquot of competent bacteria, which was then incubated at 37°C for 10 min. 10 – 100 ng/ml DNA was then added and the transformation mixture was incubated at 32°C for 30 min followed by 2 – 4 h at 37°C. Bacteria were plated onto blood agar without antibiotics and grown overnight at 37°C in 95% air, 5% CO_2. Colonies were

subsequently patched in duplicate onto blood agar with and without the relevant antibiotic to select for transformants in which resistance to the antibiotic had been lost.

2.5.3 Preparation of competent *E. coli* and transformation

Competent cells were prepared by growth in LB medium at 37°C to OD_{600} 0.6, followed by an incubation of 30 min at 4°C. After centrifugation, the cell pellet was resuspended in cold 100 mM $MgCl_2$, followed by another centrifugation step and resuspension in 100 mM $CaCl_2$. After another 30 min at 4°C, 30% v/v glycerol was added and aliquots were frozen at −80°C. For transformation, an aliquot was thawed and 50 µl of bacteria were mixed with 1 – 10 ng of plasmid DNA in a volume of 5 µl. This was incubated at 4°C for 15 min, then at 42°C for 3 min, then at 4°C for 15 min again. 500 µl LB was added and the culture was incubated at 37°C for 1 h with vigorous shaking followed by plating on LB-agar containing the appropriate antibiotic(s).

2.6 Expression and purification of proteins

2.6.1 Expression of pneumococcal proteins

One litre of the *E. coli* expression strain was grown to high density in Terrific Broth at 37°C. Protein expression was induced with 1 mM IPTG [BioVectra, Prince Edward Island, Canada] for 2 h at 37°C. Bacterial pellets were collected via centrifugation and frozen at −20°C.

2.6.2 Purification of pneumococcal proteins

Pellets were resuspended in cell lysis buffer (10 mM sodium phosphate, cOmplete EDTA free protease inhibitor cocktail [Roche], 10 µg/ml DNAse I [Roche], pH 7.0). The mixture was homogenised using a tissue grinder [Wheaton, New Jersey, USA]. The cells were lysed using a Cell Disruptor [Constant Systems, Daventry, UK] at 20 kpsi and 1 mM PMSF [Sigma] was added. The lysate was centrifuged at 20,000 × g for 30 min and the supernatant was collected. 1 M NaCl and 20 mM imidazole were added and the pH was adjusted to 8.0. This was applied to a column containing a 1 ml bed of Ni-NTA agarose [Qiagen] which had been equilibrated with 20 ml equilibration buffer (10 mM sodium phosphate, 1 M NaCl, 20 mM imidazole, pH 8.0). The column was washed with 20 ml of

wash buffer (10 mM sodium phosphate, 1 M NaCl, 30 mM imidazole, pH 6.0). The his-tagged protein was eluted from the column in 5 ml fractions with wash buffer containing a gradient of increasing imidazole concentration (0 – 250 mM). Fractions were analysed by SDS-PAGE and Western blot to check for the presence of the desired protein and to assess its purity. Buffer exchange was performed by repeated dilution with 10 mM sodium phosphate buffer at pH 7.4 using Amicon Ultra-15 centrifugal filter units [Merck Millipore, VIC, Australia] and proteins were stored at −20°C with 50% v/v glycerol. Protein concentration was measured using a Nanodrop 1000 spectrophotometer [Thermo Fisher Scientific].

2.6.3 Cloning, expression and purification of factor H and SCR domain proteins

Factor H and related proteins were cloned, expressed and purified by Dr Penelope Adamson and Professor David Gordon (Department of Microbiology and Infectious Diseases, Flinders University, South Australia) as follows. Full length factor H was purified from human serum using anti-factor H affinity chromatography. The coding region for recombinant SCR 1-7 was amplified by PCR, digested with *EcoRI* and *XbaI* [New England Biolabs], cloned into the multiple cloning site of the yeast expression vector pPICZαA [Life Technologies, VIC, Australia] downstream of the AOX1 methanol-inducible promoter, and transformed into *E. coli* DH5α. Sequence analysis confirmed that the construct was correct. Up to 10 µg of *SacI*-linearised SCR 1-7/pPICZαA DNA was electroporated into *Pichia pastoris* strain X33 and transformants were selected with 100 µg/ml zeocin [Life Technologies]. Expression of recombinant protein was induced for three to four days in the presence of 2% v/v methanol according to the manufacturer's instructions [Life Technologies]. Recombinant protein was purified from the cell culture supernatant by nickel affinity chromatography. The SCR1-7 B mutant was produced from the recombinant SCR 1-7 construct by introducing amino acid substitutions, R386A and K387A, using splice overlap extension PCR as described previously (Giannakis *et al*., 2003). Other truncated factor H proteins were cloned, expressed and purified as described previously (Duthy *et al*., 2002; Okemefuna *et al*., 2008).

2.7 Enzyme-linked immunosorbent assay

To detect protein:protein interactions, pneumococcal proteins were diluted to 5 μg/ml in TSA buffer (132 mM NaCl, 25 mM Tris-HCl, 0.05% w/v NaN_3, pH 7.5) and allowed to adsorb onto the wells of Nunc MaxiSorp 96 well trays [Thermo Fisher Scientific] overnight at 4°C. Blocking was performed using 1% w/v bovine serum albumin (BSA) dissolved in PBS for 2 h at 37°C. Factor H or different SCR domain proteins were then introduced for 4 h at RT at 5 μg/ml unless specified otherwise. Polyclonal anti-factor H goat serum [Calbiochem, Merck Millipore] was diluted 1:2000 v/v in PBS and incubated in the tray overnight at 4°C. Rabbit anti-goat alkaline phosphatase conjugated secondary antibody [Bio-Rad] was diluted 1:3000 v/v in PBS and incubated for 2 h at RT. Lastly, 4-nitrophenyl phosphate disodium salt hexahydrate [Sigma] was diluted in substrate buffer (10% v/v diethanolamine [Sigma], 1 M $MgCl_2$, 0.02% w/v NaN_3, pH 9.8) to 500 μg/ml and incubated at RT in the tray until a yellow colour developed, at which point trays were read at 405 nm using a Spectramax M2 microplate reader [Molecular Devices, California, USA]. Trays were washed five times with PBS between each step.

For ELISAs used to measure antibody titres from mouse serum, coating of the target proteins onto the wells and blocking were performed as above. This was followed by introducing serial dilutions of pooled mouse serum overnight at 4°C, followed by detection with rabbit anti-mouse alkaline phosphatase conjugated secondary antibody [Bio-Rad] and substrate as above. Titres (dilution of mouse serum resulting in half-maximal response) were determined using Prism [GraphPad Software, California, USA].

2.8 Surface plasmon resonance

Optimal pH values for protein immobilisations were determined by pH scouting experiments. SCR 1-7 was transferred into 10 mM sodium acetate buffer at pH 5.8 by serial concentration and dilution in this buffer using Vivaspin 500 centrifugal concentrators [Sartorius, VIC, Australia]. 500 response units (RU) were immobilised onto a CM5 chip [Biacore, GE Healthcare, NSW, Australia] using an amine coupling kit [Biacore] on a T-100 system [Biacore]. A blank immobilisation was performed using a different flow cell and the response obtained from binding of analytes to this flow cell was subtracted from the response of the flow cell with immobilised protein. PhtD and polyclonal anti-factor H goat serum were diluted in 0.45 μm filtered HBS buffer (10 mM HEPES, 150 mM NaCl,

0.005% v/v surfactant P20 [Biacore], pH 7.4) and injected over the chip surface for 1 min at a flow rate of 30 µl/min.

Reverse experiments (in which PhtD was used as the ligand and SCR 1-7 the analyte) were performed essentially as described above. PhtD was exchanged into 10 mM sodium acetate buffer at pH 4.2, and an immobilisation level of 1000 RU was achieved. For analyte binding experiments, SCR 1-7 and polyclonal anti-PhtD murine serum were diluted into HBS buffer.

2.9 Flow cytometry

Bacteria were grown in THY to OD_{600} 0.3. For measurements of SCR 1-7 binding, they were incubated with 25 µg/ml SCR 1-7 for 1 h at 37°C followed by polyclonal anti-factor H goat serum [Calbiochem] for 1 h at 37°C. Alexa Fluor® 488 donkey anti-goat IgG (H+L) [Life Technologies] was used for 30 min at 4°C to detect binding. Three washes with 1 ml PBS were performed between each step and all antibodies were diluted 1:100 v/v in PBS. Fluorescence measurements from 10,000 events were collected using a BD FACSCanto flow cytometer [BD Biosciences, NSW, Australia]. Data were analysed using the software package FlowJo [Tree Star, Oregon, USA].

Other flow cytometry experiments were performed essentially as described above. For complement deposition measurements, bacteria were incubated with naïve mouse serum (collected as described in Section 2.19.2) diluted 1:10 v/v in gelatin veronal buffer (141 mM NaCl, 3.4 mM barbitone, 1.6 mM sodium barbitone, 0.5 mM $MgCl_2$, 0.15 mM $CaCl_2$, 0.1% w/v gelatin, pH 7.4) for 10 min at 37°C. FITC-conjugated goat anti-mouse C3 [MP Biomedicals, NSW, Australia] was used for 30 min at 4°C to detect complement C3 deposition. For PhtD exposure experiments, bacteria were incubated with murine anti-PhtD serum for 1 h at 37°C followed by Alexa Fluor® 488 rabbit anti-mouse IgG (H+L) [Life Technologies] for 30 min at 4°C.

2.10 Preparation of bacterial lysates and precipitation of proteins from culture supernatants

Pneumococci were grown in 5 ml THY to OD_{600} 0.3 and centrifuged at 2000 × *g* for 5 min. After one wash with PBS, the bacterial pellet was resuspended in PBS with 0.1% sodium

deoxycholate and incubated for 1 h at 37°C. 1 ml of culture supernatant was centrifuged again at 13,000 × *g* for 10 min to ensure no contaminating bacteria remained; 900 µl of this was collected trichloroacetic acid was added to a final concentration of 10% w/v. After 1 h at 4°C, precipitated proteins were pelleted by centrifugation at 13,000 × *g* for 10 min and resuspended in PBS. 1/10th volume of SDS-PAGE loading buffer (25% v/v 2-mercaptoethanol [Merck Millipore], 600 mM Tris, 10% w/v SDS, 65% v/v glycerol, 0.05% w/v bromophenol blue [BioRad]) was added to bacterial lysates and supernatant proteins; 1 µl of 2 M sodium hydroxide was added to the latter to neutralise any remaining acid. All samples were then heated to 95°C for 5 min.

2.11 Cell wall digestion assay

This assay was based on the method of Price and Camilli (2009). Pneumococci were grown in 50 ml THY to OD_{600} 0.5 and centrifuged at 5000 × *g* for 10 min. Bacterial pellets were resuspended in 200 µl of cell wall digestion buffer (10 mM Tris, 30% w/v sucrose, cOmplete EDTA free protease inhibitor cocktail [Roche], pH 7.5) with or without 1 U/µl mutanolysin [Sigma] and/or 1 mg/ml lysozyme [Sigma] and incubated for 2 h at 37°C on a windmill circular rotator. Protoplasts were then separated from digested cell wall components by centrifugation at 13,000 × *g* for 10 min.

2.12 Assay for release of PhtD over time

A 100 ml culture of wild-type pneumococci was grown in THY to OD_{600} 0.3. At this point the culture was split in half and 30 µg/ml chloramphenicol was added to one of the cultures. 5 ml samples were taken from each culture at this starting point and then again at hourly intervals for 4 h, as well as once more after incubation overnight. The cultures were kept at 37°C throughout the experiment and the optical density was monitored to observe the growth of the bacteria. Proteins were precipitated from the supernatants and bacterial lysates were prepared as described in Section 2.10 and Western blotting was performed to detect PhtD and AdcR as described in Section 2.13.

2.13 SDS-PAGE and Western blotting

Samples were loaded into 4 – 12% polyacrylamide gels and electrophoresis was performed at 180 V using the NuPAGE® SDS-PAGE gel system [Life Technologies]. For staining of

proteins, gels were incubated with 0.06% w/v Coomassie Brilliant Blue R-250 [Bio-Rad] dissolved in 10% v/v glacial acetic acid and 25% v/v methanol, followed by destaining with several washes of 10% v/v acetic acid and 10% v/v isopropanol. Alternatively, proteins were transferred to a nitrocellulose membrane using the iBlot system [Life Technologies] according to the manufacturer's instructions, followed by blocking with 5% w/v skim milk powder dissolved in TTBS for 30 min at RT. Primary antibodies were incubated in TTBS overnight at 4°C, followed by a 1:50,000 dilution of anti-mouse IRDye 800 in TTBS [LI-COR Biosciences, Nebraska USA] for 1 h at RT. Blots were dried at 37°C and scanned using an Odyssey infrared imaging system [LI-COR Biosciences]. Band intensities were measured after subtraction of background using the manufacturer's application software. Alternatively, for CpsD, a 1:5,000 dilution of anti-rabbit alkaline phosphatase conjugated secondary antibody [BioRad] was used followed by detection using 1.7 mg 5-bromo-4-chloro-3-indolyl phosphate [Roche] and 2.5 mg nitro blue tetrazolium chloride [Roche] dissolved in buffer (100 mM Tris, 100 mM NaCl, 50 mM $MgCl_2$, pH 9.5).

2.14 Inductively coupled plasma mass spectrometry

2.14.1 Purified proteins

Purified protein samples were dialysed three times in TSA buffer (50 mM MOPS, 150 mM NaCl, pH 7.2) supplemented with a 100:1 molar ratio of EDTA:protein then three times in TSA buffer without EDTA using Slide-a-Lyzer Dialysis Cassettes [Thermo Scientific] with a nominal molecular weight cut-off of 10 kDa. Dialysis was performed at 4°C. Proteins were diluted to 5 μM with 3.5% HNO_3 and heated to 95°C for 20 min. Samples were allowed to cool to RT then centrifuged for 20 min at 13,000 × *g*. Metal ion content was measured on an Agilent 7500cx ICPMS [Adelaide Microscopy, University of Adelaide] and metal to protein molar ratios were calculated.

2.14.2 Pneumococcal cultures

Bacteria were grown in C+Y medium to OD_{600} 0.3. Bacterial pellets were washed three times with PBS containing 5 mM EDTA (to chelate ions bound loosely to the surface) then twice with PBS alone, with centrifugation for 5 min at 20,000 × *g* between each wash.

Pellets were desiccated at 80°C overnight and weighed before being heated to 95°C in 1 ml of 35% HNO_3 for 30 min. Samples were diluted into 3.5% HNO_3 in duplicate and metal ion content was measured using an Agilent 7500cx ICPMS [Adelaide Microscopy, University of Adelaide]. Metal quantities were normalised by dry weight of bacterial pellet.

2.15 Thermal shift assay

Proteins were dialysed as described in Section 2.14.1. Proteins were then diluted to 10 μM using TSA buffer and 5 × SYPRO Orange [Life Technologies] was added. Samples were pre-incubated for 10 min with 1 mM of various metal ions in triplicate and then subjected to thermal unfolding from 37°C to 97°C at a heating rate of 1°C per min using a LC480 Real-Time Cycler [Roche]. Fluorescence data were collected at 570 nm after excitation at 470 nm. After subtraction of the background fluorescence recorded from the buffer alone, the first derivative of the fluorescence data was calculated using Prism [GraphPad Software] to determine the inflection point of the melting transition.

2.16 Growth curve assays

Wild-type *S. pneumoniae* D39 and mutant strains were grown to OD_{600} 0.3 in C+Y. They were then sub-cultured into 200 μl C+Y supplemented with various concentrations of $ZnSO_4$ or TPEN. The bacteria were incubated at 37°C and growth was monitored by measurement of the OD_{600} at 30 min intervals.

2.17 Zeta potential measurements

Bacteria were grown in THY medium to OD_{600} 0.3. After two washes with PBS, approximately 2×10^7 CFU were diluted into 1 ml of PBS or 150 mM sodium phosphate buffer. Electrophoretic measurements were taken at 25°C using a Zetasizer Nano [Malvern Instruments, Worcestershire, UK] and zeta potentials were calculated with the Smoluchowski model using the manufacturer's software.

2.18 Circular dichroism spectroscopy

Proteins were diluted to 0.15 mg/ml in 10 mM sodium phosphate buffer at pH 7.4. Absorbance in the ultraviolet spectrum was measured using a J-815 Spectropolarimeter

[Jasco Analytical Instruments, Maryland, USA] according to the manufacturer's instructions. Calculations of proportions of secondary structural elements were performed using the DichroWeb online analysis tool (available at http://dichroweb.cryst.bbk.ac.uk/html/home.shtml) using the CDSSTR programme.

2.19 *In vivo* models of pneumococcal disease

2.19.1 Mice

Five to six week old female CD1 (Swiss) mice were obtained from the Laboratory Animal Services breeding facility at the University of Adelaide. This strain of mice was used in all experiments except where otherwise noted. Ethics approval for all experiments was granted by the Animal Ethics Committee of the University of Adelaide; experiments were conducted in compliance with the Australian Code of Practice for the Care and Use of Animals for Scientific Purposes (7th edition, 2004) and the South Australian Animal Welfare Act 1985.

2.19.2 Generation of polyclonal antisera

Purified protein antigens were mixed with aluminium hydroxide and magnesium hydroxide [Imject® Alum; Thermo Scientific] and PBS for 30 min at RT. Three mice were immunised intraperitoneally on day 0, 14 and 28. Each dose contained 10 μg of protein and 100 μg alum. Mice were euthanised on day 35 and blood was collected from the posterior vena cava. The blood was allowed to coagulate at RT for 30 min before collection of serum by centrifugation. Equal volumes of serum from each of the three mice were pooled. Serum from unimmunised mice for complement deposition experiments was also collected in this manner, and was split into single use aliquots and frozen at −80°C.

2.19.3 Intranasal challenge

Mice were anaesthetised by intraperitoneal injection of pentobarbital sodium [Nembutal; Rhone-Merieux, QLD, Australia] at a dose of 66 μg/g body weight, then given 50 μl of bacteria suspended in serum broth intranasally by pipetting onto the nares. The challenge dose was confirmed by retrospectively diluting and plating the culture on blood agar. For virulence experiments, the mice were monitored and survival times recorded. For

pathogenesis and competition experiments, mice were euthanised at the pre-determined time points by CO_2 asphyxiation. The trachea was exposed and 1 ml of PBS containing 0.5% w/v trypsin was inserted into the tracheal end of the upper respiratory tract and collected from the nose. Blood was collected from the aorta. Following perfusion with PBS, the lungs and the nasopharynx/upper palate were excised. These samples were homogenised in 1 ml PBS using a Precellys® 24 tissue homogeniser [Bertin Technologies, France]. Samples of the nasal wash, nasal tissue, blood and lungs were then serially diluted in serum broth and colonies were enumerated after overnight growth on blood agar plates containing gentamycin and other antibiotics as appropriate. For competition experiments, colonies were enumerated from plates with and without antibiotic to allow the numbers of each strain used to infect the mice to be calculated.

2.19.4 Immunisation experiments

For the sepsis model experiments, mice were immunised intraperitoneally three times with 10 μg of protein mixed with 100 μg Imject® Alum [Thermo Scientific] in 100 μl final volume on days 0, 14 and 28. On day 35, approximately 100 μl of blood was collected by submandibular bleeding. This was allowed to coagulate at RT for 30 min before collection of serum by centrifugation. Equal volumes of serum from each mouse were pooled for antibody titre analysis. On day 42, mice were injected intraperitoneally with 100 μl of serum broth containing the appropriate CFU of wild-type pneumococci and survival times were recorded.

For the colonisation model experiment, mice were immunised intranasally with 10 μl containing 10 μg of protein and 0.2 μg *E. coli* heat labile toxin B subunit (gift from Tom Duthy, University of Adelaide) on days 0, 14 and 28. On day 42, mice were challenged intranasally as described in Section 2.19.3.

Chapter 3: Interaction of Pht proteins and PspA with the human complement regulator Factor H-Like Protein 1

3.1 Introduction

The first experimental evidence for a function of the Pht proteins was the observation that a Δ*phtABDE* mutant strain attracted more deposition of the complement protein C3 onto its surface from fresh naïve mouse serum than an isogenic wild-type strain (Ogunniyi *et al*., 2009). This was suggested to be caused by the recruitment of factor H to the pneumococcal surface by Pht proteins, and direct binding between the purified proteins was demonstrated by ELISA and Western blotting, although the amount of factor H bound was much less than that bound by PspC (Ogunniyi *et al*., 2009). Factor H is the major negative regulator of the alternative pathway of complement deposition; it binds to sialic acid residues on host cells and subsequently displaces factor B from C3b:Bb convertases, as well as acting as a cofactor for factor I, a protease that cleaves C3b to the inactive iC3b (Buhé *et al*., 2010). These effects protect the host from potentially damaging spontaneous activation of complement.

Factor H is the founding member of a protein family comprising seven members (for reviews see Zipfel *et al*., 2002 and Jozsi and Zipfel, 2008), all of which are made up of repetitive domains called short consensus repeats (SCRs). Factor H consists of 20 such domains, which are joined by short linker regions. Various regulatory activities and the ability to bind to certain ligands have been attributed to particular SCR domains within factor H (see Figure 3.1), and these can be shared by other factor H family proteins that contain homologous SCR domains. For example, factor H-like protein 1 (FHL-1) is produced as a splice variant of factor H and is composed of the first seven SCR domains alone; FHL-1 therefore shares the C3b binding, decay-accelerating activity and co-factor activity that these domains contribute to the full length protein's function (Giannakis *et al*., 2001).

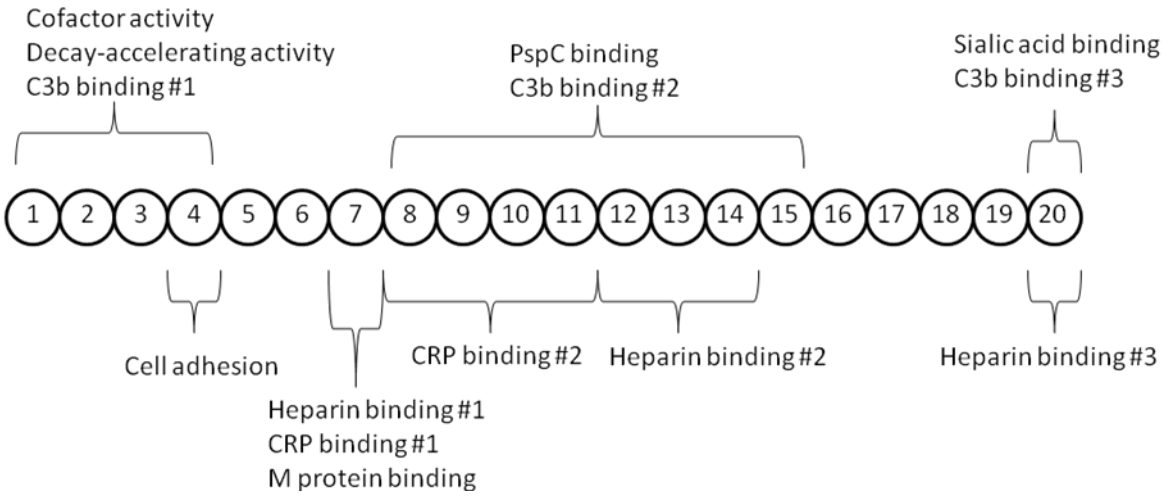

Figure 3.1: SCR domains of factor H and their known binding and catalytic activities.

The 20 SCR domains of factor H are represented schematically and sites of ligand binding and catalytic activity are indicated. Some ligands such as C3b and heparin can interact with multiple regions of factor H as shown. Adapted from Giannakis *et al*., 2001.

Recruitment of factor H family molecules by bacterial surface proteins is used by several pathogenic species as a strategy to prevent the deposition of C3 on the bacterial surface (Zipfel *et al*., 2008); examples include Fba and M protein of *S. pyogenes* (Blackmore *et al*., 1998; Pandiripally *et al*., 2003), CRASPs of *Borrelia spps*. (Kraiczy *et al*., 2001) and PspC of *S. pneumoniae* itself (Dave *et al*., 2001). Interestingly, such interactions can also be used to promote bacterial adherence to host surfaces and invasion of host cells (Pandiripally *et al*., 2003; Quin *et al*., 2007; Agarwal *et al*., 2010).

As mentioned above, the Pht proteins of *S. pneumoniae* have been shown to bind factor H (Ogunniyi *et al*., 2009). In addition to this, the group 1 Pht protein family member streptococcal histidine triad protein (Sht) found in group B *Streptococcus* has also been identified as a factor H binding protein (Maruvada *et al*., 2009). However, another study only detected differences in factor H binding and complement C3 deposition between wild-type and Pht-deficient bacteria in one out of five strains of *S. pneumoniae* tested (Melin *et al*., 2010). Furthermore, whilst weak factor H binding to PhtD was shown by surface plasmon resonance with purified proteins, no binding was found with PhtA, B or E with this technique, nor could binding between any Pht protein and factor H be found using ELISA, despite the detection of strong binding to PspC. It was therefore concluded that the contribution of Pht proteins to factor H binding and evasion of complement deposition is much lower than that of PspC, and that this contribution is dependent on the presence of other pneumococcal proteins and the genetic background (Melin *et al*., 2010).

When this work began, the observations of Melin *et al.* were yet to be published, and as such the aim of this work was to delineate which domains of factor H are involved in binding to Pht proteins, as well as to compare wild-type and Δ*phtABDE* mutant pneumococci in mouse models of disease to establish a basic understanding of the role of the Pht proteins in virulence and pathogenesis. Subsequently, this work also aimed to shed light onto the seemingly contradictory findings of Ogunniyi *et al.* and Melin *et al.* regarding binding of factor H to Pht proteins, and to assess the relative contribution of this interaction to evasion of complement deposition in comparison with those of PspC and PspA.

3.2 Virulence of the Δ*phtABDE* mutant strain in a murine sepsis model

To gain insight into the contribution of Pht proteins to the pathogenicity of *S. pneumoniae*, a virulence experiment was performed in which two groups of 12 male C57BL/6 mice were challenged intraperitoneally with 5×10^5 CFU of wild-type or Δ*phtABDE S. pneumoniae* strain D39. The construction of this mutant has been described previously (Ogunniyi *et al*., 2009). The survival times of the mice were recorded (see Figure 3.2).

The mutant strain showed a modest but statistically significant increase in survival time, indicating that the Pht proteins are required for full virulence in this model. The magnitude of the difference is relatively small; this may be partly due to the use of a very high challenge dose relative to the susceptibility of this strain of mice to invasive pneumococcal disease, leading to an overwhelming infection and short survival times of less than 20 hours.

3.3 *In vivo* competition between wild-type and the Δ*phtABDE* mutant strain

To gain further insights into the role of the Pht proteins in pneumococcal pathogenicity, a competition experiment was performed between wild-type D39 and the Δ*phtABDE* mutant (see Section 2.19.3). Mice were challenged intranasally with a mixed culture of the wild-type and mutant (2.5×10^6 CFU of each strain), and nasal wash, nasal tissue, lungs and blood were collected after 24 and 48 h. Competitive indices (the ratio of Δ*phtABDE* to wild-type pneumococci) were calculated for each sample; these are shown in Figure 3.3. All groups were significantly different from the null hypothesis mean competitive index of 1 ($P < 0.0001$ in all cases; one sample *t*-tests, one-tailed), indicating an attenuation of the ability of the mutant strain to survive and/or multiply in all niches.

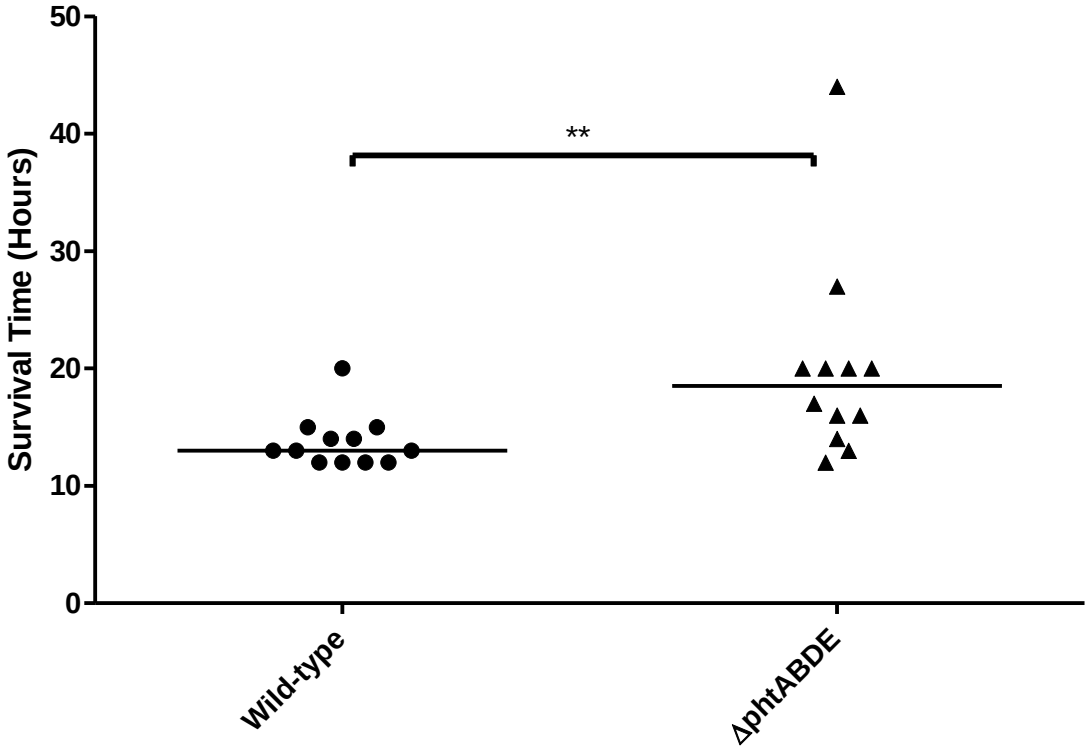

Figure 3.2: Survival times of mice challenged with wild-type or Δ*phtABDE* pneumococci of strain D39.

Groups of 12 mice were challenged intraperitoneally and survival times were recorded. **, $P < 0.01$.

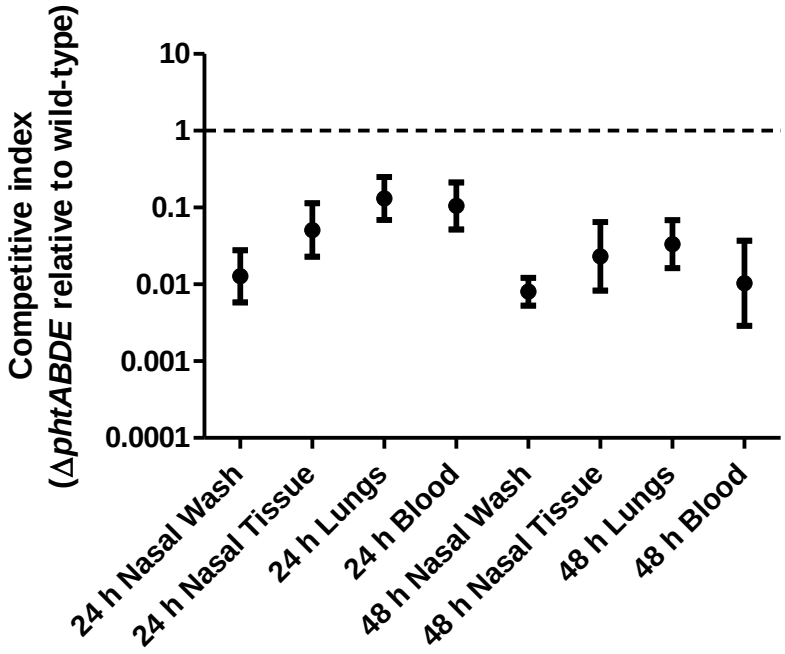

Figure 3.3: Competitive indices between wild-type and Δ*phtABDE* pneumococci from a murine intranasal infection model.

Nasal wash, nasal tissue, lung and blood samples were collected from mice at each time point and wild-type and mutant pneumococci enumerated from each sample as described in Section 2.19.3. Competitive indices were calculated and the geometric means and 95% confidence intervals are shown above on a $\log_{10}$ scale as Δ*phtABDE* relative to wild-type. The dotted black line represents a competitive index of 1, which would indicate no difference in fitness between the two strains.

3.4 Pht proteins and PspA bind to SCR 1-7 of factor H

Having established that loss of the *pht* genes leads to a decrease in virulence and competitive disadvantage of *S. pneumoniae*, experiments were aimed at examining how the proteins might contribute to pathogenicity. It has been reported previously that the Pht proteins bind to factor H (Ogunniyi *et al*., 2009), and it was of interest to determine which regions of factor H are involved in this interaction. Therefore, factor H and truncated proteins representing SCR 1-7, SCR 8-15 and SCR 16-20 were titrated in ELISA against immobilised purified Pht proteins and control proteins PspA and PspC. Proteins were purified as described in Section 2.6. SCR 1-7 was found to bind to all four Pht proteins and PspA but not to PspC (see Figure 3.4), which bound full length factor H and SCR 8-15, consistent with previous observations (Duthy *et al*., 2002). Little to no binding of full length factor H was observed for the Pht proteins; the amount of time that the ELISA substrate was allowed to develop may have needed to be longer to detect such interactions. However, the data indicate that the interaction of the Pht proteins and PspA with SCR 1-7 is much greater than with factor H, and since *in vivo* the SCR 1-7 domains are expressed as a separate protein (FHL-1) from factor H by alternative splicing, it seems likely that the preferential physiological ligand for the Pht proteins and PspA is FHL-1 rather than the much more weakly interacting factor H.

3.5 Binding of SCR 1-7 to Pht proteins and PspA occurs via ionic interaction with SCR 7

To further characterise the interaction of the pneumococcal proteins with SCR 1-7, further ELISAs were performed. Firstly, binding was tested in PBS with increasing concentrations of sodium chloride added to assess whether the interaction was ionic in nature (see Figure 3.5). There was a general trend of decreasing binding with increasing salt concentration, especially in the range of 0 – 400 mM added NaCl, indicating that the interaction between SCR 1-7 and Pht proteins or PspA is at least partly electrostatic in nature.

To further narrow down the binding site within SCR 1-7, binding was next compared between SCR 1-5 and SCR 1-7 (Figure 3.6). Effectively no binding was found between

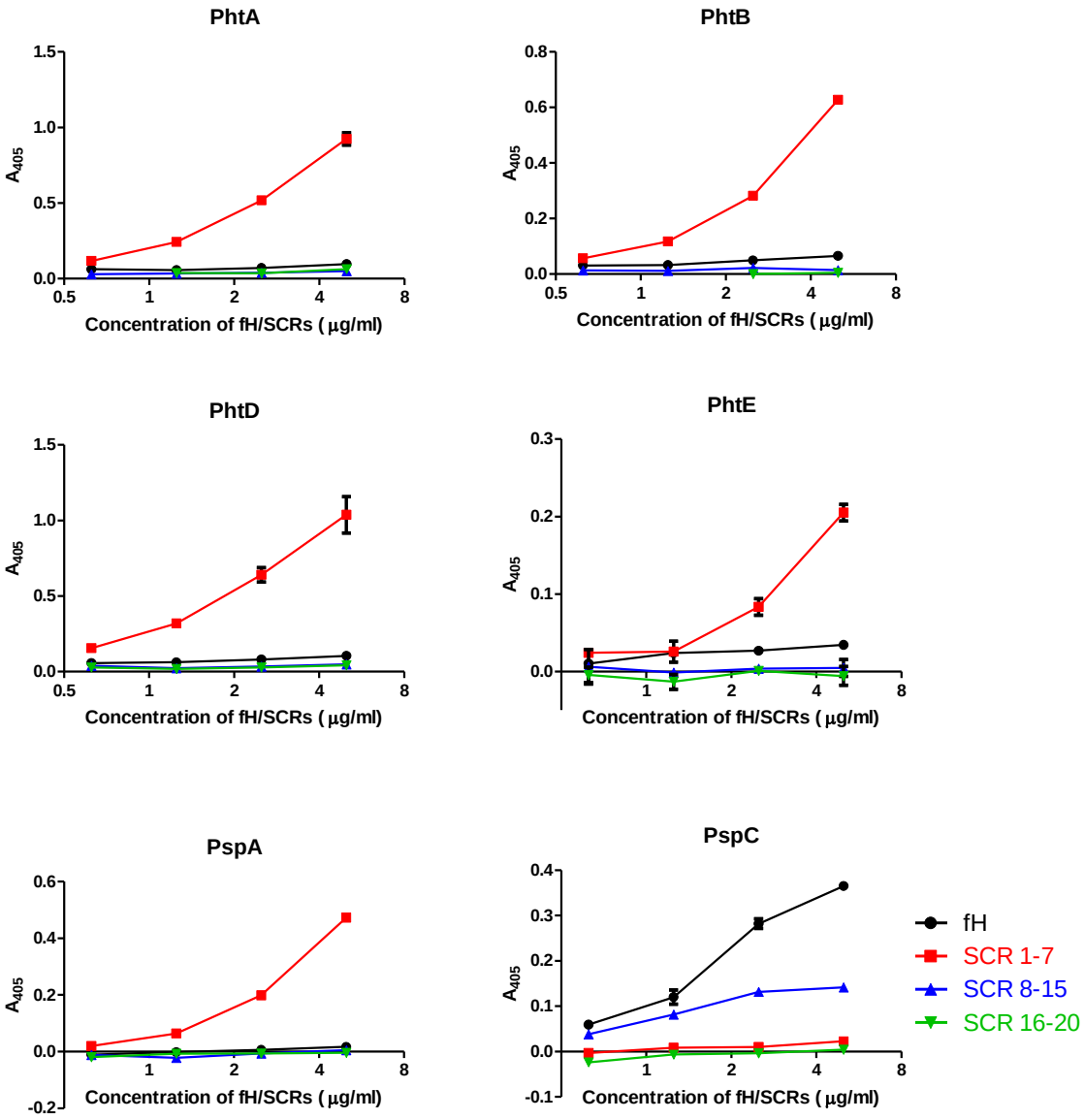

Figure 3.4: Binding of factor H and domains within factor H to Pht proteins, PspA and PspC.

Binding between proteins was assessed by ELISA by incubating immobilised pneumococcal proteins with proteins comprising SCR domains 1-7, 8-15 or 16-20 of factor H, or the full length protein. Binding was detected using an anti-factor H polyclonal antibody and alkaline phosphatase-conjugated secondary antibody.

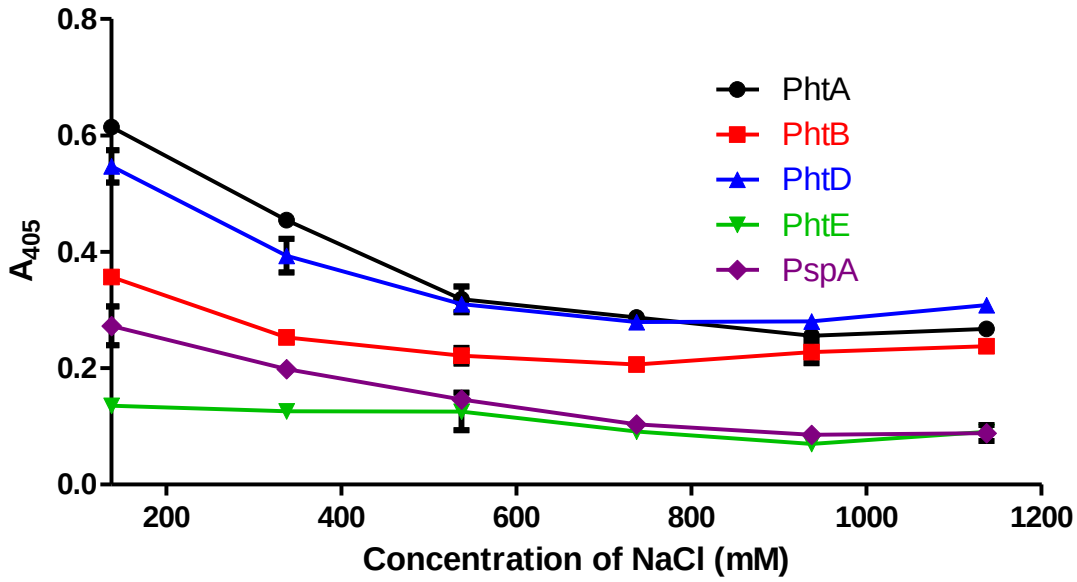

Figure 3.5: Inhibition of SCR 1-7 binding to Pht proteins and PspA by increasing concentrations of NaCl.

Binding between proteins was assessed by ELISA by incubating immobilised pneumococcal proteins with SCR 1-7 in PBS (which contained 137 mM NaCl) with extra NaCl added in 200 mM increments. Binding was detected using an anti-factor H polyclonal antibody and alkaline phosphatase-conjugated secondary antibody.

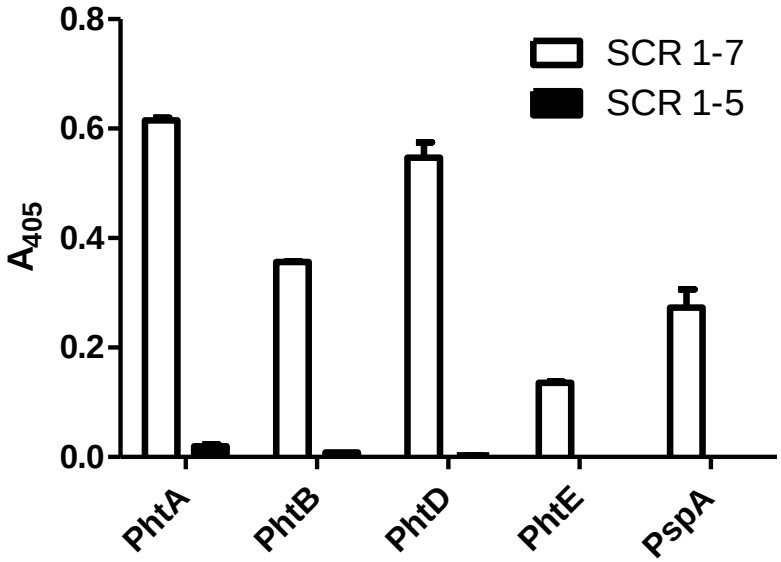

Figure 3.6: Binding of SCR 1-5 and SCR 1-7 to Pht proteins and PspA.

Binding between proteins was assessed by ELISA by incubating immobilised pneumococcal proteins with proteins comprised of SCR domains 1-5 or 1-7 of factor H. Binding was detected using an anti-factor H polyclonal antibody and alkaline phosphatase-conjugated secondary antibody.

SCR 1-5 and any of the Pht proteins or PspA, indicating that SCR domains 6 and/or 7 are critical for the interaction with FHL-1.

3.6 Non-conserved charged residues of SCR 7 are critical for binding

SCR 7 contains a cluster of positively charged residues that are not conserved in other SCR domains and are known to mediate interactions with multiple ligands such as heparin, M protein and C-reactive protein (Giannakis *et al*., 2001). It was therefore hypothesised that these same residues could be involved in binding of Pht proteins and PspA. This hypothesis was tested with a purified recombinant SCR 1-7 construct with the amino acid substitutions R386A and K387A ('B mutant'; see Figure 3.7).

Binding of the mutant form of SCR 1-7 to all four Pht proteins as well as PspA was markedly reduced compared to that with wild-type SCR 1-7 (see Figure 3.8), indicating that residues R386 and/or K387 are necessary for a strong interaction. The requirement for these charged residues also supports the previous observation that the interaction is mediated by ionic forces.

3.7 Surface plasmon resonance measurement of the interaction of SCR 1-7 with Pht proteins and PspA

Whilst the ELISA data above showed that Pht proteins and PspA can bind SCR 1-7, there was a degree of variability between experiments as to the apparent relative binding strengths for the different proteins with SCR 1-7. This may have been due to variability in the efficiency of the proteins adsorbing to the wells of the ELISA tray. Binding was therefore also assessed by surface plasmon resonance (SPR) using immobilised SCR 1-7 as described in Section 2.8. Initially, PhtD was used as the analyte, but no binding could be detected using concentrations of PhtD up to 13.7 μM. As a control, polyclonal anti-factor H goat serum (commercially available from Calbiochem) was used, and this resulted in an increase in response units corresponding to binding of antibodies to the SCR 1-7 on the surface of the chip (data not shown). This indicated that the protein had indeed been successfully immobilised. Since it was feasible that binding of PhtD could have been

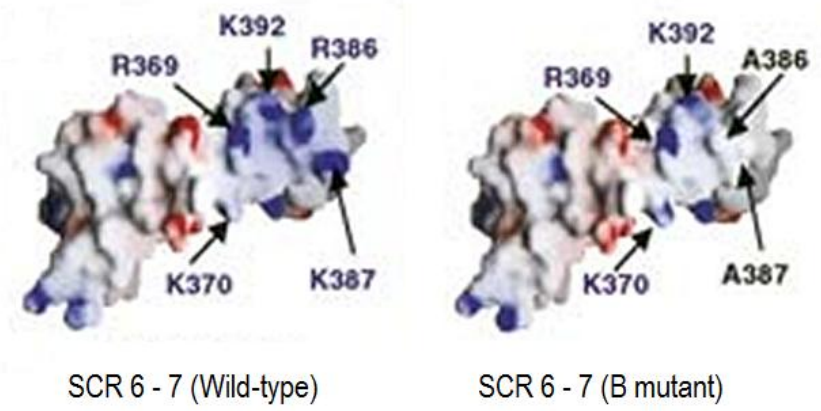

Figure 3.7: Surface electrostatic potentials of molecular models of wild-type and B mutant SCR 1-7.

Giannakis *et al.*(2003) used the NMR structure of SCR 15–16 as a template for a molecular model of SCR 6–7, both for wild-type (left) and the B mutant (which has amino acid substitutions R386A and K387A, shown right). The surface electrostatic potentials are shown with red denoting negative charge and blue denoting positive charge. The positively charged residues on SCR 7 are indicated with arrows as are the substitutions at site B. Adapted from Giannakis *et al*., 2003, with permission.

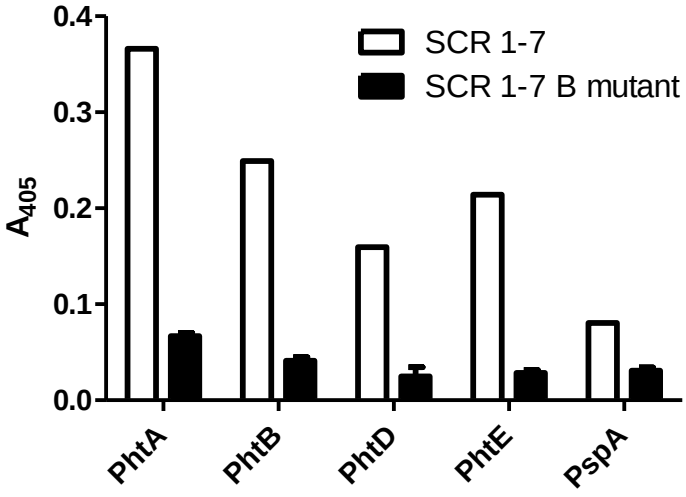

Figure 3.8: Binding of pneumococcal proteins to wild-type or 'B mutant' SCR 1-7.

Binding between proteins was assessed by ELISA by incubating immobilised pneumococcal proteins with proteins comprised of SCR domains 1-7 of factor H, either wild-type or with the amino acid substitutions R386A and K387A. Binding was detected using an anti-factor H polyclonal antibody and alkaline phosphatase-conjugated secondary antibody.

prevented by conformational changes in SCR 1-7 resulting from the immobilisation process, PhtD was then immobilised onto a chip and SCR 1-7 used as the analyte. No binding could be detected even at the highest concentration of SCR 1-7 used (7 μM). Again, a polyclonal antiserum (in this case raised against PhtD in mice) was used as a control, and this showed binding (data not shown).

3.8 Flow cytometric measurements of the interaction of SCR 1-7 with Pht proteins and PspA

To test the binding of SCR 1-7 to whole pneumococci of strain D39, flow cytometric assays were performed as described in Section 2.9. Briefly, bacteria were incubated with 25 μg/ml purified SCR 1-7 before detection of its binding to the cell surface with an anti-factor H antibody and a fluorescent secondary antibody. FHL-1 is thought to be present at between 10 – 50 μg/ml in blood serum, hence 25 μg/ml was chosen as a concentration representative of the *in vivo* scenario (Kuhn and Zipfel, 1996; Hellwage *et al*., 1997). The mutant strains used in these experiments had been constructed previously (Graham and Paton, 2006; Ogunniyi *et al*., 2009). In the first experiment, wild-type pneumococci were incubated with SCR 1-7, SCR 1-7 B mutant or PBS. As shown in Figure 3.9 A, there was an increase in fluorescence when SCR 1-7 was used as opposed to negative controls PBS and SCR 1-7 B mutant, indicating binding of SCR 1-7 to the surface of the bacteria. Next, Δ*phtABDE* and Δ*pspA* strains were compared to wild-type for SCR 1-7 binding, and were both found to show a decrease (Figure 3.9 B). Lastly, binding was compared between strains lacking *pht* genes as well as *adcR*, which is a negative transcriptional regulator known to repress *pht* gene expression (see Section 1.5.2). Δ*adcR* strains are known to express Pht proteins at a very high level (Ogunniyi *et al*., 2009). The Δ*adcR* strain bound more SCR 1-7 than wild-type, consistent with its greater expression of Pht proteins and their interaction with SCR 1-7 (Figure 3.9 C), while the Δ*adcR* Δ*phtABDE* strain bound a similar level as the Δ*phtABDE* mutant, confirming that other potential transcriptional changes caused by loss of AdcR were not the cause of the increased binding observed for the Δ*adcR* strain.

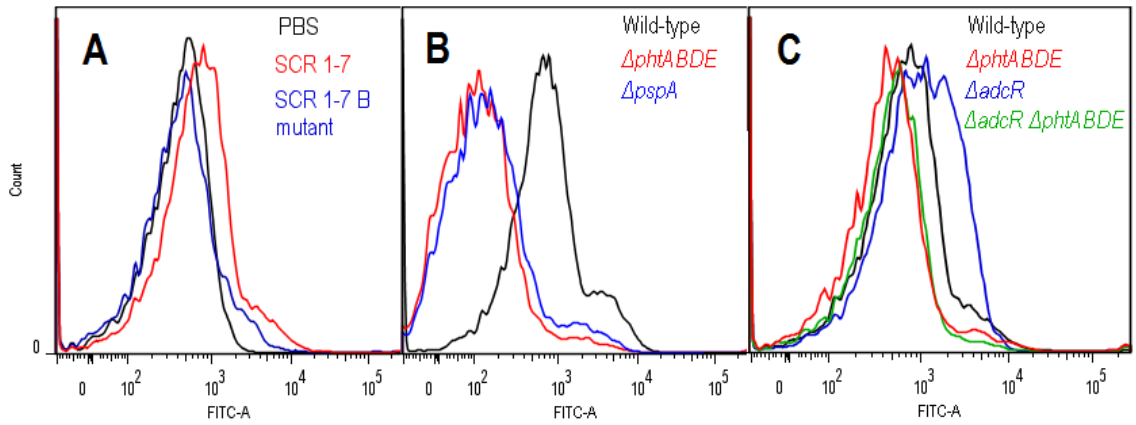

Figure 3.9: Binding of purified SCR 1-7 to the pneumococcal surface.

Bacteria were incubated with SCR 1-7 and its binding to the surface was detected with an anti-factor H antibody followed by a fluorescent secondary antibody and flow cytometry analysis. **A**: Comparison of SCR 1-7 and SCR 1-7 B mutant binding to wild-type pneumococci with negative control (PBS alone). **B**: Comparison of binding of SCR 1-7 to wild-type, Δ*phtABDE* and Δ*pspA* strains. **C**: Comparison of binding of SCR 1-7 to wild-type, Δ*phtABDE*, Δ*adcR* and Δ*adcR*Δ*phtABDE* strains.

3.9 Contributions of Pht proteins, PspA and PspC to evasion of complement deposition

Mutant strains lacking either *phtABDE*, *pspA* or *pspC* had been constructed previously (Graham and Paton, 2006; Ogunniyi *et al*., 2009). Strains lacking combinations of these genes were created by amplifying the relevant genetic loci (which contained antibiotic resistance genes in place of the pneumococcal gene) by PCR and transforming the other strains such that mutants lacking all permutations of *phtABDE*, *pspA* and *pspC* genes were created (see Table 2.1). The deposition of complement protein C3b onto the strains was then assessed by flow cytometry after incubation with naïve mouse serum as described in Section 2.9. Since variation in colony opacity phenotype can affect interactions of pneumococci with the complement system (Li *et al*., 2012), opaque variants of all strains were selected on THY-catalase agar plates for all experiments. Replicate experiments yielded similar trends in fluorescence changes between strains but different absolute values of fluorescence; to account for this, each set of measurements was normalised to the relevant measurement of the wild-type strain. As shown in Figure 3.10, all mutant strains showed increased deposition of C3b compared to wild-type. The difference was significant ($P < 0.05$) for all strains except Δ*pspC* and Δ*phtABDE*Δ*pspC* (comparisons were made by one-sample *t*-test with a theoretical mean of 1), indicating that the Pht proteins and PspA do contribute to evasion of complement deposition in this model. There was a trend towards greater complement deposition on the Δ*pspC* and Δ*phtABDE*Δ*pspC* strains, and it was apparent that the normalized mean fluorescence for the Δ*phtABDE*Δ*pspC* strain was similar to that of the Δ*phtABDE* strain, with only the large standard error of the former preventing a significant difference from being observed. More measurements may therefore be required to accurately elucidate the phenotypes of the Δ*pspC* and Δ*phtABDE*Δ*pspC* strains.

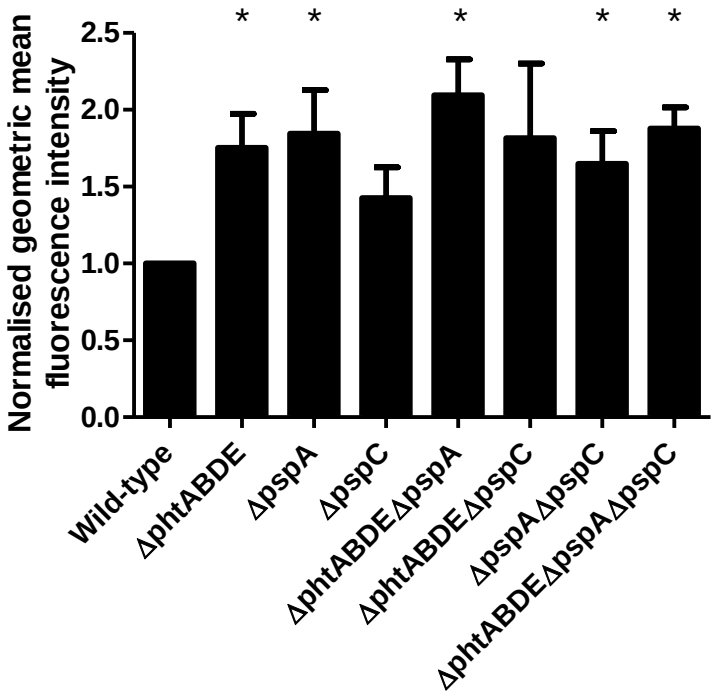

Figure 3.10: Deposition of complement C3b from murine serum onto pneumococcal strains lacking surface proteins.

Wild-type D39 and mutant pneumococcal strains were incubated with naïve mouse serum then C3b deposition was detected by flow cytometry as described in Section 2.9. Results are shown as geometric mean and standard error of fluorescence normalised to wild-type and are representative of six replicate sets of measurements taken over four independent experiments.

3.10 Discussion

The Pht proteins have previously been shown to be virulence factors in murine models of pneumococcal sepsis and pneumonia (Ogunniyi *et al*., 2009). In this work, the requirement for *pht* genes for full virulence was confirmed in a murine sepsis model, and a competition experiment showed that the Δ*phtABDE* mutant was highly attenuated in all niches examined after 24 and 48 h. This experiment supports the hypothesis that Pht proteins play a role in pneumococcal colonisation of the nasopharynx. Consistent with this, it has previously been shown that immunisation with Pht proteins can protect against pneumococcal colonisation (Godfroid *et al*., 2011). It cannot be inferred from the competition experiment alone whether Pht proteins have a role during sepsis, since the competitive indices measured for the blood are affected not only by pneumococcal fitness in this niche, but also by the relative numbers of wild-type and mutant pneumococci that survive in the nasopharynx and lungs. This is because the bacteria are transmitted to the blood from the nasopharynx and lungs, and thus unequal numbers in these niches would be likely to affect the numbers that reach the blood. Nevertheless, the sepsis model experiment implies that the Pht proteins have a function during this stage of infection as well. Thus, they are likely to contribute to virulence throughout the course of infection, from colonisation through to pneumonia and sepsis. Previous reports indicate that Pht proteins have multiple functions, such as in binding factor H, zinc homeostasis and adherence to host surfaces (Ogunniyi *et al*., 2009; Rioux *et al*., 2010; Khan and Pichichero, 2012), and these may all contribute to varying extents at different times during infection in different niches.

Factor H is composed of 20 SCR domains, and it was of interest to determine which of these domains are involved in binding to the Pht proteins. Following an approach similar to one used previously for PspC (Duthy *et al*., 2002), it was found that the Pht proteins bind to SCR 1-7. This interaction was much more readily detectable than the interaction of Pht proteins with the full length factor H protein, to which little binding was detected. A study by Melin *et al*. (2011) also failed to detect *in vitro* binding of purified Pht proteins to factor H, despite an earlier report of this being the case (Ogunniyi *et al*., 2009). The data presented in Figure 3.4 show slightly higher A_{405} readings for Pht proteins with factor H than with SCR 8-15 or 16-20, and comparisons using two-tailed paired *t*-tests showed that

the differences were statistically significant. It is possible that, if the substrate were given a longer time to develop, a clearer interaction with factor H would have been observed. Furthermore, due to the differences in molecular weight of factor H and the truncated proteins, the molar concentration of the full length protein was approximately three times less than the others, which may also have contributed to the low level of binding observed. Nevertheless, based on this experiment, the preferential physiological ligand for the Pht proteins *in vivo* is likely to be FHL-1.

Further ELISA experiments suggested that binding occurs via ionic interactions between Pht proteins and SCR 7. Whilst a crystal structure for the entire factor H protein is not available, modelling studies based on structures determined for various SCR regions suggest that factor H adopts a conformation in which it is bent back upon itself (Aslam and Perkins, 2001; Arlaud *et al*., 2007). This could explain the specificity of Pht proteins in binding FHL-1 over factor H, since access to SCR 7 may be blocked by other SCR domains in factor H, but not in FHL-1.

PspA was initially included in the ELISA experiments as it was expected to act as a negative control; however, it was also found to bind SCR 1-7 and was similarly dependent on electrostatic interaction with SCR 7. In Figure 3.4, PspC (which has previously been shown to bind to SCR 13-15 (Duthy *et al*., 2002)) did not show an interaction with SCR 1-7, and thus acted as a negative control, implying that the results from the other samples were not false positives. Interestingly, coiled-coil domains are thought to be present in the Pht proteins, PspA and PspC. Such domains have been implicated in binding factor H and/or FHL-1 in surface proteins of a number of other bacterial species, such as FhbA of *Borrelia hermsii* (Hovis *et al*., 2008), OspE of *Borrelia burgdorferi* (McDowell *et al*., 2004), Fba of *Streptococcus pyogenes* (Pandiripally *et al*., 2003) and FhbB of *Treponema denticola* (McDowell *et al*., 2009). Coiled-coils may therefore be a favourable structural feature that allows binding to SCR domains, and could account for the common binding of Pht proteins and PspA to SCR 7.

Flow cytometry experiments showed that SCR 1-7 is able to bind to the pneumococcal surface, and that this binding is decreased in the absence of Pht proteins or PspA. This was an important demonstration, since binding of the proteins *in vitro* does not take into accounts factors such as the conformation and orientation of the proteins on the bacterial

surface or steric hindrance by other factors such as other surface proteins or the capsule layer. However, binding could not be detected between SCR 1-7 and PhtD using surface plasmon resonance when either protein was used as the immobilised ligand. This could be due to the immobilisation procedure, which was performed using amine coupling (and thus involves either the N-terminus of the protein or lysine residues, which are plentiful in both proteins). Immobilisation may have resulted in changes to both proteins' conformations that led to a loss of binding activity. A different technique should be used to confirm *in vitro* binding of SCR 1-7 to the Pht proteins and PspA, preferably one that does not involve immobilisation of either protein, such as microscale thermophoresis. This would also allow comparisons of dissociation constants for the interactions of the different pneumococcal proteins with SCR 1-7. However, due to time constraints such experiments could not be performed in this study.

Finally, an assay for complement deposition using mouse serum as the source of complement suggested that Pht proteins and PspA, but not PspC, contributed to decreased C3b accumulation on the pneumococcal surface. PspC has been shown to specifically bind human factor H, and not to factor H molecules of other species, including mice (Lu *et al*., 2008a). This may explain the lack of effect seen for loss of *pspC* in this experiment. To further investigate the contribution of the proteins to evasion of complement deposition, it would be necessary to be repeat the experiment using human serum as a source of complement; this, however, would be complicated by the presence of anti-pneumococcal antibodies in the serum (which almost all humans develop during infancy) which could activate complement via the classical pathway and/or bind to the surface proteins being examined and block their function. The experiment performed here, however, has demonstrated a role for PspA and Pht proteins in defence against complement; in terms of Pht proteins, this is in agreement with the findings of Ogunniyi *et al.* (2009) and contradicts the conclusion of Melin *et al*. (2011). The inconsistencies in the literature are likely to be due to small differences in the protocols used to measure C3b deposition and the different dynamic ranges of C3b deposition that the experiments would be able to detect. Overall, given that Melin *et al*. (2011) found that one out of five *pht*-deficient strains accumulated more C3b than the wild-type strain, and with the findings presented here and those of Ogunniyi *et al.*, it appears likely that Pht proteins do play a role in

defence against complement deposition, which may be mediated via binding of FHL-1, but further work is required before this can be concluded with a high level of confidence.

Chapter 4: The relationship between Pht proteins and zinc

4.1 Introduction

Pht proteins were hypothesised to bind metal ions from as early as the first report of their discovery (Adamou *et al*., 2001). This is due to the presence of multiple histidine triad motifs (HxxHxH) in the proteins and the known ability of the imidazole groups of histidine to bind to transition metal ions, especially Zn^{2+}. Complexed metal ions are often necessary for correct folding and/or enzymatic activity of proteins. However, it is not clear whether this is the case for the Pht proteins, or whether the proteins may instead be involved in acquisition of metal ions from the environment and their transport into the cell.

A possible role for Pht proteins in zinc homeostasis was first implied by the identification of binding sites for AdcR (a zinc-binding transcriptional repressor) upstream of *pht* genes and the discovery that the external Zn^{2+} concentration affects the level of expression of Pht proteins (Panina *et al*., 2003; Ogunniyi *et al*., 2009; Shafeeq *et al*., 2011). One report found that the level of *pht* gene expression was increased when 100 μM Zn^{2+} was added to the growth medium (Ogunniyi *et al*., 2009), whereas others found increased expression below approximately 30 - 50 μM zinc (Rioux *et al*., 2010; Loisel *et al*., 2011; Shafeeq *et al*., 2011). It has been suggested that this apparent inconsistency in the literature could be resolved by taking the level of expression of AdcR itself into consideration (Plumptre *et al*., 2012). Since expression of the *adcRCBA* operon has been shown to be repressed at high zinc concentrations (Shafeeq *et al*., 2011), pneumococci grown under such conditions should mimic an *adcR* mutant phenotype, whereby *pht* gene expression is high due to the absence of its repressor AdcR. Over a lower range of external Zn^{2+} (0 – 50 μM), AdcR is present and causes zinc-dependent repression of *pht* gene expression. Together, these two effects could lead to a 'U' shaped profile of *pht* expression levels over the 0 – 200 μM range of external zinc (Plumptre *et al*., 2012).

As well as affecting the transcription of *pht* genes, zinc has been shown to interact directly with Pht proteins *in vitro*. PhtD has been found to bind zinc ions at a ratio of cation:protein of 4.6:1, consistent with all five histidine triad motifs being occupied (Loisel

et al., 2011). Furthermore, a Δ*phtABDE* mutant has been shown to be unable to grow as effectively as the wild-type in minimal medium without supplementation of Zn^{2+} (Rioux *et al*., 2010). Surprisingly, however, growth could also be restored by supplementing with Mn^{2+} or, to a certain extent, Fe^{2+}. The authors proposed that Pht proteins could therefore act as metal 'scavengers'; according to this hypothesis, they would bind metal ions when they are abundant in the environment, and then release them to metal ion importers at a later time when the bacteria are in a situation where they are starved of the ions (Rioux *et al*., 2010). PhtD has also been suggested to interact directly with AdcAII (Loisel *et al*., 2011); this will be addressed in Chapter 5.

This chapter aims to investigate possible functions of Pht proteins beyond the FHL-1 binding and evasion of complement deposition discussed in Chapter 3. In particular, it aims to further our understanding of the relationship between Pht proteins and metal ions by addressing the current disagreement in the literature regarding the direction of influence of zinc on expression of *pht* genes, as well as by examining the hypothesis that Pht proteins bind and scavenge metal ions.

4.2 Effect of zinc concentration on expression levels of Pht proteins and AdcR

Wild-type *S. pneumoniae* D39 were grown in C+Y medium with up to 100 μM zinc sulphate added, or alternatively with up to 12 μM of the Zn^{2+} specific metal ion chelator TPEN. From ICPMS measurements made in our laboratory, C+Y medium is known to contain just over 10 μM Zn^{2+} (data not shown), although the exact value can vary slightly from one batch of medium to another; in the batch used for these experiments the addition of more than 12 μM TPEN prevented any bacterial growth and thus C+Y with 12 μM TPEN presumably represented medium with almost no available zinc. Bacterial lysates were prepared from the cultures as well as concentrated samples of protein from the culture supernatants as described in Section 2.10, and Western blotting was performed to quantify the relative amounts of PhtD and AdcR in each sample. Western blots and quantifications of band intensities are shown in Figure 4.1 and Figure 4.2 respectively. Whilst no AdcR was detected in the culture supernatants as expected for an intracellular protein, it was interesting to note that PhtD was detected in these samples. The proportion of PhtD

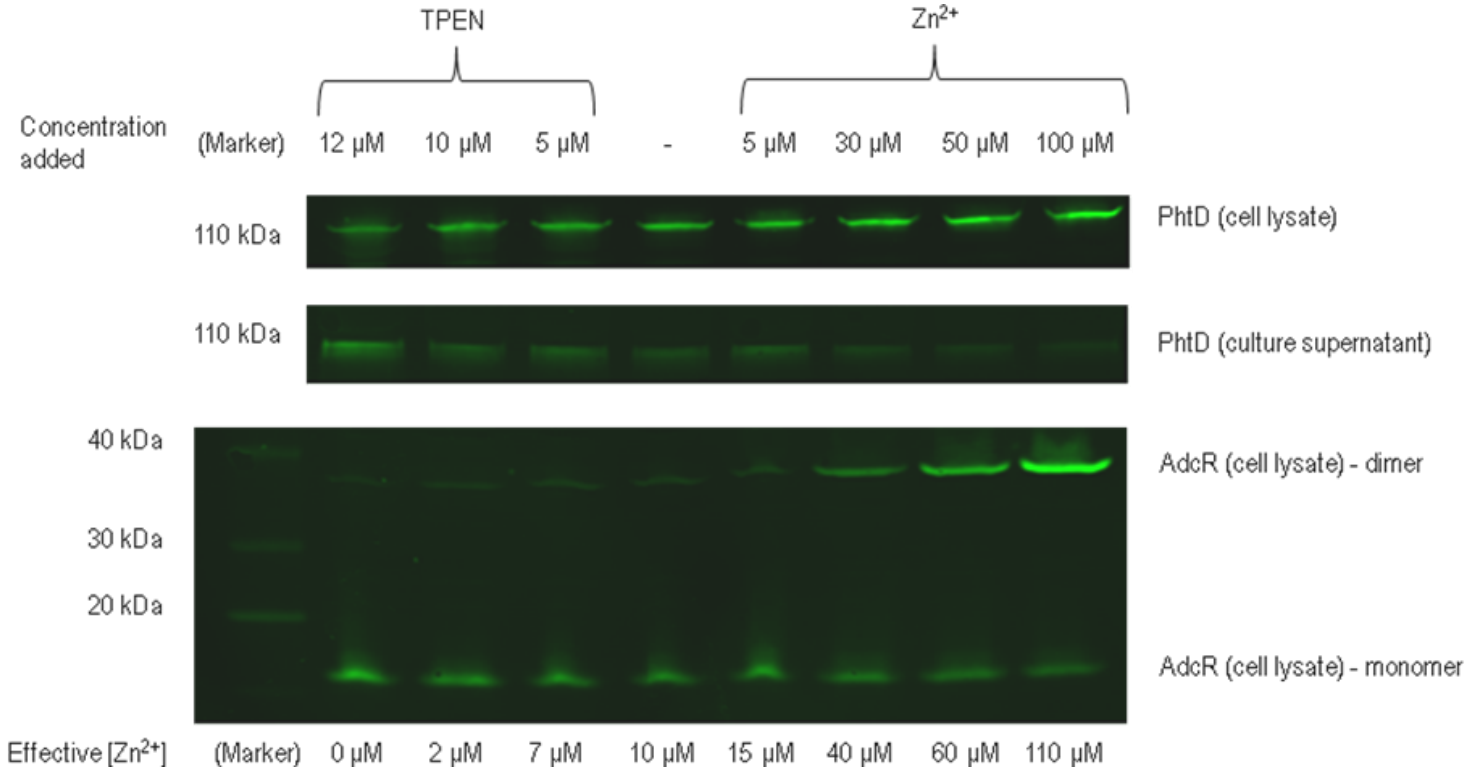

Figure 4.1: Expression of PhtD and AdcR across a range of zinc concentrations.

Wild-type D39 pneumococci were grown in C+Y medium supplemented with varying concentrations of TPEN or zinc sulphate. Bacterial lysates were prepared and proteins precipitated from the culture supernatants. Samples were run on SDS-PAGE followed by Western blotting to detect PhtD and AdcR. Molecular sizes of standard markers are indicated on the left; approximate concentrations of available zinc (based on the C+Y media containing 10 - 12 µM zinc when unsupplemented) are indicated at the bottom.

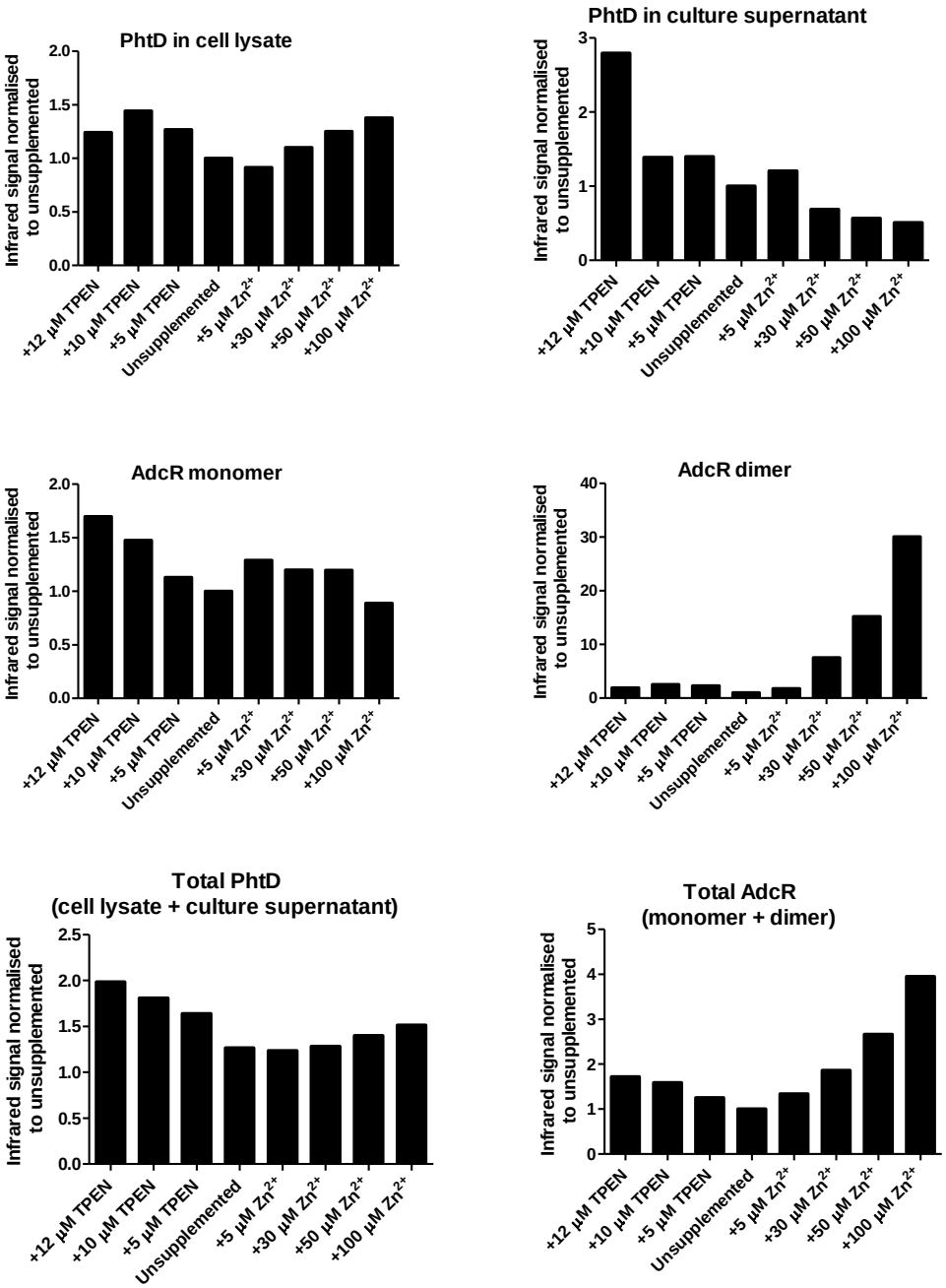

Figure 4.2: Quantitation of Western blot band intensities for expression of PhtD and AdcR across a range of zinc concentrations.

Odyssey software [LI-COR Biosciences] was used to quantify band intensities from the Western blots in Figure 4.1. Background fluorescence was subtracted and the signals were normalised to the signal detected for bacteria grown in unsupplemented C+Y medium.

detected in the supernatant was considerable: extracellular PhtD represented 9% of the total amount of the protein for medium with 100 μM zinc, and 37% of the total for medium with 12 μM TPEN. Observations related to secretion/release of PhtD will be investigated further in Chapter 7. There was a general trend of a decrease in PhtD in the supernatant with increasing external zinc concentration; however, in the lysates and when the total amount of protein was calculated by adding the amounts in the lysate and supernatant (appropriately normalised for the relative amounts of those fractions loaded onto the gel), it was apparent that the amount of PhtD followed a U-shaped pattern, with greater expression at either very low or very high amounts of zinc.

The blot for AdcR revealed the presence of two main bands, one at around 16 kDa corresponding to the predicted monomeric molecular weight of the protein, and one at a little under 40 kDa. This band is likely to represent dimeric AdcR. Two distinct dimers of AdcR have been described previously. In the first, the AdcR monomers are joined by ionic forces to form an active repressor that can bind to DNA, whilst in the other, monomers are covalently bonded together, but the resultant dimer is not thought to be able to act as a transcriptional repressor (Reyes-Caballero *et al*., 2010). Since the samples were heated to 95°C in the presence of 2-mercaptoethanol before loading onto the gel, the dimer observed here is likely to be the latter form. There is a general trend of a decrease in the amount of monomeric AdcR with increasing zinc concentration, whilst the amount of dimeric AdcR detected increases very strongly at 30 μM added Zn^{2+} and above. The total amount of AdcR (monomeric plus dimeric) is also somewhat U-shaped. These results support the hypothesis that the expression of PhtD is affected by both the level of expression of AdcR and its activity, both of which are zinc-dependent and together give rise to a U shaped expression profile of PhtD across the range of zinc concentrations examined. These observations will be discussed further in Section 4.7.

4.3 Binding of metal ions by purified Pht proteins

To examine the metal-binding abilities of the Pht proteins *in vitro*, inductively coupled plasma mass spectrometry (ICPMS) and thermal shift assays (TSA) were performed on purified Pht proteins. For ICPMS, untreated proteins were compared with protein that had been dialysed three times with buffer containing a 100:1 molar ratio of EDTA:protein, then three times in buffer without EDTA. Protein samples were prepared for ICPMS analysis as

described in Section 2.14.1. The amounts of Mg^{2+}, Mn^{2+}, Fe^{2+}/Fe^{3+} (these two ions cannot be distinguished using this apparatus), Co^{2+}, Ni^{2+}, Cu^{2+} and Zn^{2+} associated with the proteins were determined. Results, expressed as the ratio of molar concentrations of metal:protein, are shown in Table 4.1 for nickel and zinc. Only very small amounts of the other metal ions were present in all samples (less than 0.3 metal:protein molar ratio) and thus those results were omitted for clarity. Due to the range of metal concentrations used to generate the standard curve, measurements above 1.5 moles of metal per mole of protein could not be made accurately, and are simply reported here as > 1.5.

These data show that after expression and purification from *E. coli*, the Pht proteins were associated with a large amount of zinc and a small amount of nickel, which is likely to have come from the use of Ni^{2+} in the affinity column during purification. Furthermore, dialysis with EDTA removed effectively all of the nickel, but was only able to remove zinc to below 1.5 moles per mole of protein for PhtA and PhtD, and even these two proteins were still associated with a considerable amount of the metal. These results are consistent with nickel being loosely associated with the surface of the proteins after purification but being chelated by the EDTA during dialysis. In contrast, zinc remained associated with the proteins after dialysis, suggesting that it could be bound at sites within the protein that are not readily accessible to the exterior solvent phase, which prevented it from being chelated by EDTA. This may particularly be the case for PhtB and PhtE, since these two proteins retained the greatest amounts of zinc after dialysis, followed by PhtA and PhtD.

In order to measure the ability of the Pht proteins to interact with various transition metal ions, thermal shift assays were performed as described in Section 2.15. This assay is designed to measure the unfolding of proteins as they are heated; a difference in the temperature at which unfolding occurs at its maximum rate between samples incubated with and without a certain metal ion implies that the metal ion can interact with the protein and affect its structure (Cummings *et al*., 2006; McDevitt *et al*., 2011). Whilst the proteins contained histidine tags which could potentially interact with metal ions, such interactions would be unlikely to stabilise the protein's tertiary structure and thus would not contribute to the readout of the assay. Indeed, this technique has previously been applied to histidine-tagged proteins (McDevitt *et al*., 2011). Samples of buffer alone, protein without any metal ions or protein with EDTA were analysed as controls. The protein samples used in this experiment were from the same batch of EDTA-dialysed proteins used in the ICPMS

analysis, and therefore contained varying quantities of zinc as a baseline level. To account for this, the thermal stability of each protein incubated with metal ions was compared to that of the same protein without added metal ions. The results (Figure 4.3) show that the Pht proteins are quite promiscuous metal ion binders, with all the metal ions tested except Fe^{3+} able to stabilise at least one Pht protein to some extent. The EDTA controls showed no differences to the protein on its own. Amongst the metal ions, zinc, cadmium, nickel and cobalt consistently showed the greatest effects on thermal stability. Incubation with zinc led to a slight decrease in the thermal stability of PhtA and PhtE, indicating that this metal ion could interact with the proteins in some way even though it did not stabilise their structures.

Table 4.1: Nickel and zinc content of purified Pht proteins before and after dialysis with EDTA.

Protein	$[Ni^{2+}]$:[Protein] in non-EDTA treated samples	$[Ni^{2+}]$:[Protein] in EDTA treated samples	$[Zn^{2+}]$:[Protein] in non-EDTA treated samples	$[Zn^{2+}]$:[Protein] in EDTA treated samples
PhtA	0.82	< 0.01	> 1.5	1.49
PhtB	0.30	< 0.01	> 1.5	> 1.5
PhtD	0.82	< 0.01	> 1.5	0.70
PhtE	1.27	< 0.01	> 1.5	> 1.5

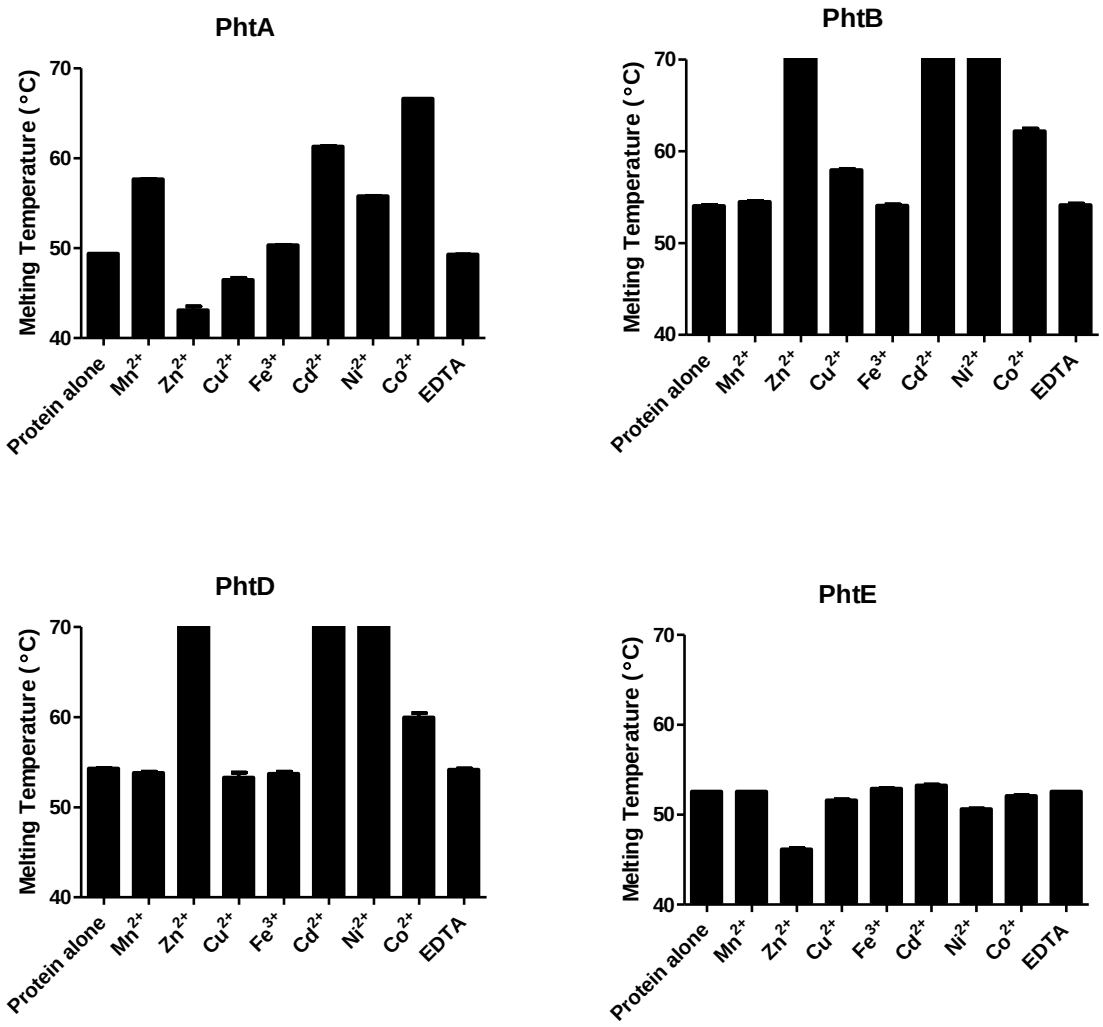

Figure 4.3: Thermal stability of the Pht proteins during unfolding in the presence of transition metal ions.

Proteins were heated in the presence of the indicated metal ions or EDTA and unfolding was measured as a function of temperature. The mean temperature at which the rate of unfolding was maximal is plotted for triplicate samples for each combination of protein and metal ion.

4.4 Metal ion accumulation of the Δ*phtABDE* mutant strain

Given that Pht proteins bind metals *in vitro*, the accumulation of metal ions by wild-type and Δ*phtABDE* pneumococci was investigated by ICPMS (see Section 2.14.2). For this analysis, the bacteria were grown in either unsupplemented C+Y medium or C+Y with 12 μM TPEN to assess the phenotype of the strains under conditions of zinc starvation. After growth, the bacteria were washed with PBS containing 5 mM EDTA to remove loosely associated metal ions from the bacterial surface. Results for zinc and nickel are shown in Figure 4.4; concentrations of magnesium, manganese, iron, cobalt and copper were also measured but no differences were found between wild-type and Δ*phtABDE* pneumococci for these metal ions (data not shown). The results show that growth of either strain in medium containing TPEN led to significantly less zinc accumulation than for the respective strain grown in unsupplemented C+Y; it can also be seen that the Δ*phtABDE* mutant strain accumulated significantly less zinc than wild-type when grown in medium containing TPEN, and less nickel than wild-type when grown in either medium.

In order to examine the relative amounts of loosely surface-bound versus tightly-bound and internal metal ions in these strains, ICPMS was again performed comparing bacteria washed with buffer either with or without 5 mM EDTA; the only metal ion to show significant differences between groups after this analysis was zinc, the results of which are shown in Figure 4.5. It should be noted that this experiment was performed with a different batch of C+Y medium, and it is known that the zinc concentration of this medium varies from batch to batch; this is the most likely reason for the discrepancy in total zinc content of the samples in this experiment, compared to those shown in Figure 4.4. The results show a small drop in cell-associated zinc after EDTA washing versus PBS; however, this effect occurs for both the wild-type and Δ*phtABDE* mutant strain, and there are no significant differences between the two strains, indicating that the amounts of loosely surface-bound zinc as well as the total amount of zinc associated with the bacteria are independent of the presence of Pht proteins.

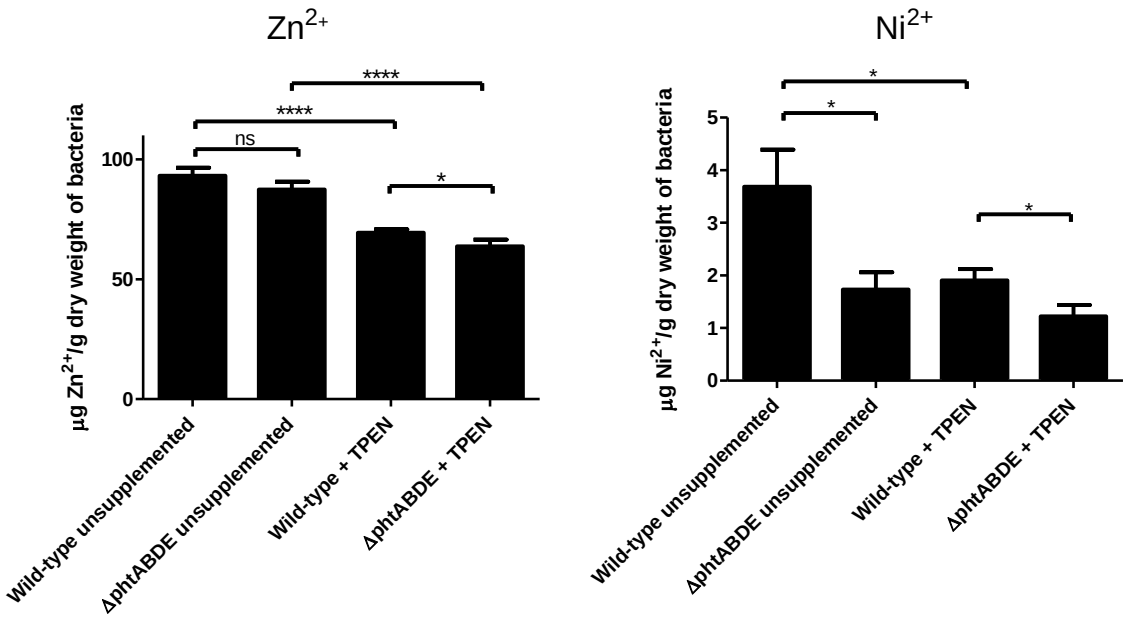

Figure 4.4: Zinc and nickel accumulation of wild-type and Δ*phtABDE* strains.

Wild-type and Δ*phtABDE* strains were grown in unsupplemented C+Y or C+Y with 12 µM TPEN and analysed by ICPMS to measure their metal ion content. Results are normalised by dry weight of the cell pellet of each sample. Results shown are the mean and standard error of the metal content of four biological replicate cultures, each measured in technical duplicate. Significant differences are indicated where present, as measured by one-tailed unpaired *t*-tests (ns, not significant; *, $P < 0.05$; ****, $P < 0.0001$).

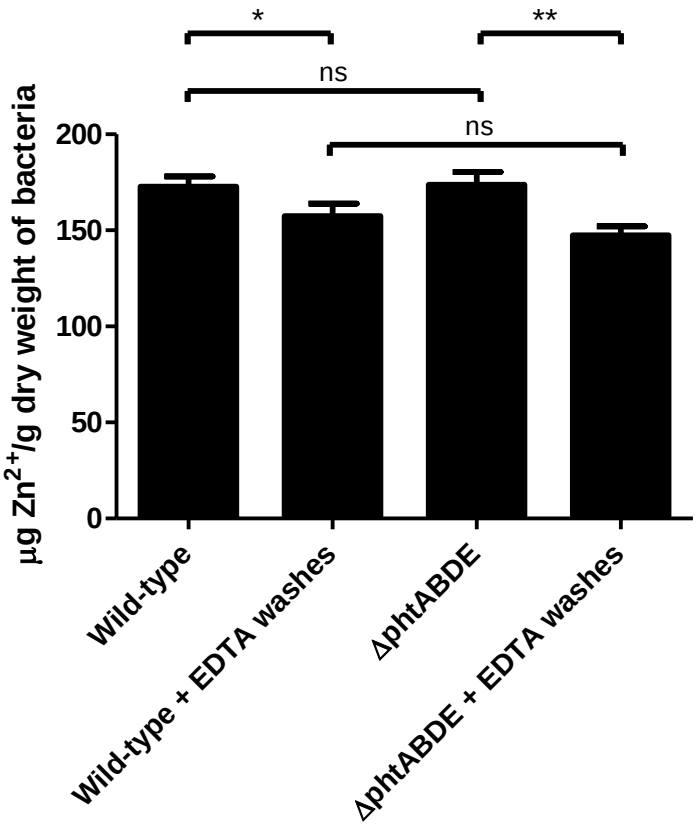

Figure 4.5: Accumulation of zinc of wild-type and Δ*phtABDE* mutant with or without EDTA washes.

Wild-type and Δ*phtABDE* mutant of strain D39 were grown in C+Y medium then washed three times with PBS or PBS with 5 mM EDTA. ICPMS analysis was performed to measure total zinc content after these treatments. Results are normalised by dry weight of the cell pellet of each sample. Results shown are the mean and standard error of the metal content of four biological replicate cultures, each measured in technical duplicate. Significant differences are indicated where present, as measured by one-tailed unpaired *t*-tests (*, $P < 0.05$; **, $P < 0.01$).

4.5 Growth of the Δ*phtABDE* mutant strain over a range of zinc concentrations

The most obvious functional role for zinc binding by Pht proteins would be in scavenging zinc when it is present at a low concentration in the extracellular environment; another plausible scenario is that Pht proteins could provide some form of defence against zinc toxicity when the metal ion is abundant. These two possibilities were tested by measuring the growth of wild-type and the Δ*phtABDE* mutant strain in medium containing a range of zinc and manganese concentrations. Firstly, growth in C+Y medium with high zinc:manganese ratios was measured, since it has been shown that pneumococcal infection leads to an increase in this ratio *in vivo,* which hinders bacterial growth by blocking acquisition of manganese by PsaA (McDevitt *et al*., 2011). Bacteria were prepared for growth curve measurements as described in Section 2.16. Growth was measured in unsupplemented medium or medium with 64 or 128 μM zinc sulphate added. It should be noted that due to the baseline concentrations of zinc and manganese in C+Y medium, the Zn^{2+}:Mn^{2+} ratios tested in this experiment were approximately 10:1, 70:1 and 130:1. As can be seen in Figure 4.6, an increase in the Zn^{2+}:Mn^{2+} ratio decreased the rate of growth and the maximum OD_{600} reached for both strains, and there were no substantial differences between the wild-type and Δ*phtABDE* mutant. It was therefore concluded that Pht proteins do not play a role in protecting against the toxic effects of excess zinc.

Similar experiments were performed examining the growth of wild-type and the Δ*phtABDE* mutant under conditions of very low availability of zinc. For this analysis C+Y was supplemented with various concentrations of TPEN to chelate the zinc present in the medium. As shown in Figure 4.7, 11 μM TPEN increased the time taken for both strains to reach exponential phase slightly, whilst 12.4 μM substantially inhibited growth and 13.6 μM completely abolished it. Interestingly, at 12.4 μM, there was a large difference between the growth of the wild-type and Δ*phtABDE* strains; the wild-type reached exponential phase much more quickly and grew to a higher maximum OD_{600}. These results suggest that the Pht proteins could play a role in allowing growth of pneumococci when zinc is extremely low in abundance; this is in agreement with the data in Figure 4.4, showing that the Δ*phtABDE* strain is less able to accumulate zinc than wild-type under conditions of very low zinc availability.

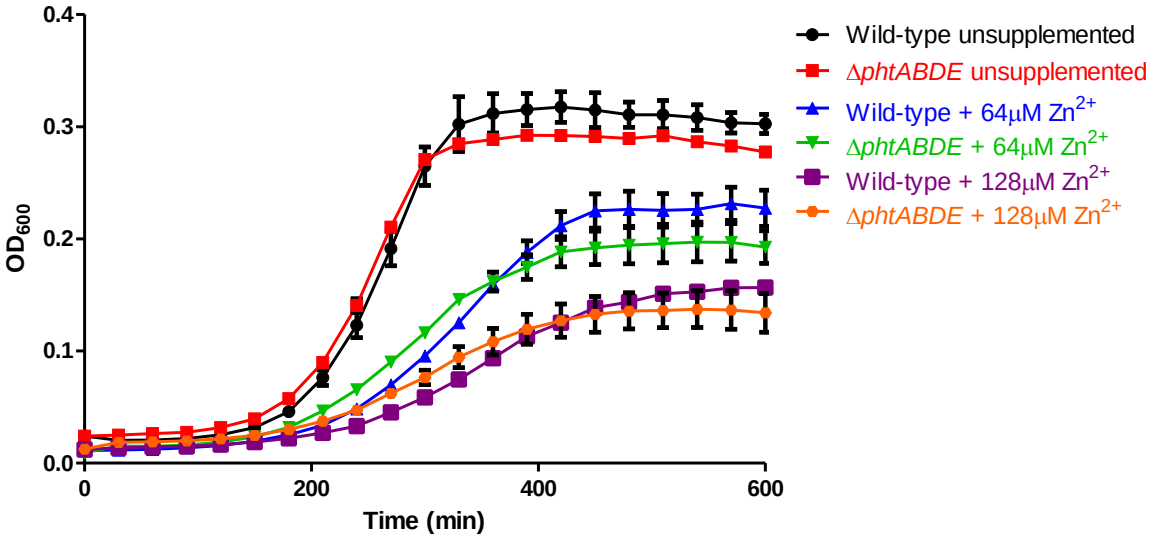

Figure 4.6: Growth of wild-type and Δ*phtABDE* mutant in C+Y with high Zn^{2+}:Mn^{2+} ratios.

Strains were grown in C+Y with varying concentrations of zinc sulphate to examine the effect of high Zn^{2+}:Mn^{2+} ratios on growth rate. Automated measurements of the OD_{600} were taken every 30 min. Mean and standard error are plotted for duplicate samples for each curve. The results are representative of three independent experiments.

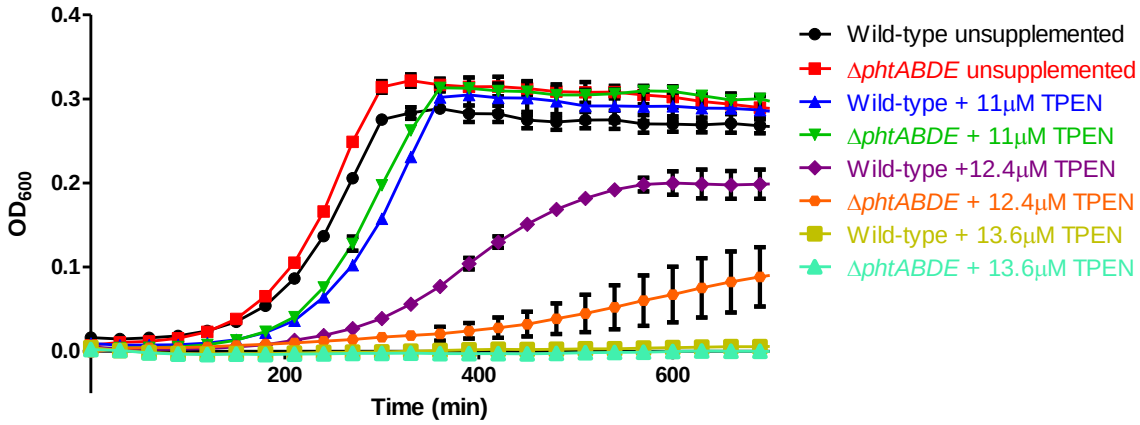

Figure 4.7: Growth of wild-type and Δ*phtABDE* mutant strain in C+Y with very low zinc availability.

Strains were grown in C+Y either unsupplemented or with 11 μM, 12.4 μM, 13.6 μM TPEN added. Automated measurements of the OD_{600} were taken every 30 minutes. Mean and standard error are plotted for duplicate samples for each curve. The results are representative of three independent experiments.

4.6 Surface charge of the Δ*phtABDE* mutant strain

Since Pht proteins are surface-localised and able to bind charged metal ions, it was hypothesised that they may have an effect on the overall surface charge of *S. pneumoniae*. Surface charge is an important property for bacteria as it can strongly influence various processes such as the ability of antimicrobial peptides to bind, the propensity of the bacteria to be phagocytosed and their adherence to biological and non-biological surfaces (Wilson *et al*., 2001; Strevett and Chen, 2003). Measurement of the zeta potential is commonly used as an indication of the surface charge of small particles and this technique can be applied to bacteria (Wilson *et al*., 2001).

The zeta potential of wild-type and Δ*phtABDE* pneumococci of strains D39 and WCH43 was measured as described in Section 2.17. In an initial pilot experiment, one culture of each strain was grown and the zeta potential measured in technical quadruplicate with the bacteria suspended in PBS at pH 7.4; the results are shown in Figure 4.8. The zeta potential of WCH43 was significantly more negative than that of D39; however, no difference in zeta potential was observed between wild-type and the Δ*phtABDE* mutant in either the D39 or WCH43 background.

Since pH can have a strong influence on the zeta potential, a more comprehensive experiment was performed subsequently in which cultures of wild-type and Δ*phtABDE* pneumococci of strain D39 were grown in triplicate, and the zeta potential was measured with the bacteria suspended in 150 mM sodium phosphate buffer ranging from pH 6 to pH 8 (see Figure 4.9). Again, no significant difference in zeta potential was observed between the two strains at any of the pH values examined.

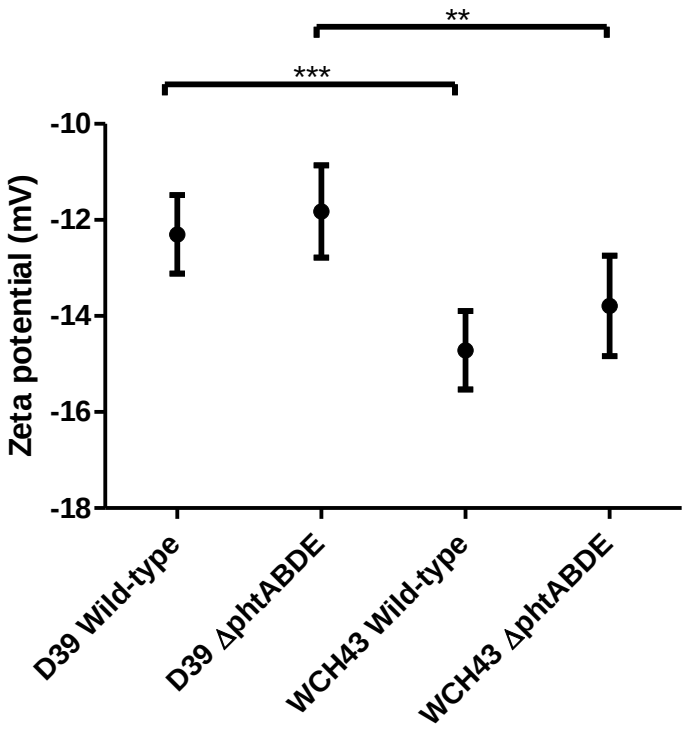

Figure 4.8: Zeta potential of D39 and WCH43 wild-type and Δ*phtABDE* strains.

Zeta potential was measured in PBS at pH 7.4 in technical quadruplicate. Results are shown as mean zeta potential with error bars representing the 95% confidence interval. Two tailed unpaired *t*-tests were used to show significant differences (**, $P < 0.01$; ***, $P < 0.001$); no significant difference was found between wild-type and Δ*phtABDE* in either D39 or WCH43.

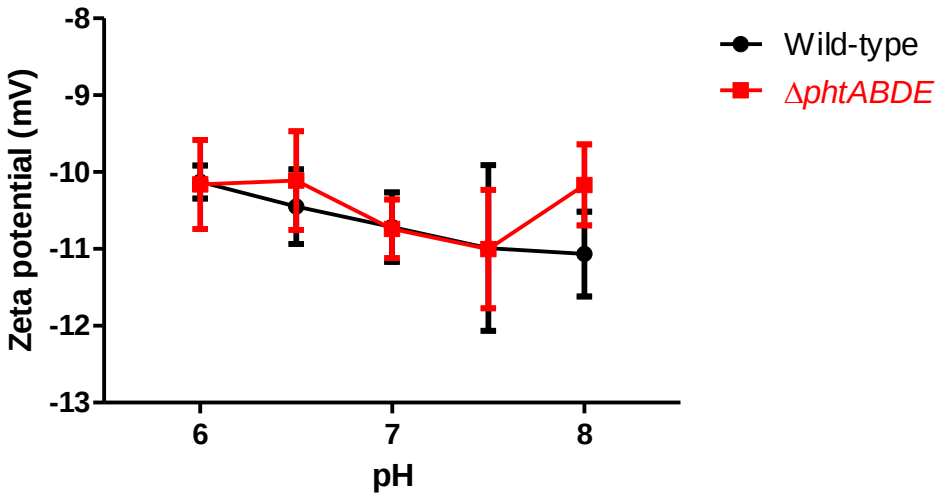

Figure 4.9: Zeta potential of wild-type and Δ*phtABDE* D39 pneumococci over the pH range 6 to 8.

Bacteria were grown in THY medium, washed and resuspended in sodium phosphate buffer before measurement of the zeta potential. The data points and error bars represent the means and standard errors for biological triplicates.

4.7 Discussion

In this chapter several aspects of the relationship between Pht proteins and transition metal ions, principally Zn(II), were investigated. Firstly, the effect of the external concentration of zinc on the expression of PhtD and AdcR was measured by quantitative Western blotting. This showed that total and cell-associated PhtD expression follows a U shaped trend with greater levels of expression at very low (< 5 μM) and very high (> 60 μM) levels of zinc compared to moderate (~10 μM) levels, as predicted previously (Plumptre *et al*., 2012). This experiment shows the value in comprehensively examining PhtD expression over a range of physiological zinc concentrations, rather than comparison at only two or three concentrations of zinc as has been the case previously (Ogunniyi *et al*., 2009; Rioux *et al*., 2010; Loisel *et al*., 2011; Shafeeq *et al*., 2011). Interestingly, a considerable proportion of the PhtD (ranging from approximately 10% to 40% depending on the level of TPEN or zinc supplementation) was found in the culture supernatants, with a trend of decreasing amounts in the supernatant with increasing zinc concentration. Secretion and/or release of Pht proteins from the bacterial surface has been reported to occur previously (Zhang *et al*., 2001), but later publications have neglected this observation. It should be noted that AdcR, an intracellular protein, could not be detected in the culture supernatants, indicating that the presence of Pht proteins in this fraction was not due to pneumococcal autolysis. Secretion and/or release of Pht proteins will be investigated further in Chapter 7.

Expression of AdcR was also found to be affected by the external concentration of zinc. Interestingly, a considerable amount of an apparent dimer of AdcR was detected when ≥ 30 μM Zn(II) was added to the medium. AdcR is known to form a homodimer in solution (Reyes-Caballero *et al*., 2010), but this is usually mediated by ionic or hydrophobic forces, which would have been disrupted when the samples were heated to 95°C with SDS-PAGE loading buffer. This implies that the dimer detected here may be stabilised by the formation of a covalent bond. The formation of an AdcR dimer from a purified protein sample that was resistant to reduction by dithiothreitol has been reported in a denaturing SDS-PAGE experiment previously; the dimer could not be detected in a C30A mutant of AdcR however, indicating that this cysteine residue is likely to mediate the formation of a covalent bond to another AdcR monomer (Reyes-Caballero *et al*., 2010). This is consistent

with the resistance of the dimer seen here to heating with 2-mercaptoethanol, which was also present in the SDS-PAGE loading buffer. Since strains encoding the C30A mutant form of AdcR showed the same phenotype as wild-type in terms of growth rate and total zinc content, the C30A mutation does not appear to affect the ability of AdcR to function *in vivo*, and thus covalent bonding of AdcR monomers to form a dimer may not be physiologically necessary for the function of AdcR (Reyes-Caballero *et al*., 2010). It is unclear whether covalently-bonded dimers of AdcR would be able to bind DNA and repress gene expression. However, given that PhtD expression was greater in samples in which the dimer was detected compared to samples grown in unsupplemented medium, we may speculate that this dimeric form is non-functional, since if functional it would be expected to repress transcription of PhtD and lead to a lower level of protein expression, which was not found to be the case.

The U shaped pattern of PhtD expression is therefore likely to be caused by an interplay between the level of AdcR (in the 'active' form detected here as monomeric), and its activity, for which it must bind zinc to allow binding to DNA to repress transcription of its target genes. The following model can be proposed. At low external zinc concentrations, the AdcR monomer was more abundant, but was unable to bind to DNA due to the low concentration of zinc in the cell, and could therefore not repress transcription effectively, leading to a high level of PhtD expression. At high external zinc, the amount of AdcR monomer itself was low, also allowing a high level of PhtD expression. At intermediate levels of zinc, however, AdcR was abundant and active enough to repress PhtD expression, leading to less of the protein compared to other samples grown with either very high or very low amounts of zinc. It is interesting to note that the total amount of AdcR (considering both monomeric and dimeric forms) was at its highest when the medium contained the highest level of zinc. In contrast to this, by using a transcriptomic approach, Shafeeq *et al.* (2011) found a 5.4 fold higher amount of *adcR* mRNA after growth in chemically defined medium lacking zinc compared to medium with 0.2 mM zinc sulphate added. The apparent discrepancy between the results presented in Section 4.2 and those of Shafeeq *et al*. (2011) may be due to differences in growth media or concentrations of zinc used or the possibility that the level of *adcR* mRNA is not proportional to the total amount of monomeric and dimeric AdcR protein. This could be the case if the level of monomeric AdcR were regulated by both its rate of translation from

mRNA and by some form of degradation of the protein, and if this could only break down the monomer but not the reduction-resistant dimer. Such a scenario would result in a gradual buildup of this dimer over time, leading to a higher total amount of AdcR (monomer plus dimer) present in the bacteria (e.g. the bacteria grown with 100 μM zinc added in Section 4.2) compared to another culture in which the level of transcription of *adcR* were similar or higher but the dimerisation was not occurring (e.g. the bacteria grown in unsupplemented C+Y in Section 4.2) .

In vitro measurements of purified Pht proteins indicated that, after purification, the proteins contained considerable quantities of zinc and a small amount of nickel. Dialysis with EDTA removed all of the nickel and a large proportion of the zinc. Thermal shift analysis revealed that a number of metal ions can interact with the Pht proteins. Of these, some of the largest shifts in melting temperature were observed with Zn(II), and since this ion is by far the most abundant transition metal ion found in the body (Versieck, 1985), it seems likely that the Pht proteins would have a physiological role related to zinc binding over binding to any other metal ion. However, a complete analysis of this issue would require a detailed characterisation of the proteins' affinity constants for the various metal ions.

Examination of the metal ion content of wild-type and Δ*phtABDE* strains showed that the Δ*phtABDE* mutant strain only accumulated less zinc when grown in medium with TPEN, representing conditions of zinc starvation. Under such conditions, the growth of the mutant was also impaired compared to wild-type (see Figure 4.7). There was no difference in zinc content when bacteria were grown in unsupplemented medium, nor when washes with EDTA were omitted. These observations indicate that Pht proteins could play a role in zinc homeostasis and aid in the acquisition of the metal ion, but only when it is very scarce. The physiological relevance of these observations is unclear, since the amount of bioavailable zinc that the pneumococcus would encounter during colonisation or disease cannot be measured with current approaches. Whilst homogenised nasopharyngeal and lung tissues of uninfected mice have been reported to contain approximately 41 μM and 44 μM Zn^{2+} respectively (McDevitt *et al*., 2011), it is unlikely that pneumococci in these niches would have access to such concentrations of the metal, given that the majority of the metal may be held intracellularly and/or tightly bound by eukaryotic proteins. However, since the release of zinc by the host to induce zinc toxicity in pneumococci has been

postulated to occur during infection (McDevitt *et al*., 2011), it seems likely that zinc deficiency would be a greater issue for the bacteria during initial colonisation. Further experiments will be required to determine whether Pht proteins do contribute to zinc acquisition *in vivo*; additional findings related to this topic will be presented and discussed in Chapter 5.

Whilst a role for Pht proteins in zinc homeostasis at very low external concentrations of the metal is supported by the evidence presented here, the importance of Pht proteins at high concentrations was also examined (Figure 4.6). A high external ratio of Zn(II):Mn(II) has been shown to be toxic to the pneumococcus due to the zinc competing for binding to PsaA, the SBP of the high affinity manganese uptake ABC transporter system, thus starving the bacteria of manganese (McDevitt *et al*., 2011). It was hypothesised that Pht proteins might help defend against this phenomenon by binding some of the zinc, thereby preventing it from binding to PsaA. However, this does not seem to be the case, since wild-type and Δ*phtABDE* pneumococci showed equally attenuated growth phenotypes in medium with high Zn(II):Mn(II).

The ICPMS experiments indicated that the strain lacking Pht proteins accumulated less Ni(II) than the wild-type. This metal ion was also capable of interacting with the Pht proteins in the thermal shift analysis. Whilst nickel homeostasis has been recognized as important for microorganisms due to their requirement for the metal in certain enzymes, as well as its toxicity at high concentrations (for reviews see Kaluarachchi *et al.*, 2010 and Macomber and Hausinger, 2011), its significance is thought to be mainly associated with bacteria surviving in more extreme environments such as contaminated soils around industrial parks. There has been little research into the effects of nickel on *S. pneumoniae* since the organism is not thought to come into contact with significant amounts of the metal in the human nasopharynx (its major niche). This is in contrast to zinc, which has been shown to exert a toxic effect on the pneumococcus *in vivo* (McDevitt *et al*., 2011). Thus, while a role for Pht proteins in nickel homeostasis cannot be ruled out, it appears unlikely that the observations here relating to nickel binding reflect a genuine physiological function.

Lastly, the zeta potential of wild-type and Δ*phtABDE* pneumococci was measured in two different strains and over a range of pH conditions. This experiment was performed to

test the hypothesis that Pht proteins, in binding multiple positively charged zinc ions at the bacterial surface, might alter the net surface charge of the bacteria. This is an important property, since it affects the ability of antimicrobial peptides to bind, the propensity of bacteria to be phagocytosed and their adherence to biological and non-biological surfaces (Wilson *et al*., 2001; Strevett and Chen, 2003). It has previously been shown that loss of the choline-binding proteins can affect surface charge and hydrophobicity (Swiatlo *et al*., 2002). The values for the zeta potential of D39 found here were similar to the result of −11.3 mV found for this strain by Swiatlo *et al*. (2002). Whilst it was also found that WCH43 was more negatively charged than D39, and that the zeta potential of the bacteria decreased slightly with increasing pH, no significant differences were found between the wild-type and Δ*phtABDE* strains. This indicated that Pht proteins are not a significant determinant of surface potential, at least in the strains and conditions examined here.

In summary, this chapter has provided information on the expression of PhtD and AdcR over a large range of zinc concentrations, at least partially resolving some seemingly conflicting observations in the literature, and has shown that Pht proteins may play a role in zinc acquisition when the metal is scarce in the environment. The precise mechanism of this activity is unclear, but could be via 'scavenging' of metal ions when they are abundant for use at a later time when they are in short supply, as has been proposed previously (Rioux *et al*., 2010). Alternatively, they may work with the high affinity zinc binding protein AdcAII to aid zinc import directly, as suggested by Loisel *et al*., (2008). This hypothesis will be examined experimentally in the following chapter.

Chapter 5: AdcA, AdcAII and the import of zinc

5.1 Introduction

In the previous chapter the relationship between Pht proteins and zinc was investigated. In this chapter this analysis has been extended to include AdcA and AdcAII. These proteins are SBPs of ABC transporter systems and belong to cluster A-1 of this family of molecules (Dintilhac and Claverys, 1997; Dintilhac *et al*., 1997; Berntsson *et al*., 2010). AdcA, which is encoded in the *adcRCBA* operon, shares 26% amino acid sequence identity with AdcAII, which is encoded as an orphan SBP immediately upstream of *phtD*. The latter two genes have been shown to be co-transcribed in an operon that also includes *ccdA* (which is involved in the biogenesis of cytochrome c), *spr0904* (which shows homology with thioredoxin), and *yfnA* (a putative amino acid transporter belonging to the cationic APC superfamily) (Loisel *et al*., 2008; Rioux *et al*., 2010). The transcriptional repressor AdcR controls the expression of *adcRCBA* and *adcAII-phtD* as well as that of the other *pht* genes, in response to environmental zinc concentrations (as discussed in Section 4.2) (Shafeeq *et al*., 2011).

In terms of function, the *adcCBA* operon has been shown to encode an ABC-type zinc permease required for the pneumococcus to acquire sufficient zinc for growth and to allow transformation (Dintilhac *et al*., 1997), whilst AdcAII specifically binds zinc *in vitro*, and was also shown by X-ray crystallography to contain a canonical metal-binding site containing zinc (Loisel *et al*., 2008). AdcA and AdcAII both contain a loop structure near the metal binding site characteristic of zinc importers, but only the loop of AdcA contains a cluster of positively charged histidine residues that has been hypothesised to either facilitate the sequestration of zinc or to sense environmental zinc levels (Loisel *et al*., 2008). AdcA also contains a domain at its C-terminal end that is not present in AdcAII; this domain is homologous to ZinT, which has been characterised in Gram-negative bacteria as contributing to zinc acquisition via ZnuABC (an ABC transporter system homologous to AdcCBA) (Gabbianelli *et al*., 2011; Lim *et al*., 2011).

It has been proposed that AdcAII and PhtD have a direct joint function, given data interpreted as showing *in vitro* cross-linking and apparent co-localisation on the bacterial

surface (Loisel *et al*., 2011). However, in the cross-linking experiments in which purified PhtD and AdcAII were the only proteins present, only a small proportion of the PhtD became associated with AdcAII, despite the latter being present in eight-fold molar excess. It is also not clear that AdcAII and PhtD are co-localised, given that AdcAII was found exclusively in the membrane fraction, whilst the majority of the PhtD was found in the cell wall fraction, with only a minority associated with the cell membrane (Plumptre *et al*., 2012).

An investigation into the possible functional link between AdcAII and Pht proteins was therefore undertaken. In addition to this, the hypothesis that AdcAII is redundant with AdcA in acting as a SBP specific for zinc, based on the high homology of the two proteins, was also examined.

5.2 Construction of mutants

Mutants lacking *adcA*, *adcAII*, *adcCBA*, *phtABDE* and combinations thereof were constructed in strain D39. This was performed by overlap extension PCR to fuse the flanking regions of the gene(s) to an antibiotic resistance gene cassette, followed by transformation in which the flanking regions undergo homologous recombination with the bacterial chromosome, replacing the gene with the antibiotic resistance cassette (see Figure 5.1). The primers used to make mutants in the indicated genes are shown in Table 5.1. Primer sequences are listed in Table 2.2.

In this manner *adcA* and *adcCBA* were replaced with a gene conferring resistance to chloramphenicol, whilst *adcAII* and *adcAIIphtDE* were replaced with a gene conferring resistance to spectinomycin. For the Δ*adcAII* mutant, the spectinomycin resistance gene was then removed. This was done so that transcription of *phtD*, which is usually co-transcribed with *adcAII*, would not be affected by the presence of the antibiotic resistance gene upstream of it. Overlap extension PCR was again used to achieve this as explained in Figure 5.2.

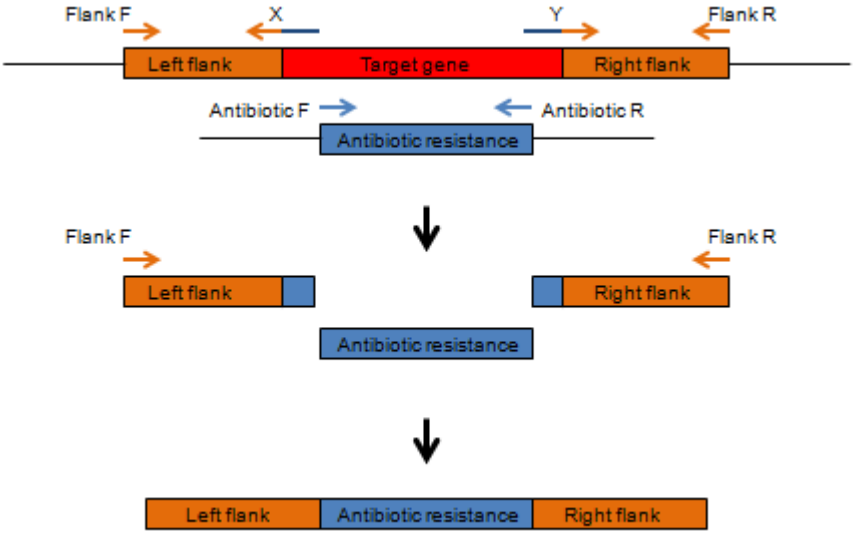

Figure 5.1: Overlap extension PCR.

Regions flanking either side of the gene of interest are amplified by PCR using primers 'Flank F' with 'X' and 'Flank R' with 'Y'. 'X' and 'Y' contain sequences complementary to an antibiotic resistance gene cassette, which itself is amplified separately with 'Antibiotic F' and 'Antibiotic R'. The flanks and antibiotic resistance cassette are mixed and another PCR is performed using primers 'Flank F' and 'Flank R' to fuse the three products. The resulting product can recombine with the bacterial chromosome through the homology of the flanking regions; this leads to replacement of the target gene with the antibiotic resistance cassette and allows selection of mutants by the addition of the antibiotic to the growth medium.

Table 5.1: Primers used to construct mutant strains.

Gene(s)	Flank F primer	X primer	Y primer	Flank R primer
adcA	CP1	CP2	CP7	CP8
adcAII	CP3	CP4	CP9	CP10
adcCBA	CP5	CP6	CP11	CP12
adcAIIphtDE	CP3	CP4	PhtE Spec Y	AD82

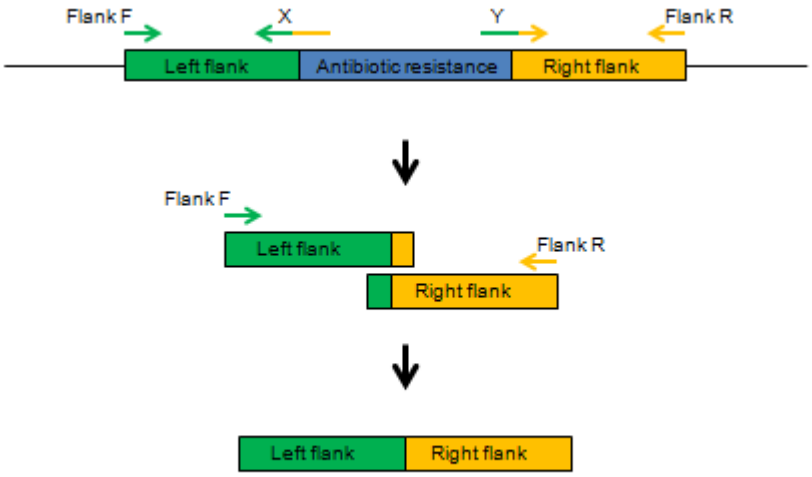

Figure 5.2: Overlap extension PCR to remove an antibiotic resistance gene.

Regions flanking either side of the antibiotic resistance gene are amplified by PCR using primers 'Flank F' with 'X' and 'Flank R' with 'Y'. 'X' and 'Y' contain sequences complementary to one another, allowing a product consisting of the two flanks fused together to be created in a subsequent PCR using primers 'Flank F' and 'Flank R'. The resulting product can recombine with the bacterial chromosome through the homology of the flanking regions; this removes the antibiotic resistance gene. Mutants are selected by screening for loss of resistance to the antibiotic.

Once these mutant strains had been constructed, the relevant loci were amplified using the 'Flank F' and 'Flank R' primers, and the resulting products were used to transform the other mutants such that all relevant combination mutants were made. The Δ*adcAIIphtDE* mutant locus was used to transform a previously generated Δ*phtAB* mutant (Ogunniyi *et al*., 2009).

5.3 Growth of mutants under zinc-limiting conditions

Growth experiments were performed as described in Section 2.16 to determine the ability of the various mutants to grow in environments with low concentrations of zinc. As a starting point, mutants lacking *adcA*, *adcAII*, *adcCBA* and combinations thereof were tested using C+Y medium, which was either unsupplemented or had had 5 μM or 40 μM zinc sulphate added. The results (Figure 5.3) show that the Δ*adcA*Δ*adcAII*, Δ*adcCBA* and Δ*adcAII*Δ*adcCBA* strains were not able to grow effectively in unsupplemented C+Y, whereas the addition of 5 μM zinc sulphate could partially reconstitute growth, and 40 μM allowed full recovery. In contrast, the growth phenotypes of the Δ*adcA* and Δ*adcAII* single mutant strains were similar to that of the wild-type. These results imply that AdcA and AdcAII are functionally redundant under the conditions tested, since loss of one has no effect on phenotype, whereas loss of both has a dramatic effect. Furthermore, it also appears that AdcB and/or AdcC are required for the import of zinc via AdcAII, since the Δ*adcCBA* mutant had a similar phenotype to that of the Δ*adcA*Δ*adcAII* strain. It is interesting to note that the Δ*adcCBA* mutant showed less recovery of growth than the Δ*adcA*Δ*adcAII* and Δ*adcAII*Δ*adcCBA* strains when medium was supplemented with only 5 μM zinc sulphate; this is likely to be due to sequestration of zinc by AdcAII in the Δ*adcCBA* mutant preventing the metal being available for transport into the cell by low affinity secondary transporters.

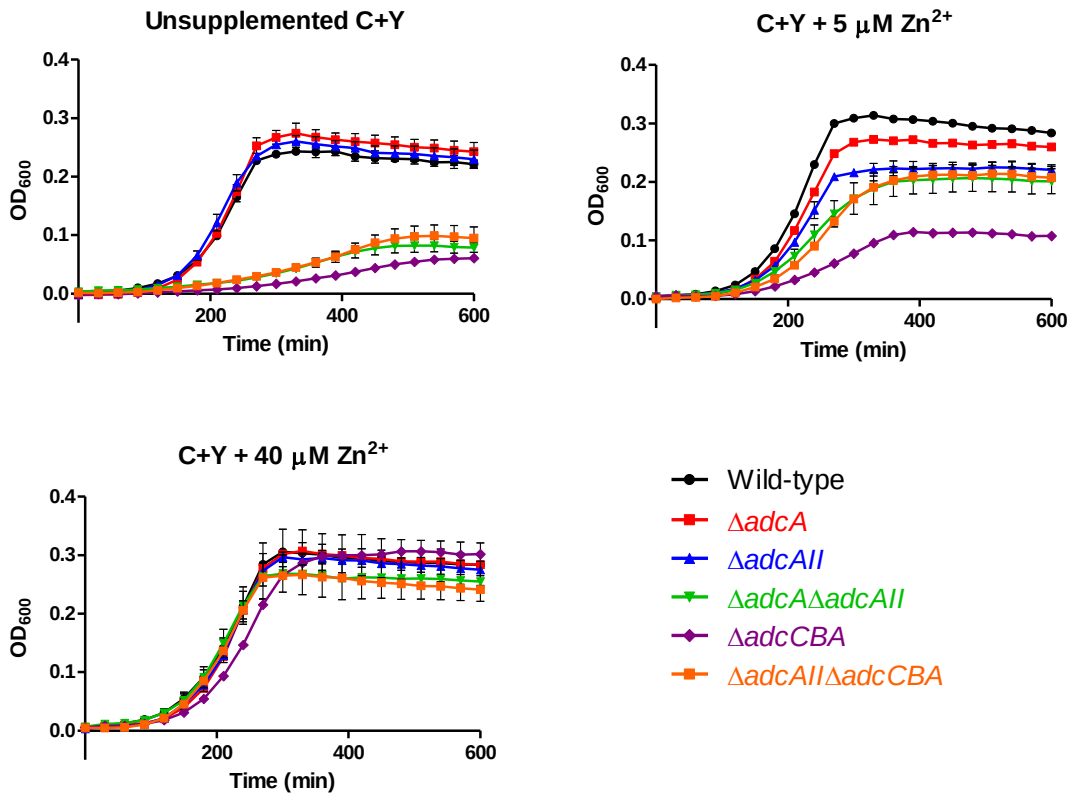

Figure 5.3: Growth curves of Δ*adc* mutants in C+Y supplemented with Zn^{2+}.

Equal CFU of wild-type and mutant strains were sub-cultured into 200 µl C+Y (either unsupplemented or with 5 or 40 µM Zn^{2+} added) in a 96 well tray. The bacteria were incubated at 37°C and growth was monitored via measurement of the OD_{600} every 30 min. Mean and standard error are plotted for duplicate samples for each curve. Results are representative of three independent experiments.

In subsequent experiments, the growth phenotypes of mutants lacking combinations of *adcA*, *adcAII* and *phtABDE* were examined in C+Y supplemented with 11 μM TPEN. As can be seen in Figure 5.4, all of the strains grew normally in unsupplemented C+Y except for Δ*adcA*Δ*adcAII* and Δ*adcA*Δ*adcAII*Δ*phtABDE*. Importantly, in this medium, no differences in growth could be observed when comparing strains that had *pht* genes intact to those in which the *pht* genes had been deleted. In the presence of 11 μM TPEN, growth of all strains was slightly delayed compared to zinc-replete conditions. Growth of the Δ*adcA* and Δ*adcAII* strains was similar to that of wild-type. There was a slight delay in growth of Δ*phtABDE* and Δ*adcAII*Δ*phtABDE* strains, and lower maximum OD_{600} values were reached compared to wild-type. The Δ*adcA*Δ*phtABDE* strain showed a much more serious growth defect, and the Δ*adcA*Δ*adcAII* and Δ*adcA*Δ*adcAII*Δ*phtABDE* strains were unable to grow at all during the initial 400 min of the experiment. These results indicated that loss of the Pht proteins can have an effect on growth under conditions of low zinc availability; moreover, they show that this effect is highly exacerbated when AdcA is also absent, but not when AdcAII is also absent. These data are consistent with the Pht proteins playing a role in facilitating zinc acquisition by the SBPs, and this role being more important for the acquisition of zinc by AdcAII than by AdcA. Structural differences between AdcA and AdcAII may account for this interesting disparity (discussed in Section 5.6).

After 400 min, the Δ*adcA*Δ*adcAII*Δ*phtABDE* strain began to grow, whereas the Δ*adcA*Δ*adcAII* mutant did not. This discrepancy may indicate that when the high affinity SBPs and the Pht proteins are absent, secondary transporters are eventually able to import some zinc into the bacteria to allow growth; when the Pht proteins are present, they may sequester the metal from the secondary transporters, thereby preventing growth, as seen for the Δ*adcA*Δ*adcAII* strain.

Further experiments focussed on the relationships between AdcA, AdcAII, zinc import and pathogenesis of pneumococcal disease, since it was important to gain a better understanding of these relationships before examining how the Pht proteins fit into the system.

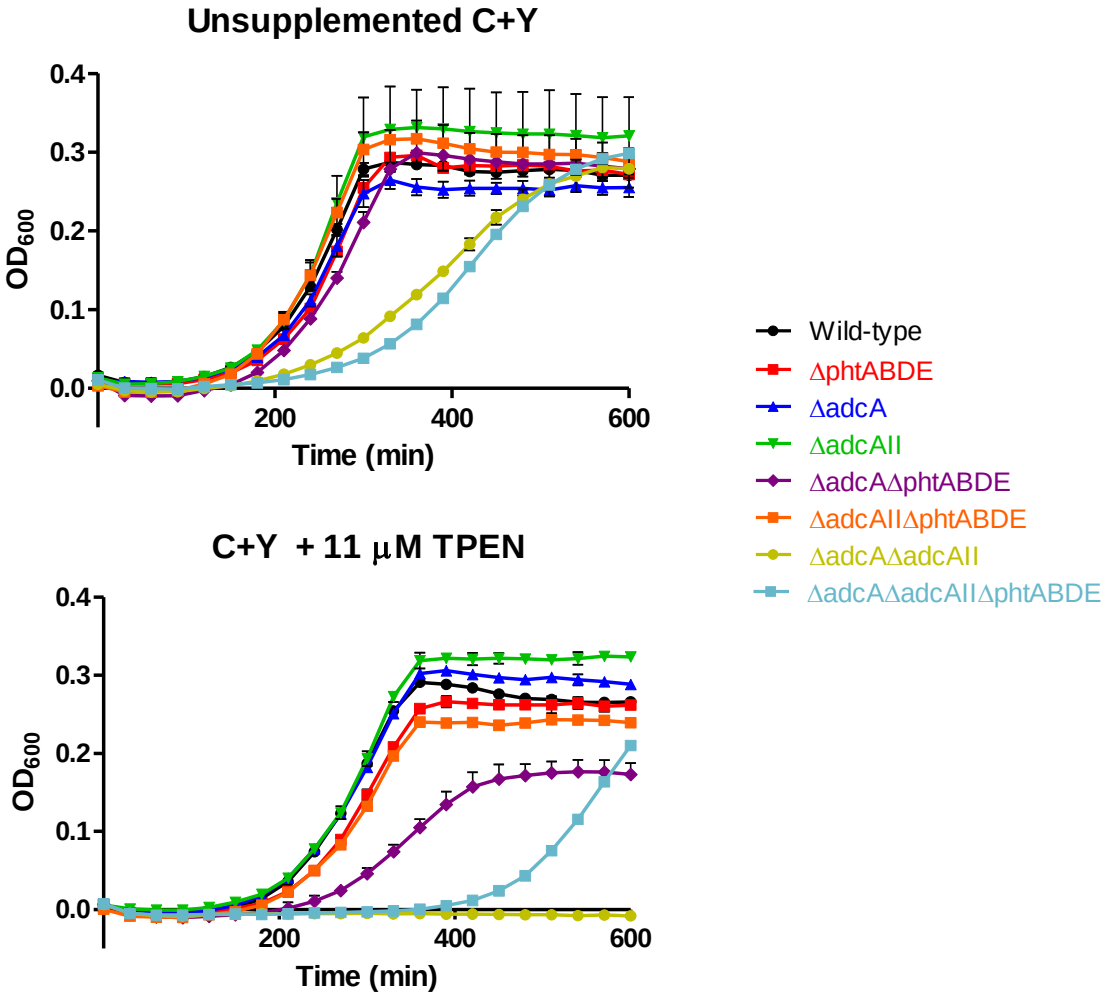

Figure 5.4: Growth curves of Δ*adc*Δ*phtABDE* combination mutants in C+Y supplemented with zinc or TPEN.

Equal CFU of wild-type and mutant strains were sub-cultured into 200 µl C+Y (either with or without 11 µM TPEN) in a 96 well tray. The bacteria were incubated at 37°C and growth was monitored via measurement of the OD_{600} every 30 min. Mean and standard error are plotted for duplicate samples for each curve. Results are representative of three independent experiments.

5.4 ICPMS analysis of Δ*adc* mutants

Given the growth defects of the Δ*adc* mutants, the intracellular accumulation of zinc in the various strains was examined by inductively-coupled plasma mass spectrometry as described in Section 2.14.2. For this analysis, bacteria were grown in C+Y supplemented with 20 μM zinc sulphate. Results are displayed in Figure 5.5. There were no differences in zinc accumulation between wild-type and either the Δ*adcA* or the Δ*adcAII* single mutants. However, the Δ*adcA*Δ*adcAII*, Δ*adcCBA* and Δ*adcAII*Δ*adcCBA* mutants all showed significantly less intracellular zinc than the wild-type. These results are consistent with the growth curves, in that the single mutants did not show significant defects whereas the latter three combination mutants did.

The concentrations of other metal ions were also measured in the samples at the same time as zinc. Interestingly, the Δ*adcCBA* and Δ*adcAII*Δ*adcCBA* mutants showed significantly elevated amounts of manganese compared to the other samples (see Figure 5.6). It was hypothesised that this might be explained by a difference in the expression of PsaA, the allocrite binding subunit of the major manganese import system of the pneumococcus (McAllister *et al*., 2004). To address this, bacterial lysates were prepared from the strains (grown under the same conditions as they were for the ICPMS analysis) and quantitative Western blotting with an anti-PsaA mouse serum was performed as described in Section 2.13. As shown in Figure 5.7, there were no differences in the level of PsaA expression between any of the strains.

The only other metal ion to show differences between strains in the ICPMS analysis was cobalt (see Figure 5.8). Co^{2+} levels were significantly elevated in the Δ*adcA*Δ*adcAII*, Δ*adcCBA* and Δ*adcAII*Δ*adcCBA* mutant strains. These are the same strains which showed decreased zinc content. Since they are starved of zinc, these strains are likely to have reduced levels of the metal ion efflux protein CzcD, the expression of which is known to be affected by both Zn^{2+} and Co^{2+} (Kloosterman *et al*., 2007). Less CzcD allows the pneumococci to retain more of their imported zinc, whilst another consequence is that less cobalt is exported, leading to its elevated levels seen in Figure 5.8.

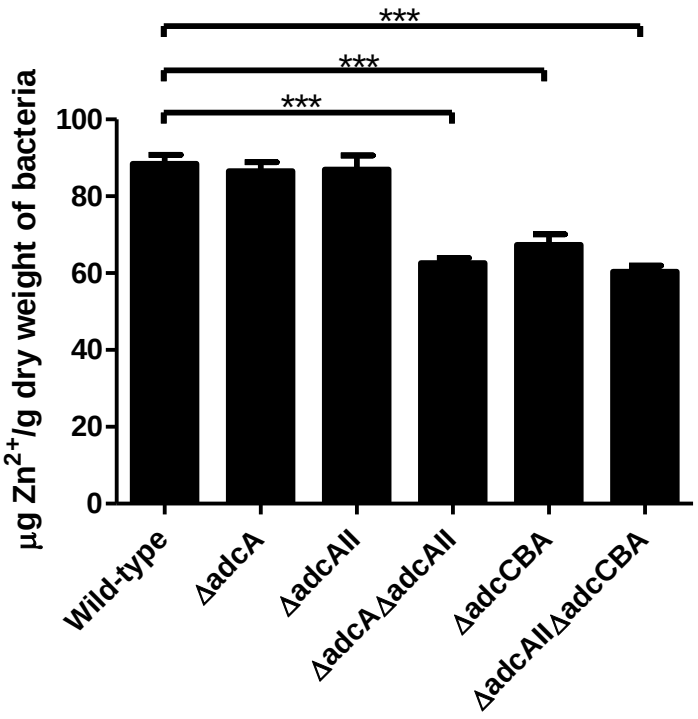

Figure 5.5: Zinc ion content of Δ*adc* mutants analysed by ICPMS.

Strains were grown in C+Y medium to OD_{600} 0.3. The bacteria were washed three times with PBS containing 5 mM EDTA, then twice with normal PBS. Zn^{2+} content was determined by ICPMS as described in Section 2.14.2. Results are normalised by dry weight of bacterial pellets and are presented as mean and standard error of data obtained from four biological replicate cultures of each strain. Where applicable, significant differences in the mean amounts of Zn^{2+} are shown as judged by two-tailed unpaired *t*-tests (***, $P < 0.001$).

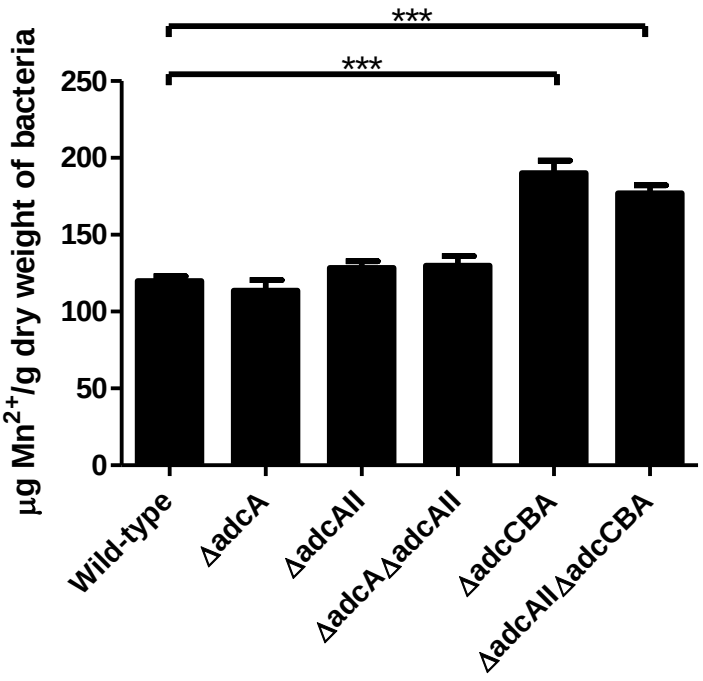

Figure 5.6: Manganese ion content of Δ*adc* mutants analysed by ICPMS.

Strains were grown in C+Y medium to OD_{600} 0.3. The bacteria were washed three times with PBS containing 5 mM EDTA, then twice with normal PBS. Mn^{2+} content was determined by ICPMS as described in Section 2.14.2. Results are normalised by dry weight of bacterial pellets and are presented as mean and standard error of data obtained from four biological replicate cultures of each strain. Where applicable, significant differences in the mean amounts of Mn^{2+} are shown as judged by two-tailed unpaired *t*-tests (***, P <0.001).

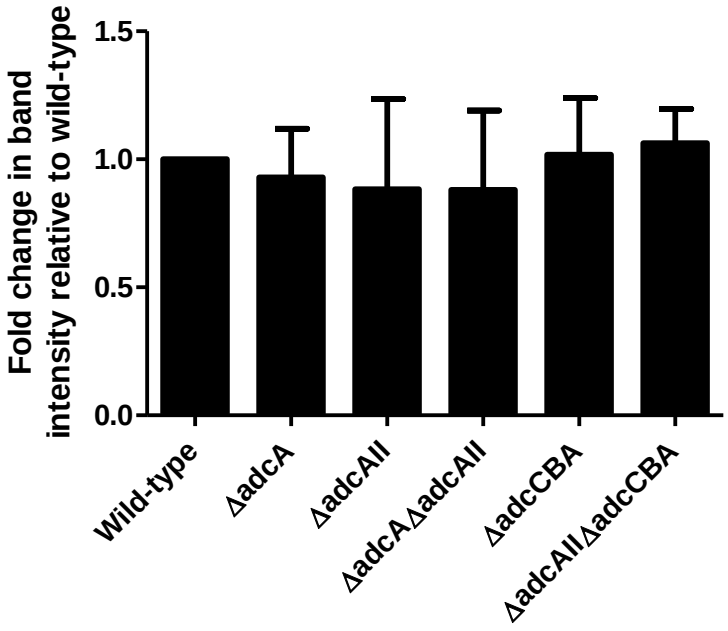

Figure 5.7: Expression levels of PsaA.

Bacterial strains were grown as for ICPMS analysis and cell lysates were prepared. The amount of PsaA was detected by quantitative Western blotting as described in Section 2.13. The results have been normalised to wild-type, and are presented as mean and standard error of data obtained from biological duplicate cultures.

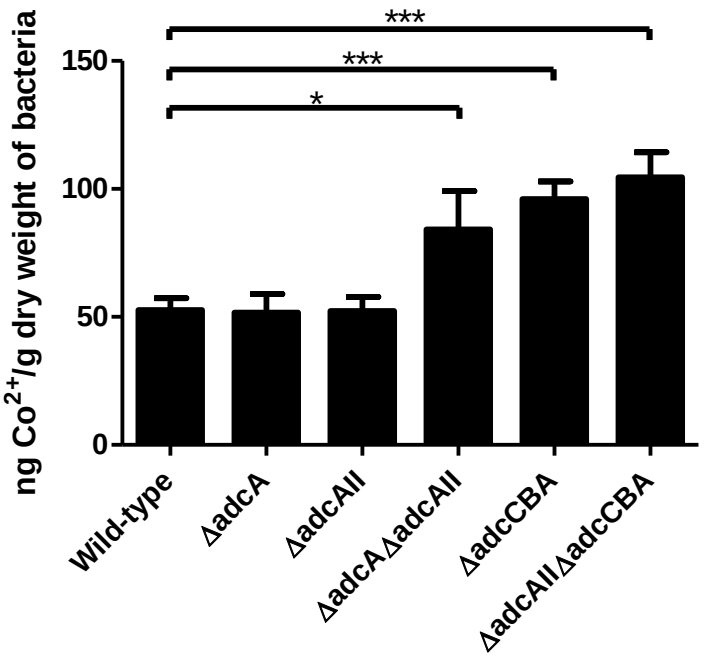

Figure 5.8: Cobalt ion content of Δ*adc* mutants analysed by ICPMS.

Strains were grown in C+Y medium to OD_{600} 0.3. The bacteria were washed three times with PBS containing 5 mM EDTA, then twice with normal PBS. Co^{2+} content was determined by ICPMS as described in Section 2.14.2. Results are normalised by dry weight of bacterial pellets and are presented as mean and standard error of data obtained from four biological replicate cultures of each strain. Where applicable, significant differences in the mean amounts of Co^{2+} are shown as judged by two-tailed unpaired *t*-tests (*, $P < 0.05$; ***, $P < 0.001$).

5.5 Virulence of Δ*adc* mutants in mouse models of pneumococcal disease

To investigate whether the defects in the mutants seen *in vitro* affect their phenotype *in vivo,* and in particular to probe the relationship and proposed redundancy between AdcA and AdcAII, the Δ*adcA,* Δ*adcAII* and Δ*adcA*Δ*adcAII* mutants were assessed in mouse models of pneumococcal disease. Given the *in vitro* data, it was hypothesised that the loss of either *adcA* or *adcAII* would not decrease invasiveness or virulence *in vivo*, but that the double mutant would be highly attenuated.

5.5.1 Pathogenesis of Δ*adc* mutants

To investigate possible niche-specific decreases in virulence of the mutants, an intranasal challenge model was used. Groups of ten mice were anaesthetised and challenged with ~10^7 CFU of wild-type, Δ*adcA*, Δ*adcAII* or Δ*adcA*Δ*adcAII* pneumococci intranasally. At 24 and 48 hour timepoints, mice were euthanised and bacteria were enumerated from nasal wash, blood, lungs and nasal tissue as described in Section 2.19.3. Results after 24 and 48 hours of infection are shown in Figure 5.9 and Figure 5.10 respectively.

After 24 hours, the three mutant strains were all attenuated compared to the wild-type in the nasal wash, nasal tissue and lungs; in the blood, the Δ*adcA*Δ*adcAII* strain was the only strain to be significantly attenuated. After 48 hours, the Δ*adcA* and Δ*adcAII* strains were not attenuated in any niches, except for Δ*adcA* in the lungs. In contrast, the Δ*adcA*Δ*adcAII* mutant was seriously and significantly attenuated in each niche. These results suggest that AdcA and AdcAII are not entirely functionally redundant *in vivo*, since each one appears to be required for full virulence during the first 24 hours after infection. However, the loss of both genes leads to a much greater decrease in bacterial fitness than the loss of just one. This is the case both for colonisation of the nasopharynx and for invasion into deeper tissues.

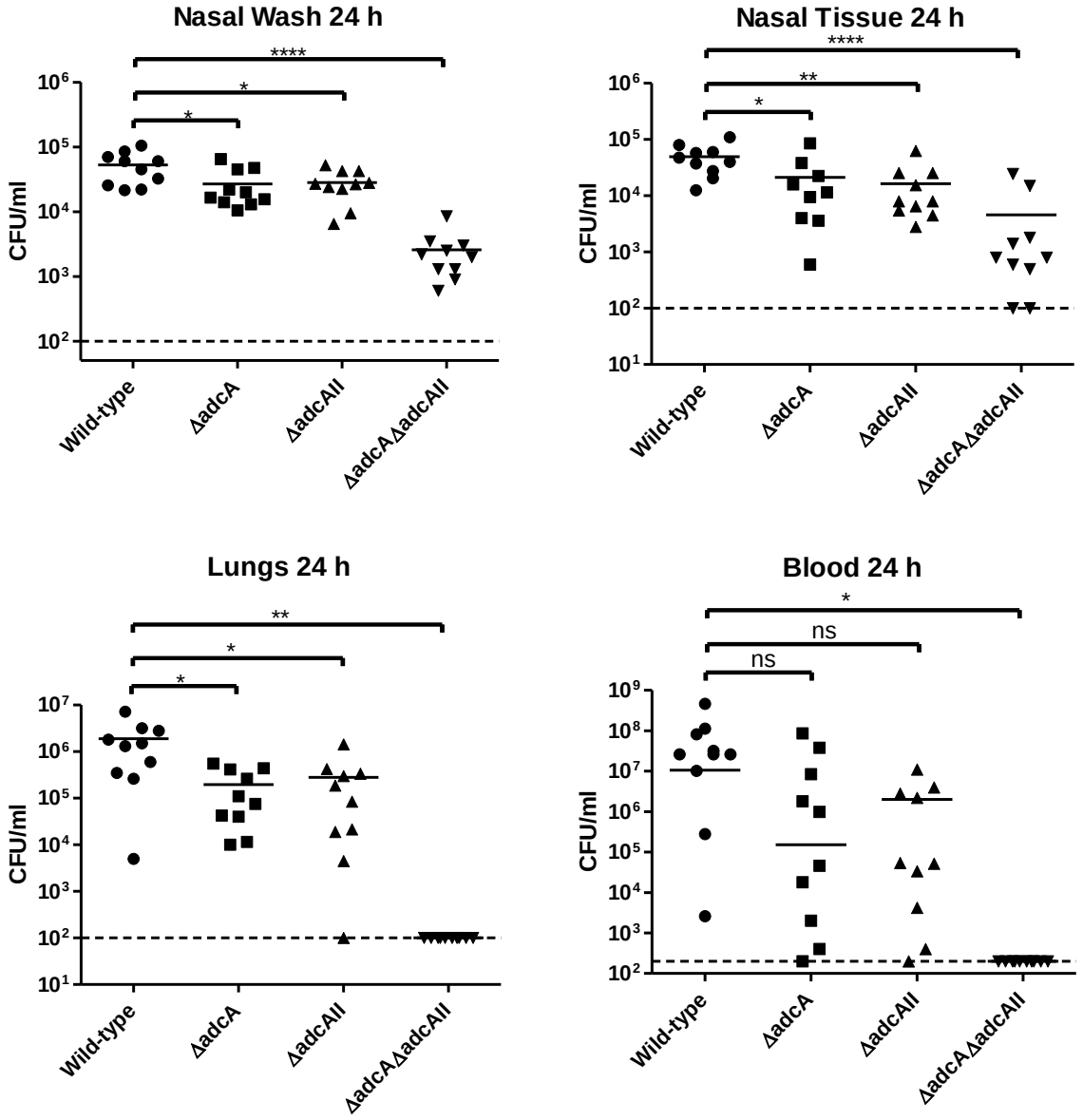

Figure 5.9: Numbers of pneumococci recovered from infected mice 24 h after challenge.

Groups of 10 mice were anaesthetised and challenged with ~10^7 CFU of the indicated strains via the intranasal route. The numbers of pneumococci in each niche after 24 h are plotted (one point represents one niche from one mouse). Solid lines denote geometric means of each group; dashed lines denote the limit of detection. Statistical differences from the wild-type are indicated, as assessed by unpaired one-tailed *t*-tests (ns, not significant; *, $P < 0.05$; **, $P < 0.01$; ****, $P < 0.0001$).

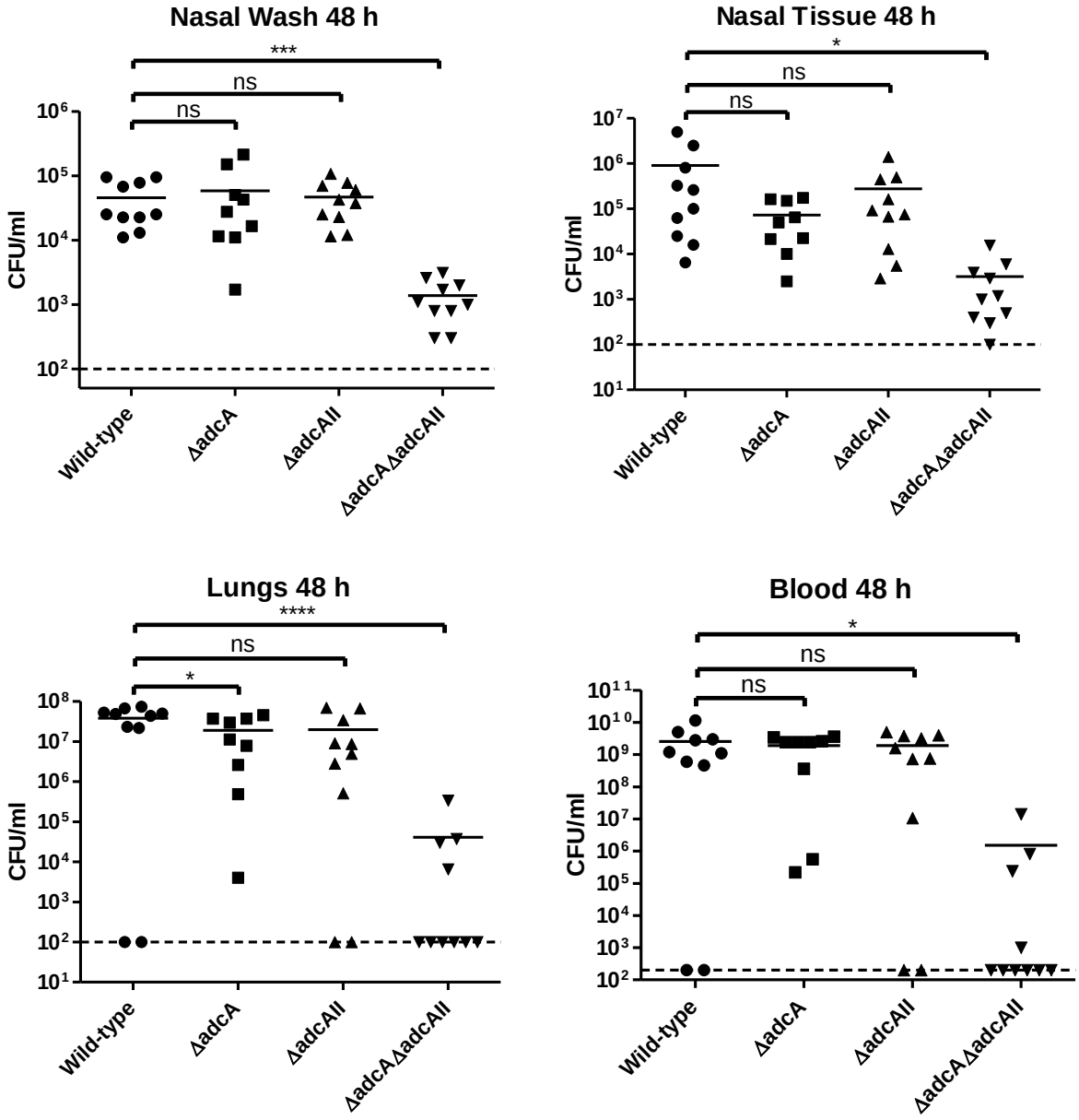

Figure 5.10: Numbers of pneumococci recovered from infected mice 48 h after challenge.

Groups of 10 mice were anaesthetised and challenged with ~10^7 CFU of the indicated strains via the intranasal route. The numbers of pneumococci in each niche after 48 h are plotted (one point represents one niche from one mouse). Solid lines denote geometric means of each group; dashed lines denote the limit of detection. Statistical differences from the wild-type are indicated, as assessed by unpaired one-tailed *t*-tests (ns, not significant; *, $P < 0.05$; **, $P < 0.01$; ****, $P < 0.0001$).

5.5.2 Virulence of Δ*adc* mutants after intranasal challenge

In order to assess whether there are also differences in the abilities of the mutant strains to cause fulminant disease, a virulence experiment was performed. Groups of 15 mice were infected intranasally with ~2 × 10^7 CFU of the same four strains as in the previous experiment, and survival times were recorded for up to two weeks after challenge. As can be seen in Figure 5.11, only one mouse infected with the Δ*adcA*Δ*adcAII* mutant died during the experiment, whereas none of the mice infected by wild-type survived beyond 72 hours. In contrast, the Δ*adcA* and Δ*adcAII* groups showed survival curves that were not significantly different to that of the wild-type group (comparison to wild-type using the log-rank Mantel-Cox test gives $P > 0.05$ in both cases). Therefore, loss of a*dcA* or a*dcAII* alone does not significantly affect pneumococcal virulence in this model, whereas loss of both causes a very large decrease in virulence.

5.5.3 *In vivo* competition between Δ*adcA* and Δ*adcAII* mutants

Lastly, *in vivo* competition between the Δ*adcA* and Δ*adcAII* mutants was assessed in order to see if there could be any small differences in fitness between the two mutants that might give a greater understanding of the relative importance of the two SBPs. For this experiment, ten mice were infected with a mixed culture of Δ*adcA* and Δ*adcAII* mutant strains. A sample of this mixed culture was diluted and spread on a blood agar plate; colonies from this plate were patched onto a blood agar plate containing chloramphenicol and a normal blood agar plate. Since only the Δ*adcA* mutant was resistant to chloramphenicol, this allowed the proportion of Δ*adcA* and Δ*adcAII* bacteria in the mixed culture to be calculated, which gave the input ratio. It should be noted that this experiment would usually be performed by plating a diluted sample of the mixed culture directly onto chloramphenicol- and normal blood agar plates, but in this case the Δ*adcA* mutant, which was confirmed to contain the chloramphenicol acetyl transferase gene in place of *adcA*, seemed unable to grow on the chloramphenicol-containing plates without being patched from a normal plate. This may be due to a lack of expression of the chloramphenicol resistance cassette when the bacteria are plated directly onto chloramphenicol blood agar plates from liquid culture, or only a small proportion of the bacteria expressing the resistance cassette at any one time.

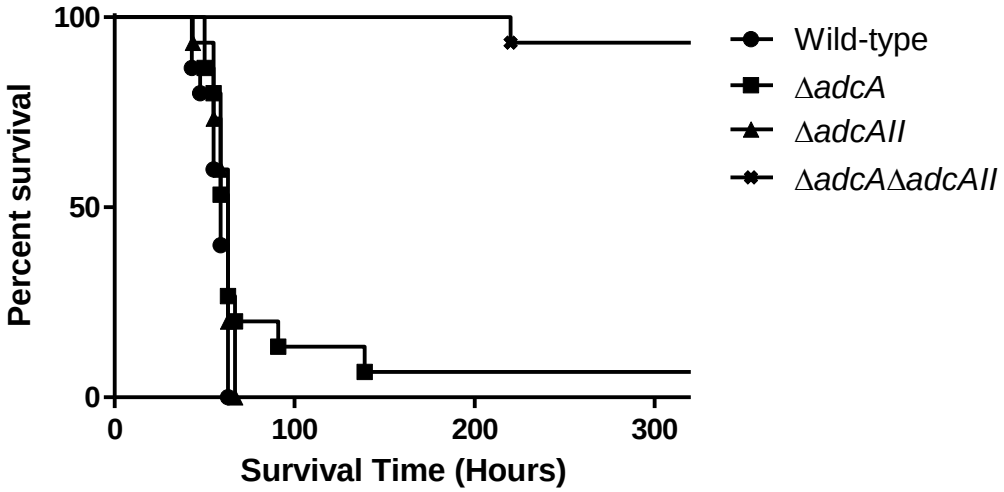

Figure 5.11: Survival times of mice after infection with wild-type and Δ*adc* mutant pneumococcal strains.

Groups of 15 mice were infected intranasally while anaesthetised with 2×10^7 CFU of the indicated strains. Mice were monitored and survival times were recorded over two weeks.

At 24 and 48 hours post-challenge, ten mice were euthanised and nasal wash, nasal tissue, lungs and blood were collected. Nasal tissue and lungs were homogenised in PBS; all samples were serially diluted and spotted onto blood agar plates. Colonies were patched onto chloramphenicol and normal blood agar plates to calculate the proportion of Δ*adcA* and Δ*adcAII* bacteria, as for the input ratio above. The competitive index (defined in this case as Δ*adcA* relative to Δ*adcAII*) for each niche for each mouse was calculated by dividing the relevant output ratio by the input ratio; the results of these calculations are shown in Figure 5.12. No bacterial colonies grew from a small number of samples, implying that the infection had been cleared from that mouse in that niche; in such cases the competitive index could not be calculated and so the sample was excluded. The results show that the Δ*adcA* mutant strain was marginally but significantly less competitive than the *ΔadcAII* strain after 24 h in the nasal wash, but was significantly more competitive after 48 h in the lungs and blood. This implies that the AdcAII protein could be slightly more important in allowing pneumococci to cause invasive disease over 48 h in this model.

5.6 Discussion

The work described in this chapter initially sought to examine whether AdcA and/or AdcAII could have a joint role with Pht proteins in terms of zinc homeostasis. This was suggested for AdcAII and PhtD by Loisel *et al.* (2011) on the basis of co-repression of transcription of the two genes by zinc, their apparent co-localisation at the bacterial surface, and their ability to be cross-linked *in vitro* (Loisel *et al*., 2011). These data, however, have been criticized, as described in Section 5.1. Experiments to provide evidence regarding the possibility of a joint function for Pht proteins and AdcAII were therefore required. Through the creation of mutant strains lacking *adcA, adcAII, adcCBA* or *phtABDE* genes, and combinations thereof, and testing the ability of these strains to grow in semi-synthetic medium with varying concentrations of zinc, it was concluded in Section 5.3 that Pht proteins may indeed support the function of AdcA and AdcAII in the import of zinc. This was shown by the superior growth of the Δ*adcA* and Δ*adcAII* single mutant strains compared to that of the Δ*adcA*Δ*phtABDE* and Δ*adcAII*Δ*phtABDE* combination mutants. However, this effect was only seen when almost all of the available zinc in the medium was chelated by TPEN. It is therefore not presently clear whether these observations are physiologically relevant, since the concentrations of bioavailable zinc that

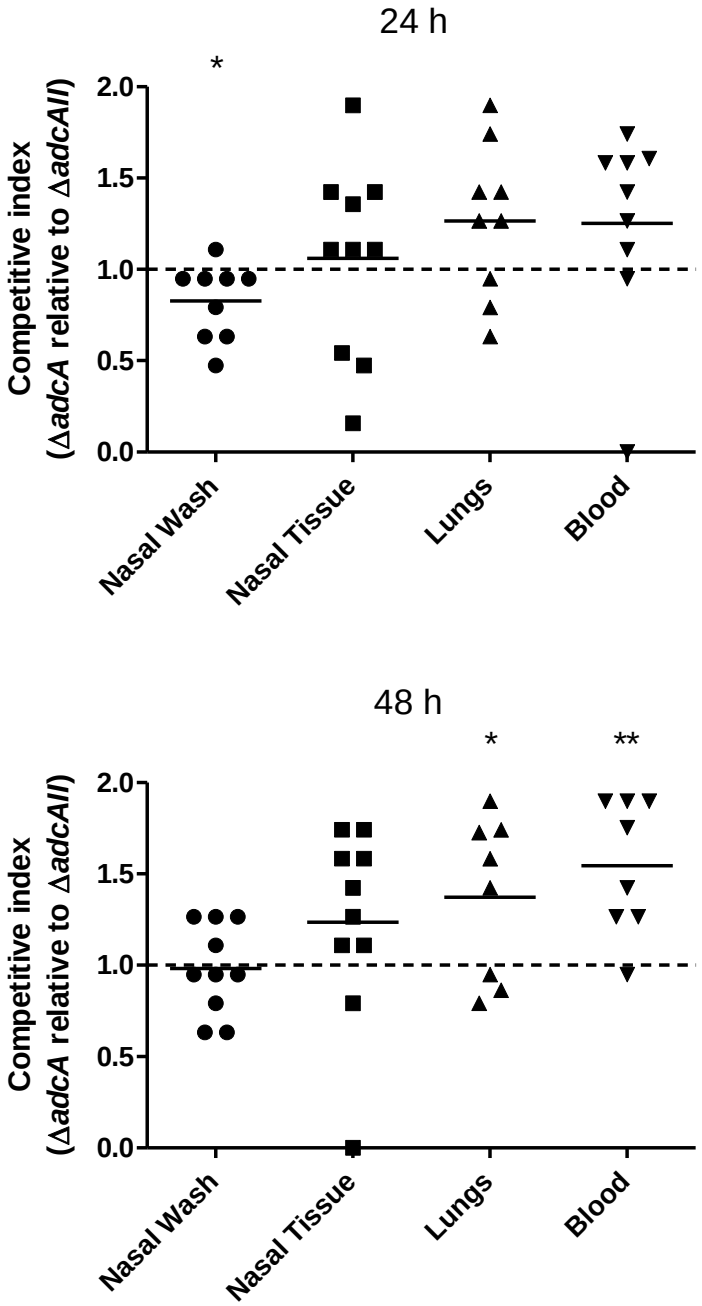

Figure 5.12: Competitive indices between Δ*adcA* and Δ*adcAII* mutants.

Anaesthetised mice were challenged intranasally with a mixed culture of Δ*adcA* and Δ*adcAII* mutant strains. After 24 and 48 h, ten mice were euthanised and bactetria enumerated from nasal wash, nasal tissue, lungs and blood. The mean competitive index for each niche was compared to a theoretical value of 1 (expected if there is no difference in fitness between the two strains) by two-tailed one-sample *t*-tests; significant differences are indicated where present (*, $P < 0.05$; **, $P < 0.01$).

pneumococci would encounter *in vivo* are not readily determinable, as discussed in Section 4.7. Nonetheless, we may speculate that the conservation of a high affinity zinc uptake system, indeed one with two SBPs (AdcA and AdcAII), amongst pneumococci implies that obtaining sufficient zinc is a challenge for the bacteria, most likely during initial colonisation.

A much clearer phenotypic difference in the growth curve experiments was found between wild-type and the Δ*adcA*Δ*adcAII*, Δ*adcCBA* and Δ*adcAII*Δ*adcCBA* strains. It was therefore decided that further experiments would focus on characterizing these mutants in order to gain an improved understanding of the roles and possible functional redundancy of AdcA and AdcAII. A later investigation could then build on this by including mutants lacking *pht* genes, but this could not be achieved within the timeframe of this project. Functional redundancy *in vitro* between AdcA and AdcAII is implied by the large impairment in growth of the Δ*adcA*Δ*adcAII* double mutant strain without zinc supplementation, compared to the lack of defects in the Δ*adcA* and Δ*adcAII* single mutants. Given the high homology of these proteins, this is perhaps unsurprising. Despite having an intact *adcAII* gene, the Δ*adcCBA* strain shares the same phenotype as the Δ*adcA*Δ*adcAII* strain. This implies that AdcAII requires AdcB and/or AdcC to be able to function; presumably, since AdcAII is an orphan SBP, it uses the AdcB transmembrane transport protein and AdcC nucleotide binding protein to form a functional ABC transporter capable of mediating the import of zinc. The results of the ICPMS analysis support these conclusions, since the same strains that were shown to require zinc supplementation for efficient growth accumulated significantly less intracellular zinc than the wild-type strain.

Interestingly, the ICPMS analysis also showed that the Δ*adcCBA* and Δ*adcII*Δ*adcCBA* strains accumulate more Mn^{2+} under the growth conditions used in the experiment compared to wild-type and other mutant strains. This effect appears to be specific to the loss of *adcB* and/or *adcC* rather than linked to the decreased ability to import zinc, as the Δ*adcA*Δ*adcAII* mutant did not show elevated manganese content. This could not be explained by differences in the level of PsaA expression. One possible hypothesis is that AdcBC and PsaBC compete for binding to PsaA, with only the interaction of manganese-loaded PsaA with PsaBC being productive for transport of the metal ion into the cell. In this model, loss of *adcBC* increases the chance of PsaA binding to its cognate transporter

PsaBC, increasing the efficiency of manganese import and leading to the elevated manganese levels observed here. This hypothesis could be further investigated by looking for structural features common to AdcA, AdcAII and PsaA that may allow them to all dock with AdcBC.

Having established that AdcA and AdcAII could act redundantly *in vitro,* the phenotypes of the Δ*adcA*, Δ*adcAII* and Δ*adcA*Δ*adcAII* mutants were assessed *in vivo*. Pathogenesis and virulence experiments showed that the double mutant was highly attenuated in its ability to survive in mice and to cause fulminant disease, whilst loss of *adcA* or *adcAII* alone had a smaller effect on the ability of the bacteria to survive and multiply during infection. These experiments therefore suggest that AdcA and AdcAII perform complementary roles *in vivo,* and are not entirely redundant.

A competition experiment between the Δ*adcA* and Δ*adcAII* mutant strains showed small but significant differences in the importance of these two genes for bacterial fitness in different niches at different times after infection. This is an interesting finding, since while AdcA and AdcAII are highly similar, there are two notable structural differences. Firstly, the flexible 15 amino acid loop region near the N terminus of AdcA is rich in histidine residues, whilst the loop region of AdcAII is not. It has been speculated that the histidine rich loop could help with the acquisition of zinc or could act to sense the environmental zinc concentration (Loisel *et al*., 2008). Secondly, AdcA contains a C-terminal domain with homology to ZinT, a protein that in Gram negative bacteria is free in the periplasm and contributes to zinc uptake via the ZnuABC system (Gabbianelli *et al*., 2011; Lim *et al*., 2011). AdcAII does not contain such a domain. It is interesting to speculate that the Pht proteins could fulfil an analogous role to ZinT in an initial acquisition of zinc from the environment, which raises the local concentration of the metal ion at the cell surface and facilitates its binding by AdcA and/or AdcAII. Given that AdcA contains a ZinT-like domain, we might expect AdcAII to be more dependent on the presence of the Pht proteins than AdcA to be able to acquire zinc. Indeed, the growth curve experiments support this interpretation (Figure 5.4), since the Δ*adcA*Δ*phtABDE* mutant was less able to grow when TPEN was present in the medium than the Δ*adcAII*Δ*phtABDE* mutant. That is, when the Pht proteins are absent, AdcA alone is better able to acquire zinc for the pneumococcus that when AdcAII is present alone. Another competition experiment

in the mouse model comparing the Δ*adcA*Δ*phtABDE* mutant with the Δ*adcAII*Δ*phtABDE* mutant would provide important evidence to further investigate this issue.

Since this work was carried out, related findings have been published by another group (Bayle *et al*., 2011). In this paper, it was shown through the use of a fluorescent zinc probe that Δ*adcA*, Δ*adcAII* and Δ*adcA*Δ*adcAII* mutant strains in the R6 background import zinc at slower rates than wild-type. Whilst the single mutants in the work presented in this chapter did not show delayed growth or lower total zinc accumulation, kinetic measurements of zinc import were not made, only 'endpoint' measurements of total zinc accumulation after several hours of growth. This difference in the type of experiment performed is likely to account for the finding of phenotypic differences between wild-type and the single mutants by Bayle *et al*, where none were found *in vitro* here. In the published study, AdcA and AdcAII were shown to mediate zinc import via AdcB, and loss of both SBPs affected pneumococcal morphology and cell division. Lastly, the Δ*adcA*Δ*adcAII* mutant was shown to be avirulent using colonisation, sepsis and pneumonia models of disease. The findings presented in this chapter are largely in agreement with results published by Bayle *et al*., although there are some differences in the interpretations. Bayle *et al.* conclude that AdcA and AdcAII are redundant, whereas from the data presented here it must be concluded that the proteins are complementary, since loss of either one decreased the efficiency of pneumococcal colonisation compared to wild-type.

Chapter 6: Vaccination using truncated derivatives of PhtA and PhtD

6.1 Introduction

Pht proteins are promising vaccine candidates for use against the pneumococcus. They have been demonstrated to confer protective immunity against pneumococcal disease in mouse models of nasopharyngeal and lung colonisation, pneumonia and sepsis, as well as in a rhesus macaque model of pneumonia (Adamou *et al*., 2001; Denoël *et al*., 2011b; Godfroid *et al*., 2011). PhtD has been the focus of the greatest attention since it is conserved in all strains tested to date (PhtA, B and E were found in 62%, 81% and 97% of strains respectively, out of 107 tested), shows little variability, and elicits protective immunity against pneumococcal colonisation that is superior to that of the other family members (Rioux *et al*., 2010; Godfroid *et al*., 2011).

At 110 kDa, PhtD is a relatively large surface protein, and is thought to be anchored to the surface via attachment to the cell wall (Loisel *et al*., 2011). It therefore seems highly likely that certain regions of PhtD, and indeed the other Pht proteins, will show a varying degree of exposure on the bacterial surface due to the orientation and topology of the protein and the presence of the capsule layer hindering access to certain regions. Flow cytometry experiments have indicated that regions of the Pht proteins at the C-termini are more exposed on the bacterial surface than the N-termini (Adamou *et al*., 2001; Hamel *et al*., 2004). Furthermore, immunisation with a fusion protein consisting of the C-termini of PhtB and PhtE was found to elicit an improved antibody response compared to when the individual truncated protein components were used to immunise mice (Hamel *et al*., 2004). However, this analysis was far from comprehensive and was not performed for PhtD, the most promising vaccine candidate of the family.

In order to increase understanding of the topology of Pht proteins as well as the contribution to vaccine efficacy of different regions of Pht proteins, a series of truncated derivatives of PhtA and PhtD were created and examined as detailed below.

6.2 Design of truncated derivatives

Primers with restriction endonuclease recognition sites incorporated were designed to amplify truncated derivatives of PhtA and PhtD lacking approximately 200 amino acids and multiples thereof from both the C- and N-termini. The first 57 nucleotides, which are predicted to encode the signal peptides of both proteins, were excluded from all constructs. In order to minimise potential disruption to overall protein structure, the exact positions of the truncations were designed to fall between protein domains as predicted by the Coils server (Lupas *et al*., 1991) (see Figure 6.1 and Figure 6.2 for the output for PhtA and PhtD respectively). The truncated derivatives that were constructed are listed in Table 6.1 and are represented diagrammatically in Figure 6.3.

6.3 Cloning, expression and purification of truncated derivatives

Truncated genes were amplified by PCR, digested, ligated into pQE plasmids [Qiagen] and transformed into *E. coli* BL21 (DE3) *lpxM*$^{-}$ as described in Section 2.5. Proteins were expressed and purified as described in Section 2.6. Truncated proteins are shown in Figure 6.4 (PhtA) and Figure 6.5 (PhtD); with the exception of PhtA C2, all were judged to be > 90% pure.

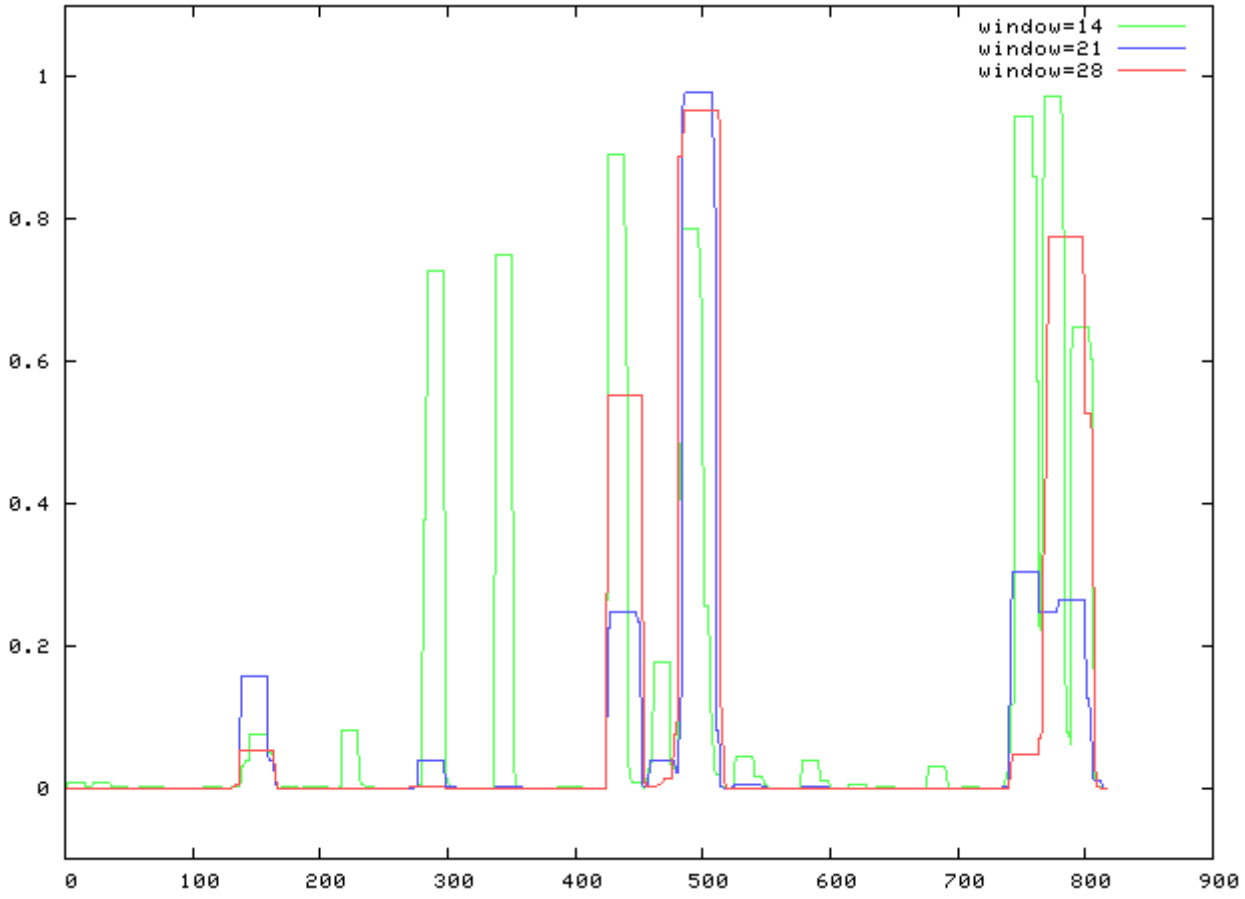

Figure 6.1: Coils prediction server output for PhtA.

The Coils server (http://embnet.vital-it.ch/software/COILS_form.html) was used to compare the amino acid sequence of PhtA to a database of proteins known to form coiled-coils to yield a prediction of which regions (if any) will fold in this conformation. The x-axis represents the position in the protein by amino acid number (starting at the N-terminus) and the y-axis shows how strongly that region is predicted to form a coiled coil. 'Window' refers to the width of the amino acid 'window' that is scanned at one time.

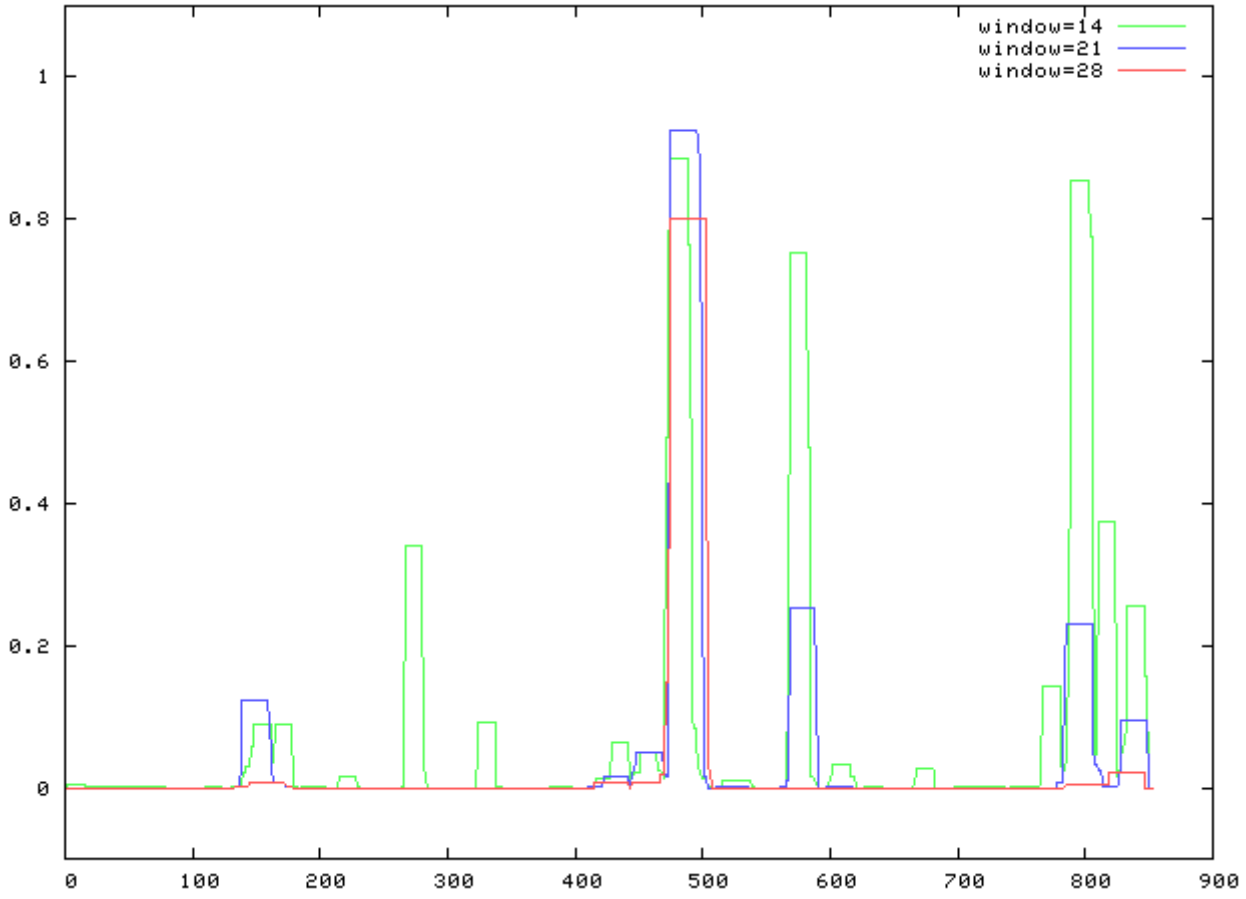

Figure 6.2: Coils prediction server output for PhtD.

The Coils server (http://embnet.vital-it.ch/software/COILS_form.html) was used to compare the amino acid sequence of PhtD to a database of proteins known to form coiled-coils to yield a prediction of which regions (if any) will fold in this conformation. The x-axis represents the position in the protein by amino acid number (starting at the N-terminus) and the y-axis shows how strongly that region is predicted to form a coiled coil. 'Window' refers to the width of the amino acid 'window' that is scanned at one time.

Table 6.1: List of starting and ending amino acids of PhtA and PhtD truncated derivatives.

Protein	Starting amino acid	Last amino acid
PhtA C1	Cys20	Ala616
PhtA C2	Cys20	Arg416
PhtA C3	Cys20	Pro216
PhtA C4	Cys20	Gly124
PhtA N1	Asp195	Asn816
PhtA N2	Val310	Asn816
PhtA N3	Asp542	Asn816
PhtA N4	Lys671	Asn816
PhtD C1	Cys20	Phe655
PhtD C2	Cys20	Ser445
PhtD C3	Cys20	Asn247
PhtD N1	Pro248	Gln853
PhtD N2	Asp446	Gln853
PhtD N3	Asp656	Gln853

Amino acids are shown using standard three letter codes. Numbers refer to the number of the amino acid in the parent protein (PhtA or PhtD). The full length PhtA protein has 816 amino acids, and the full length PhtD protein has 853. All purified Pht protein derivatives omit the putative N-terminal signal peptide (amino acids 1 - 19).

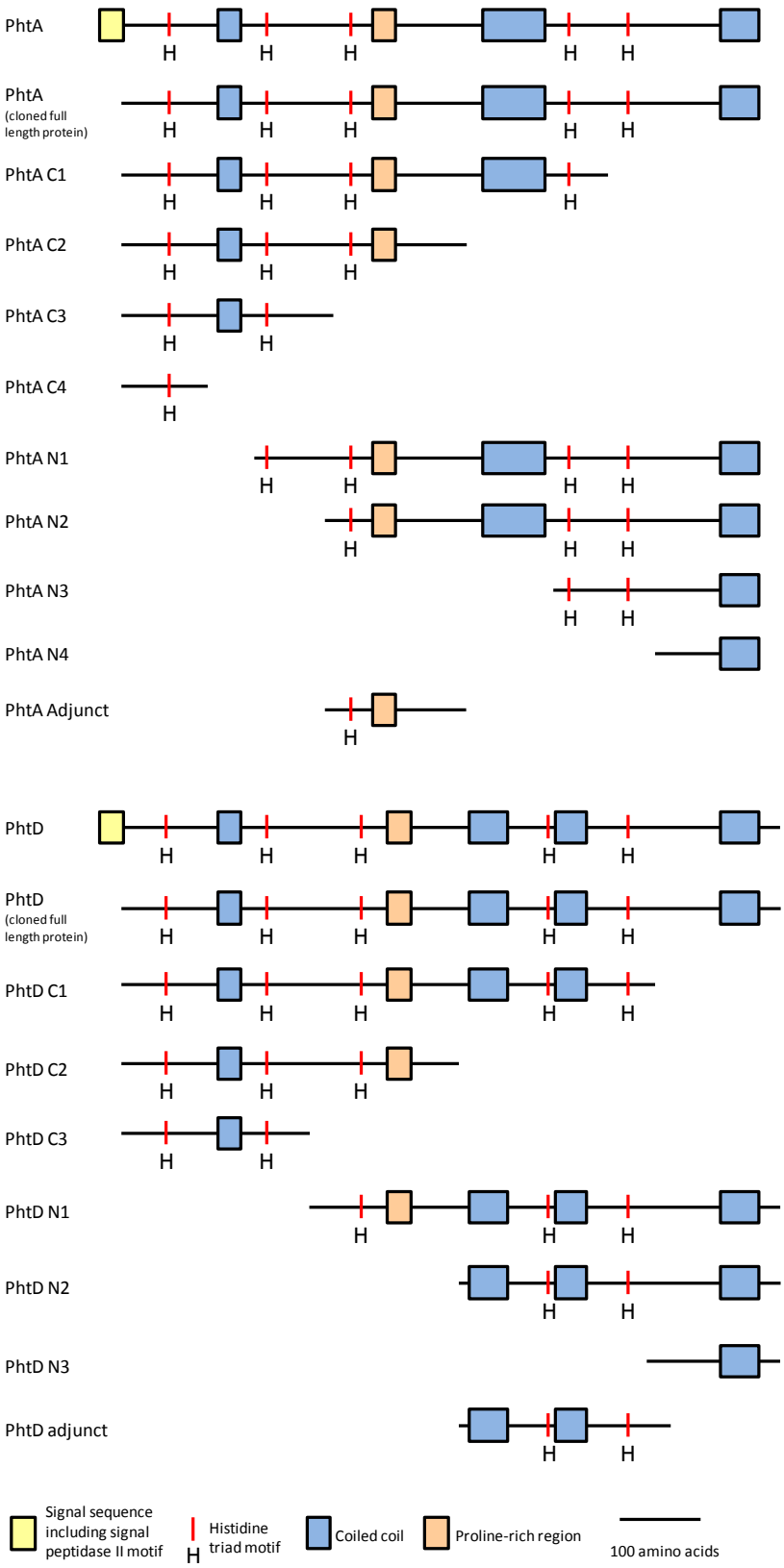

Figure 6.3: Truncated derivatives of PhtA and PhtD used in this study.

Diagrammatic representation of truncated derivatives of PhtA and PhtD cloned for expression and purification in this study. The N termini are to the left.

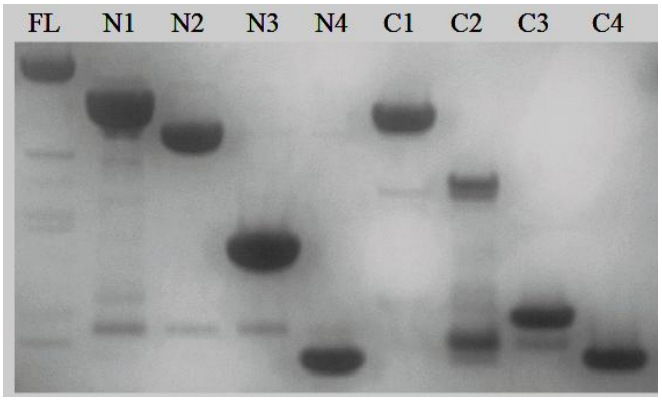

Figure 6.4: SDS-PAGE analysis of purified truncated derivatives of PhtA.

Truncated derivatives of PhtA were analysed by SDS-PAGE using a 12% acrylamide gel and subsequently stained using Coomassie R250. 1 µg of each protein was used. The identity of the protein is indicated above each lane (FL; full length).

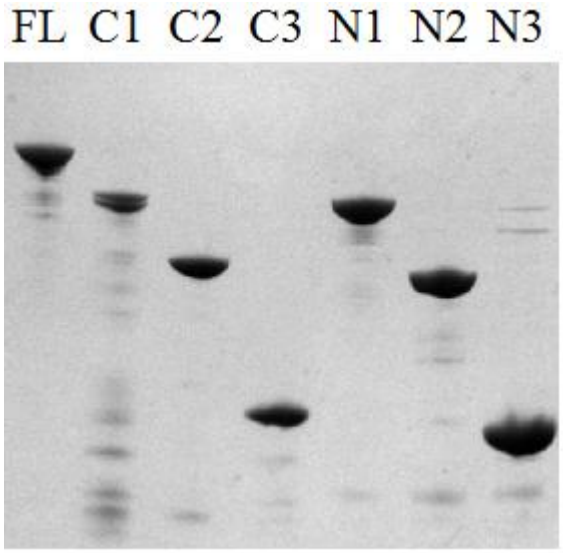

Figure 6.5: SDS-PAGE analysis of purified truncated derivatives of PhtD.

Truncated derivatives of PhtD were analysed by SDS-PAGE using a 12% acrylamide gel and subsequently stained using Coomassie R250. 1 µg of each protein was used. The identity of the protein is indicated above each lane (FL; full length).

6.4 Binding of antibodies to truncated derivatives of PhtA and PhtD

ELISAs were performed to examine the extent of binding of an antiserum to the truncated derivatives of PhtA and PhtD. Wells of the trays were coated with the full length proteins or truncated derivatives and various dilutions of polyclonal anti-PhtA or anti-PhtD sera were introduced. The antisera had been generated by immunizing mice three times with the relevant full length protein and collecting pooled serum, as described in Section 2.19.2. Results are shown in Figure 6.6 and Figure 6.7. The truncated derivatives can be grouped based on the ability of antibodies in the antisera to bind to them relative to the full length protein. For PhtA, C1, N1 and N2 show high binding (close to that observed for full length PhtA), C2 shows intermediate binding and C3, C4, N3 and N4 show low binding. Similarly for PhtD, C1, N1 and N2 show high binding whilst C2, C3 and N3 show markedly lower binding. Interestingly, the region of PhtD between Asp446 and Phe655 is common to C1, N1 and N2 (the high antibody binders) but is lacking in C2, C3 and N3 (the low antibody binders). These results are consistent with the region being highly immunogenic. A similar case can be made for the region of PhtA between Val310 and Arg416.

6.5 Design and antibody reactivity of the PhtA and PhtD adjunct regions

These regions of PhtA and PhtD (Val310 to Arg416 and Asp446 to Phe655 respectively, hereafter referred to as PhtA adjunct and PhtD adjunct), which appear to be particularly immunogenic, were therefore cloned, expressed and purified as for the other truncated derivatives. Antibody binding to the adjuncts was examined as for the truncated derivatives in Section 6.4. Results are shown in Figure 6.8. Antibody binding to the PhtD adjunct was as strong as to the full length protein; however, this was not the case for the PhtA adjunct, which was bound to a lesser extent that the full length PhtA.

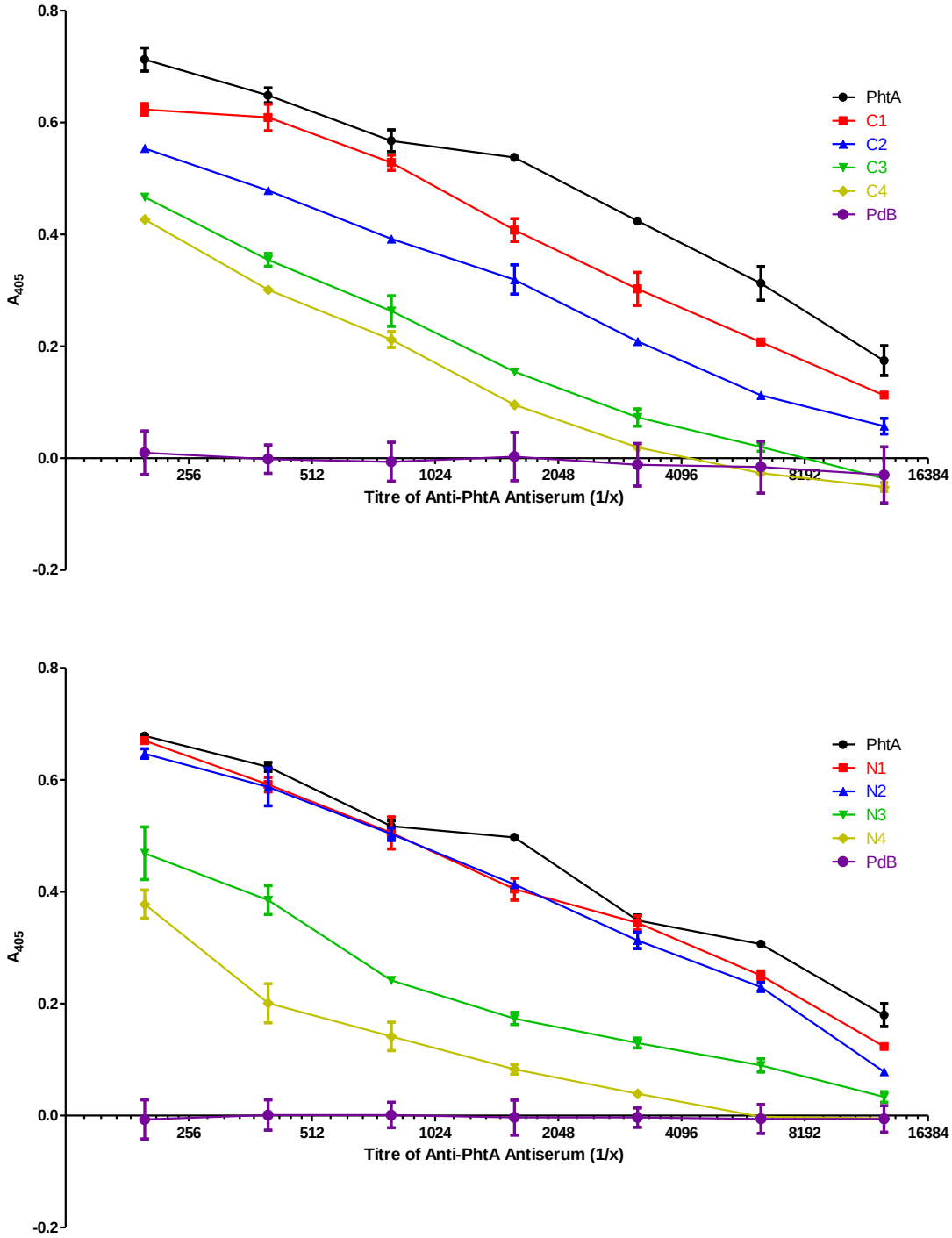

Figure 6.6: Binding of polyclonal anti-PhtA serum to PhtA and truncated derivatives.

ELISA examining binding of anti-PhtA serum to PhtA and truncated derivatives. Binding was detected by measuring the absorbance at 405 nm. PdB is an unrelated negative control protein (genetic toxoid derivative of pneumolysin) to which no binding is expected.

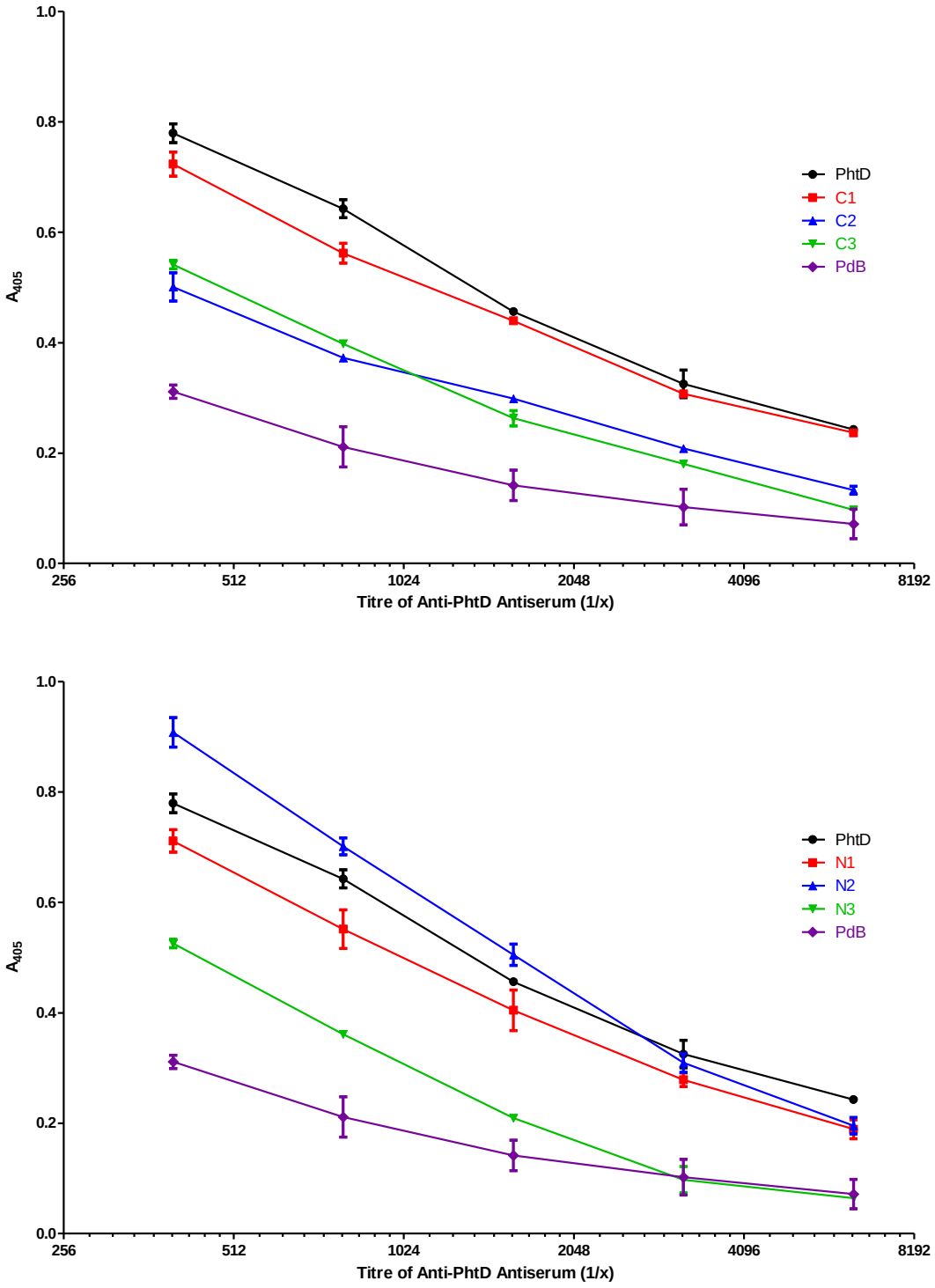

Figure 6.7: Binding of polyclonal anti-PhtD serum to PhtD and truncated derivatives.

ELISA examining binding of anti-PhtD serum to PhtD and truncated derivatives. Binding was detected by measuring the absorbance at 405 nm. PdB is an unrelated negative control protein (genetic toxoid derivative of pneumolysin) to which no binding is expected.

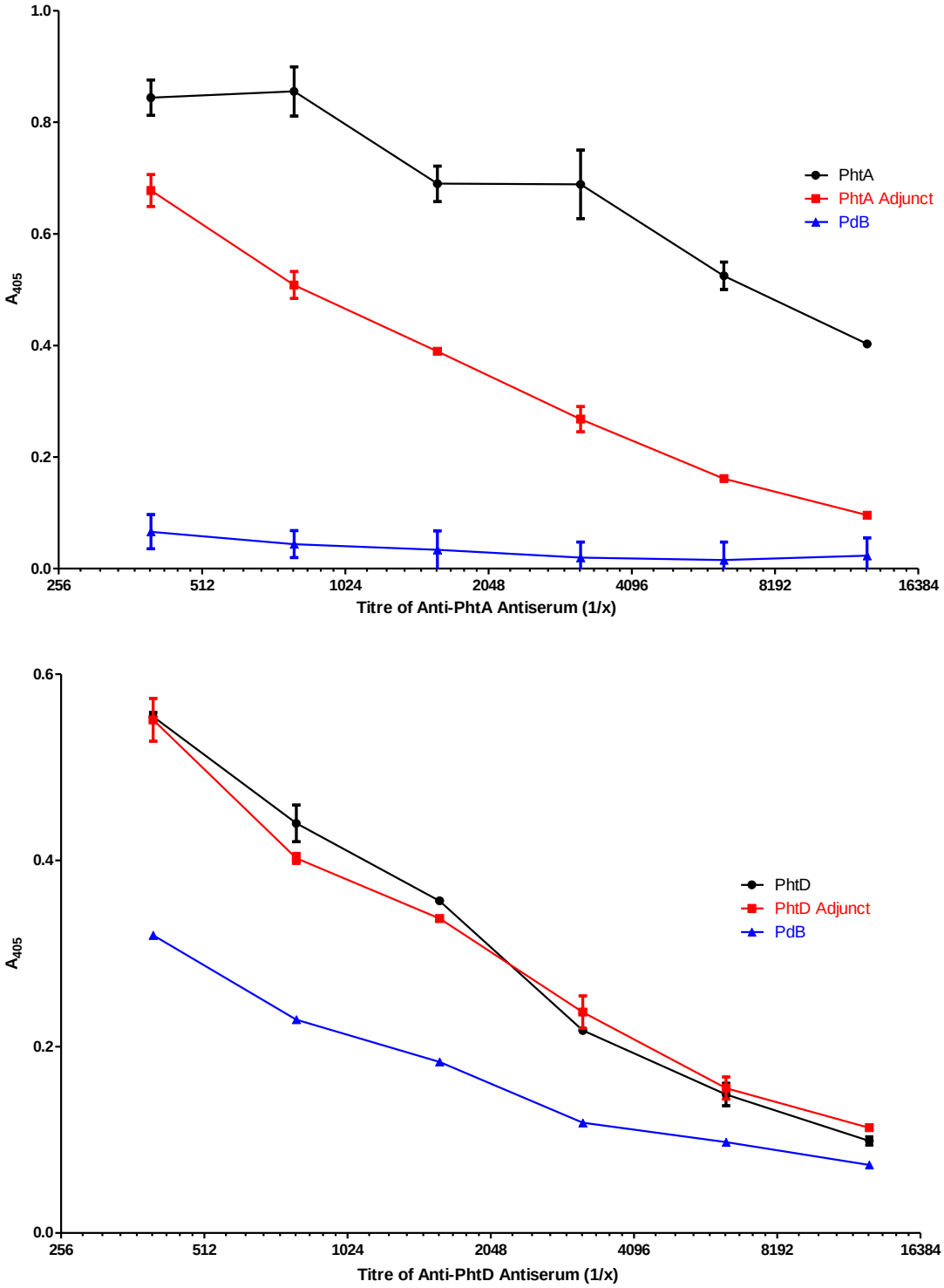

Figure 6.8: Binding of polyclonal antiserum to PhtA and PhtD adjuncts.

ELISA examining binding of anti-PhtA or anti-PhtD antiserum to respective full length proteins and adjuncts. Binding was detected by measuring the absorbance at 405 nm. PdB is an unrelated negative control protein (genetic toxoid derivative of pneumolysin) to which no binding is expected.

6.6 CD spectroscopy of truncated forms of PhtD

During the course of this project, observations that PhtD is more conserved and better able to elicit protective immunity in a nasopharyngeal colonisation model than PhtA, PhtB and PhtE were published (Godfroid *et al.*, 2011; Rioux *et al.*, 2010); furthermore, the PhtD adjunct showed stronger antibody binding than the PhtA adjunct, making it a more promising vaccine candidate. It was therefore decided that PhtD would be the main focus of the remaining experiments in this work. Circular dichroism spectroscopy was used to examine the truncated derivatives of PhtD and the full length protein. Data on absorbance in the ultraviolet spectrum were collected and analysed using the CDSSTR algorithm via DichroWeb (Compton and Johnson, 1986; Whitmore and Wallace, 2004, 2008). This was performed to determine whether the truncated derivatives were disordered in their secondary structural elements, or whether they were folded in a manner representative of the full length protein. Results showing the proportions of each protein predicted to be in alpha-helical, beta-strand, beta-turn or unordered conformations are shown in Table 6.2. All of the truncated derivatives were found to contain similar proportions in an unordered conformation as the full length protein, consistent with the proteins assuming a correctly folded structure. In addition, the results reveal that PhtD has a high proportion of α-helix in the C-terminal half of the protein, since PhtD N1, N2 and the PhtD adjunct had high proportions of this secondary structural element. This is in agreement with Figure 6.2, which also predicted a high degree of α-helical content (in the form of coiled-coils) in this region.

Table 6.2: Circular dichroism spectroscopy analysis of PhtD and truncated derivatives.

Protein	α-helix	β-strand	β-turn	Unordered
PhtD	0.36	0.18	0.18	0.28
PhtD C1	0.25	0.26	0.20	0.30
PhtD C2	0.20	0.26	0.21	0.33
PhtD C3	0.16	0.29	0.21	0.34
PhtD N1	0.49	0.09	0.17	0.25
PhtD N2	0.56	0.07	0.14	0.23
PhtD N3	0.44	0.11	0.20	0.26
PhtD Adjunct	0.51	0.18	0.13	0.18

Results are shown as proportions of each protein predicted to be folded in each of the indicated secondary structural conformations, or predicted to be unordered.

6.7 Immunisation with truncated derivatives of PhtA and PhtD

6.7.1 D39 sepsis model

Given that the PhtD adjunct protein bound a high amount of antibody from the polyclonal antiserum, it was of interest to determine whether it could induce protective immunity against systemic pneumococcal disease. Whilst the antibody binding capacity of the PhtA adjunct was not as great, it was also included in the experiment. Groups of 12 female Swiss mice were immunised with full length PhtA or PhtD, the adjunct proteins, or combinations thereof as described in Section 2.19.4. Control groups were immunised with adjuvant (Imject® Alum, Thermo Scientific) alone, a combination of all four full length Pht proteins, or a combination of PdT (a genetic toxoid derivative of pneumolysin), PspA and PspC (shown previously to be a highly effective combination by Ogunniyi *et al*. (2007)). Mice were challenged two weeks after the final immunisation with 5×10^4 wild-type pneumococci of strain D39, injected intraperitoneally. Survival times of the mice were measured and the results are shown in Figure 6.9. Only the groups given the PhtA adjunct or PhtD adjunct proteins individually, or the combination of PdT, PspA and PspC, showed significant increases in median survival time relative to that of the alum control group ($P < 0.05$ for adjunct proteins and $P < 0.001$ for the PdT, PspA and PspC combination; Mann-Whitney U tests, one-tailed). Titres of antibodies specific for each antigen in pooled sera from each group of mice were measured by ELISA and the results are shown in Table 6.3.

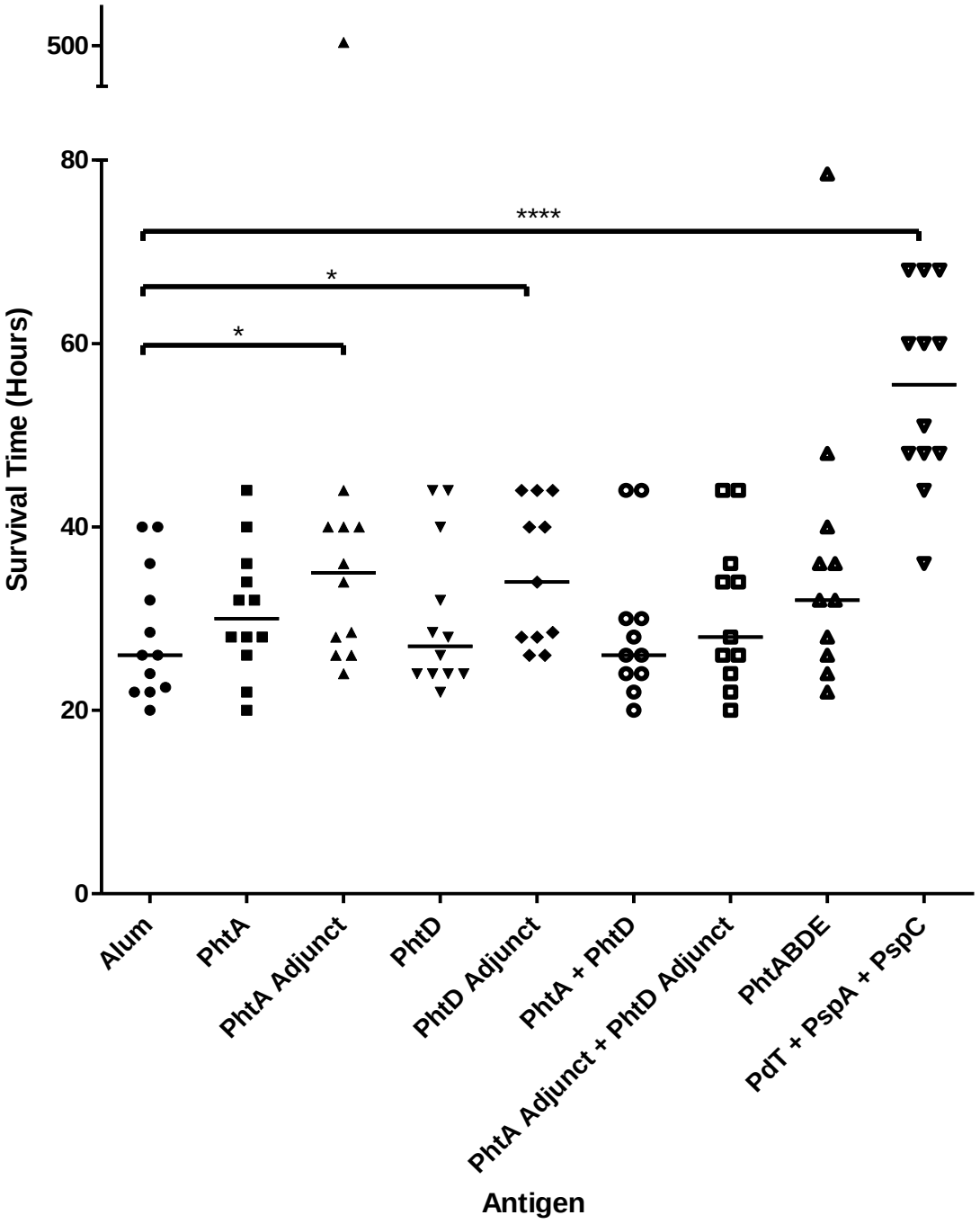

Figure 6.9: Survival times of mice challenged with D39 after immunisation with the indicated antigens.

Median survival time is indicated by horizontal lines. Significant differences from the alum only control group are indicated (*, $P < 0.05$; ***, $P < 0.001$); all other groups did not show a significant difference.

Table 6.3: Antibody titres of pooled sera from immunised mice before challenge with D39.

Mouse Group	Antigen	Titre
PhtA	PhtA	15,000
PhtA Adjunct	PhtA Adjunct	14,000
PhtD	PhtD	10,000
PhtD Adjunct	PhtD Adjunct	54,000
PhtA + PhtD	PhtA	29,000
PhtA + PhtD	PhtD	14,000
PhtA Adjunct + PhtD Adjunct	PhtA Adjunct	10,000
PhtA Adjunct + PhtD Adjunct	PhtD Adjunct	210,000
PhtABDE	PhtA	16,000
PhtABDE	PhtB	17,000
PhtABDE	PhtD	12,000
PhtABDE	PhtE	66,000
PdT + PspA + PspC	PdT	8,800
PdT + PspA + PspC	PspA	3,800
PdT + PspA + PspC	PspC	5,900

Antibody titres were measured via ELISA. Antigens were coated onto wells of a 96-well tray, and these were exposed to serial dilutions of the pooled mouse sera. Binding was detected using alkaline phosphatase-conjugated anti-mouse IgG secondary antibody and measurement of A_{405} after the addition of substrate. Titre was defined as the dilution of mouse serum giving half-maximal absorbance, and was rounded to two significant figures.

6.8 Immunisation with truncated derivatives of PhtD

6.8.1 D39 colonisation model

To further investigate the protective role of different regions of PhtD, protection against colonisation by *S. pneumoniae* was examined in another mouse model. Groups of eight mice were immunised three times via the intranasal route using 0.2 μg *E. coli* labile toxin B subunit (LTB) per dose as adjuvant. 10 μg of PhtD was given per dose; amounts of truncated derivatives of PhtD were adjusted such that equimolar quantities of these antigens to that of full-length PhtD were given. Control groups were immunised with adjuvant alone (negative control) or with adjuvant and PspA (positive control). Mice were subsequently challenged with 6.5×10^6 CFU of strain D39 intranasally under anaesthesia. After 96 hours, mice were euthanised and numbers of pneumococci in the nasopharynx were enumerated as described in Section 2.19.3. This model was chosen since immunisation with PhtD has previously been shown to significantly reduce pneumococcal colonisation under similar experimental conditions (Godfroid *et al*., 2011). Results are shown in Figure 6.10. A small number of mice died from invasive pneumococcal disease before the 96 hours had elapsed; results from these mice were excluded. Whilst modest differences in median CFU recovered can be seen between groups, statistical analysis (by Mann-Whitney U test) revealed that none of the groups were significantly different from the adjuvant alone negative control group. This includes the PhtD and PspA positive control groups, which was unexpected since these antigens have previously been shown to confer protective immunity in this model (Godfroid *et al*., 2011).

6.8.2 P9 sepsis model

Since PhtD and its truncated derivatives did not show any significant protection in the colonisation experiment of Section 6.8.1, a different model was required to evaluate the capacity of the antigens to act as a vaccine. A sepsis model using strain P9 was chosen due to the previously demonstrated ability of PhtD to confer protective immunity in sepsis models of infection (Adamou *et al*., 2001) and the clinical relevance of serotype 6A strains.

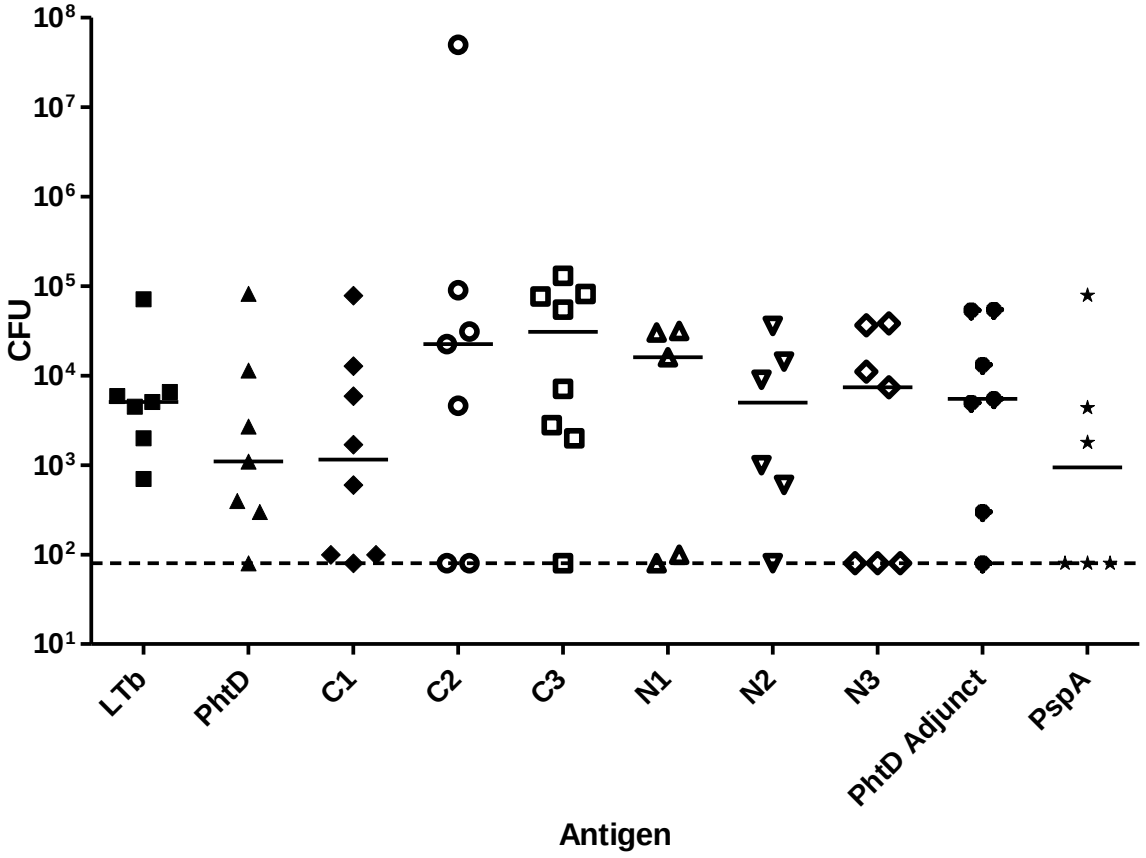

Figure 6.10: CFU of pneumococci recovered from the nasopharynges of vaccinated mice.

After three immunisations with the indicated antigens, mice were challenged intranasally with 6.5 × 10^6 CFU of wild-type D39 pneumococci. After 96 hours, pneumococci from the nasopharynx were enumerated. Median CFU recovered is indicated by the solid lines; the dashed line indicates the limit of detection.

First, the presence and immunological cross-reactivity of Pht proteins in this strain with Pht proteins of D39 were checked. Western blots were performed using whole-cell lysates of wild-type P9 and D39, as well as of a D39 Δ*phtABDE* mutant, with anti-PhtD or anti-PhtABDE (from animals immunised with a combination of all four Pht proteins) polyclonal murine sera. As shown in Figure 6.11, there were only small differences in the presence or reactivity of bands corresponding to Pht proteins between D39 and P9, implying that murine antibodies generated by immunisation with Pht proteins (which were cloned from D39) were likely to be able to bind P9 in the sepsis model. A band at around 80 kDa was detected in both Western blots; it is not clear whether this represents PhtA (which has a predicted molecular weight of approximately 92 kDa) or a partly degraded form of a full length Pht protein.

Flow cytometry using wild-type D39 and P9 strains showed that anti-PhtD and anti-PhtABDE sera actually bound more readily to P9 than to D39, as shown by a greater shift in fluorescence for P9 relative to the P9 negative control (normal mouse serum), compared to the shift for D39 samples relative to the D39 negative control. This suggested there was greater expression and/or exposure of PhtD on the surface of P9 than on D39, auguring well for antibody-mediated protective immunity (Figure 6.12).

Groups of 12 mice were therefore immunised with PhtD or equimolar amounts of truncated derivatives with Imject® Alum (Thermo Scientific) as the adjuvant. Further groups were immunised with alum alone (negative control) or PdT (positive control). Groups immunised with a combination of PhtD and PdT or PhtD adjunct and PdT were also included to assess whether these antigens could confer additive or synergistic protection. Survival times were recorded after intraperitoneal challenge with 2×10^5 CFU of wild-type P9. Data are shown in Figure 6.13. To confirm that an antibody response against the proteins had been induced, antibody titres of pooled sera (collected before challenge) from each group of mice were measured against the relevant protein(s) by ELISA, and these data are shown in Table 6.4. Whilst marginal increases in median survival time were observed for a number of groups, only groups immunised with PhtD N1, PdT, PhtD and PdT or PhtD adjunct and PdT showed statistically significant differences compared to that of the alum group. This implies that the N-terminal region of PhtD that PhtD N1 lacks is not needed for protection. Furthermore, not only was the full-length PhtD protein not effective in conferring significant protection on its own, it also did

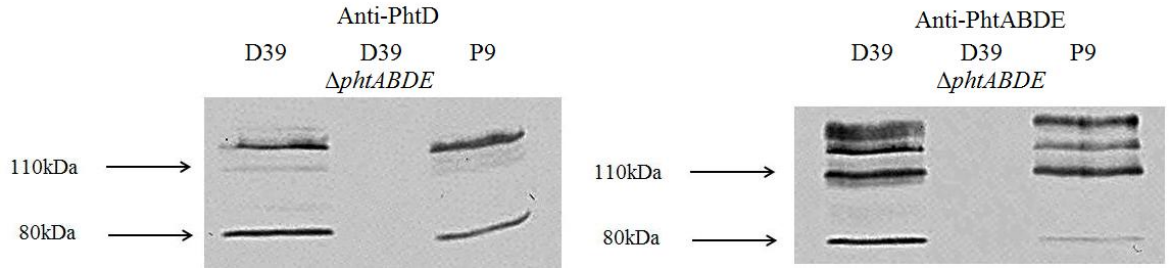

Figure 6.11: Expression of Pht proteins in D39 and P9.

Western blots were performed using pneumococcal cell lysates with anti-PhtD (left) or anti-PhtABDE (right) polyclonal sera. Mobilities of molecular size markers are indicated.

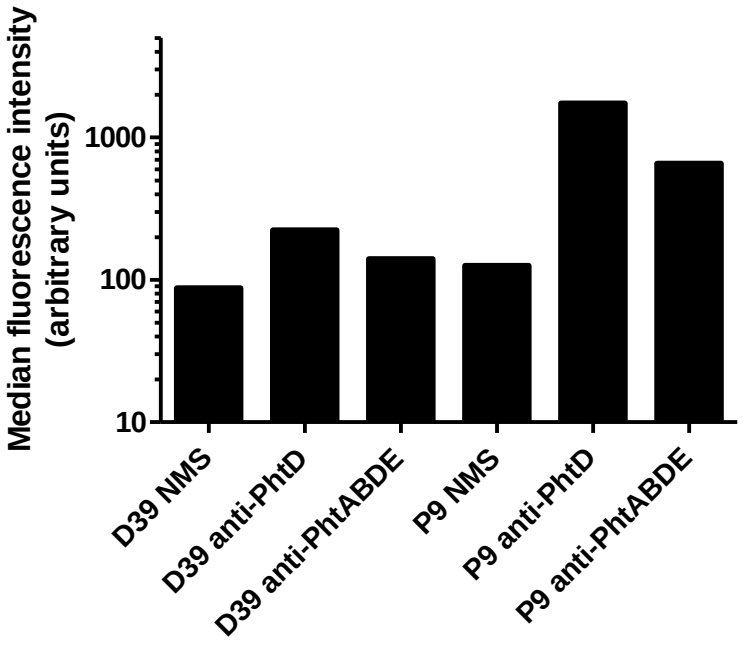

Figure 6.12: Surface exposure of Pht proteins on D39 and P9.

Wild-type D39 and P9 were incubated with normal mouse serum (NMS), anti-PhtD serum or anti-PhtABDE serum, followed by anti-mouse Alexa 488 secondary antibody. Fluorescence was measured by flow cytometry; median fluorescence intensities for 10000 events are displayed.

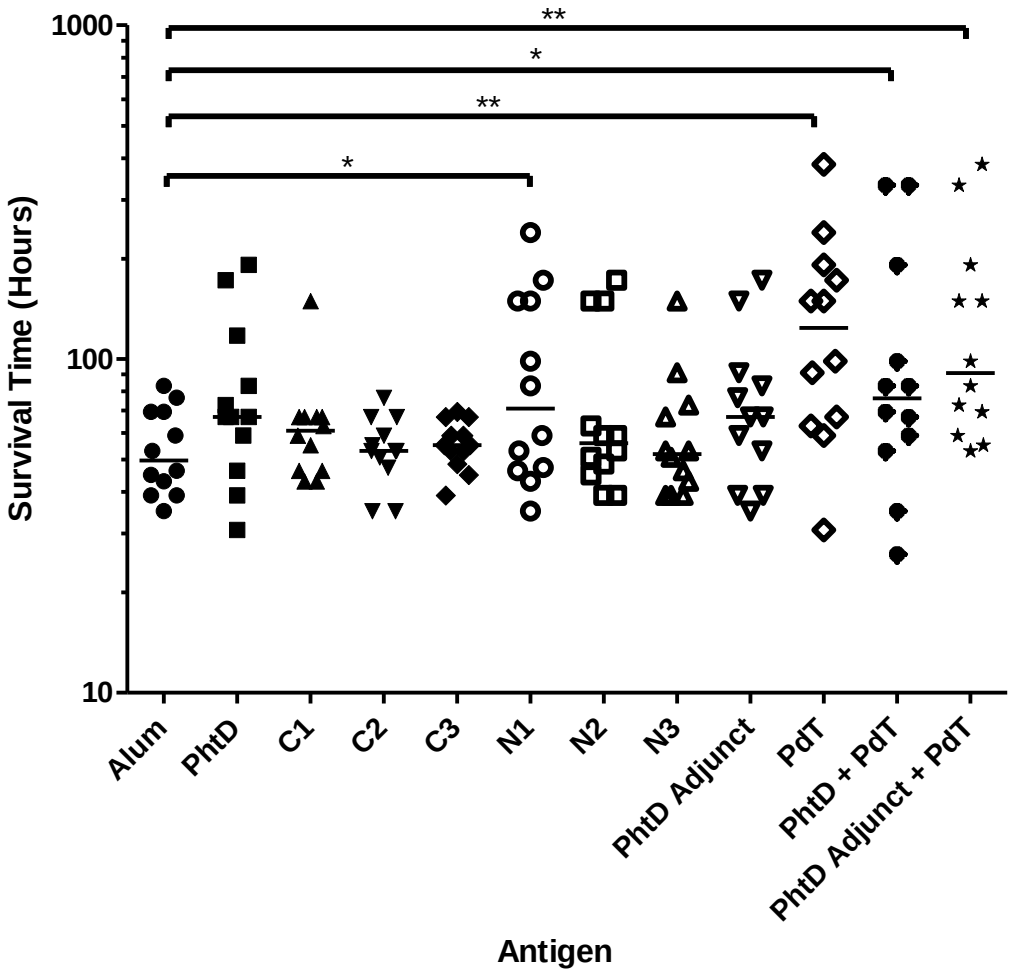

Figure 6.13: Survival times of mice challenged with P9 after immunisation with the indicated antigens.

Mice were immunised three times with alum as an adjuvant before challenge. The y-axis is displayed using a log scale. All groups were compared to the alum group using one-tailed Mann-Whitney tests; significant differences relative to the alum control group are indicated (*, $P < 0.05$; **, $P < 0.01$).

Table 6.4: Antibody titres of pooled sera from immunised mice before challenge with P9.

Mouse Group	Antigen	Titre
PhtD	PhtD	22,000
PhtD + PdT	PhtD	8,400
PhtD C1	PhtD C1	23,000
PhtD C2	PhtD C2	10,000
PhtD C3	PhtD C3	4,700
PhtD N1	PhtD N1	9,700
PhtD N2	PhtD N2	8,600
PhtD N3	PhtD N3	6,400
PhtD Adjunct	PhtD Adjunct	110,000
PhtD Adjunct + PdT	PhtD Adjunct	110,000
PdT	PdT	9,300
PhtD + PdT	PdT	10,000
PhtD Adjunct + PdT	PdT	8,900

Antibody titres were measured by ELISA. Antigens were coated onto wells of a 96 well tray, and these were exposed to serial dilutions of the pooled mouse sera. Binding was detected using alkaline phosphatase-conjugated anti-mouse IgG secondary antibody and measurement of A_{405} after the addition of substrate. Titre was defined as the dilution of mouse serum giving half-maximal absorbance.

not increase the survival time of mice immunised with PhtD and PdT, compared with PdT alone. The same was true of the PhtD adjunct. This is despite the induction of strong antibody responses (especially for the PhtD adjunct) as shown by the titres in Table 6.4. It was therefore concluded that PhtD is not a good candidate for a protein vaccine component in this model of pneumococcal disease, relative to PdT.

6.9 Discussion

In this chapter truncated derivatives of PhtA and PhtD were produced in order to assess the capacity of different regions of the proteins to interact with polyclonal antisera generated against the full length proteins. This allowed an evaluation of the immunogenicity of these regions independent of their level of exposure on the pneumococcal surface.

6.9.1 Secondary structural elements and immunogenicity of truncated proteins

CD spectroscopy was used to show that the PhtD truncated derivative proteins had a similar proportion of unordered regions to that of the full length protein, indicative of correct folding. In addition, the data showed a high level of alpha helix to be located in the C-terminal half of PhtD. This is in concordance with the prediction of coiled-coils being found in this region. The PhtD adjunct protein (Asp446 to Phe655 of the full length protein) was found to be highly immunogenic and to contain a large proportion of alpha helix, potentially in a coiled coil arrangement. It is encouraging that such a region should be so immunogenic, since it is also likely that an elongated structure such as a coiled coil would extend out from the pneumococcal surface and would therefore be exposed and available to be bound by antibodies *in vivo*. These two characteristics – immunogenicity and exposure on the surface – are critical for a successful vaccine antigen. As an aside, it is interesting to note that another leading protein vaccine candidate for the pneumococcus, PspA, also contains coiled-coil motifs that are thought to be immunogenic and exposed (McDaniel *et al*., 1994). This common structural feature may be necessary to allow these proteins to penetrate the capsule layer access the extracellular milieu in order to interact with host surfaces and/or carry out their respective functions, but could also be an ‘Achilles heel’ that could be exploited by vaccination. There is some apprehension that antibodies against the coiled-coil regions of PspA could be cross-reactive with cardiac

myosin, which also forms a coiled-coil structure. However, such concerns can be allayed somewhat by the fact that there are no known associations between pneumococcal infections and autoimmune conditions, even though the majority of adults have significant levels of antibodies to PspA in their serum (Briles and Hollingshead, 2006).

The data from the initial ELISAs were largely consistent with the antibody titre data from the D39 and P9 sepsis model experiments (see Table 6.3 and Table 6.4). These both showed that mice immunised with the PhtD adjunct developed a very high titre of IgG, showing that this region is indeed highly immunogenic. In the D39 experiment, equal masses of the full length and adjunct proteins were used to immunise the mice, whereas in the P9 experiment equimolar quantities were used. However, in both experiments the titres of sera from the mice immunised with the PhtD adjunct were greater than those of mice immunised with the full length protein, indicating that the quantity of protein used to immunise the mice may not have played a major role in determining the titre that was elicited.

6.9.2 Protective immunity elicited by immunisation with truncated proteins in D39 sepsis model

Immunisation with the PhtA or PhtD adjuncts elicited significant increases in median survival time of mice after challenge with D39, whereas immunisation with the respective full length proteins did not. Whilst it might be expected that the full length proteins would either be equal or superior to any truncated forms in terms of vaccine efficacy, since they contains all potential epitopes, this result could be explained by an effect of the dose of protein given. In this experiment, mice were immunised with 10 μg of each protein per dose, which implies that the dose of the adjunct proteins was approximately four-fold greater in molar terms than that of the full length proteins, due to the difference in molecular weight of the full length and adjunct proteins. Consistent with the ELISA data showing that the PhtD adjunct is immunodominant (a high proportion of antibodies in the polyclonal antiserum generated against the full length protein could bind to the PhtD adjunct), the titre of pooled mouse serum from the PhtD adjunct group against the adjunct protein was much greater than that of the PhtD group against the full length protein. This difference in the level of antibody in the mice could account for the increase in survival time, since antibodies against pneumococcal proteins are known to be a major correlate of

protective immunity against invasive disease (Ogunniyi *et al*., 2000; Malley and Anderson, 2012).

However, this line of reasoning cannot be used to explain the increased survival time of the PhtA adjunct group versus the PhtA group, since the antibody titres in this case were similar. Another unexpected outcome of this experiment was the lack of difference in median survival time of the group immunised with both adjuncts, when either adjunct given alone could increase survival time. A similar phenomenon whereby combinations of PhtB and/or PhtE with PspA and the pneumolysoid PdB did not give additive protection over the single antigens given alone has been reported previously (Ogunniyi *et al*., 2007). In this case, the only explanations that could be given were steric hindrance between antibody binding sites or an unknown mechanism(s). In a similar vein, it is unclear as to why a combination of the two adjunct proteins was not protective in this study.

6.9.3 Failure to elicit protective immunity in D39 colonisation and P9 sepsis models

Disappointingly, almost no protective effects were seen in either the D39 colonisation or the P9 sepsis models. The result of the former is particularly surprising given that Godfroid *et al.* (2011) showed that immunisation with PhtD decreases the bacterial load in the nasopharynx. The two experiments used the same adjuvant, immunisation schedule and challenge strain (D39). There were differences in the challenge dose (7×10^4 in the published study versus 6.5×10^6 here) and strain of mice (BALC/c versus CD1) used. BALB/c mice have been shown to be more resistant to pneumococcal infections than several other mouse strains, and this is associated with a more vigorous immune response (Kadioglu and Andrew, 2005). However, CD1 mice, which are outbred, were not tested in that study. Genetic differences between the two mouse strains giving rise to quantitatively different immune responses to the vaccine antigens and the bacteria may be responsible for the difference in vaccine efficacy seen by Godfroid *et al*. and in this study.

In the P9 sepsis model, PhtD N1 was the only PhtD derivative that significantly increased survival time compared to the alum control group. This confirms that critical immunogenic epitopes are not located at the N-terminus. However, it cannot be concluded that the PhtD N1 protein was actually more able to induce protective immunity than the full length protein or any truncated derivatives, since there were no statistically significant

differences in survival time between the N1 group and any of these other groups. Neither full-length PhtD nor any of the other truncated derivatives conferred significant protective effects compared to the alum control group. This is surprising, given that substantial IgG titres were generated against PhtD and its truncated derivatives, and *in vitro* PhtD was found to be highly accessible to antibodies on the surface of P9 as shown by flow cytometry. It is possible that Pht proteins make a lesser contribution to the pathogenicity of P9 than they do to other strains such as D39, which would mean that blockade of their function via antibody binding would have a lesser effect on the course of disease.

When combined with the pneumolysoid PdT, neither full-length PhtD nor the PhtD adjunct increased the median survival time compared to when PdT was given alone. As mentioned above, a similar absence of additive protection has previously been reported from attempts to combine PhtB and PhtE with PspA and PdB (Ogunniyi *et al*., 2007). In light of the results found here, it may be that none of the Pht proteins elicit additive or synergistic protection when combined with other antigens. It was concluded from these findings that PhtD is not an effective vaccine antigen, at least in the models examined in the present study. For this reason, it was decided that it was not ethically justifiable to continue to perform mouse experiments to try to gain further insight into which regions of PhtD are the most immunogenic. The results in this chapter have therefore identified a potentially important region in PhtD that is highly immunogenic and likely to be surface exposed, but have also cast doubt on the efficacy of PhtD as a vaccine candidate relative to other antigens such as pneumolysoids, PspA and PspC. If PhtD is to be investigated further as a vaccine candidate by other groups, the adjunct region should be considered as a replacement for the full length protein, given its potential to elicit superior antibody responses and protective immunity.

Chapter 7: Surface attachment of PhtD

7.1 Introduction

Targeting of prokaryotic proteins for insertion into the plasma membrane or cell wall layers generally depends upon the presence of a signal peptide in the protein, which directs the protein to the export machinery. In Gram positive bacteria, the major export pathway is thought to involve the signal recognition particle, which binds to the nascent protein's signal sequence and targets it to the Sec translocon, allowing the protein to pass through the cell membrane (Scott and Barnett, 2006). Whilst there are significant variations in the length and position of signal peptides of different proteins, they are generally between 15 and 50 amino acids long and are found at the N terminus. Their characteristic features include a polar region of net positive charge followed by a hydrophobic core and another polar region. Once the protein has been exported via the general secretory (Sec) pathway described above, the signal peptide is cleaved off at the latter polar region. This is mediated by either a type I or a type II signal peptidase, resulting in a mature protein which may be secreted or attached to the cell membrane or cell wall by further modifications (Martoglio and Dobberstein, 1998; Hedge and Bernstein, 2006). In *S. pneumoniae*, such further modifications may be the addition of an *N*-acyl diacylglyceryl group, which anchors the protein to the cell membrane, or the covalent attachment of the protein to the cell wall by a sortase enzyme. A further group of surface proteins are not chemically altered after secretion but contain a conserved choline binding domain, which attaches the protein to phosphorylcholine moieties in the cell wall teichoic acid or membrane lipoteichoic acid by non-covalent attractions (Pérez-Dorado *et al*., 2012).

The Pht proteins were initially discovered via a genomic search for proteins with signal sequences and motifs indicative of attachment to the cell surface, and a number of flow cytometry studies have confirmed that the proteins are surface exposed (Adamou *et al*., 2001; Wizemann *et al*., 2001; Zhang *et al*., 2001; Reid *et al*., 2003). It is assumed that the proteins make use of the Sec pathway to traverse the cell membrane, but this has not been experimentally verified. Despite containing a type II signal peptidase motif (LxxC) which typically leads to the addition of an *N*-acyl diacylglyceryl group to anchor the protein in the cell membrane, the Pht proteins are not lipoproteins (they are not labelled by ^{3}H-

palmitate), but instead are embedded in the cell wall (Adamou *et al*., 2001; Hamel *et al*., 2004; Loisel *et al*., 2011). The mechanism of attachment is not clear, since they do not contain a C-terminal LPxTG motif characteristic of sortase-dependent anchoring (Paterson and Mitchell, 2004), nor a choline-binding domain, which is the only other mode of cell wall attachment known to be employed by pneumococcal proteins. An investigation into which region(s) of the Pht proteins are required for attachment to the surface was therefore undertaken, using PhtD as a model for the family.

7.2 Signal peptide prediction for PhtD

As a starting point for further experiments, bioinformatic software was used to predict which regions of PhtD could be acting as a signal peptide. The amino acid sequence of PhtD from strain D39 (SPD_0889 from the Kyoto Encyclopaedia of Genes and Genomes) was analysed using the SignalP and LipoP programs, available online at http://www.cbs.dtu.dk/services/ (Juncker *et al*., 2003; Petersen *et al*., 2011). The N terminal region of the protein was predicted to encode a signal peptide by SignalP, albeit somewhat weakly and without a single, confidently predicted type I signal peptidase cleavage site (see Figure 7.1). The output for LipoP (Figure 7.2), shows a strong prediction of a type II signal peptidase cleavage site at amino acid 20, corresponding to the LxxC motif that is known to be non-functional in making PhtD a lipoprotein (Adamou *et al*., 2001). A number of weak potential type I signal peptidase cleavage sites were also predicted. From these analyses, it appears that PhtD has an atypical signal peptide region, since neither program could confidently or accurately predict the signal peptide and cleavage site.

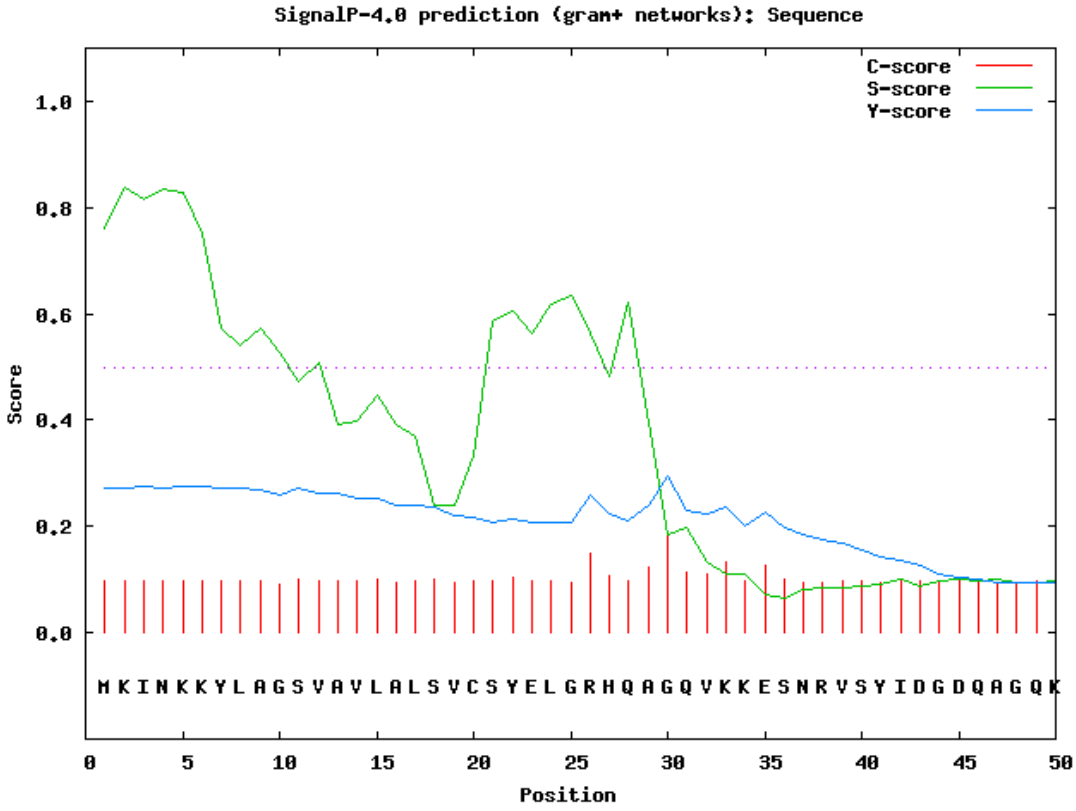

Figure 7.1: SignalP output for PhtD.

The amino acid sequence of PhtD was analysed with SignalP (available online at http://www.cbs.dtu.dk/services/SignalP-4.0/). The S-score (green) is high for amino acids predicted to be part of the signal peptide and low for amino acids predicted to be in the mature protein. The C-score (red) indicates the prediction of any type I signal peptidase cleavage site. The Y-score (blue) is a derivative of the S- and C-scores, in theory giving better prediction of the cleavage site. Thus for PhtD, the SignalP program predicts that the first 30 amino acids form the signal peptide, with a type I signal peptidase cleavage site between A29 and G30. However, the predictions have relatively low scores. Only the first 50 amino acids are shown, since the rest of the protein was not predicted to contain any regions which could act as a signal peptide.

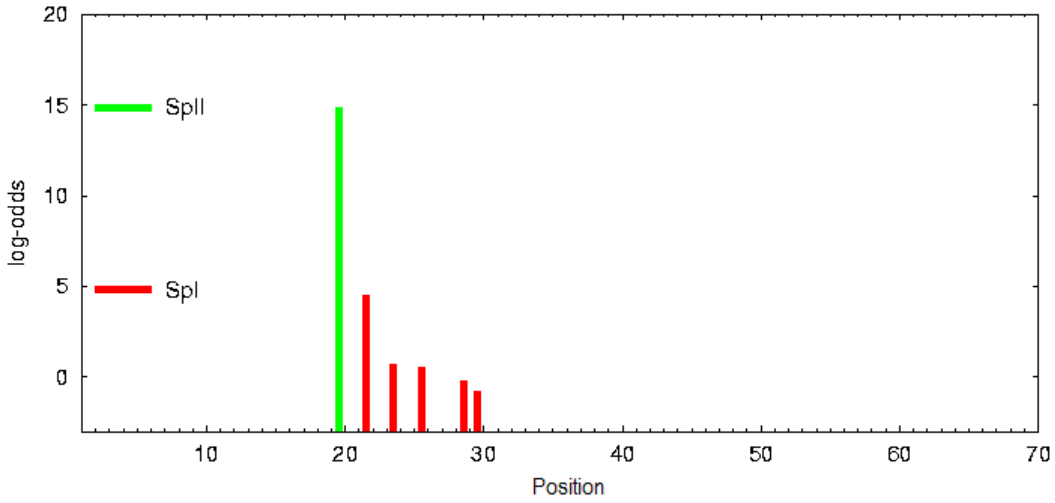

Figure 7.2: LipoP output for PhtD.

The amino acid sequence of PhtD was analysed with LipoP (available online at http://www.cbs.dtu.dk/services/LipoP/). The green bar represents a predicted type II signal peptidase cleavage site, whilst the red bars indicate predicted type I signal peptidase cleavage sites, with the height of the bar indicating the confidence of the prediction. Beyond amino acid 70, no other sites were predicted to encode cleavage sites.

7.3 Construction of Δ*phtABDE* strains complemented with altered forms of *phtD*

To assess which region(s) of PhtD mediate attachment to the cell surface, the Δ*phtABDE* strain was complemented with altered forms of *phtD* that lacked nucleotide sequences of interest. This was done in the Δ*phtABDE* mutant strain background rather than just a Δ*phtD* mutant to ensure subsequent Western blotting and flow cytometry experiments using anti-PhtD murine serum did not detect a signal due to the presence of the other Pht proteins with which the antiserum may cross-react. The procedure used for creating the mutant strains is explained in Figure 7.3. Primers were designed to amplify two regions: the first, using primer F and primer X, started approximately 2 kb upstream of *phtD* and ended within the gene, whilst the second, using primer Y and primer R, started within the gene and extended around 2 kb downstream. The positions of primers X and Y could be varied to create mutants lacking different regions of *phtD*. Primer Y contained an overhanging region complementary to primer X, allowing fusion of the two PCR products by an overlap extension PCR reaction. This product was then used to transform Δ*phtABDE* bacteria, in which the *phtD* locus has been replaced by a tetracycline resistance gene, as described in Section 2.5.2. By screening transformants for sensitivity to tetracycline, bacteria in which the *phtD* construct had replaced the *tetM* gene were identified; mutants were then confirmed by DNA sequencing.

7.4 Deletion of amino acid stretches causing loss of surface attachment of PhtD

The first mutant strain created by this procedure lacked amino acids S40 to P95 (inclusive) and was referred to as ‘N50’ since it lacked 50 amino acids near the N-terminus. Amino acids near the N terminus were chosen to be deleted because previous evidence suggested that the C-terminal end of the Pht proteins is more exposed on the pneumococcal surface, indicating that attachment is likely to be mediated at or near the N-terminus (Hamel *et al*., 2004 and Chapter 6 of this thesis). Since the signal peptide and cleavage site could not be accurately predicted, the deletion was designed to start significantly downstream of amino acid G30, which was the best guess for the cleavage site, to ensure that the signal peptide

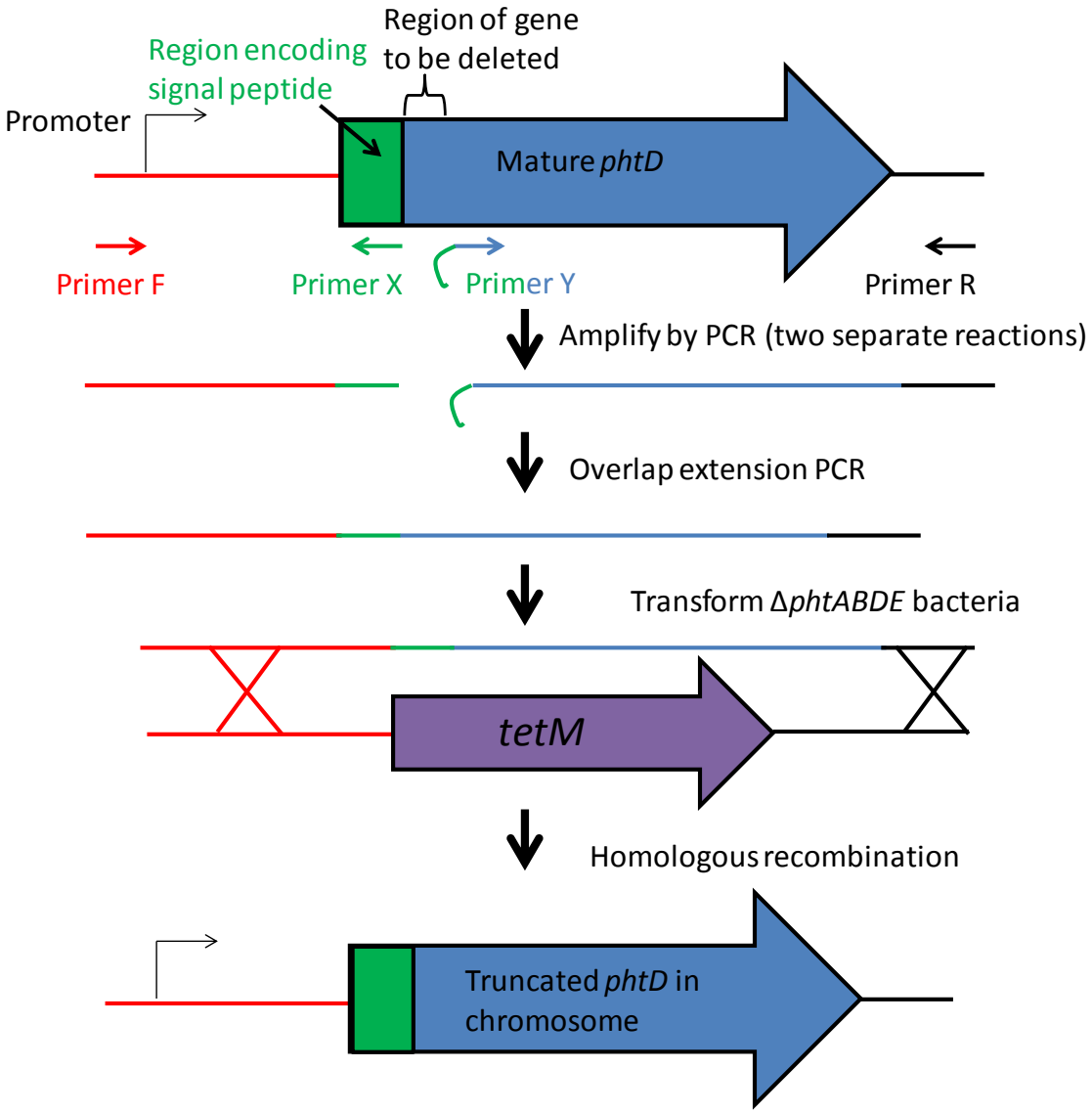

Figure 7.3: Construction of strains complemented with altered forms of *phtD*.

The phtD gene locus was amplified by PCR in two sections, omitting a small region between the two. These two regions were then joined by overlap extension PCR, and this product was used to transform Δ*phtABDE* bacteria followed by selection for tetracycline sensitivity.

was not disrupted. A control strain was complemented with the full length, unaltered *phtD* gene and referred to as 'N full'.

The level of exposure of PhtD on the surface of the wild-type, Δ*phtABDE*, N full and N50 strains was assessed by flow cytometry as described in Section 2.9; the results, shown in Figure 7.4, reveal that the N full and N50 strains have PhtD attached and exposed on the surface to a similar level as the wild-type, whereas the Δ*phtABDE* negative control strain does not. Thus, amino acids S40 to P95 are not required for surface attachment of PhtD.

Two further mutant strains were therefore created that lacked regions closer to the N-terminus than S40. The first, referred to as SP+, lacked V32 to V39, whilst the second lacked R26 to V39, and was referred to as SP-. These amino acids were chosen based on the signal peptide prediction in Figure 7.1; SP+ lacks amino acids immediately following the potential cleavage site at G30, whilst SP- also lacks the putative cleavage site. It was therefore predicted that the PhtD in the SP- mutant strain would not be able to be exported or attached to the surface due to disruption of the signal peptide. Flow cytometry was performed as before, as well as Western blotting of bacterial lysates and culture supernatants to look for the presence of PhtD in these fractions. Results are shown in Figure 7.5 and Figure 7.6 respectively.

The flow cytometry results indicated that the SP+ mutant had PhtD at its surface at similar levels to wild-type and the N full mutant, and that the SP- mutant did not have PhtD present at the surface. Interestingly, the Western blots showed that all strains except the Δ*phtABDE* mutant had PhtD present in the culture supernatant, indicating a degree of secretion and/or release of the protein from the cells. Furthermore, the SP- mutant showed an increased level of PhtD in the supernatant compared to the other strains. This implied that the amino acid stretch RHQAGQ that was absent in the SP- mutant but present in the SP+ strain was not required for the signal peptide to function correctly, since the protein could still be exported from the bacteria. However, the increased amount of PhtD in the supernatant and the lack of detection of PhtD at the surface of the bacteria by flow cytometry in the SP- mutant both suggested that these amino acids could be required to mediate attachment of PhtD to the surface. The Western blots also revealed a small amount of protein with an estimated molecular weight of approximately 70 kDa that was reactive with the anti-PhtD antiserum. This was found for all strains (except the Δ*phtABDE*

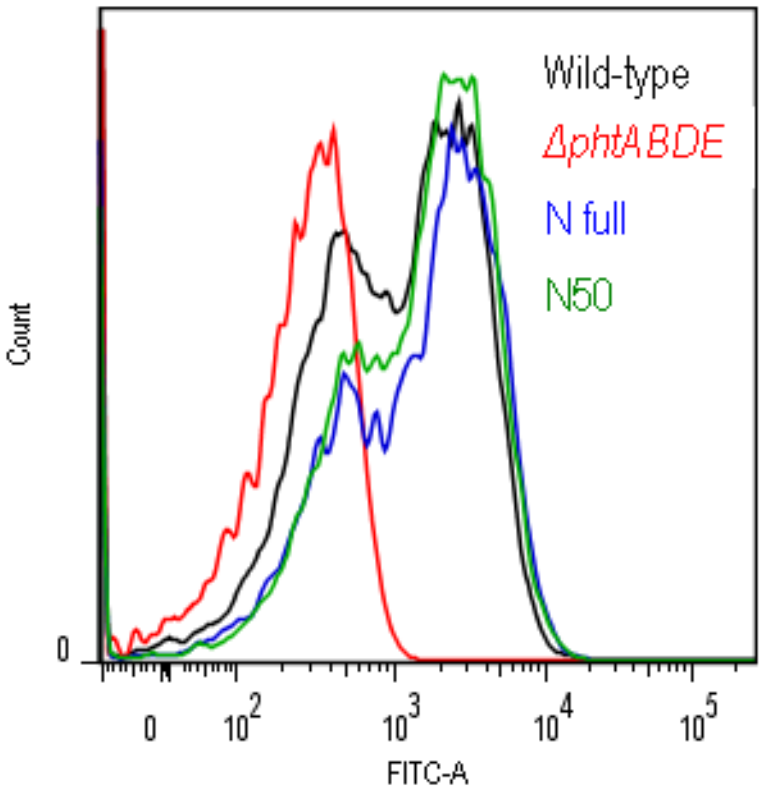

Figure 7.4: Surface attachment of PhtD in the N50 mutant strain.

Wild-type, Δ*phtABDE*, N full and N50 strains were analysed for PhtD surface attachment and exposure by flow cytometry as described in Section 2.9. A representative histogram of fluorescence profiles for each strain is shown.

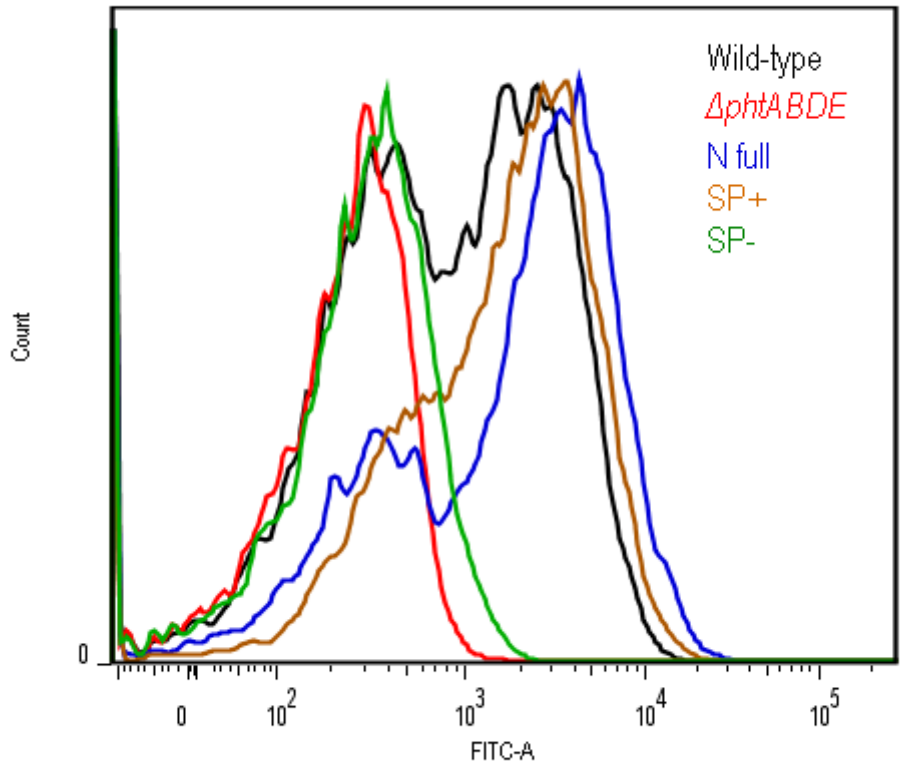

Figure 7.5: Surface attachment of PhtD in SP+ and SP- mutants.

Wild-type, Δ*phtABDE*, N full, SP+ and SP- strains were analysed for PhtD surface attachment and exposure by flow cytometry as described in Section 2.9. A representative histogram of fluorescence profiles for each strain is shown.

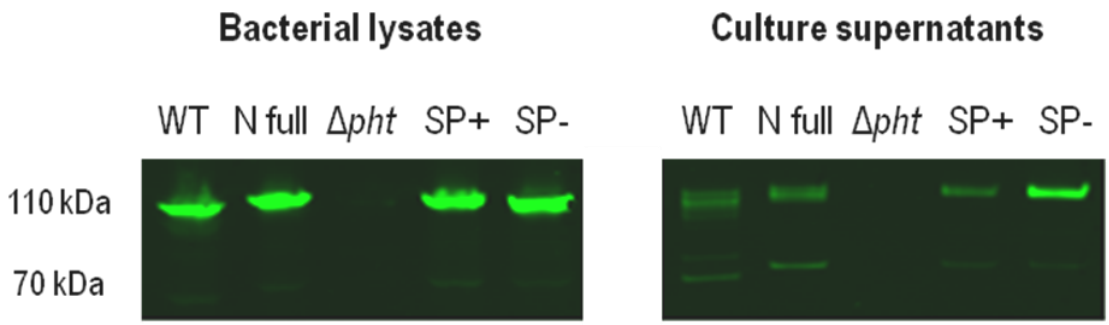

Figure 7.6: Western blotting for PhtD in bacterial lysates and culture supernatants of SP+ and SP- mutants.

The level of PhtD in lysates and culture supernatants of wild-type, N full, Δ*phtABDE*, SP+ and SP- strains was measured by Western blot as described in Section 2.13. Approximate molecular sizes are indicated on the left; these were estimated based on the mobilities of standard markers (not shown).

mutant) and was more prominent in the culture supernatant fractions. This may indicate that some of the PhtD is cleaved by a protease at some stage after its production.

To check that the PhtD detected in the culture supernatants was not an artefact of autolysis of the pneumococci, Western blots were performed to detect CpsD, an intracellular protein (Morona *et al*., 2000) (see Figure 7.7). CpsD was only detected in the bacterial lysates, indicating lysis had not occurred. 110 kDa and 70 kDa forms of PhtD were present once again; the 70 kDa form was particularly prominent in the N full strain.

7.5 Site-directed mutagenesis in PhtD leading to loss of attachment

To confirm that the RHQAGQ amino acid stretch from the SP- mutant is indeed critical for attachment of PhtD to the bacterial surface, site-directed mutagenesis was performed. This was carried out as described in Section 7.3, with the only difference being that primers X and Y were designed not to delete any amino acids, but to encode a form of PhtD with the amino acid substitutions R26A, H27A and Q28A. This strain, once checked by DNA sequencing, was referred to as the '3 alanine' mutant. Out of the six amino acids RHQAGQ, the first three were chosen for mutagenesis based on an alignment of this region across the four pneumococcal Pht proteins (see Figure 7.8), which showed that the histidine and first glutamine were conserved in three out of four of the proteins, whilst the arginine was also chosen because of its charged side-chain. R26, H27 and Q28 were considered to be the most likely amino acids of the six to mediate attachment, although it was interesting to note that none of the six amino acids were completely conserved amongst the four Pht proteins, despite the fact that the proteins show 32% identity overall, and 62% identity in their N-terminal regions (Adamou *et al*., 2001).

The 3 alanine mutant was tested by flow cytometry and Western blotting as for the previous mutants (see Figure 7.9 and Figure 7.10). PhtD was not attached to the surface of this mutant strain, and was only present in the supernatant. This indicates that R26, H27 and/or Q28 are required for attachment of the protein to the bacterial surface. Interestingly, the phenotypes of the SP- mutant and the 3 alanine mutant were not identical, with the SP- mutant showing a small amount of surface-localised PhtD, with a large amount of the protein in the bacterial lysate where the 3 alanine mutant had none.

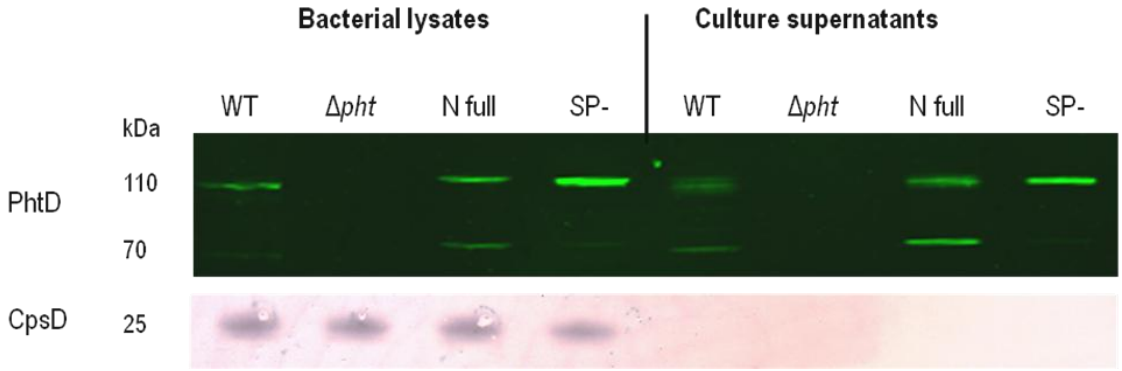

Figure 7.7: Western blotting for PhtD and CpsD in bacterial lysates and culture supernatants to check for pneumococcal autolysis.

PhtD and CpsD was detected in lysates and culture supernatants of wild-type, N full, Δ*phtABDE* and SP- strains by Western blotting as described in Section 2.13.

PhtA	**L**	**Y**	**Q**	**A**	**R**	**T**
PhtB	**L**	**H**	**Q**	**A**	**Q**	**T**
PhtD	**R**	**H**	**Q**	**A**	**G**	**Q**
PhtE	**Q**	**H**	**R**	**S**	**Q**	**E**

Figure 7.8: Alignment of putative attachment motif in PhtD with homologous regions in PhtA, PhtB and PhtE.

The Pht proteins of *S. pneumoniae* D39 were aligned using ClustalW2 (available online at http://www.ebi.ac.uk/Tools/msa/clustalw2/) (Larkin *et al*., 2007; Goujon *et al*., 2010). Only the six amino acids corresponding to RHQAGQ from PhtD are shown. Colours indicate physiochemical properties of classes of amino acids (red, small/hydrophobic; blue, acidic; black, basic; green, hydroxyl/sulphhydryl/amine).

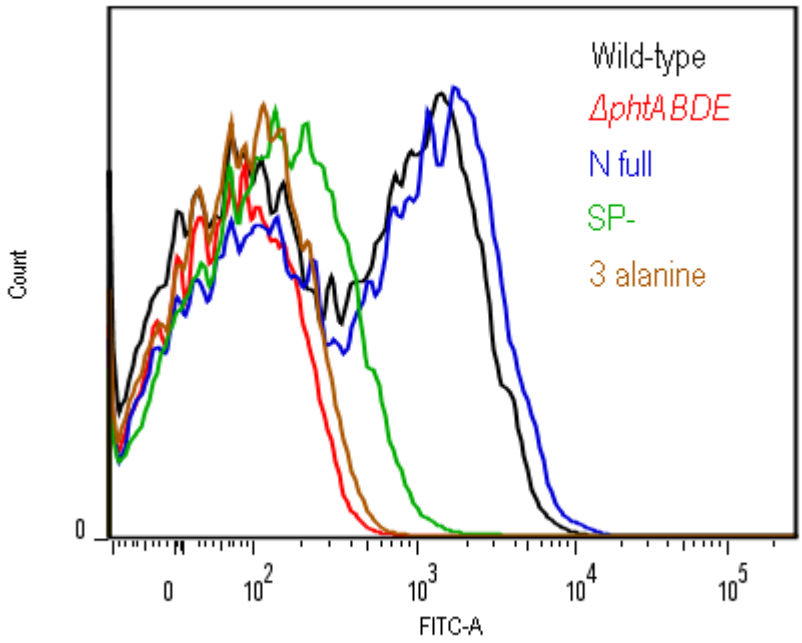

Figure 7.9: Surface attachment of PhtD in 3 alanine mutant.

Wild-type, Δ*phtABDE*, N full, SP+ and SP- strains were analysed for PhtD surface attachment and exposure by flow cytometry as described in Section 2.9. A representative histogram of fluorescence profiles for each strain is shown.

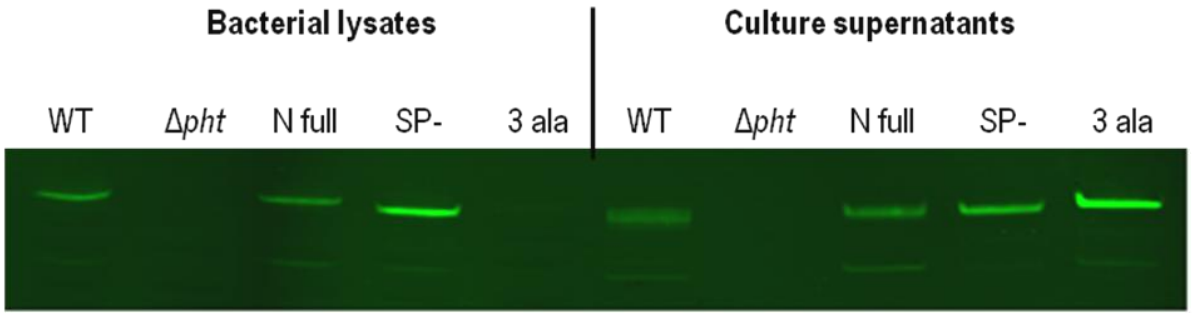

Figure 7.10: Western blotting for PhtD in bacterial lysates and culture supernatants of 3 alanine mutant.

The level of PhtD in lysates and culture supernatants of wild-type, N full, Δ*phtABDE*, SP- and 3 alanine strains was measured by Western blot as described in Section 2.13.

7.6 Assessment of the chemical nature of attachment by released protein assay

Having identified a short stretch of amino acids apparently required for attachment to the bacterial surface, other aspects of the attachment mechanism were examined. Firstly, the nature of the interaction of PhtD with the surface was probed by incubating wild-type bacteria for 15 min at RT with various compounds in an assay that has been described previously (Price and Camilli, 2009). Sodium chloride (4 M) was used to disrupt ionic interactions and dithiothreitol (DTT; 10 mM) and sodium carbonate (100 mM) to disrupt disulphide and thioester bonds of cysteine residues respectively. Urea (8 M) was used to examine whether the protein needed to be in a folded conformation for attachment and SDS (0.1% v/v) tested whether the interaction was mediated by hydrophobic attractions. Water was used as a control. CpsD was again used as a control for bacterial lysis. As can be seen in Figure 7.11, CpsD could be detected in all of the wash fractions, indicating a certain amount of lysis under all the conditions tested. In contrast to results obtained by Price and Camilli (2009), SDS appeared to cause significantly more cell lysis than other compounds, and because of this the increased level of PhtD detected in the SDS wash cannot be interpreted as meaning that PhtD interacts hydrophobically with the cell surface. PhtD, in both 110 kDa and 70 kDa forms, can also be detected in all of the other washes, but it is not clear whether this is entirely due to autolysis or whether the chemical treatments contributed to the release of the protein. However, the fact that none of the treatments led to a substantially greater release of PhtD than any other (with the exception of SDS, as mentioned above) could be interpreted as implying that the interaction is neither strongly ionic, nor dependent upon disulphide or thioester bonds, nor reliant upon the protein being in a folded conformation.

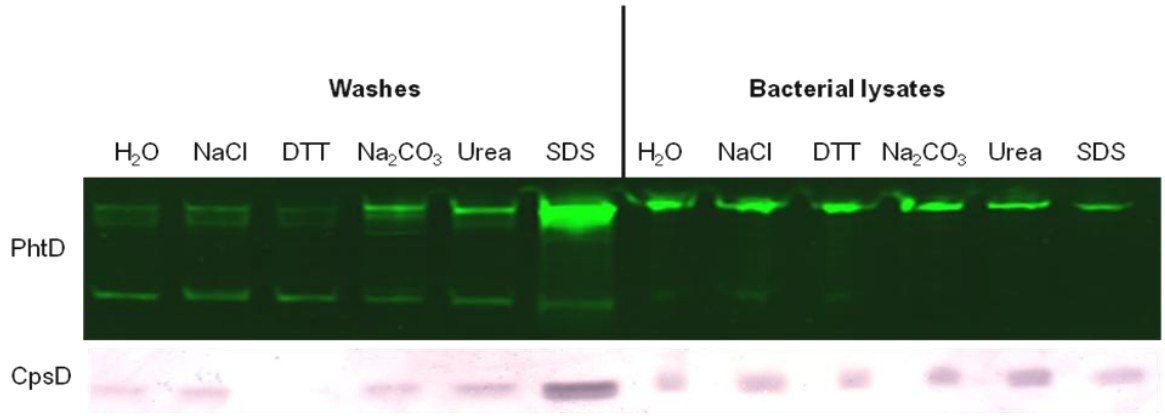

Figure 7.11: Released protein assay for PhtD with CpsD as a control for bacterial lysis.

Wild-type pneumococci were washed with the indicated compounds and the washes were separated from the bacteria. PhtD and CpsD were detected in the samples by Western blotting as described in Section 2.13.

7.7 Digestion of the cell wall leads to release of PhtD

To corroborate the previous finding of Loisel *et al.* (2011) that PhtD is associated with the cell wall, wild-type, N full and SP- strains were separated into protoplast and cell wall fractions by digestion with mutanolysin and lysozyme, using a previously published protocol (Price and Camilli, 2009; Price *et al*., 2012; see Section 2.11). The presence of PhtD in samples of these fractions and in the culture supernatant was detected by Western blotting as described in Section 2.13 (see Figure 7.12). Equivalent proportions of the culture supernatant, and supernatant and pellet fractions from after the cell wall had been digested, were loaded onto the gel such that the band intensities reflect the relative proportions of PhtD in the respective fractions. The results showed that PhtD is released by digestion of the cell wall. No bands were observed in the protoplast fractions except for a weak band for the SP- mutant strain, indicating that PhtD is not anchored in the cell membrane and is not present at high levels in the cytoplasm. Considerable quantities of PhtD were observed in the culture supernatants, especially for the SP- mutant. However, the proportion of PhtD released by digestion of the cell wall of this strain appeared lower than that for the wild-type or N full strains. This is in agreement with the previous detection of a low level of surface accessible PhtD in the SP- mutant and its presence in the bacterial lysate (Figure 7.9 and Figure 7.10). It is not clear why the wild-type strain showed a lower level of PhtD in the culture supernatant in this experiment; nevertheless, it was still detectable in this fraction.

A 70 kDa protein was observed in the culture supernatants and supernatants after cell wall digestion for each strain, consistent with previous experiments. In addition to this, there were further proteins in the cell wall fractions that reacted with the anti-PhtD murine serum, all of which migrated with apparent molecular weights that were smaller than the 110 kDa of full length PhtD. Whilst inhibitors of cysteine and serine proteases (cOmplete EDTA-free Protease Inhibitor Cocktail Tablets, Roche) were included in the cell wall digestion buffer, it is possible that other types of proteases could be responsible for these bands. These could have been contaminants in the cell wall digestion mix, or may have been produced by the bacteria themselves and have been released by the digestion of the cell wall.

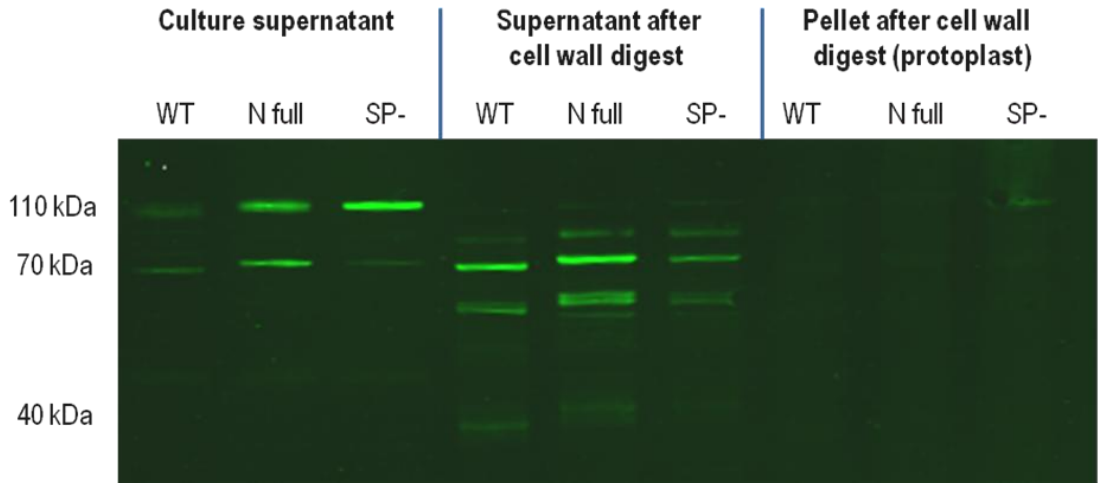

Figure 7.12: Detection of PhtD in culture supernatant, cell wall and protoplast fractions.

Wild-type, N full and SP- strains were incubated with mutanolysin and lysozyme to digest the cell wall and subsequently separated into supernatant (containing cell wall material) and pellet (containing protoplasts) fractions. Proteins were also precipitated from the supernatants of the original culture medium. PhtD was detected by Western blotting as described in Section 2.13.

To investigate the source of the protease activity, the experiment was repeated with the wild-type strain with either mutanolysin or lysozyme alone, or with both or neither enzyme, as shown in Figure 7.13. It should be noted that the cell wall digestion buffer used in this experiment has been reported to induce spontaneous spheroplast formation even in the absence of mutanolysin and lysozyme, and that this was dependent on its sucrose content (Lacks and Neuberger, 1975). Consistent with this, PhtD was found in the supernatant after bacteria were incubated in buffer without mutanolysin or lysozyme. The protein was present in several forms at different molecular weights below 110 kDa, consistent with the hypothesis that proteases produced by the pneumococci had cleaved the protein into smaller fragments. In previous experiments, the majority of the PhtD had been detected in the 110 kDa band, whereas the supernatant after cell wall digestion lanes in this experiment showed extensively digested PhtD, with only a small proportion of the protein detectable at 110 kDa. This is likely to be a reflection of the considerable length of time over which cell wall digestion was performed (2 h), during which the proteases could extensively degrade the PhtD. There was no difference in the amount or molecular sizes of PhtD fragments detected when lysozyme was present or absent, indicating that this enzyme may not have an effect on the pneumococcal cell wall beyond that of the buffer alone. In contrast, the addition of mutanolysin led to further proteolysis of PhtD, potentially indicating that the stock of mutanolysin was contaminated with additional proteases.

7.8 Culture supernatant swaps show that PhtD does not reversibly detach from and re-attach to the cell surface

Numerous experiments had indicated that the Pht proteins can be found in the bacterial culture supernatants, even where autolysis had not occurred. It has previously been demonstrated that the pneumococcal alpha-enolase protein can re-attach to the bacteria when present in the external soluble phase (Bergmann *et al*., 2001). It was therefore hypothesised that the PhtD present in the culture supernatants may be able to reassociate with the bacterial surface, and that PhtD is in a dynamic equilibrium between surface bound and soluble forms. To test this hypothesis, cultures of wild-type, Δ*phtABDE*, and N full strains were grown. Δ*phtABDE* bacteria were then incubated with filtered supernatant from the wild-type and N full cultures or recombinantly expressed purified PhtD for 1 h at 37°C. Flow cytometry was performed to detect any PhtD attached to the surface of the

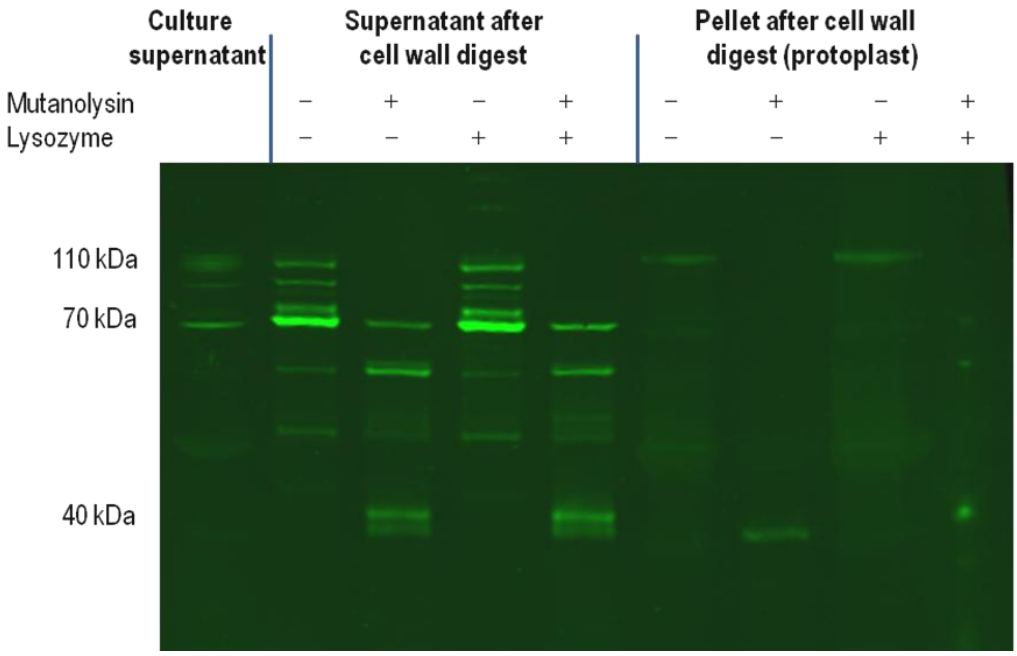

Figure 7.13: Detection of PhtD in culture supernatant, cell wall and protoplast fractions after digestion with mutanolysin or lysozyme.

Wild-type pneumococci were incubated with mutanolysin and/or lysozyme (as indicated) to digest the cell wall and subsequently separated into cell wall and protoplast fractions. PhtD was detected by Western blotting as described in Section 2.13.

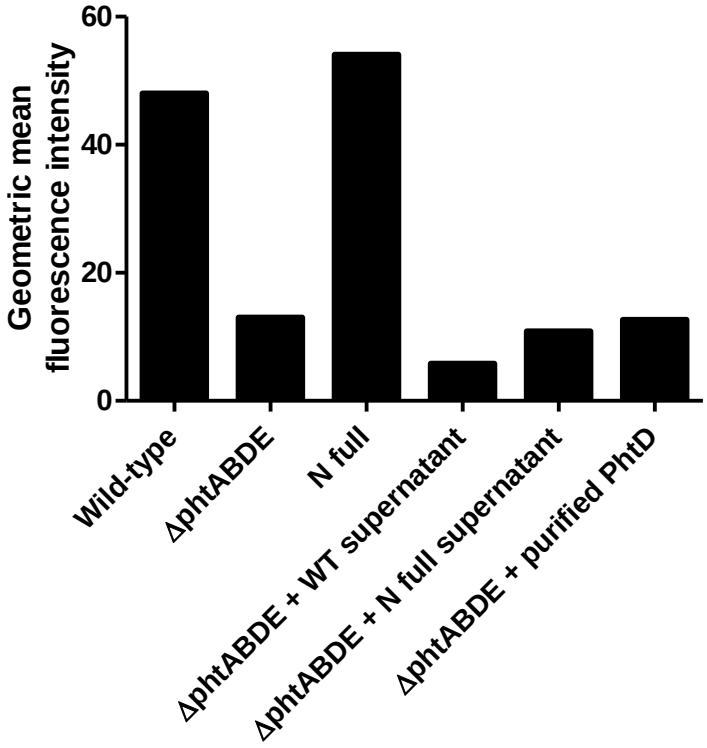

Figure 7.14: Detection of PhtD by flow cytometry after swapping supernatants between cultures.

Flow cytometry was performed as described in Section 2.9 to detect PhtD on the surface of wild-type, Δ*phtABDE* and N full strains, as well as samples of Δ*phtABDE* bacteria that had been incubated with supernatant from wild-type or N full cultures, or with purified PhtD. Geometric mean fluorescence intensities for 10,000 events are shown.

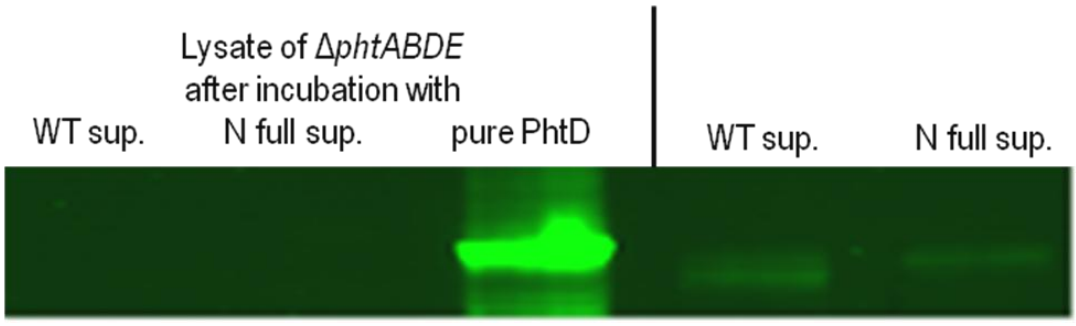

Figure 7.15: Detection of PhtD associated with Δ*phtABDE* bacteria after swapping supernatants between cultures.

After incubation with supernatant from wild-type or N full cultures or purified PhtD, lysates were prepared from the Δ*phtABDE* bacteria and PhtD detected by Western blotting (first three lanes). On the right, samples of precipitated protein from the culture supernatants after incubation are shown, indicating that PhtD was still present in these supernatants.

strains, and Western blotting was used to look for the protein in the bacterial lysates and supernatants. The flow cytometry results (shown in Figure 7.14) indicate that PhtD from either culture's supernatant or the recombinantly expressed purified protein did not reassociate with the bacteria, since the mean fluorescence intensities of these samples were similar to the untreated Δ*phtABDE* strain. Similarly, Western blotting (Figure 7.15) showed that PhtD from the supernatants was not associated with the bacteria after incubation with culture supernatants and preparation of lysates. A large amount of PhtD was detected in the lysate of the Δ*phtABDE* bacteria after incubation with purified PhtD, but since no PhtD was detected on the bacterial surface after this treatment, this band is in fact likely to result from some of the purified protein having aggregated and thus having been spun down into a pellet with the bacteria during centrifugation. A test centrifugation of a sample of purified protein alone revealed the formation of a small pellet, confirming this explanation. This experiment therefore showed that PhtD is not able to reassociate with the bacterial surface after release.

7.9 PhtD is released over time

From the above experiments, it is not clear whether the pool of PhtD found in culture supernatants comes from protein that was previously attached to the cell surface or whether the protein was secreted directly from the cytoplasm without being transiently attached. To address this, wild-type pneumococci were grown to OD_{600} 0.3 and samples collected every hour thereafter for 4 h, as described in Section 2.12. Cell lysates and supernatants were prepared from these samples for SDS-PAGE as described in Section 2.10. This also allowed the possible relationship of release/secretion of PhtD with different growth phases to be investigated. Chloramphenicol was added to a duplicate culture at OD_{600} 0.3 and samples collected from this culture at the same timepoints. This allowed the levels of PhtD in lysates and supernatants to be monitored over time without further protein synthesis occurring. Western blotting was performed to detect PhtD as well as the intracellular transcriptional regulator AdcR to control for pneumococcal autolysis. The results are shown in Figure 7.16 and Figure 7.17. Total amounts of PhtD and AdcR were quantified from the Western blots; both proteins increased in abundance over time when chloramphenicol was absent but remained at a stable level when chloramphenicol was present, indicating that treatment with the antibiotic had been effective at inhibiting new

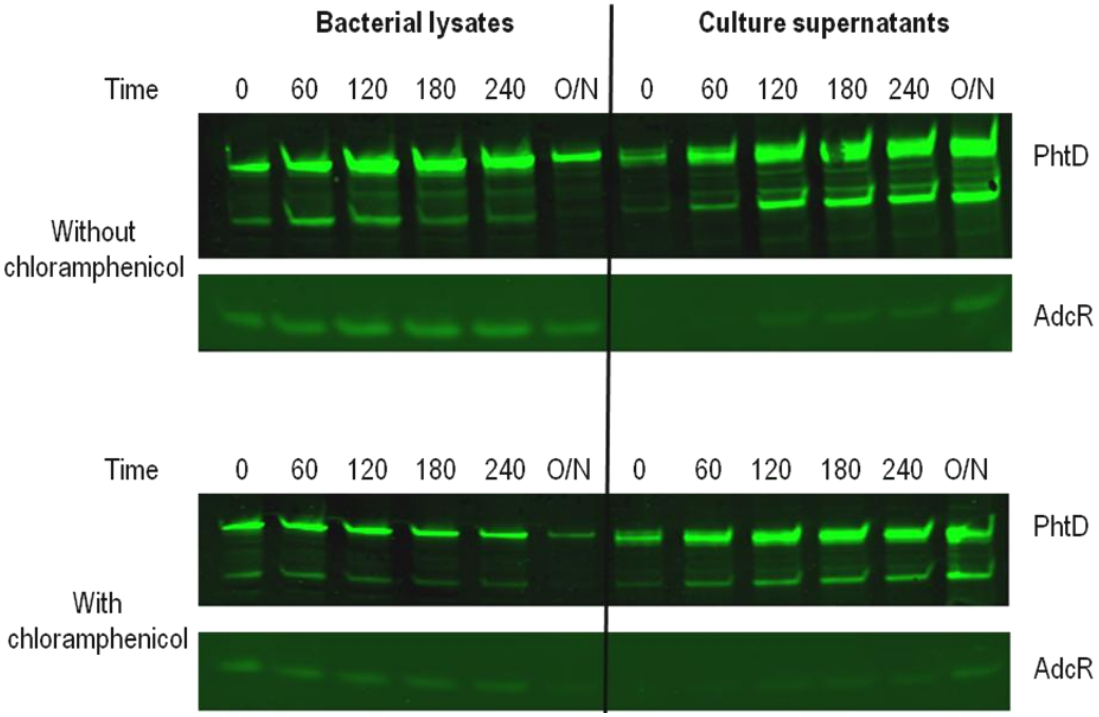

Figure 7.16: Release of PhtD from the bacterial surface over time.

Bacteria were grown and incubated with or without chloramphenicol. Samples were collected every hour or after overnight (O/N) incubation as described in Section 2.12. PhtD and AdcR were detected in bacterial lysates and culture supernatants by Western blotting. Equal proportions of bacterial lysate and culture supernatant were loaded in each lane.

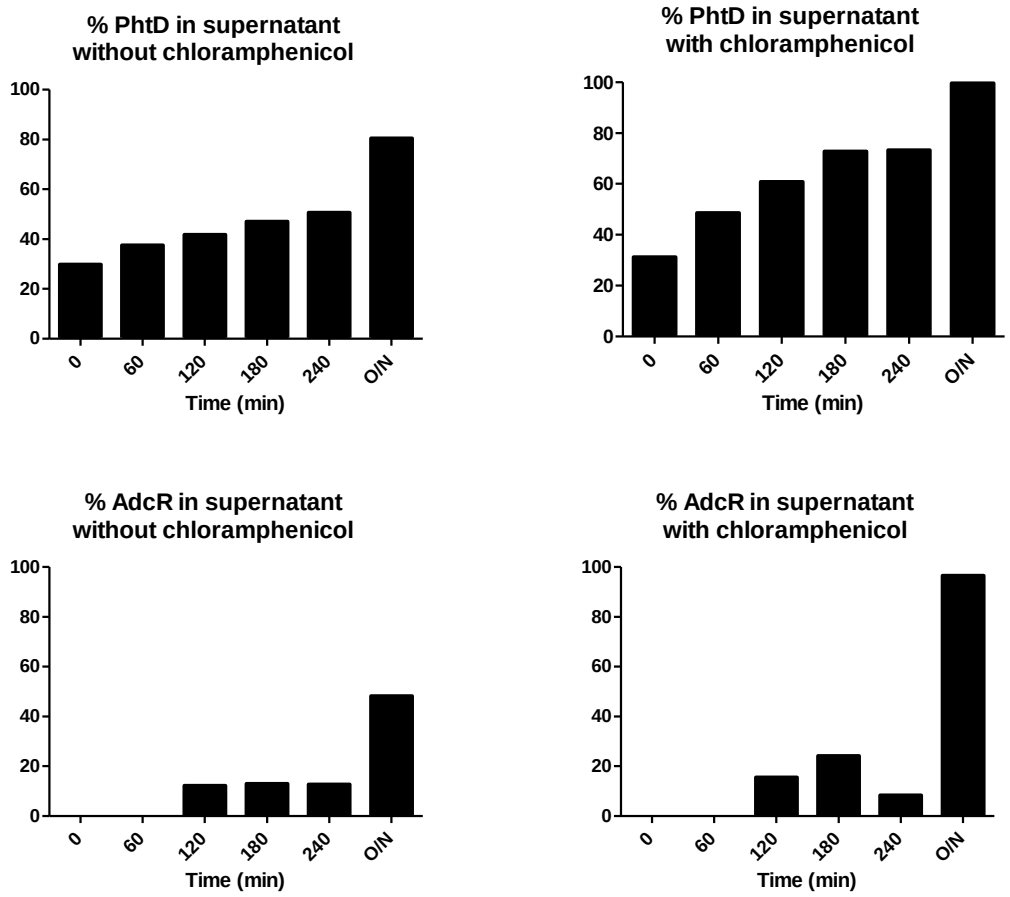

Figure 7.17: Percentages of PhtD and AdcR in culture supernatants from bacteria incubated with or without chloramphenicol.

Band intensities were quantified from the Western blots shown in Figure 7.16 and the percentage of protein found in culture supernatant for each timepoint was calculated as described in Section 2.13. For PhtD, intensities of both the 110 kDa band and the 70 kDa band were measured and added together.

protein synthesis (data not shown).

After 1 h, the bacteria without chloramphenicol were still in log phase, whereas after 2 h stationary phase had been reached. In the presence of chloramphenicol, the growth of the bacteria was arrested at around OD_{600} 0.3. The results for bacteria grown without chloramphenicol revealed a small amount of AdcR in the culture supernatant from 2 h onwards, indicative of a low level of autolysis from this time. Extensive autolysis occurred after overnight culture as expected. The percentage of PhtD found in the supernatant from the bacteria cultured without chloramphenicol increased over time from approximately 30% initially to approximately 50% after 4 h. The absolute amount of protein found in both lysates and supernatants was gradually increasing. The percentage of PhtD found in the supernatant of bacteria cultured with chloramphenicol showed a slightly greater rate of increase over time, peaking at approximately 70% after 4 h. This was caused by an increase in the amount of PhtD found in the supernatant over time and a decreasing amount in the bacterial lysates. This was not the result of autolysis since the level of AdcR found in the culture supernatants did not consistently increase over time. These results indicate that there is a steady turnover of PhtD, with the protein being continually lost from the surface. This is supported by the gradual increase in percentage of PhtD in the supernatants, which occurred regardless of whether chloramphenicol was present or absent. It should be noted that the calculations of the percentage of protein in the supernatant assume that the procedures used to prepare bacterial lysates and precipitate proteins from culture supernatants are 100% efficient in terms of yield of protein.

7.10 Comparison of levels of PhtD in the culture supernatants of four pneumococcal strains

Since all of the above experiments had been performed with one pneumococcal strain (D39), it was desirable to confirm that release of PhtD into the culture supernatant is a general characteristic of pneumococci and not just a feature of D39. To do this, strains WCH43 (serotype 4), P9 (serotype 6A) and WU2 (serotype 3), as well as D39 (serotype 2) as a control, were grown in THY to OD_{600} 0.5. Samples of culture supernatant and bacterial lysate were prepared for SDS-PAGE as described in Section 2.10, and PhtD and

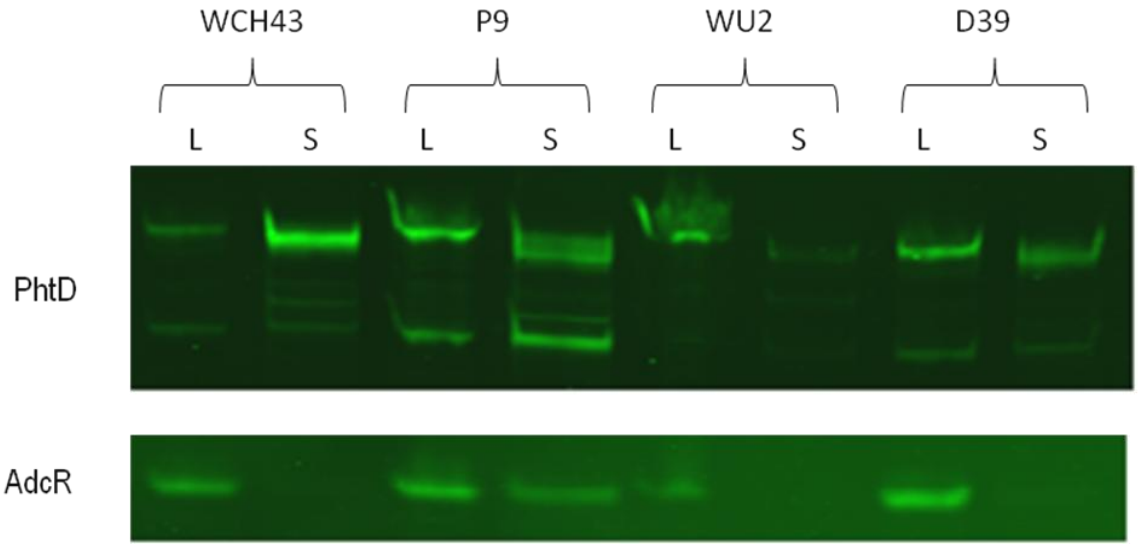

Figure 7.18: Comparison of the amounts of PhtD released by four pneumococcal strains.

Strains WCH43, P9, WU2 and D39 were grown in THY to OD_{600} 0.5 and PhtD and AdcR were detected in samples of bacterial lysate (L) and culture supernatant (S) by Western blotting.

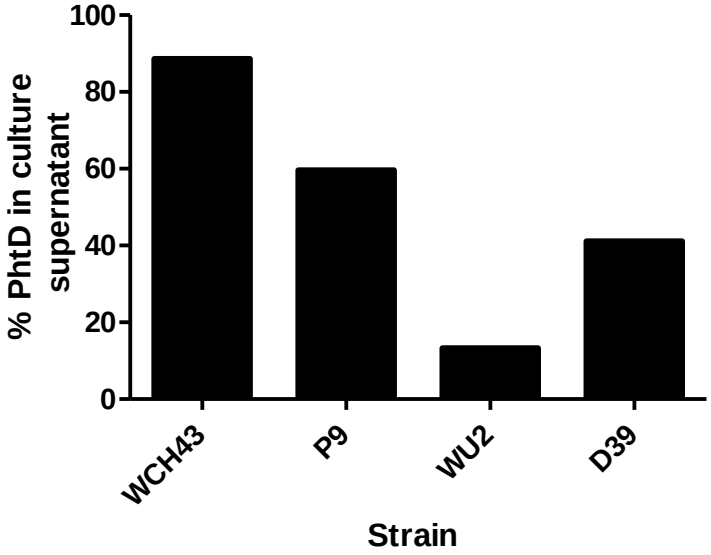

Figure 7.19: Percentage of PhtD found in culture supernatants of four pneumococcal strains.

Band intensities were quantified from the Western blot shown in Figure 7.18, and the percentages of PhtD found in the culture supernatant out of the total amount of PhtD were calculated. For PhtD, intensities of both the 110 kDa band and the 70 kDa band were measured and added together.

AdcR were quantified by Western blotting (see Figure 7.18 and Figure 7.19). All four strains showed some release of PhtD into the culture supernatant. Another common feature was the presence of major bands with apparent molecular sizes of both 110 kDa and 70 kDa. Interestingly, there were marked differences in the proportion of the protein detected in the supernatant. WCH43 showed a very high level of PhtD release, with almost 90% of the protein being found in the supernatant, whereas for WU2 only approximately 10% of the protein was released. As in the previous experiment, around 40% of the PhtD was found in the culture supernatant for D39. For P9, approximately 60% of the PhtD had been released. However, AdcR was also detected in the P9 culture supernatant, indicating that some autolysis had occurred, making interpretation difficult.

7.11 Discussion

Pneumococcal surface proteins are thought to fall into four major groups (Pérez-Dorado *et al*., 2012). The first two, both of which are common to many Gram-positive bacteria, are the lipoproteins, which attach to the cell membrane via a post-translationally added *N*-acyl diacylglyceryl group, and the LPxTG sortase-dependent proteins, which are covalently anchored to the cell wall. *S. pneumoniae* also produces choline binding proteins, which are attached via non-covalent interactions of conserved choline binding domains with phosphorylcholine residues in teichoic acids of the cell wall or lipoteichoic acids embedded in the cell membrane. Lastly, there is a group of non-classical surface proteins, which can be loosely defined as proteins traditionally thought to be cytoplasmic that lack conventional secretion or anchoring sequences, but are nonetheless found to be exposed on the cell surface (Nobbs *et al*., 2009; Henderson and Martin, 2011; Pérez-Dorado *et al*., 2012). The Pht proteins, however, do not appear to fit into any of these groups. They contain a type II signal peptidase cleavage site consensus motif, but do not appear to be attached to the membrane and are not lipoproteins (Adamou *et al*., 2001; Hamel *et al*., 2004; Loisel *et al*., 2011), whilst they do not contain choline binding domains nor any motifs thought to be recognised by sortases. They do, however, contain a signal peptide and are not thought to play a role intracellularly, thus excluding them from the non-classical surface protein group. They are therefore thought to use a novel mechanism to attach to the cell surface. A greater understanding of PhtD's mechanism of attachment and

surface exposure is important for its development as a vaccine candidate, as well as for our knowledge of the biology of surface protein attachment in general.

In the first half of this chapter, the amino acids R26, H27 and/or Q28 were found to be critical for the association of PhtD with the bacterial surface. Although the released protein assay of Section 7.6 suggested that PhtD is not attached via ionic, hydrophobic or cysteine-mediated bonds, the chemical nature of any bond formed with a surface 'anchor' molecule is unclear. However, the reactivity of the arginine and/or histidine positively charged side-chains may play a role. Interestingly, as shown in Figure 7.8, none of the other Pht proteins of *S. pneumoniae* contain identical amino acids at the same positions as R26, H27 and Q28 in PhtD. This may indicate either that each protein's mechanism of attachment is different, or alternatively that only amino acids with similar chemical properties are required; for instance, all four proteins contain positively charged and/or polar amino acids in their respective regions. Further point mutants would need to be generated and their phenotype examined to determine whether each of R26, H27 and Q28 are required for the protein to be associated with the cell surface. Furthermore it would be interesting to determine whether any of the amino acids between M1 to Q28 are also required, and whether M1 to Q31 is sufficient for the association of a protein with the surface or whether other residues in PhtD are also required. This could be done by cloning the nucleotides encoding this region upstream of a tag protein and assessing pneumococci encoding this construct for surface exposure of the tag. This would preferably be performed using a tag protein that pneumococci are known to be capable of exporting, since some proteins such as pneumolysin cannot be exported even when fused to a signal peptide known to be sufficient to allow export of other proteins (Price *et al*., 2012). Zinc may also play a role in the surface attachment and release of PhtD, since the experiments shown in Figure 4.1 and Figure 4.2 show that more of the protein was present in the culture supernatant when the extracellular concentration of the ion was low.

Incubation of pneumococci in buffer containing a high concentration of sucrose, which has previously been shown to induce spheroplast formation (Lacks and Neuberger, 1975), led to release of PhtD from the bacteria. This indicates that the protein may either be attached to the cell wall or may be non-specifically encased within or beneath this layer (discussed below). In the experiments of Section 7.7, the majority of the PhtD was found in a band with an approximate molecular size of 70 kDa, suggesting that a protease that

cleaves the protein was also present in the cell wall. Since the digestion buffer contained a protease inhibitor cocktail targeted at serine and cysteine proteases, other types of protease such as metallo or aspartic proteases are likely to be responsible for the cleavage of PhtD. The experiment could be repeated in the presence of EDTA to inhibit metalloprotease activity to show whether this type of protease is involved. A 70 kDa band could also be detected in all of the other Western blots in this chapter, and was usually more prominent in culture supernatants than bacterial lysates. It is therefore feasible that PhtD is cleaved from 110 kDa into a 70 kDa form when the protein reaches the bacterial surface.

Intriguingly, significant quantities of PhtD (up to 40% of the total amount of the protein for D39) could be detected in culture supernatants in all of the above experiments, and this was not caused by pneumococcal autolysis. There has been one previous report that Pht proteins are released or secreted, and this was demonstrated for a number of strains of different serotypes, although no control was performed to show that this effect was not due to autolysis (Zhang *et al*., 2001). In Section 7.10 it was confirmed that release of PhtD occurs in a number of pneumococcal strains, and other results presented in this chapter suggest that released PhtD cannot re-attach to the bacteria and that the protein is continually being lost from the cell surface independent of new protein synthesis. These results imply that the Pht proteins may not be surface attached in the normal sense, but instead, after being translocated through the cell membrane, may be prevented from diffusing away from the surface by a combination of weak ionic and/or hydrophobic forces and steric hindrance by the cell wall peptidoglycan and teichoic acid. In this model, the residues identified in Section 7.5 as being important for attachment may simply contribute to the weak ionic forces that retard the spontaneous loss of the proteins. This hypothesis could be tested by mechanically lysing a washed culture of wild-type pneumococci in a French pressure cell and separating cell debris (which would include the cell wall and cell membrane fractions) from supernatant by ultracentrifugation, before examining both the pellet and supernatant for PhtD content by Western blotting. If Pht proteins are tightly attached to the cell wall (for instance by a covalent bond), they would be present in the pellet fraction; however if they are only loosely bound, or trapped under the cell wall layer, a significant proportion would be found in the supernatant.

There were sizeable differences in the proportion of PhtD found to be extracellular between different pneumococcal strains, (e.g. approximately 90% for the serotype 4 strain

WCH43 compared with only 10% for the serotype 3 strain WU2). It is interesting to note that measurements of capsule size have indicated that serotype 4 strains have relatively small capsules, whereas serotype 3 strains are thought to produce large quantities of capsular polysaccharide (Hammerschmidt *et al*., 2005; Weinberger *et al*., 2009). It could therefore be speculated that the thickness of the capsule layer may play a role in retarding the diffusion of Pht proteins away from the bacterial surface, and the varying chemical composition of polysaccharides of different capsular serotypes may also contribute. More work, such as examination of mutants deficient in capsule production, will be required to provide definitive evidence for this hypothesis.

A constant loss of Pht proteins from the cell surface would be metabolically wasteful if the released protein did not play a role that is beneficial to pneumococci. Assuming that secretion of PhtD also occurs during infections *in vivo*, i.e. that it is not an artefact of growing bacteria in liquid culture, there are several possible hypotheses that could be proposed to explain the role of the released protein. Firstly, release of Pht proteins could be important in the context of a biofilm. During planktonic growth the propensity of released Pht proteins to diffuse away from the bacteria would lead to them being lost very quickly, whereas the extracellular matrix of the biofilm may prevent such diffusion and trap the proteins in the local environment. They may then function to retain and/or recruit zinc to the biofilm. It is also feasible that the released Pht proteins could interact with receptors on host cells to trigger inflammatory responses, or could bind factor H or FHL-1 in such a way as to inactivate it, leading to non-specific complement activation in the local area. Further investigation of these issues is clearly warranted, since they are potentially very important for our understanding of the functions and roles of Pht proteins. Furthermore, they may have consequences for the use of the proteins in vaccine formulations, since if Pht proteins are released *in vivo* during infection, their perceived usefulness as vaccine candidates may be diminished. This is because a proportion of antibodies generated against the proteins during vaccination would bind to soluble rather than cell-associated forms of the proteins during infection, leading to reduced opsonophagocytic activity.

Chapter 8: Final Discussion

8.1 Importance of research into Pht proteins

The polyhistidine triad proteins, and PhtD in particular, have emerged as leading vaccine candidates for future protein-based pneumococcal vaccines. Indeed, clinical trials of PhtD have already been undertaken, and have so far shown the protein to be safe and immunogenic (Ferreira *et al*., 2011; Bologa *et al*., 2012; Seiberling *et al*., 2012). However, understanding of the biology of these proteins is seriously lacking, and lags far behind their development for use in vaccine formulations. It is important that our knowledge of the structure and function of these proteins be improved to allow informed decisions regarding which combinations of proteins to use as immunogens in future vaccines. The proteins are also highly intriguing in a purely academic sense because of their unique histidine triad motifs, apparent redundancy, importance for pneumococcal virulence, tantalizing range of putative functions and conservation across different streptococcal species. The work reported in this thesis was therefore designed to address these issues in several ways.

8.2 Functions of Pht proteins

8.2.1 Binding of FHL-1 and defence against complement deposition

In Chapter 3 it was demonstrated by ELISA and flow cytometry that Pht proteins and PspA bind FHL-1, a negative regulator of the alternate pathway of the complement system, and that loss of these proteins significantly increases the deposition of complement protein C3 from mouse serum onto bacteria lacking them. Interestingly, factor H has been shown to oligomerise in the presence of high concentrations of zinc (Nan *et al*., 2008). Putative zinc binding sites are located in SCR 6 and 7 (Nan *et al*., 2011), potentially providing a link between the metal-binding properties of the Pht proteins and their ability to bind FHL-1. However, no binding between FHL-1 and PhtD could be detected by surface plasmon resonance. This confounding result may be due to the immobilisation of the SCR 1-7 by amine coupling that is required for this technique, which could have altered the conformation of the protein such that the interaction with PhtD could no longer occur. When PhtD was used as the ligand protein, binding with FHL-1 could still not be detected.

It is feasible that the conformation of PhtD was also affected to such an extent that FHL-1 could not bind. Due to constraints on the maximum protein concentrations that could be achieved, the upper limit of detection for the K_D between PhtD and FHL-1 in the surface plasmon resonance experiments was around 10 μM, and it is possible that the interaction could have a higher K_D than this. However, if this were the case then it would be questionable whether such a weak interaction would be physiologically relevant. Overall, it does seem that Pht proteins play a role in defence against complement deposition, but more experiments are required to give a greater confidence that Pht proteins and PspA do indeed interact with FHL-1.

8.2.2 Role in zinc homeostasis

Prior to this work, it had been suggested that Pht proteins are required for zinc transport (Rioux *et al*., 2010), but there was a lack of evidence to distinguish this hypothesis from the possibility that the metal ion is merely required for the proteins to form the correct conformation to allow some other function. The evidence presented in Chapter 4 supports the hypothesis that Pht proteins are involved in zinc transport, since a defect in the growth of the Δ*phtABDE* strain was detected at very low external zinc concentrations, and ICPMS revealed significantly lower zinc content of the mutant strain under these conditions. Rioux *et al.* (2011) suggested that Pht proteins could act as metal scavengers, storing zinc and manganese when they are abundant and releasing them to high affinity zinc transporters when required. However, the data here do not support this, since there were no differences between wild-type and Δ*phtABDE* mutant in zinc content when EDTA washes were included or excluded, nor any difference in surface potential of the strains. Both of these experiments indicate that the Pht proteins do not retain a 'pool' of metal ions at the pneumococcal surface, and favour a model in which Pht proteins release zinc relatively quickly after binding it. However, the former scenario cannot be ruled out based on these two experiments alone.

Loisel *et al.* (2011) proposed that PhtD and AdcAII could interact, with the implication that PhtD might directly pass zinc onto the SBP. Whilst the experiments in Chapter 5 focussed more on dissecting the relative roles of AdcA and AdcAII in zinc import independent of the Pht proteins, it is interesting to note that, under zinc-limiting conditions (see Figure 5.4), the Δ*adcA*Δ*phtABDE* and the Δ*adcAII*Δ*phtABDE* strains were attenuated

for growth compared to the Δ*adcA* and Δ*adcAII* single mutants. This provides further evidence that Pht proteins do play a role in acquisition of zinc when the external concentration of the metal is extremely low. Furthermore, growth of the Δ*adcA*Δ*phtABDE* strain was impaired to a greater extent than that of the Δ*adcAII*Δ*phtABDE* strain. Interestingly, AdcA contains a histidine rich loop region near its high affinity metal binding site, as well as a domain homologous to the *E. coli* periplasmic protein ZinT at its C terminus. The histidine rich loop and the ZinT protein have been implicated in aiding the acquisition of zinc by the high affinity zinc transporter ZnuA (which is highly homologous to AdcA) in *E. coli* (Petrarca *et al*., 2010; Gabbianelli *et al*., 2011). Although otherwise highly similar to AdcA, AdcAII contains neither the histidine rich loop nor the C terminal domain homologous to ZinT. It can therefore be hypothesised that Pht proteins act by reversibly binding zinc from the external environment and facilitating its diffusion through the cell wall towards the cell membrane, where the high affinity SBPs AdcA and AdcAII can then bind it and deliver it to the permease AdcB. AdcAII may rely on this activity to a greater extent than AdcA, because AdcAII lacks the histidine rich loop and ZinT-like domain that facilitate the acquisition of zinc by the SBP. This would explain the greater impairment in growth of the AdcAII-only containing strain (Δ*adcA*Δ*phtABDE*) than the AdcA-only containing strain (Δ*adcAII*Δ*phtABDE)*. However, further experiments will be required to determine whether Pht proteins and AdcAII do indeed bind to one another or whether the delivery of zinc does not involve a direct interaction.

8.3 Use of Pht proteins as protective immunogens

As mentioned above, clinical trials using PhtD as an immunogen have begun. Numerous experiments testing the ability of Pht proteins to elicit protective immunity in animal models of disease have been undertaken, with the majority, especially for PhtD, demonstrating significant protective effects. However, in Chapter 6, the full length PhtD protein did not show a significantly protective effect in any of the three animal model experiments, despite there being a trend towards protection in each case. The failure to demonstrate significant protection in these experiments compared to the relatively high number of successes seen in the literature may be due to the high virulence of the challenge strains (D39 and P9) used in these experiments. Of course, studies which demonstrate significant protection for a given antigen are more likely to be published than those in

which such protection is not found. Nonetheless, the ability of the PhtD adjunct region to elicit significant protective immunity (as seen in Figure 6.9) warrants further evaluation of this antigen compared to the full length protein, perhaps in models in which protective effects of the full length protein have previously been demonstrated.

More worrying, perhaps, was the observation that vaccination with a combination of PhtD with the pneumolysoid PdT did not significantly increase survival time compared to PdT alone. For an effective protein based-vaccine, it is clear that several proteins will have to be administered in order to confer sufficiently strong protection against invasive disease. These proteins should have additive or synergistic protective effects when given in combination. However, from Figure 6.13 and a previously published study (Ogunniyi *et al*., 2007), this does not appear to be the case with Pht proteins. It will be of great interest to see the results of clinical trials at phase 2 and beyond that are using Pht proteins as immunogens, since this will reveal much more regarding whether the proteins are able to induce sufficient protective immunity in humans for them to be used in an effective vaccine.

8.4 Surface attachment and release of PhtD

Despite encoding a type II signal peptidase cleavage site consensus motif characteristic of lipoproteins, the Pht proteins are associated with the pneumococcal cell wall (Loisel *et al*., 2011). They contain an atypical signal peptide and no known sortase motifs, and hence are thought to attach via a novel mechanism. In this thesis, the amino acids R26, H27 and/or Q28 of PhtD were shown to contribute to the protein's association with the surface. However, a considerable amount of PhtD could be found in the culture supernatants, including of wild-type bacteria. This effect was not specific to one type of growth medium as it was observed when using either THY or C+Y, and occurred to varying extents in all four pneumococcal strains tested. In D39, the proportion of the protein that was found to be extracellular was greater at lower external zinc concentrations (Figure 4.1) and increased throughout the log and stationary phases of growth (Section 7.9). In Section 7.11, a model was proposed in which the Pht proteins are not tightly bound to any molecule on the cell surface, but instead are held in or under the cell wall layer by a combination of weak ionic and/or hydrophobic forces and steric hindrance from the cell wall itself preventing diffusion of the proteins away from the cell surface. This would be in

keeping with observations that, over time, an increasing proportion of the proteins are found in the culture supernatant, including when protein synthesis is not occurring (Section 7.9).

The presence of Pht proteins in culture supernatants has been briefly reported in one publication (Zhang *et al*., 2001), but has otherwise been overlooked. However, this phenomenon could have important implications for our understanding of the role of Pht proteins in pneumococcal pathogenicity (assuming that it occurs for the other Pht proteins as well as PhtD, and that it takes place *in vivo)*. A number of hypotheses can be proposed regarding the role(s) of the released protein molecules. For instance, they may be involved in sequestration of zinc from host cells, engagement of receptors on host cells to trigger inflammatory reactions, regulation of metal homeostasis in the context of pneumococcal biofilms, or binding of factor H or FHL-1 in a conformation that renders them inactive, leading to nonspecific complement deposition in the vicinity of the bacteria and its subsequent depletion. These suggestions are of course speculative, and it should be noted that extracellular forms of Pht proteins are unlikely to mediate their most important functions, because the Δ*phtABDE* mutant strain was severely attenuated compared to wild-type in the *in vivo* competition model (Figure 3.3). This would not be the case if soluble forms of Pht proteins performed the major function(s) of the proteins, since the protein released by the wild-type would be expected to complement the Δ*phtABDE* mutant bacteria, leading to a smaller or no difference in fitness between the two strains and thus competitive indices much closer to one.

As discussed in Section 8.2.2, the Pht proteins appear to play an analogous role to ZinT in facilitating the acquisition of zinc by high affinity SBPs (AdcAII and ZnuA respectively). It is therefore interesting to note that ZinT has been reported to be secreted from the cell when the extracellular availability of the metal ion is low (Ho *et al*., 2008; Gabbianelli *et al*., 2011), as has been found for PhtD in this work; furthermore neither protein can reattach once it has been secreted. The mechanism of export of ZinT is not clear, as there are conflicting reports as to whether the type 2 secretion system is responsible (Ho *et al*., 2008; Gabbianelli *et al*., 2011). It has been suggested that the role of ZinT secretion could be to interact with intestinal epithelial zinc-containing proteins to aid bacterial colonisation by some undefined mechanism. Thus, it will be of interest to

determine whether released forms of the Pht proteins play an analogous role in aiding pneumococcal colonisation of the nasopharynx.

8.5 Future directions

Given that this project included work on a number of different aspects of the biology of Pht proteins, there are a number of potential future directions in which the research could proceed, and as such only a subset of the most promising will be discussed. In terms of the binding of Pht proteins and PspA with FHL-1, it is important that the interaction is measured using a different method, such as microscale thermophoresis (which would circumvent the requirement for one protein to be immobilised). Should binding be detected, dissociation constants for the binding of SCR 1-7 by different Pht proteins and PspA could be measured and compared. It would also be useful to measure dissociation constants for the interaction of these proteins with factor H, since this may help to resolve apparent disagreements in the published literature. Lastly, complement deposition on the mutant strains deficient in Pht proteins, PspA and PspC could also be performed using human serum as the source of complement. Since any human donor is likely to have been colonised at some point in their life by *S. pneumoniae* and have generated antibodies against the bacteria that could interfere with the assay by activating the classical pathway of complement deposition, EGTA and magnesium ions could be included with the serum to inhibit the classical pathway.

To further investigate the hypothesis that Pht proteins facilitate the acquisition of zinc by the zinc-specific SBPs, and AdcAII in particular, kinetic assays examining the uptake of zinc over time (as described by Loisel *et al*. (2011)) could be performed with the mutants lacking combinations of *pht*, *adcA* and *adcAII* genes to see if there are differences between the Δ*adcA* and Δ*adcAII* single mutants and the Δ*adcA*Δ*phtABDE* and Δ*adcAII*Δ*phtABDE* strains. It would also be of interest to perform *in vivo* competition experiments between pairs of these strains, and between the Δ*adcA*Δ*phtABDE* and Δ*adcAII*Δ*phtABDE* mutants in particular, as this would reveal whether the difference between them found in growth curve analysis (Figure 5.4) is reflected in a difference in fitness during infection. This would potentially reveal the importance of the histidine rich loop and ZinT-like domain of AdcA and provide solid evidence either for or against the hypothesis that AdcAII requires Pht proteins to facilitate zinc acquisition.

As discussed in Section 7.11, it would be informative to investigate whether the signal peptide of PhtD with or without R26 to Q31 is sufficient for the association of a different protein with the cell surface. This could be done by cloning the signal peptide with or without nucleotides encoding R26 to Q31 upstream of a tag protein, inserting the construct into Δ*phtABDE* pneumococci, and determining whether the tag is surface localised by flow cytometry and Western blotting. Looking for the presence of the protein in the culture supernatant would also provide insight into whether the release of PhtD is dependent upon its signal peptide region, or whether other regions of the protein are required for this phenomenon. Furthermore, the model of Pht proteins being only loosely held in or under the cell wall layer by a combination of weak ionic or hydrophobic forces and steric hindrance from the cell wall preventing their diffusion away from the surface could be tested by mechanically lysing a culture of bacteria (e.g. using a French pressure cell), separating cell debris from supernatant by ultracentrifugation, and performing Western blotting on the two fractions. If the proteins are tightly bound to the cell wall, they would be expected to mostly be found in the pellet fraction, whereas if the model is correct, the majority should be found in the supernatant fraction.

It is both surprising and fascinating that the pneumococcus encodes a family of four highly related proteins each with so many histidine triad motifs. Why should this be the case? If the four proteins are entirely redundant in function, production of all of them would surely represent a wasteful metabolic burden that would have been removed by natural selection. This implies that the proteins must exhibit some differences in function, despite their high similarity. Clearly, further structural and functional characterisation of individual Pht protein family members will be an important area for future study.

References

Adamou, J.E., Heinrichs, J.H., Erwin, A.L., Walsh, W., Gayle, T., Dormitzer, M., Dagan, R., Brewah, Y.A., Barren, P., Lathigra, R., *et al*. (2001). Identification and characterization of a novel family of pneumococcal proteins that are protective against sepsis. Infect. Immun. *69*, 949–958.

Agarwal, V., Asmat, T.M., Luo, S., Jensch, I., Zipfel, P.F., and Hammerschmidt, S. (2010). Complement regulator factor H mediates a two-step uptake of *Streptococcus pneumoniae* by human cells. J. Biol. Chem.

Agency for Healthcare Research and Quality (AHRQ) (2010). Management of acute otitis media: evidence report/technology assessment number 15.

Alexander, J.E., Lock, R.A., Peeters, C.C., Poolman, J.T., Andrew, P.W., Mitchell, T.J., Hansman, D., and Paton, J.C. (1994). Immunization of mice with pneumolysin toxoid confers a significant degree of protection against at least nine serotypes of *Streptococcus pneumoniae*. Infect. Immun. *62*, 5683–5688.

Ali, Y.M., Lynch, N.J., Haleem, K.S., Fujita, T., Endo, Y., Hansen, S., Holmskov, U., Takahashi, K., Stahl, G.L., Dudler, T., *et al*. (2012). The lectin pathway of complement activation is a critical component of the innate immune response to pneumococcal infection. PLoS Pathog. *8*, e1002793.

American Academy of Pediatrics and American Academy of Family Physicians (2004). Diagnosis and management of acute otitis media. Pediatrics *113*, 1451–1465.

Anderton, J.M., Rajam, G., Romero-Steiner, S., Summer, S., Kowalczyk, A.P., Carlone, G.M., Sampson, J.S., and Ades, E.W. (2007). E-cadherin is a receptor for the common protein pneumococcal surface adhesin A (PsaA) of *Streptococcus pneumoniae*. Microb. Pathog. *42*, 225–236.

Andreini, C., Banci, L., Bertini, I., and Rosato, A. (2006). Zinc through the three domains of life. J. Proteome Res. *5*, 3173–3178.

Arlaud, G.J., Barlow, P.N., Gaboriaud, C., Gros, P., and Narayana, S. V (2007). Deciphering complement mechanisms: the contributions of structural biology. Mol. Immunol. *44*, 3809–3822.

Aslam, M., and Perkins, S.J. (2001). Folded-back solution structure of monomeric factor H of human complement by synchrotron X-ray and neutron scattering, analytical ultracentrifugation and constrained molecular modelling. J. Mol. Biol. *309*, 1117–1138.

Avery, O.T., Macleod, C.M., and McCarty, M. (1944). Studies on the chemical nature of the substance inducing transformation of pneumococcal types : induction of transformation by a desoxyribonucleic acid fraction isolated from pneumococcus type III. J. Exp. Med. *79*, 137–158.

Balachandran, P., Hollingshead, S.K., Paton, J.C., and Briles, D.E. (2001). The autolytic enzyme LytA of *Streptococcus pneumoniae* is not responsible for releasing pneumolysin. J Bacteriol. *183*, 3108–3116.

Van Bambeke, F., Reinert, R.R., Appelbaum, P.C., Tulkens, P.M., and Peetermans, W.E. (2007). Multidrug-resistant *Streptococcus pneumoniae* infections: current and future therapeutic options. Drugs *67*, 2355–2382.

Bayle, L., Chimalapati, S., Schoehn, G., Brown, J., Vernet, T., and Durmort, C. (2011). Zinc uptake by *Streptococcus pneumoniae* depends on both AdcA and AdcAII and is essential for normal bacterial morphology and virulence. Mol. Microbiol. *82*, 904–916.

Bergmann, S., Rohde, M., Chhatwal, G.S., and Hammerschmidt, S. (2001). alpha-Enolase of *Streptococcus pneumoniae* is a plasmin(ogen)-binding protein displayed on the bacterial cell surface. Mol. Microbiol. *40*, 1273–1287.

Berntsson, R.P.-A., Smits, S.H.J., Schmitt, L., Slotboom, D.-J., and Poolman, B. (2010). A structural classification of substrate-binding proteins. FEBS Lett. *584*, 2606–2617.

Berry, A.M., Alexander, J.E., Mitchell, T.J., Andrew, P.W., Hansman, D., and Paton, J.C. (1995). Effect of defined point mutations in the pneumolysin gene on the virulence of *Streptococcus pneumoniae*. Infect. Immun. *63*, 1969–1974.

Berry, A.M., and Paton, J.C. (1996). Sequence heterogeneity of PsaA, a 37-kilodalton putative adhesin essential for virulence of *Streptococcus pneumoniae*. Infect. Immun. *64*, 5255–5262.

Berry, A.M., Yother, J., Briles, D.E., Hansman, D., and Paton, J.C. (1989). Reduced virulence of a defined pneumolysin-negative mutant of *Streptococcus pneumoniae*. Infect. Immun. *57*, 2037–2042.

Blackmore, T.K., Fischetti, V.A., Sadlon, T.A., Ward, H.M., and Gordon, D.L. (1998). M protein of the group A *Streptococcus* binds to the seventh short consensus repeat of human complement factor H. Infect. Immun. *66*, 1427–1431.

Bogaert, D., De Groot, R., and Hermans, P.W. (2004). *Streptococcus pneumoniae* colonisation: the key to pneumococcal disease. Lancet Infect. Dis. *4*, 144–154.

Bologa, M., Kamtchoua, T., Hopfer, R., Sheng, X., Hicks, B., Plevic, V., Yuan, T., and Gurunathan, S. (2012). Safety and immunogenicity of pneumococcal protein vaccine candidates: monovalent choline-binding protein A (PcpA) vaccine and bivalent PcpA-pneumococcal histidine triad protein D vaccine. Vaccine *30*, 7461–7468.

Briles, D.E., Ades, E., Paton, J.C., Sampson, J.S., Carlone, G.M., Huebner, R.C., Virolainen, A., Swiatlo, E., and Hollingshead, S.K. (2000). Intranasal immunization of mice with a mixture of the pneumococcal proteins PsaA and PspA is highly protective against nasopharyngeal carriage of *Streptococcus pneumoniae*. Infect. Immun. *68*, 796–800.

Briles, D.E., and Hollingshead, S.K. (2006). Surface proteins of *Streptococcus pneumoniae*: their roles in virulence and potential as vaccines. In Program and Abstracts of the 2006 Euroconference on Infections and Lung Diseases, (Paris, France.),.

Briles, D.E., Hollingshead, S.K., Paton, J.C., Ades, E.W., Novak, L., Van Ginkel, F.W., and Benjamin Jr., W.H. (2003). Immunizations with pneumococcal surface protein A and pneumolysin are protective against pneumonia in a murine model of pulmonary infection with *Streptococcus pneumoniae*. J. Infect. Dis. *188*, 339–348.

Briles, D.E., Nahm, M., Schroer, K., Davie, J., Baker, P., Kearney, J., and Barletta, R. (1981). Antiphosphocholine antibodies found in normal mouse serum are protective against intravenous infection with type 3 *Streptococcus pneumoniae*. J. Exp. Med. *153*, 694–705.

Briles, D.E., Tart, R.C., Wu, H.Y., Ralph, B.A., Russell, M.W., and McDaniel, L.S. (1996). Systemic and mucosal protective immunity to pneumococcal surface protein A. Ann. N. Y. Acad. Sci. *797*, 118–126.

Brooks-Walter, A., Briles, D.E., and Hollingshead, S.K. (1999). The pspC gene of *Streptococcus pneumoniae* encodes a polymorphic protein, PspC, which elicits cross-reactive antibodies to PspA and provides immunity to pneumococcal bacteremia. Infect. Immun. *67*, 6533–6542.

Brown, J.S., Hussell, T., Gilliland, S.M., Holden, D.W., Paton, J.C., Ehrenstein, M.R., Walport, M.J., and Botto, M. (2002). The classical pathway is the dominant complement pathway required for innate immunity to *Streptococcus pneumoniae* infection in mice. Proc. Natl. Acad. Sci. USA *99*, 16969–16974.

Brundage, J.F., and Shanks, G.D. (2008). Deaths from bacterial pneumonia during 1918-19 influenza pandemic. Emerg. Infect. Dis. *14*, 1193–1199.

Buhé, V., Loisel, S., Pers, J.O., Le Ster, K., Berthou, C., and Youinou, P. (2010). Updating the physiology, exploration and disease relevance of complement factor H. Int. J. Immunopathol. Pharmacol. *23*, 397–404.

Chen, H., Ma, Y., Yang, J., O'Brien, C.J., Lee, S.L., Mazurkiewicz, J.E., Haataja, S., Yan, J.-H., Gao, G.F., and Zhang, J.-R. (2008). Genetic requirement for pneumococcal ear infection. PLoS One *3*, e2950.

Chien, Y.-W., Klugman, K.P., and Morens, D.M. (2009). Bacterial pathogens and death during the 1918 influenza pandemic. N. Engl. J. Med. *361*, 2582–2583.

Chien, Y.-W., Klugman, K.P., and Morens, D.M. (2010). Efficacy of whole-cell killed bacterial vaccines in preventing pneumonia and death during the 1918 influenza pandemic. J. Infect. Dis. *202*, 1639–1648.

Cognet, I., De Coignac, A.B., Magistrelli, G., Jeannin, P., Aubry, J.P., Maisnier-Patin, K., Caron, G., Chevalier, S., Humbert, F., Nguyen, T., *et al*. (2003). Expression of recombinant proteins in a lipid A mutant of *Escherichia coli* BL21 with a strongly reduced

capacity to induce dendritic cell activation and maturation. J. Immunol. Methods. *272*, 199–210.

Compton, L.A., and Johnson, W.C. (1986). Analysis of protein circular dichroism spectra for secondary structure using a simple matrix multiplication. Anal. Biochem. *155*, 155–167.

Cummings, M.D., Farnum, M.A., and Nelen, M.I. (2006). Universal screening methods and applications of ThermoFluor. J. Biomol. Screen. *11*, 854–863.

Cundell, D.R., Gerard, N.P., Gerard, C., Idanpaan-Heikkila, I., and Tuomanen, E.I. (1995). *Streptococcus pneumoniae* anchor to activated human cells by the receptor for platelet-activating factor. Nature *377*, 435–438.

Dave, S., Brooks-Walter, A., Pangburn, M.K., and McDaniel, L.S. (2001). PspC, a pneumococcal surface protein, binds human factor H. Infect. Immun. *69*, 3435–3437.

Denoël, P., Godfroid, F., Hermand, P., Verlant, V., and Poolman, J. (2011a). Combined protective effects of anti-PhtD and anti-pneumococcal polysaccharides. Vaccine *29*, 6451–6453.

Denoël, P., Philipp, M.T., Doyle, L., Martin, D., Carletti, G., and Poolman, J.T. (2011b). A protein-based pneumococcal vaccine protects rhesus macaques from pneumonia after experimental infection with *Streptococcus pneumoniae*. Vaccine *29*, 5495–5501.

Dintilhac, A., Alloing, G., Granadel, C., and Claverys, J.P. (1997). Competence and virulence of *Streptococcus pneumoniae*: Adc and PsaA mutants exhibit a requirement for Zn and Mn resulting from inactivation of putative ABC metal permeases. Mol. Microbiol. *25*, 727–739.

Dintilhac, A., and Claverys, J.P. (1997). The *adc* locus, which affects competence for genetic transformation in *Streptococcus pneumoniae*, encodes an ABC transporter with a putative lipoprotein homologous to a family of streptococcal adhesins. Res. Microbiol. *148*, 119–131.

Douglas, R.M., Paton, J.C., Duncan, S.J., and Hansman, D.J. (1983). Antibody response to pneumococcal vaccination in children younger than five years of age. J. Infect. Dis. *148*, 131–137.

Duthy, T.G., Ormsby, R.J., Giannakis, E., Ogunniyi, A.D., Stroeher, U.H., Paton, J.C., and Gordon, D.L. (2002). The human complement regulator factor H binds pneumococcal surface protein PspC via short consensus repeats 13 to 15. Infect. Immun. *70*, 5604–5611.

Elsner, A., Kreikemeyer, B., Braun-Kiewnick, A., Spellerberg, B., Buttaro, B.A., and Podbielski, A. (2002). Involvement of Lsp, a member of the LraI-lipoprotein family in *Streptococcus pyogenes*, in eukaryotic cell adhesion and internalization. Infect. Immun. *70*, 4859–4869.

Enserink, M. (2009). Global health. Some neglected diseases are more neglected than others. Science *323*, 700.

Felmingham, D., Cantón, R., and Jenkins, S.G. (2007). Regional trends in beta-lactam, macrolide, fluoroquinolone and telithromycin resistance among *Streptococcus pneumoniae* isolates 2001-2004. J. Infect. *55*, 111–118.

Ferreira, D.M., Jambo, K.C., and Gordon, S.B. (2011). Experimental human pneumococcal carriage models for vaccine research. Trends Microbiol. *19*, 464–470.

Ferreira, D.M., Oliveira, M.L.S., Moreno, A.T., Ho, P.L., Briles, D.E., and Miyaji, E.N. (2010). Protection against nasal colonization with *Streptococcus pneumoniae* by parenteral immunization with a DNA vaccine encoding PspA (Pneumococcal surface protein A). Microb. Pathog. *48*, 205–213.

Fischer Walker, C., and Black, R.E. (2004). Zinc and the risk for infectious disease. Annu. Rev. Nutr. *24*, 255–275.

Gabbianelli, R., Scotti, R., Ammendola, S., Petrarca, P., Nicolini, L., and Battistoni, A. (2011). Role of ZnuABC and ZinT in *Escherichia coli* O157:H7 zinc acquisition and interaction with epithelial cells. BMC Microbiol. *11*, 36.

Giannakis, E., Jokiranta, T.S., Male, D.A., Ranganathan, S., Ormsby, R.J., Fischetti, V.A., Mold, C., and Gordon, D.L. (2003). A common site within factor H SCR 7 responsible for binding heparin, C-reactive protein and streptococcal M protein. Eur. J. Immunol. *33*, 962–969.

Giannakis, E., Male, D.A., Ormsby, R.J., Mold, C., Jokiranta, T.S., Ranganathan, S., and Gordon, D.L. (2001). Multiple ligand binding sites on domain seven of human complement factor H. Int. Immunopharmacol. *1*, 433–443.

Giefing, C., Meinke, A.L., Hanner, M., Henics, T., Bui, M.D., Gelbmann, D., Lundberg, U., Senn, B.M., Schunn, M., Habel, A., *et al*. (2008). Discovery of a novel class of highly conserved vaccine antigens using genomic scale antigenic fingerprinting of pneumococcus with human antibodies. J. Exp. Med. *205*, 117–131.

Godfroid, F., Hermand, P., Verlant, V., Denoël, P., and Poolman, J.T. (2011). Preclinical evaluation of the Pht proteins as potential cross-protective pneumococcal vaccine antigens. Infect. Immun. *79*, 238–245.

Goujon, M., McWilliam, H., Li, W., Valentin, F., Squizzato, S., Paern, J., and Lopez, R. (2010). A new bioinformatics analysis tools framework at EMBL-EBI. Nucleic Acids Res. *38*, W695–699.

Graham, R.M., and Paton, J.C. (2006). Differential role of CbpA and PspA in modulation of *in vitro* CXC chemokine responses of respiratory epithelial cells to infection with *Streptococcus pneumoniae*. Infect. Immun. *74*, 6739–6749.

Gray, B.M., and Dillon, H.C. (1986). Clinical and epidemiologic studies of pneumococcal infection in children. Pediatr. Infect. Dis. *5*, 201–207.

Hamel, J., Charland, N., Pineau, I., Ouellet, C., Rioux, S., Martin, D., and Brodeur, B.R. (2004). Prevention of pneumococcal disease in mice immunized with conserved surface-accessible proteins. Infect. Immun. *72*, 2659–2670.

Hammerschmidt, S., Bethe, G., Remane, P.H., and Chhatwal, G.S. (1999). Identification of pneumococcal surface protein A as a lactoferrin-binding protein of *Streptococcus pneumoniae*. Infect. Immun. *67*, 1683–1687.

Hammerschmidt, S., Talay, S.R., Brandtzaeg, P., and Chhatwal, G.S. (1997). SpsA, a novel pneumococcal surface protein with specific binding to secretory immunoglobulin A and secretory component. Mol. Microbiol. *25*, 1113–1124.

Hammerschmidt, S., Wolff, S., Hocke, A., Rosseau, S., Müller, E., and Rohde, M. (2005). Illustration of pneumococcal polysaccharide capsule during adherence and invasion of epithelial cells. Infect. Immun. *73*, 4653–4667.

Hansman, D., Glasgow, H., Sturt, J., Devitt, L., and Douglas, R. (1971). Increased resistance to penicillin of pneumococci isolated from man. N. Engl. J. Med. *284*, 175–177.

Harvey, R.M., Ogunniyi, A.D., Chen, A.Y., and Paton, J.C. (2011a). Pneumolysin with low hemolytic activity confers an early growth advantage to *Streptococcus pneumoniae* in the blood. Infect. Immun. *79*, 4122–4130.

Harvey, R.M., Stroeher, U.H., Ogunniyi, A.D., Smith-Vaughan, H.C., Leach, A.J., and Paton, J.C. (2011b). A variable region within the genome of *Streptococcus pneumoniae* contributes to strain-strain variation in virulence. PLoS One *6*, e19650.

Hava, D.L., and Camilli, A. (2002). Large-scale identification of serotype 4 *Streptococcus pneumoniae* virulence factors. Mol. Microbiol. *45*, 1389–1406.

Hava, LeMieux, J., and Camilli, A. (2003). From nose to lung: the regulation behind *Streptococcus pneumoniae* virulence factors. Mol. Microbiol. *50*, 1103–1110.

Hedge, R.S., and Bernstein, H.D. (2006). The surprising complexity of signal sequences. Trends Biochem. Sci. *31*, 563–571.

Hellwage, J., Kuhn, S., and Zipfel, P.F. (1997). The human complement regulatory factor-H-like protein 1, which represents a truncated form of factor H, displays cell-attachment activity. Biochem J. *326 Pt 2*, 321–327.

Henderson, B., and Martin, A. (2011). Bacterial virulence in the moonlight: multitasking bacterial moonlighting proteins are virulence determinants in infectious disease. Infect. Immun. *79*, 3476–3491.

Ho, T.D., Davis, B.M., Ritchie, J.M., and Waldor, M.K. (2008). Type 2 secretion promotes enterohemorrhagic *Escherichia coli* adherence and intestinal colonization. Infect. Immun. *76*, 1858–1865.

Hollingshead, S.K., Becker, R., and Briles, D.E. (2000). Diversity of PspA: mosaic genes and evidence for past recombination in *Streptococcus pneumoniae*. Infect. Immun. *68*, 5889–5900.

Holmlund, E., Quiambao, B., Ollgren, J., Jaakkola, T., Neyt, C., Poolman, J., Nohynek, H., and Kayhty, H. (2009). Antibodies to pneumococcal proteins PhtD, CbpA, and LytC in Filipino pregnant women and their infants in relation to pneumococcal carriage. Clin. Vaccine Immunol. *16*, 916–923.

Holmlund, E., Simell, B., Jaakkola, T., Lahdenkari, M., Hamel, J., Brodeur, B., Kilpi, T., and Kayhty, H. (2007). Serum antibodies to the pneumococcal surface proteins PhtB and PhtE in Finnish infants and adults. Pediatr. Infect. Dis. J. *26*, 447–449.

Hood, M.I., and Skaar, E.P. (2012). Nutritional immunity: transition metals at the pathogen–host interface. Nat. Rev. Microbiol. *10*, 525–537.

Hovis, K.M., Freedman, J.C., Zhang, H., Forbes, J.L., and Marconi, R.T. (2008). Identification of an antiparallel coiled-coil/loop domain required for ligand binding by the *Borrelia hermsii* FhbA protein: additional evidence for the role of FhbA in the host-pathogen interaction. Infect. Immun. *76*, 2113–2122.

Hsu, H.E., Shutt, K.A., Moore, M.R., Beall, B.W., Bennett, N.M., Craig, A.S., Farley, M.M., Jorgensen, J.H., Lexau, C.A., Petit, S., *et al*. (2009). Effect of pneumococcal conjugate vaccine on pneumococcal meningitis. N. Engl. J. Med. *360*, 244–256.

Ibrahim, Y.M., Kerr, A.R., Silva, N.A., and Mitchell, T.J. (2005). Contribution of the ATP-dependent protease ClpCP to the autolysis and virulence of *Streptococcus pneumoniae*. Infect. Immun. *73*, 730–740.

Janulczyk, R., Iannelli, F., Sjoholm, A.G., Pozzi, G., and Bjorck, L. (2000). Hic, a novel surface protein of *Streptococcus pneumoniae* that interferes with complement function. J. Biol. Chem. *275*, 37257–37263.

Jarva, H., Janulczyk, R., Hellwage, J., Zipfel, P.F., Björck, L., and Meri, S. (2002). *Streptococcus pneumoniae* evades complement attack and opsonophagocytosis by expressing the pspC locus-encoded Hic protein that binds to short consensus repeats 8-11 of factor H. J. Immunol. *168*, 1886–1894.

Jedrzejas, M.J. (2007). Unveiling molecular mechanisms of bacterial surface proteins: *Streptococcus pneumoniae* as a model organism for structural studies. Cell. Mol. Life. Sci. *64*, 2799–2822.

Jozsi, M., and Zipfel, P.F. (2008). Factor H family proteins and human diseases. Trends Immunol. *29*, 380–387.

Juncker, A.S., Willenbrock, H., Von Heijne, G., Brunak, S., Nielsen, H., and Krogh, A. (2003). Prediction of lipoprotein signal peptides in Gram-negative bacteria. Protein Sci. *12*, 1652–1662.

Kadioglu, A., and Andrew, P.W. (2005). Susceptibility and resistance to pneumococcal disease in mice. Brief. Funct. Genomic. Proteomic. *4*, 241–247.

Kadioglu, A., Weiser, J.N., Paton, J.C., and Andrew, P.W. (2008). The role of *Streptococcus pneumoniae* virulence factors in host respiratory colonization and disease. Nat. Rev. Microbiol. *6*, 288–301.

Kaluarachchi, H., Chan Chung, K.C., and Zamble, D.B. (2010). Microbial nickel proteins. Nat. Prod. Rep. *27*, 681–694.

Kehl-Fie, T.E., Chitayat, S., Hood, M.I., Damo, S., Restrepo, N., Garcia, C., Munro, K.A., Chazin, W.J., and Skaar, E.P. (2011). Nutrient metal sequestration by calprotectin inhibits bacterial superoxide defense, enhancing neutrophil killing of *Staphylococcus aureus*. Cell Host Microbe *10*, 158–164.

Kehl-Fie, T.E., and Skaar, E.P. (2010). Nutritional immunity beyond iron: a role for manganese and zinc. Curr. Opin. Chem. Biol. *14*, 218–224.

Khan, M.N., and Pichichero, M.E. (2012). Vaccine candidates PhtD and PhtE of *Streptococcus pneumoniae* are adhesins that elicit functional antibodies in humans. Vaccine *30*, 2900–2907.

Kim, J.O., and Weiser, J.N. (1998). Association of intrastrain phase variation in quantity of capsular polysaccharide and teichoic acid with the virulence of *Streptococcus pneumoniae*. J. Infect. Dis. *177*, 368–377.

Kirkham, L.-A.S., Jefferies, J.M.C., Kerr, A.R., Jing, Y., Clarke, S.C., Smith, A., and Mitchell, T.J. (2006). Identification of invasive serotype 1 pneumococcal isolates that express nonhemolytic pneumolysin. J. Clin. Microbiol. *44*, 151–159.

Kloosterman, T.G., Van der Kooi-Pol, M.M., Bijlsma, J.J., and Kuipers, O.P. (2007). The novel transcriptional regulator SczA mediates protection against Zn2+ stress by activation of the Zn2+-resistance gene *czcD* in *Streptococcus pneumoniae*. Mol. Microbiol. *65*, 1049–1063.

Kloosterman, T.G., and Kuipers, O.P. (2011). Regulation of arginine acquisition and virulence gene expression in the human pathogen *Streptococcus pneumoniae* by transcription regulators ArgR1 and AhrC. J. Biol. Chem. *286*, 44594–44605.

Koppe, U., Suttorp, N., and Opitz, B. (2012). Recognition of *Streptococcus pneumoniae* by the innate immune system. Cell. Microbiol. *14*, 460–466.

Kraiczy, P., Skerka, C., Brade, V., and Zipfel, P.F. (2001). Further characterization of complement regulator-acquiring surface proteins of *Borrelia burgdorferi*. Infect. Immun. *69*, 7800–7809.

Kuhn, S., and Zipfel, P.F. (1996). Mapping of the domains required for decay acceleration activity of the human factor H-like protein 1 and factor H. Eur. J. Immunol. *26*, 2383–2387.

Kunin, C.M. (1993). Resistance to antimicrobial drugs--a worldwide calamity. Ann. Intern. Med. *118*, 557–561.

Kunitomo, E., Terao, Y., Okamoto, S., Rikimaru, T., Hamada, S., and Kawabata, S. (2008). Molecular and biological characterization of histidine triad protein in group A streptococci. Microbes Infect. *10*, 414–423.

Lacks, S., and Hotchkiss, R.D. (1960). A study of the genetic material determining an enzyme in Pneumococcus. Biochim. Biophys. Acta *39*, 508–518.

Lacks, S., and Neuberger, M. (1975). Membrane location of a deoxyribonuclease implicated in the genetic transformation of Diplococcus pneumoniae. J. Bacteriol. *124*, 1321–1329.

Larkin, M.A., Blackshields, G., Brown, N.P., Chenna, R., McGettigan, P.A., McWilliam, H., Valentin, F., Wallace, I.M., Wilm, A., Lopez, R., *et al*. (2007). Clustal W and Clustal X version 2.0. Bioinformatics *23*, 2947–2948.

Lau, G.W., Haataja, S., Lonetto, M., Kensit, S.E., Marra, A., Bryant, A.P., McDevitt, D., Morrison, D.A., and Holden, D.W. (2001). A functional genomic analysis of type 3 *Streptococcus pneumoniae* virulence. Mol. Microbiol. *40*, 555–571.

Li, Q., Li, Y.X., Douthitt, K., Stahl, G.L., Thurman, J.M., and Tong, H.H. (2012). Role of the alternative and classical complement activation pathway in complement mediated killing against *Streptococcus pneumoniae* colony opacity variants during acute pneumococcal otitis media in mice. Microbes Infect. *14*, 1308–1318.

Lim, J., Lee, K.-M., Kim, S.H., Kim, Y., Kim, S.-H., Park, W., and Park, S. (2011). YkgM and ZinT proteins are required for maintaining intracellular zinc concentration and producing curli in enterohemorrhagic *Escherichia coli* (EHEC) O157:H7 under zinc deficient conditions. Int. J. Food Microbiol. *149*, 159–170.

Lipsitch, M. (1997). Vaccination against colonizing bacteria with multiple serotypes. Proc. Natl. Acad. Sci. USA *94*, 6571–6576.

Lock, R.A., Zhang, Q.Y., Berry, A.M., and Paton, J.C. (1996). Sequence variation in the *Streptococcus pneumoniae* pneumolysin gene affecting haemolytic activity and electrophoretic mobility of the toxin. Microb. Pathog. *21*, 71–83.

Loisel, E., Chimalapati, S., Bougault, C., Imberty, A., Gallet, B., Di Guilmi, A.M., Brown, J., Vernet, T., and Durmort, C. (2011). Biochemical characterization of the histidine triad protein PhtD as a cell surface zinc-binding protein of pneumococcus. Biochemistry *50*, 3551–3558.

Loisel, E., Jacquamet, L., Serre, L., Bauvois, C., Ferrer, J.L., Vernet, T., Di Guilmi, A.M., and Durmort, C. (2008). AdcAII, a new pneumococcal Zn-binding protein homologous with ABC transporters: biochemical and structural analysis. J. Mol. Biol. *381*, 594–606.

Lu, L., Ma, Z., Jokiranta, T.S., Whitney, A.R., DeLeo, F.R., and Zhang, J.R. (2008a). Species-specific interaction of *Streptococcus pneumoniae* with human complement factor H. J. Immunol. *181*, 7138–7146.

Lu, Y.J., Gross, J., Bogaert, D., Finn, A., Bagrade, L., Zhang, Q., Kolls, J.K., Srivastava, A., Lundgren, A., Forte, S., *et al*. (2008b). Interleukin-17A mediates acquired immunity to pneumococcal colonization. PLoS Pathog. *4*, e1000159.

Lu, Y.J., Leite, L., Gonçalves, V.M., Dias, W. de O., Liberman, C., Fratelli, F., Alderson, M., Tate, A., Maisonneuve, J.-F., Robertson, G., *et al*. (2010a). GMP-grade pneumococcal whole-cell vaccine injected subcutaneously protects mice from nasopharyngeal colonization and fatal aspiration-sepsis. Vaccine *28*, 7468–7475.

Lu, Y.J., Yadav, P., Clements, J.D., Forte, S., Srivastava, A., Thompson, C.M., Seid, R., Look, J., Alderson, M., Tate, A., *et al*. (2010b). Options for inactivation, adjuvant, and route of topical administration of a killed, unencapsulated pneumococcal whole-cell vaccine. Clin. Vaccine Immunol. *17*, 1005–1012.

Lupas, A., Van Dyke, M., and Stock, J. (1991). Predicting coiled coils from protein sequences. Science *252*, 1162–1164.

Macomber, L., and Hausinger, R.P. (2011). Mechanisms of nickel toxicity in microorganisms. Metallomics *3*, 1153–1162.

Malley, R. (2010). Antibody and cell-mediated immunity to *Streptococcus pneumoniae*: implications for vaccine development. J. Mol. Med. *88*, 135–142.

Malley, R., and Anderson, P.W. (2012). Serotype-independent pneumococcal experimental vaccines that induce cellular as well as humoral immunity. Proc. Natl. Acad. Sci. USA *109*, 3623–3627.

Malley, R., Henneke, P., Morse, S.C., Cieslewicz, M.J., Lipsitch, M., Thompson, C.M., Kurt-Jones, E., Paton, J.C., Wessels, M.R., and Golenbock, D.T. (2003). Recognition of pneumolysin by Toll-like receptor 4 confers resistance to pneumococcal infection. Proc. Natl. Acad. Sci. USA *100*, 1966–1971.

Malley, R., Lipsitch, M., Stack, A., Saladino, R., Fleisher, G., Pelton, S., Thompson, C., Briles, D., and Anderson, P. (2001). Intranasal immunization with killed unencapsulated whole cells prevents colonization and invasive disease by capsulated pneumococci. Infect. Immun. *69*, 4870–4873.

Malley, R., Trzcinski, K., Srivastava, A., Thompson, C.M., Anderson, P.W., and Lipsitch, M. (2005). CD4+ T cells mediate antibody-independent acquired immunity to pneumococcal colonization. Proc. Natl. Acad. Sci. USA *102*, 4848–4853.

Marra, A., Asundi, J., Bartilson, M., Lawson, S., Fang, F., Christine, J., Wiesner, C., Brigham, D., Schneider, W.P., and Hromockyj, A.E. (2002). Differential fluorescence induction analysis of *Streptococcus pneumoniae* identifies genes involved in pathogenesis. Infect. Immun. *70*, 1422–1433.

Marriott, H.M., Mitchell, T.J., and Dockrell, D.H. (2008). Pneumolysin: a double-edged sword during the host-pathogen interaction. Curr. Mol. Med. *8*, 497–509.

Martoglio, B., and Dobberstein, B. (1998). Signal sequences: more than just greasy peptides. Trends Cell Biol. *8*, 410–415.

Maruvada, R., Prasadarao, N. V, and Rubens, C.E. (2009). Acquisition of factor H by a novel surface protein on group B *Streptococcus* promotes complement degradation. FASEB J. *23*, 3967–3977.

McAllister, L.J., Ogunniyi, A.D., Stroeher, U.H., Leach, A.J., and Paton, J.C. (2011). Contribution of serotype and genetic background to virulence of serotype 3 and serogroup 11 pneumococcal isolates. Infect. Immun. *79*, 4839–4849.

McAllister, L.J., Tseng, H.J., Ogunniyi, A.D., Jennings, M.P., McEwan, A.G., and Paton, J.C. (2004). Molecular analysis of the psa permease complex of *Streptococcus pneumoniae*. Mol. Microbiol. *53*, 889–901.

McDaniel, L.S., Ralph, B.A., McDaniel, D.O., and Briles, D.E. (1994). Localization of protection-eliciting epitopes on PspA of *Streptococcus pneumoniae* between amino acid residues 192 and 260. Microb. Pathog. *17*, 323–337.

McDaniel, L.S., Scott, G., Kearney, J.F., and Briles, D.E. (1984). Monoclonal antibodies against protease-sensitive pneumococcal antigens can protect mice from fatal infection with *Streptococcus pneumoniae*. J. Exp. Med. *160*, 386–397.

McDaniel, L.S., Scott, G., Widenhofer, K., Carroll, J.M., and Briles, D.E. (1986). Analysis of a surface protein of *Streptococcus pneumoniae* recognised by protective monoclonal antibodies. Microb. Pathog. *1*, 519–531.

McDevitt, C.A., Ogunniyi, A.D., Valkov, E., Lawrence, M.C., Kobe, B., McEwan, A.G., and Paton, J.C. (2011). A molecular mechanism for bacterial susceptibility to zinc. PLoS Pathog. *7*, e1002357.

McDowell, J. V, Huang, B., Fenno, J.C., and Marconi, R.T. (2009). Analysis of a unique interaction between the complement regulatory protein factor H and the periodontal pathogen *Treponema denticola*. Infect. Immun. *77*, 1417–1425.

McDowell, J. V, Wolfgang, J., Senty, L., Sundy, C.M., Noto, M.J., and Marconi, R.T. (2004). Demonstration of the involvement of outer surface protein E coiled coil structural domains and higher order structural elements in the binding of infection-induced antibody and the complement-regulatory protein, factor H. J. Immunol. *173*, 7471–7480.

Melin, M., E, D.I.P., Tikkanen, L., Jarva, H., Neyt, C., Kayhty, H., Meri, S., Poolman, J., and Vakevainen, M. (2010). Interaction of pneumococcal histidine triad proteins with human complement. Infect. Immun. *78*, 2089–2098.

Meng, J.P., Yin, Y.B., Zhang, X.M., Huang, Y.S., Lan, K., Cui, F., and Xu, S.X. (2008). Identification of *Streptococcus pneumoniae* genes specifically induced in mouse lung tissues. Can. J. Microbiol. *54*, 58–65.

Mitchell, A.M., and Mitchell, T.J. (2010). *Streptococcus pneumoniae*: virulence factors and variation. Clin. Microbiol. Infect. *16*, 411–418.

Moffitt, K.L., Gierahn, T.M., Lu, Y., Gouveia, P., Alderson, M., Flechtner, J.B., Higgins, D.E., and Malley, R. (2011). T(H)17-based vaccine design for prevention of *Streptococcus pneumoniae* colonization. Cell Host Microbe *9*, 158–165.

Moffitt, K.L., and Malley, R. (2011). Next generation pneumococcal vaccines. Curr. Opin. Immunol. *23*, 407–413.

Molzen, T.E., Burghout, P., Bootsma, H.J., Brandt, C.T., Van der Gaast-de Jongh, C.E., Eleveld, M.J., Verbeek, M.M., Frimodt-Møller, N., Østergaard, C., and Hermans, P.W.M. (2011). Genome-wide identification of *Streptococcus pneumoniae* genes essential for bacterial replication during experimental meningitis. Infect. Immun. *79*, 288–297.

Moon, S., Jambert, E., Childs, M., and Von Schoen-Angerer, T. (2011). A win-win solution?: A critical analysis of tiered pricing to improve access to medicines in developing countries. Global. Health *7*, 39.

Moreno, A.T., Oliveira, M.L.S., Ferreira, D.M., Ho, P.L., Darrieux, M., Leite, L.C.C., Ferreira, J.M.C., Pimenta, F.C., Andrade, A.L.S.S., and Miyaji, E.N. (2010). Immunization of mice with single PspA fragments induces antibodies capable of mediating complement deposition on different pneumococcal strains and cross-protection. Clin. Vaccine Immunol. *17*, 439–446.

Morens, D.M., Taubenberger, J.K., and Fauci, A.S. (2008). Predominant role of bacterial pneumonia as a cause of death in pandemic influenza: implications for pandemic influenza preparedness. J. Infect. Dis. *198*, 962–970.

Morona, J.K., Paton, J.C., Miller, D.C., and Morona, R. (2000). Tyrosine phosphorylation of CpsD negatively regulates capsular polysaccharide biosynthesis in *Streptococcus pneumoniae*. Mol. Microbiol. *35*, 1431–1442.

Mukerji, R., Mirza, S., Roche, A.M., Widener, R.W., Croney, C.M., Rhee, D.-K., Weiser, J.N., Szalai, A.J., and Briles, D.E. (2012). Pneumococcal surface protein A inhibits complement deposition on the pneumococcal surface by competing with the binding of C-reactive protein to cell-surface phosphocholine. J. Immunol. *189*, 5327–5335.

Nabors, G.S., Braun, P.A., Herrmann, D.J., Heise, M.L., Pyle, D.J., Gravenstein, S., Schilling, M., Ferguson, L.M., Hollingshead, S.K., Briles, D.E., *et al*. (2000). Immunization of healthy adults with a single recombinant pneumococcal surface protein A (PspA) variant stimulates broadly cross-reactive antibodies to heterologous PspA molecules. Vaccine *18*, 1743–1754.

Nan, R., Farabella, I., Schumacher, F.F., Miller, A., Gor, J., Martin, A.C.R., Jones, D.T., Lengyel, I., and Perkins, S.J. (2011). Zinc binding to the Tyr402 and His402 allotypes of complement factor H: possible implications for age-related macular degeneration. J. Mol. Biol. *408*, 714–735.

Nan, R., Gor, J., Lengyel, I., and Perkins, S.J. (2008). Uncontrolled zinc- and copper-induced oligomerisation of the human complement regulator factor H and its possible implications for function and disease. J. Mol. Biol. *384*, 1341–1352.

Nobbs, A.H., Lamont, R.J., and Jenkinson, H.F. (2009). *Streptococcus* adherence and colonization. Microbiol. Mol. Biol. Rev. *73*, 407–450.

O'Brien, K.L., Wolfson, L.J., Watt, J.P., Henkle, E., Deloria-Knoll, M., McCall, N., Lee, E., Mulholland, K., Levine, O.S., and Cherian, T. (2009). Burden of disease caused by *Streptococcus pneumoniae* in children younger than 5 years: global estimates. Lancet *374*, 893–902.

Ogunniyi, A.D., Folland, R.L., Briles, D.E., Hollingshead, S.K., and Paton, J.C. (2000). Immunization of mice with combinations of pneumococcal virulence proteins elicits enhanced protection against challenge with *Streptococcus pneumoniae*. Infect. Immun. *68*, 3028–3033.

Ogunniyi, A.D., Grabowicz, M., Briles, D.E., Cook, J., and Paton, J.C. (2007). Development of a vaccine against invasive pneumococcal disease based on combinations of virulence proteins of *Streptococcus pneumoniae*. Infect. Immun. *75*, 350–357.

Ogunniyi, A.D., Grabowicz, M., Mahdi, L.K., Cook, J., Gordon, D.L., Sadlon, T.A., and Paton, J.C. (2009). Pneumococcal histidine triad proteins are regulated by the Zn^{2+}-dependent repressor AdcR and inhibit complement deposition through the recruitment of complement factor H. FASEB J. *23*, 731–738.

Ogunniyi, A.D., Mahdi, L.K., Jennings, M.P., McEwan, A.G., McDevitt, C.A., Van der Hoek, M.B., Bagley, C.J., Hoffmann, P., Gould, K.A., and Paton, J.C. (2010). Central role of manganese in regulation of stress responses, physiology and metabolism in *Streptococcus pneumoniae*. J Bacteriol. *192*, 4489–4497.

Ogunniyi, A.D., Mahdi, L.K., Trappetti, C., Verhoeven, N., Mermans, D., Van der Hoek, M.B., Plumptre, C.D., and Paton, J.C. (2012). Identification of genes that contribute to pathogenesis of invasive pneumococcal disease by in vivo transcriptomic analysis. Infect. Immun. *80*, 3268–3278.

Ogunniyi, A.D., Woodrow, M.C., Poolman, J.T., and Paton, J.C. (2001). Protection against *Streptococcus pneumoniae* elicited by immunization with pneumolysin and CbpA. Infect. Immun. *69*, 5997–6003.

Okemefuna, A.I., Gilbert, H.E., Griggs, K.M., Ormsby, R.J., Gordon, D.L., and Perkins, S.J. (2008). The regulatory SCR-1/5 and cell surface-binding SCR-16/20 fragments of factor H reveal partially folded-back solution structures and different self-associative properties. J. Mol. Biol. *375*, 80–101.

Orihuela, C.J., Mahdavi, J., Thornton, J., Mann, B., Wooldridge, K.G., Abouseada, N., Oldfield, N.J., Self, T., Ala'Aldeen, D.A.A., and Tuomanen, E.I. (2009). Laminin receptor initiates bacterial contact with the blood brain barrier in experimental meningitis models. J. Clin. Invest. *119*, 1638–1646.

Orihuela, C.J., Radin, J.N., Sublett, J.E., Gao, G., Kaushal, D., and Tuomanen, E.I. (2004). Microarray analysis of pneumococcal gene expression during invasive disease. Infect. Immun. *72*, 5582–5596.

Outten, C.E., and O'Halloran, T. V (2001). Femtomolar sensitivity of metalloregulatory proteins controlling zinc homeostasis. Science *292*, 2488–2492.

Pandiripally, V., Wei, L., Skerka, C., Zipfel, P.F., and Cue, D. (2003). Recruitment of complement factor H-like protein 1 promotes intracellular invasion by group A streptococci. Infect. Immun. *71*, 7119–7128.

Panina, E.M., Mironov, A.A., and Gelfand, M.S. (2003). Comparative genomics of bacterial zinc regulons: enhanced ion transport, pathogenesis, and rearrangement of ribosomal proteins. Proc. Natl. Acad. Sci. USA *100*, 9912–9917.

Paterson, G.K., and Mitchell, T.J. (2004). The biology of Gram-positive sortase enzymes. Trends Microbiol. *12*, 89–95.

Paterson, G.K., and Orihuela, C.J. (2010). Pneumococci: immunology of the innate host response. Respirology *15*, 1057–1063.

PATH (2011). Factsheet: Accelerating New Vaccine Development Against Pneumonia.

Paton, J.C. (1996). The contribution of pneumolysin to the pathogenicity of *Streptococcus pneumoniae*. Trends Microbiol. *4*, 103–106.

Paton, J.C., and Giammarinaro, P. (2001). Genome-based analysis of pneumococcal virulence factors: the quest for novel vaccine antigens and drug targets. Trends Microbiol. *9*, 515–518.

Paton, J.C., Lock, R.A., and Hansman, D.J. (1983). Effect of immunization with pneumolysin on survival time of mice challenged with *Streptococcus pneumoniae*. Infect. Immun. *40*, 548–552.

Paton, J.C., Lock, R.A., Lee, C.J., Li, J.P., Berry, A.M., Mitchell, T.J., Andrew, P.W., Hansman, D., and Boulnois, G.J. (1991). Purification and immunogenicity of genetically obtained pneumolysin toxoids and their conjugation to *Streptococcus pneumoniae* type 19F polysaccharide. Infect. Immun. *59*, 2297–2304.

Pérez-Dorado, I., Galan-Bartual, S., and Hermoso, J.A. (2012). Pneumococcal surface proteins: when the whole is greater than the sum of its parts. Mol. Oral. Microbiol. *27*, 221–245.

Perkins, S.J., Nan, R., Okemefuna, A.I., Li, K., Khan, S., and Miller, A. (2010). Multiple interactions of complement factor H with its ligands in solution: a progress report. Adv. Exp. Med. Biol. *703*, 25–47.

Petersen, T.N., Brunak, S., Von Heijne, G., and Nielsen, H. (2011). SignalP 4.0: discriminating signal peptides from transmembrane regions. Nat. Methods *8*, 785–786.

Petrarca, P., Ammendola, S., Pasquali, P., and Battistoni, A. (2010). The Zur-regulated ZinT protein is an auxiliary component of the high-affinity ZnuABC zinc transporter that facilitates metal recruitment during severe zinc shortage. J. Bacteriol. *192*, 1553–1564.

Pilishvili, T., Lexau, C., Farley, M.M., Hadler, J., Harrison, L.H., Bennett, N.M., Reingold, A., Thomas, A., Schaffner, W., Craig, A.S., *et al*. (2010). Sustained reductions in invasive pneumococcal disease in the era of conjugate vaccine. J. Infect. Dis. *201*, 32–41.

Plumptre, C.D., Ogunniyi, A.D., and Paton, J.C. (2012). Polyhistidine triad proteins of pathogenic streptococci. Trends Microbiol. *20*, 485–493.

Poehling, K.A., Talbot, T.R., Griffin, M.R., Craig, A.S., Whitney, C.G., Zell, E., Lexau, C.A., Thomas, A.R., Harrison, L.H., Reingold, A.L., *et al*. (2006). Invasive pneumococcal disease among infants before and after introduction of pneumococcal conjugate vaccine. JAMA *295*, 1668–1674.

Polissi, A., Pontiggia, A., Feger, G., Altieri, M., Mottl, H., Ferrari, L., and Simon, D. (1998). Large-scale identification of virulence genes from *Streptococcus pneumoniae*. Infect. Immun. *66*, 5620–5629.

Van der Poll, T., and Opal, S.M. (2009). Pathogenesis, treatment, and prevention of pneumococcal pneumonia. Lancet *374*, 1543–1556.

Prasad, A.S. (2003). Zinc deficiency. BMJ *326*, 409–410.

Price, K.E., and Camilli, A. (2009). Pneumolysin localizes to the cell wall of *Streptococcus pneumoniae*. J. Bacteriol. *191*, 2163–2168.

Price, K.E., Greene, N.G., and Camilli, A. (2012). Export requirements of pneumolysin in *Streptococcus pneumoniae*. J. Bacteriol. *194*, 3651–3660.

Principi, N., Marchisio, P., Schito, G.C., and Mannelli, S. (1999). Risk factors for carriage of respiratory pathogens in the nasopharynx of healthy children. Ascanius Project Collaborative Group. Pediatr. Infect. Dis. J. *18*, 517–523.

Quin, L.R., Onwubiko, C., Moore, Q.C., Mills, M.F., McDaniel, L.S., and Carmicle, S. (2007). Factor H binding to PspC of *Streptococcus pneumoniae* increases adherence to human cell lines in vitro and enhances invasion of mouse lungs in vivo. Infect. Immun. *75*, 4082–4087.

Reichmann, P., König, A., Liñares, J., Alcaide, F., Tenover, F.C., McDougal, L., Swidsinski, S., and Hakenbeck, R. (1997). A global gene pool for high-level cephalosporin resistance in commensal Streptococcus species and *Streptococcus pneumoniae*. J. Infect. Dis. *176*, 1001–1012.

Reid, S.D., Montgomery, A.G., Voyich, J.M., DeLeo, F.R., Lei, B., Ireland, R.M., Green, N.M., Liu, M., Lukomski, S., and Musser, J.M. (2003). Characterization of an extracellular virulence factor made by group A Streptococcus with homology to the *Listeria monocytogenes* internalin family of proteins. Infect. Immun. *71*, 7043–7052.

Reyes-Caballero, H., Guerra, A.J., Jacobsen, F.E., Kazmierczak, K.M., Cowart, D., Koppolu, U.M.K., Scott, R.A., Winkler, M.E., and Giedroc, D.P. (2010). The metalloregulatory zinc site in *Streptococcus pneumoniae* AdcR, a zinc-activated MarR family repressor. J. Mol. Biol. *403*, 197–216.

Riboldi-Tunnicliffe, A., Bent, C.J., Isaacs, N.W., and Mitchell, T.J. (2004). Expression, purification and X-ray characterization of residues 18-230 from the pneumococcal histidine triad protein A (PhtA) from *Streptococcus pneumoniae*. Acta Crystallogr. D Biol. Crystallogr. *60*, 926–928.

Riboldi-Tunnicliffe, A., Isaacs, N.W., and Mitchell, T.J. (2005). 1.2 Angstroms crystal structure of the *S. pneumoniae* PhtA histidine triad domain a novel zinc binding fold. FEBS Lett. *579*, 5353–5360.

Ricci, S., Janulczyk, R., Gerlini, A., Braione, V., Colomba, L., Iannelli, F., Chiavolini, D., Oggioni, M.R., Björck, L., and Pozzi, G. (2011). The factor H-binding fragment of PspC as a vaccine antigen for the induction of protective humoral immunity against experimental pneumococcal sepsis. Vaccine *29*, 8241–8249.

Rigden, D.J., Galperin, M.Y., and Jedrzejas, M.J. (2003). Analysis of structure and function of putative surface-exposed proteins encoded in the *Streptococcus pneumoniae* genome: a bioinformatics-based approach to vaccine and drug design. Crit. Rev. Biochem. Mol. Biol. *38*, 143–168.

Rink, L., and Gabriel, P. (2001). Extracellular and immunological actions of zinc. Biometals *14*, 367–383.

Rioux, S., Neyt, C., Di Paolo, E., Turpin, L., Charland, N., Labbe, S., Mortier, M.C., Mitchell, T.J., Feron, C., Martin, D., *et al*. (2010). Transcriptional regulation, occurrence and putative role of the Pht Family of *Streptococcus pneumoniae*. Microbiology *157*, 336–348.

Rodgers, G.L., Arguedas, A., Cohen, R., and Dagan, R. (2009). Global serotype distribution among *Streptococcus pneumoniae* isolates causing otitis media in children: potential implications for pneumococcal conjugate vaccines. Vaccine *27*, 3802–3810.

Rosenow, C., Ryan, P., Weiser, J.N., Johnson, S., Fontan, P., Ortqvist, A., and Masure, H.R. (1997). Contribution of novel choline-binding proteins to adherence, colonization and immunogenicity of *Streptococcus pneumoniae*. Mol. Microbiol. *25*, 819–829.

Russell, H., Tharpe, J.A., Wells, D.E., White, E.H., and Johnson, J.E. (1990). Monoclonal antibody recognizing a species-specific protein from *Streptococcus pneumoniae*. J. Clin. Microbiol. *28*, 2191–2195.

Sampson, J.S., O'Connor, S.P., Stinson, A.R., Tharpe, J.A., and Russell, H. (1994). Cloning and nucleotide sequence analysis of *psaA*, the *Streptococcus pneumoniae* gene encoding a 37-kilodalton protein homologous to previously reported Streptococcus sp. adhesins. Infect. Immun. *62*, 319–324.

Scott, J.R., and Barnett, T.C. (2006). Surface proteins of gram-positive bacteria and how they get there. Annu. Rev. Microbiol. *60*, 397–423.

Seiberling, M., Bologa, M., Brookes, R., Ochs, M., Go, K., Neveu, D., Kamtchoua, T., Lashley, P., Yuan, T., and Gurunathan, S. (2012). Safety and immunogenicity of a

pneumococcal histidine triad protein D vaccine candidate in adults. Vaccine *30*, 7455–7460.

Shafeeq, S., Kloosterman, T.G., and Kuipers, O.P. (2011). Transcriptional response of *Streptococcus pneumoniae* to Zn^{2+} limitation and the repressor/activator function of AdcR. Metallomics *3*, 609–618.

Shankar, A.H., and Prasad, A.S. (1998). Zinc and immune function: the biological basis of altered resistance to infection. Am. J. Clin. Nutr. *68*, 447S–463S.

Shao, Z., Pan, X., Li, X., Liu, W., Han, M., Wang, C., Wang, J., Zheng, F., Cao, M., and Tang, J. (2011). HtpS, a novel immunogenic cell surface-exposed protein of *Streptococcus suis*, confers protection in mice. FEMS Microbiol. Lett. *314*, 174–182.

Shaper, M., Hollingshead, S.K., Benjamin, W.H., and Briles, D.E. (2004). PspA protects *Streptococcus pneumoniae* from killing by apolactoferrin, and antibody to PspA enhances killing of pneumococci by apolactoferrin. Infect. Immun. *72*, 5031–5040.

Sharma, S.K., Casey, J.R., and Pichichero, M.E. (2012). Reduced serum IgG responses to pneumococcal antigens in otitis-prone children may be due to poor memory B-cell generation. J. Infect. Dis. *205*, 1225–1229.

Simell, B., Ahokas, P., Lahdenkari, M., Poolman, J., Henckaerts, I., Kilpi, T.M., and Käyhty, H. (2009). Pneumococcal carriage and acute otitis media induce serum antibodies to pneumococcal surface proteins CbpA and PhtD in children. Vaccine *27*, 4615–4621.

Singleton, R.J., Hennessy, T.W., Bulkow, L.R., Hammitt, L.L., Zulz, T., Hurlburt, D.A., Butler, J.C., Rudolph, K., and Parkinson, A. (2007). Invasive pneumococcal disease caused by nonvaccine serotypes among alaska native children with high levels of 7-valent pneumococcal conjugate vaccine coverage. JAMA *297*, 1784–1792.

Spellerberg, B., Rozdzinski, E., Martin, S., Weber-Heynemann, J., Schnitzler, N., Lutticken, R., and Podbielski, A. (1999). Lmb, a protein with similarities to the LraI adhesin family, mediates attachment of *Streptococcus agalactiae* to human laminin. Infect. Immun. *67*, 871–878.

Strevett, K.A., and Chen, G. (2003). Microbial surface thermodynamics and applications. Res. Microbiol. *154*, 329–335.

Swiatlo, E., Champlin, F.R., Holman, S.C., Wilson, W.W., and Watt, J.M. (2002). Contribution of choline-binding proteins to cell surface properties of *Streptococcus pneumoniae*. Infect. Immun. *70*, 412–415.

Talkington, D.F., Brown, B.G., Tharpe, J.A., Koenig, A., and Russell, H. (1996). Protection of mice against fatal pneumococcal challenge by immunization with pneumococcal surface adhesin A (PsaA). Microb. Pathog. *21*, 17–22.

Tano, K., Grahn-Håkansson, E., Holm, S.E., and Hellström, S. (2000). Inhibition of OM pathogens by alpha-hemolytic streptococci from healthy children, children with SOM and children with rAOM. Int. J. Pediatr. Otorhinolaryngol. *56*, 185–190.

Tenenbaum, T., Spellerberg, B., Adam, R., Vogel, M., Kim, K.S., and Schroten, H. (2007). *Streptococcus agalactiae* invasion of human brain microvascular endothelial cells is promoted by the laminin-binding protein Lmb. Microbes Infect. *9*, 714–720.

Tettelin, H., Nelson, K.E., Paulsen, I.T., Eisen, J.A., Read, T.D., Peterson, S., Heidelberg, J., DeBoy, R.T., Haft, D.H., Dodson, R.J., *et al*. (2001). Complete genome sequence of a virulent isolate of *Streptococcus pneumoniae*. Science *293*, 498–506.

Tilley, S.J., Orlova, E. V, Gilbert, R.J.C., Andrew, P.W., and Saibil, H.R. (2005). Structural basis of pore formation by the bacterial toxin pneumolysin. Cell *121*, 247–256.

Tseng, H.J., McEwan, A.G., Paton, J.C., and Jennings, M.P. (2002). Virulence of *Streptococcus pneumoniae*: PsaA mutants are hypersensitive to oxidative stress. Infect. Immun. *70*, 1635–1639.

Versieck, J. (1985). Trace elements in human body fluids and tissues. Crit. Rev. Clin. Lab. Sci. *22*, 97–184.

Waldemarsson, J., Areschoug, T., Lindahl, G., and Johnsson, E. (2006). The streptococcal Blr and Slr proteins define a family of surface proteins with leucine-rich repeats: camouflaging by other surface structures. J. Bacteriol. *188*, 378–388.

Wang, S., Li, Y., Shi, H., Scarpellini, G., Torres-Escobar, A., Roland, K.L., Curtiss 3rd, R., and Curtiss, R. (2010). Immune responses to recombinant pneumococcal PsaA antigen delivered by a live attenuated *Salmonella* vaccine. Infect. Immun. *78*, 3258–3271.

Watson, D.A., Musher, D.M., Jacobson, J.W., and Verhoef, J. (1993). A brief history of the pneumococcus in biomedical research: a panoply of scientific discovery. Clin. Infect. Dis. *17*, 913–924.

Weinberger, D.M., Trzciński, K., Lu, Y.-J., Bogaert, D., Brandes, A., Galagan, J., Anderson, P.W., Malley, R., and Lipsitch, M. (2009). Pneumococcal capsular polysaccharide structure predicts serotype prevalence. PLoS Pathog. *5*, e1000476.

Weiser, J.N., Austrian, R., Sreenivasan, P.K., and Masure, H.R. (1994). Phase variation in pneumococcal opacity: relationship between colonial morphology and nasopharyngeal colonization. Infect. Immun. *62*, 2582–2589.

Whitmore, L., and Wallace, B.A. (2004). DICHROWEB, an online server for protein secondary structure analyses from circular dichroism spectroscopic data. Nucleic Acids Res. *32*, W668–73.

Whitmore, L., and Wallace, B.A. (2008). Protein secondary structure analyses from circular dichroism spectroscopy: methods and reference databases. Biopolymers *89*, 392–400.

WHO (2004). The Global Burden of Disease: 2004 Update (Geneva).

Willey, J., Sherwood, L., and Woolverton, C. (2008). Microbiology (McGraw-Hill).

Wilson, P. (2010). Giving developing countries the best shot: An overview of vaccine access and R&D. Oxfam International.

Wilson, W.W., Wade, M.M., Holman, S.C., and Champlin, F.R. (2001). Status of methods for assessing bacterial cell surface charge properties based on zeta potential measurements. J. Microbiol. Methods *43*, 153–164.

Wizemann, T.M., Heinrichs, J.H., Adamou, J.E., Erwin, A.L., Kunsch, C., Choi, G.H., Barash, S.C., Rosen, C.A., Masure, H.R., Tuomanen, E., *et al*. (2001). Use of a whole genome approach to identify vaccine molecules affording protection against *Streptococcus pneumoniae* infection. Infect. Immun. *69*, 1593–1598.

Wu, K., Zhang, X., Shi, J., Li, N., Li, D., Luo, M., Cao, J., Yin, N., Wang, H., Xu, W., *et al*. (2010). Immunization with a combination of three pneumococcal proteins confers additive and broad protection against *Streptococcus pneumoniae* infections in mice. Infect. Immun. *78*, 1276–1283.

Xu, J., Dai, W., Wang, Z., Chen, B., Li, Z., and Fan, X. (2011). Intranasal vaccination with chitosan-DNA nanoparticles expressing pneumococcal surface antigen a protects mice against nasopharyngeal colonization by *Streptococcus pneumoniae*. Clin. Vaccine Immunol. *18*, 75–81.

Zhang, J.R., Mostov, K.E., Lamm, M.E., Nanno, M., Shimida, S., Ohwaki, M., and Tuomanen, E. (2000). The polymeric immunoglobulin receptor translocates pneumococci across human nasopharyngeal epithelial cells. Cell *102*, 827–837.

Zhang, Y., Masi, A.W., Barniak, V., Mountzouros, K., Hostetter, M.K., and Green, B.A. (2001). Recombinant PhpA protein, a unique histidine motif-containing protein from *Streptococcus pneumoniae*, protects mice against intranasal pneumococcal challenge. Infect. Immun. *69*, 3827–3836.

Zipfel, P.F., Hallstrom, T., Hammerschmidt, S., and Skerka, C. (2008). The complement fitness factor H: role in human diseases and for immune escape of pathogens, like pneumococci. Vaccine *26 Suppl 8*, I67–74.

Zipfel, P.F., Skerka, C., Hellwage, J., Jokiranta, S.T., Meri, S., Brade, V., Kraiczy, P., Noris, M., and Remuzzi, G. (2002). Factor H family proteins: on complement, microbes and human diseases. Biochem. Soc. Trans. *30*, 971–978.

Publications and Conference Presentations

Plumptre, C.D., Ogunniyi, A.D., and Paton, J.C. (2012). Polyhistidine triad proteins of pathogenic streptococci. Trends Microbiol. *20*, 485–493.

Plumptre, C.D., Eijkelkamp, B.A., Behr F., O'Mara M.L., Couñago R.L.M., Ogunniyi, A.D., Kobe B., Paton J.C., McDevitt C.A. (2013). Zinc homeostasis in *Streptococcus pneumoniae* and its requirement for bacterial colonization. Manuscript submitted.

Plumptre, C.D., Ogunniyi A.D., Adamson P., Gordon D.L., Paton J.C. (23^{rd} – 26^{th} June 2011). Interaction of pneumococcal histidine triad proteins with the human complement regulator factor H-like protein 1. Poster presentation, 10^{th} European Meeting on the Molecular Biology of the Pneumococcus, Amsterdam, The Netherlands.

Plumptre, C.D., Ogunniyi A.D., Paton J.C. (1^{st} – 4^{th} July 2012). Vaccination against *Streptococcus pneumoniae* with an immunodominant region of polyhistidine triad protein D. Oral presentation, Australian Society for Microbiology Annual Scientific Meeting and Exhibition, Brisbane, Australia.